

**TOMSK POLYTECHNIC UNIVERSITY**

**S. V. Kirsanov**

**MATERIAL CUTTING AND CUTTING  
TOOLS**

**Tomsk Polytechnic University Publishing House  
2012**

UDC 621.9.01+621.9.02 (075.8)  
BBC 00000  
K00

**Kirsanov S.V.**

K00 Material cutting and cutting tools: study aid / S.V. Kirsanov; Tomsk Polytechnic University. – Tomsk: TPU Publishing House, 2012, 196 p.

The subject of this book is the machining processes. The general information about the cutting of materials, chip formation, complex cutting patterns, heat, strength, wear resistance, tool life, machinability of materials and features of the process of cutting with multiple point cutting tools and grinding tools is given in the first part. Questions of calculation and optimization of design and geometrical parameters of the common types of cutting tools, with respect to the cutting conditions, properties of cutting tool and workpiece materials, as well as the requirements for dimensional accuracy and surface finish, are examined in the second part of the book.

The book is recommended for English-speaking students following the Bachelor Degree Program in Mechanical Engineering at Tomsk Polytechnic University.

**UDC 621.9.01+621.9.02 (075.8)**  
**BBC 00000**

*Lingvistic Advisor*

Senior lecturer

Foreign Languages Chair of High Technology Physics Institute, TPU

*O.G. Maslennikova*

*Reviewers*

Doctor of Science (Technical)

Associate professor of the

Department of Automated Mechanical Manufacturing Engineering, TPU

*A.I. Afonarov*

President of Industrial Company “MION”, Limited Liability Company

*Yu.V. Volkov*

© STE HPT TPU, 2012

© Kirsanov S.V., 2012

© Design. Tomsk Polytechnic University  
Publishing House, 2012

## **Preface**

The textbook contains material necessary for the development of one of the majors, provided by the state educational standards in "Technology, equipment and automation in mechanical engineering".

The book gives an overview of the cutting of materials, issues of chip formation in free orthogonal cutting, complex cutting patterns, thermal phenomena in cutting, durability and wear of cutting tools, tool life and machinability of materials, as well as the features of the cutting process with multiple-point (milling cutters, drills) and abrasive tools.

The analysis of cutting tools designs focuses on the strengths and weaknesses of the tools, trends in cutting tool engineering, international experience and present achievements in the practice.

The textbook is illustrated with a large number of drawings and diagrams, reference materials are reduced to a minimum. All variety of cutting tools designs is reduced to the common cutters, broaches, drills, core drills, reamers, milling cutters, threading tools, gear cutting tools, grinding wheels and tools for automated production.

When writing a textbook were critically analyzed and partially used materials from textbooks, manuals, reference books, teaching materials and various publications on certain types of cutting tools.

## CONTENTS

Preface.....	3
CONTENTS .....	4
1. Basics of Cutting .....	7
1.1 Overview of the cutting process.....	7
1.2 Chip formation in cutting .....	14
1.2.1 Stresses and forces in chip formation .....	17
1.2.2 Tool-chip and tool-workpiece interactions.....	18
1.2.3 Built-up edge.....	22
1.2.4 Energy and work consumed in the cutting process .....	24
1.3 Complex schemes of cutting.....	25
1.3.1 Oblique cutting .....	25
1.3.2 Non-free cutting.....	27
1.3.3 Surface finish of the machined surface.....	29
1.4 Heat generation in cutting .....	31
1.4.1 Sources of heat and heat balance equation .....	32
1.4.2 Cutting temperature measurements .....	34
1.5 Strength and wear of the cutting tools .....	37
1.5.1 Cutting tool materials.....	37
1.5.2 Strength of cutting tools .....	40
1.5.3 Physical nature of tool wear .....	41
1.5.4 Cutting wedge failures.....	43
1.6 Cutting tool life and machinability of materials .....	44
1.6.1 Relation between tool life and cutting parameters .....	44
1.6.2 Machinability of materials .....	47
1.6.3 Application of cutting fluids in cutting.....	48
2. Basic Types of Machining.....	52
2.1 Turning Operations.....	52
2.2 Drilling operations .....	53
2.2.1 Cutting force components in drilling.....	53
2.2.2 Wear and life of drills. Calculation of drilling parameters ...	54
2.3 Milling Operations .....	57
2.3.1 Fundamentals of milling processes .....	57
2.3.2 Thickness of uncut chip for helical plain cutter. Uniform milling condition.....	60
2.3.3 Forces, work and power in plain milling .....	62



2.3.4	Forces and power in face milling .....	63
2.3.5	Milling parameters calculation .....	64
3.	Grinding Operations.....	65
3.1	Types of Grinding Operations .....	65
3.2	Types of Abrasives .....	67
3.3	Features of a Grinding Wheel as a Cutting Tool.....	68
3.4	Work of a Single Grain .....	70
3.5	Phenomenon of Self-sharpening .....	74
3.6	Principles for the Selection of a Grinding Wheel .....	74
3.7	Grinding Wheel Life .....	76
3.8	Grinding Wheels, Specification and Application .....	79
3.9	The Procedure of Selection and Calculation of Cutting Parameters and Required Power in Grinding.....	80
4.	Design and Calculation of Cutters and Broaches.....	82
4.1	Lathe Cutters.....	82
4.1.1	Constructions of turning cutters .....	82
4.1.2	Cutters with indexable inserts .....	84
4.1.3	Form cutters.....	88
4.2	Broaches.....	94
4.2.1	Common types and application of broaches .....	94
4.2.2	Calculation of the round internal pull broaches .....	96
4.2.3	Internal broaches for holes of irregular shape.....	102
4.2.4	Surface broaches.....	105
5.	Design and Calculation of Drills, Core-Drills and Reamers.....	108
5.1	Drills.....	108
5.1.1	Spade drills .....	108
5.1.2	Twist drills .....	109
5.1.3	Methods of twist drill sharpening.....	114
5.1.4	Disadvantages and correction of twist drill geometry .....	116
5.1.5	Deep hole drills .....	117
5.1.5.1	Half round drills .....	119
5.1.5.2	Gun drills.....	120
5.1.5.3	BTA drills.....	121
5.1.5.4	Ejector drills.....	122
5.1.5.5	Trepanning drills .....	123
5.2	Core drills .....	124
5.2.1	Cylindrical core drills.....	124
5.2.2	Counter bore, countersink and spot facer.....	128
5.3	Reamers .....	129
5.3.1	Straight reamers .....	131
5.3.2	Reamers of other types .....	134

<b>6. Design and Calculation of Milling Cutters .....</b>	<b>138</b>
<b>6.1 Milling cutters with pointed teeth and form-relieved teeth .....</b>	<b>139</b>
<b>6.2 Types of milling cutters.....</b>	<b>143</b>
<b>7. Design and Calculation of Thread Cutting Tools.....</b>	<b>149</b>
<b>7.1 Threading cutters and chasers .....</b>	<b>149</b>
<b>7.2 Taps.....</b>	<b>153</b>
<b>7.3 Thread dies .....</b>	<b>160</b>
<b>7.4 Thread milling cutters and inserted-chaser dies .....</b>	<b>162</b>
<b>8. Design and Calculation of Gear Cutting Tools.....</b>	<b>168</b>
<b>8.1 Involute gear cutters for form cutting.....</b>	<b>168</b>
<b>8.2 Hobs .....</b>	<b>172</b>
<b>8.3 Gear-shaper cutters.....</b>	<b>174</b>
<b>8.4 Shavers.....</b>	<b>178</b>
<b>8.5 Generating cutters for parts with non-involute profile .....</b>	<b>180</b>
<b>8.6 Calculations of spline hobbing cutters .....</b>	<b>182</b>
<b>9. Cutting Tools for Automated Production.....</b>	<b>185</b>
<b>9.1 Cutting tools for automated machining .....</b>	<b>185</b>
<b>9.2 Auxiliary tooling for CNC machines and machining centers ....</b>	<b>188</b>
<b>Conclusion .....</b>	<b>193</b>
<b>References .....</b>	<b>194</b>

# 1. Basics of Cutting

Cutting of materials is the oldest and currently one of the most common methods of machine parts manufacture, when the required shape and dimensions of the parts is produced by removing layers of material in the form of chips from surfaces of workpieces that are made by casting, forging, stamping, rolling and other methods.

The widespread use of cutting in engineering is due to the following advantages: 1) High dimensional and geometrical accuracy, fine surface finish; 2) versatility and production flexibility; 3) minimum tooling cost; 4) a favorable conditions for industrial automation; 5) relatively low power consumption, much lower compared to other methods of manufacture.

There are many types of cutting operations, which differ in design of cutting tools and machines, as well as kinematics of relative motions of the tool and the workpiece. The most widespread cutting operations include turning, planing, milling, broaching, drilling, core-drilling, reaming, thread cutting and gear cutting.

Regardless of the type of a tool, whether it is cutting or grinding, the interaction of the tool with the workpiece is based on the same general laws of the cutting process. The essence of these laws can be examined with the help of a simple single-point tool – a turning cutter.

## 1.1 Overview of the cutting process

Turning is the most widely used for machining of circular shape parts. The cutting tools involved are lathe cutters of various types. In external straight turning (Figure 1.1) the workpiece 1 is rotated around its axis and the cutter 5 is fed parallel to the axis of the workpiece at a feed rate (mm/rev). In radial turning, for example, with cut-off cutters or form cutters, the tool is moved radially along the  $Y$  axis with radial feed.

In straight turning the resultant motion of the cutting edge points is helical. In one pass of a cutter the stock (allowance) with thickness  $t$  is removed from the workpiece surface 2, called **work surface**. Surface 3, formed after the passage of the major cutting edge of a cutter, is called **transient surface**, and the surface 4 is called **machined surface**.

The definitions of the cutting tool geometrical parameters, which are also valid for other types of cutting, but with some adjustments related to their features, are examined on the example of a turning tool.

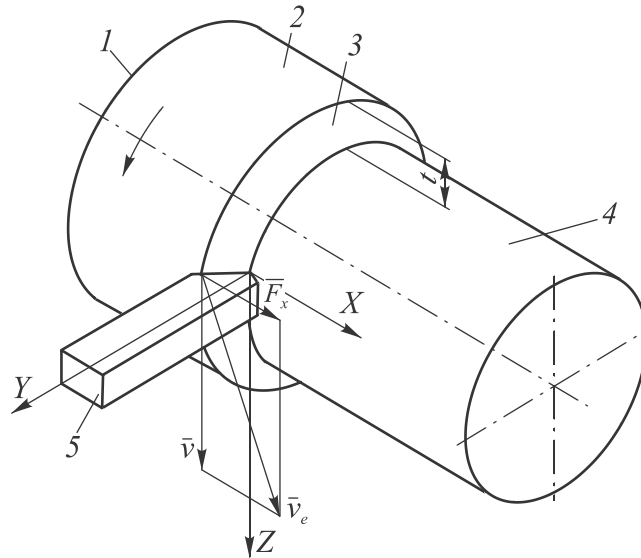


Fig. 1.1 Kinematics of external straight turning

Straight turning cutter (Figure 1.2) consists of the cutting part with the **corner 1** and shank. Surface 2, upon which the chip flows, is called **rake surface** or **face** and the other two surfaces facing the transient surface and the machined surface are called the **major flank 3** and the **minor flank 4** respectively. The intersection of the face with major and minor flanks forms the **major cutting edge 5** and the **minor cutting edge 6** respectively.

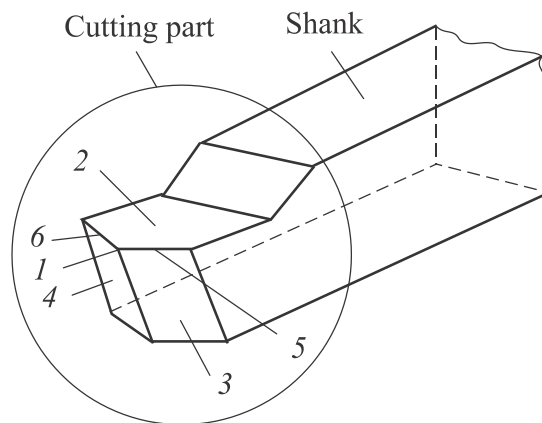


Fig. 1.2 Turning cutter

For defining, specifying and measuring angles of a cutting tool in sharpening, the two reference planes are used: the cutting edge plane and the reference plane.

The cutting edge plane passes through the major cutting edge, tangent to the transient surface and cutting velocity vector (Figure 1.3).

In straight turning the **reference plane** contains the vectors of the axial and radial feed; it is perpendicular to the cutting velocity vector and the cutting edge plane. In the particular case, this plane coincides with the base of the tool shank.

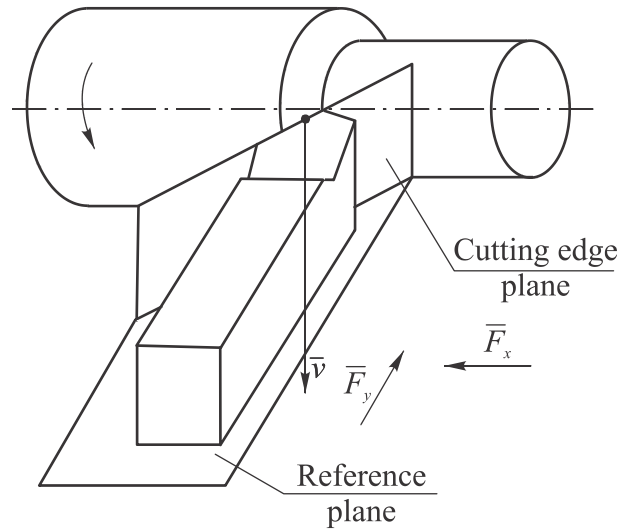


Fig. 1.3 Position of the reference and cutting edge planes

As the cutting speed in turning, the surface velocity vector  $\bar{v}$  is usually taken. The feed rate vector often an order of magnitude or more is less than the cutting velocity vector ( $\bar{f}_x \ll \bar{v}$ ), and therefore its impact on the geometric parameters of the tool is negligible. It should be noted that when, for example, drilling feed vector magnitude is comparable with the cutting velocity vector, this influence must be considered in determining the so-called **working parameters** of the tool geometry, which are measured with respect to the velocity vector of the resulting motion  $\bar{v}_e$  (Fig. 1.1).

The surface velocity of the primary motion in cutting is calculated by

$$v = \frac{\pi dn}{1000} \text{ (m/min)}, \quad (1.1)$$

where  $d$  is the diameter of the workpiece, mm;  $n$  is the speed of workpiece rotation, rpm.

Fig. 1.4 shows the plain turning cutter in the reference plane and angles in the cross sections  $N-N$  and  $N_I-N_I$ , which run perpendicular to the projections respectively of the major and minor cutting edges on the reference plane. Here the section plane  $N-N$  is called the **orthogonal plane**. The process of deformation of the material during its transformation to the chips oc-

curs in the orthogonal plane and parallel planes passing through any point of the major cutting edge.

The angles distinguished in the orthogonal plane are: the **rake angle**  $\gamma$  – the angle between the face of a tool (or a tangent to it) and the reference plane at the given point of the major cutting edge, the **clearance angle**  $\alpha$  – the angle between the flank (or tangent to it) and the cutting edge plane; **wedge angle**  $\beta$  – the angle between the face and the flank (or tangents to them) of the cutter  $\beta=90^\circ-(\alpha+\gamma)$ .

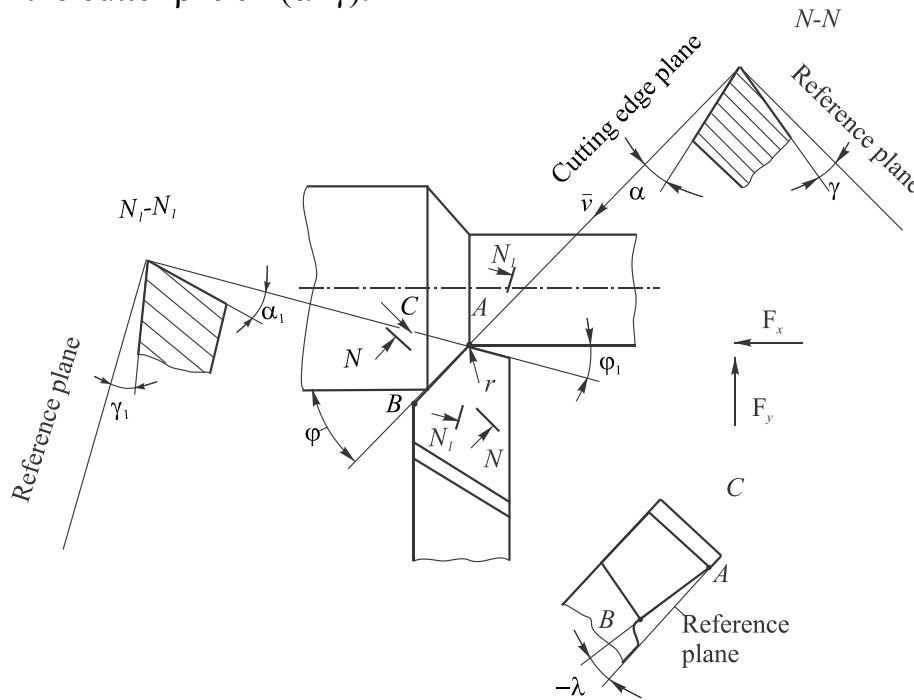


Fig. 1.4 Geometric parameters of a turning cutter

In the cutting edge plane (view A) the **cutting edge inclination angle** is measured as the angle between the major cutting edge and the reference plane.

The reference plane include the **cutting edge angle**  $\varphi$  and the **minor cutting edge angle**  $\varphi_1$  – the angles between the feed rate vector  $\overline{f_x}$  and the projections of the major and minor cutting edges on the reference plane respectively, and the included angle  $\varepsilon$  – the angle between the projections of the major and minor cutting edges on the reference plane  $\varepsilon=180^\circ-(\varphi+\varphi_1)$ .

The rake angle can have either a positive or negative value, depending on the position of the cutter face relative to the reference plane.

In turning with radial feed the values of the **working rake angle**  $\gamma_k$  and **clearance angle**  $\alpha_k$  are affected by the position of the cutting velocity vector  $\overline{v}$  through which the cutting edge plane passes.

If the tip of the cutter is shifted upward from the point  $A$  to the point  $A'$  with respect to the lathe center line (Fig. 1.5), the working rake angle  $\gamma_k$  increases ( $\gamma_k > \gamma$ ), and working clearance angle  $\alpha_k$  is reduced by the same amount ( $\alpha_k < \alpha$ ). And it is vice versa, if the cutter tip is shifted below the center line.

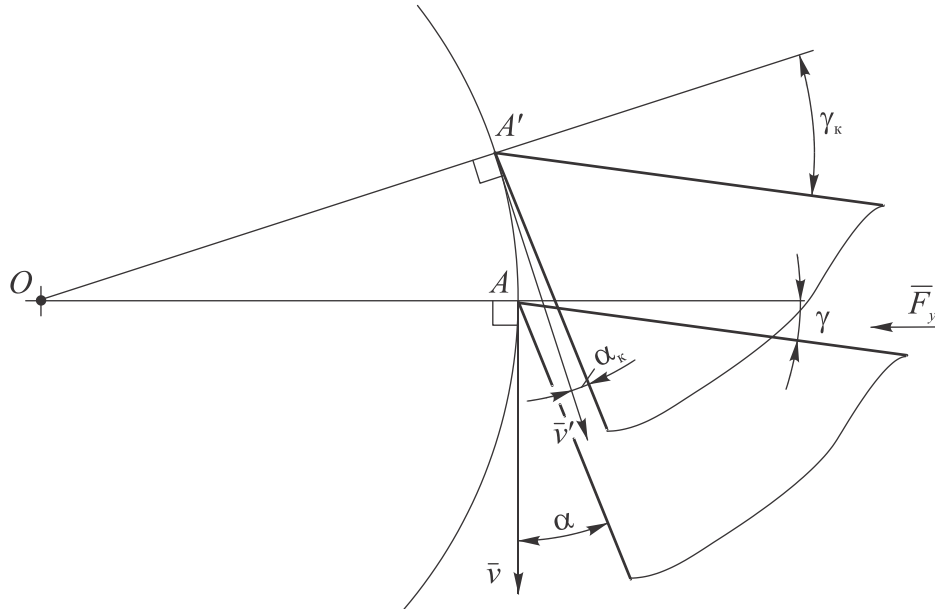


Fig. 1.5 Variation of the rake  $\gamma$  and clearance angle  $\alpha$  when the tip is placed above the center line

The clearance angle is intended to reduce friction between the transient surface and the flank of the cutting tool. With the increasing clearance angle the cutting wedge strength reduces. Therefore, accounting for the load on the cutting wedge, as well as the strength of the tool material and cutting conditions the clearance angle is often equal to  $6 \dots 10^\circ$ .

The cutting edge angles  $\phi$  and  $\phi_1$  define the dimensions of cut. i.e. ratio of the thickness and width of the uncut chip  $a/b$  ( $s/t$ ) and the roughness of the machined surface.

The inclination angle  $\lambda$  of the major cutting edge along with the rake angle  $\gamma$  influences on the process of the workpiece material deformation by changing the direction of chip flow on the face of the tool. In Russian practice, in contrast to the international case, the inclination angle  $\lambda$  is considered positive when the most vulnerable to damage part of the tool, which is its tip, is the lowest position in relation to other points of the major cutting edge (Fig. 1.6, a). Due to this position the tip of the tool is protected from damage, especially in interrupted cutting and machining with shock loads. In case viscous materials are being cut, the positive inclination angle  $\lambda$  will force the chip to flow in the direction of the machined surface, leading to scratching

and increased roughness of the latter. This is not so important in roughing, since the subsequent finishing operations will remove these micro irregularities.

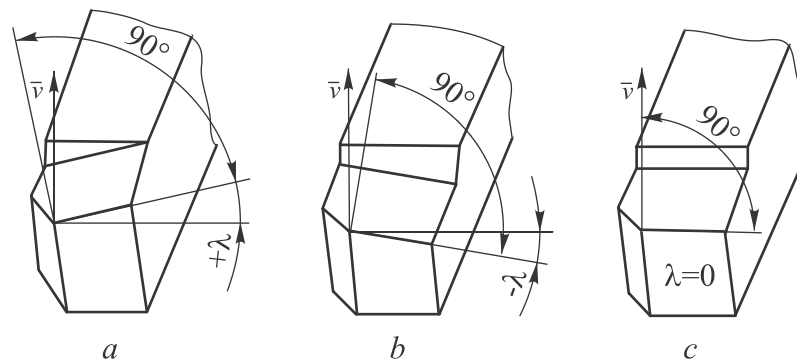


Fig. 1.6 Cutting edge inclination angle: (a)  $\lambda > 0$ ; (b)  $\lambda < 0$ ; (c)  $\lambda = 0$

During the finishing operations in order to prevent damage of the machined surface the negative inclination angle  $\lambda$  is applied (Figure 1.7, b), as in this case, the load on the cutting wedge is relatively small and the chip is directed away from the machined surface.

The **uncut chip** in longitudinal turning is defined by the thickness  $a$  and width  $b$  (Figure 1.7) that are associated with the cutting parameters: feed  $f$  and depth of cut  $t$  (Figure 1.7, a)

$$\begin{aligned} a &= f \sin \varphi; \\ b &= t / \sin \varphi. \end{aligned} \quad (1.2)$$

The nominal cross-sectional area of the uncut chip is:

$$F_N = ab = ft. \quad (1.3)$$

As it has been mentioned before, the tip of the cutter in turning follows a helical motion, and therefore the minor cutting edge is also involved in formation of the machined surface. Therefore, cross-section of the uncut chip is a truncated trapezoid in form, rather than a parallelogram (Fig. 1.7, b). The actual area of the trapezoid is decreased by the area of the micro irregularities.

It follows from Equation (1.2) that the cutting edge angle  $\varphi$  has a large effect on the  $a/b$  ratio. With the cutting edge angle decreasing, the uncut chip becomes thinner and wider, which affects the material deformation, cutting force and heat evacuation conditions.

Cutting with two or more cutting edges involved is called the **non-free cutting** (Fig. 1.7, b). In contrast to the non-free cutting, the machined surface in the **free cutting** process is formed with a single cutting edge (Fig. 1.8).



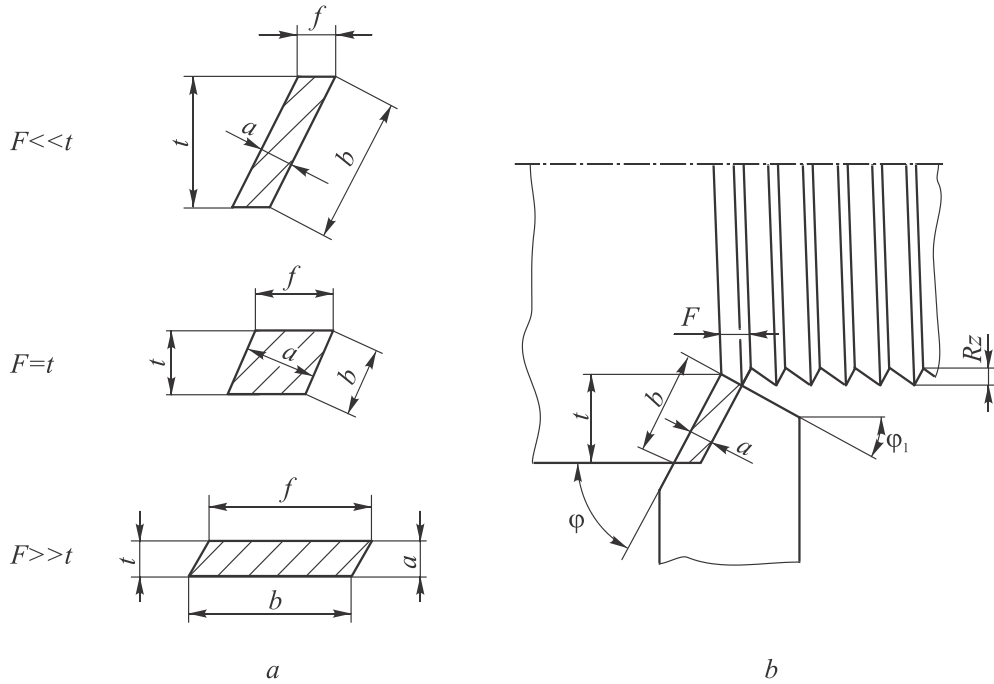


Fig. 1.7 Shapes of the uncut chip cross-sections with relation to the minor cutting edge angle: (a)  $\phi_1=0$ ; (b)  $\phi_1>0$

The **orthogonal** and **oblique cutting** schemes also can be found in machining. The latter include the cutting tool with the major cutting edge inclined at an angle  $\lambda$  with respect to the cutting velocity vector. In the orthogonal free-cutting, the chip flow direction is perpendicular to the cutting edge, and in case the inclination angle  $\lambda$  is not zero the chip flow direction deflects from the normal by about the same angle.

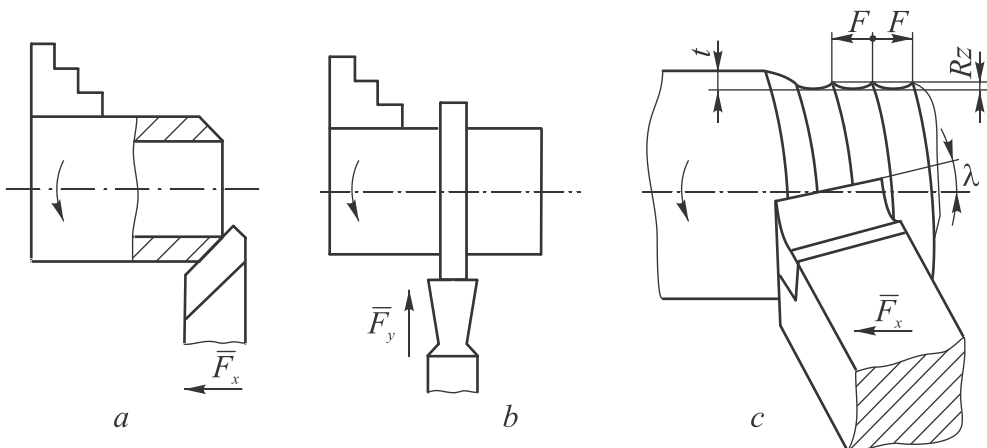


Fig. 1.8 Examples of free cutting in turning: (a) facing of a tube; (b) turning of a collar; (c) oblique finish turning with a single-edge (without corner) cutter ( $t \leq 1 \text{ mm}$ ,  $\lambda = 10 \dots 20^\circ$ )

While the deformation of work material in orthogonal cutting occurs in a plane perpendicular to the cutting edge, the deformation in oblique cutting occurs in both the parallel and normal planes.

Of all of the cutting patterns the simplest case is the scheme of free orthogonal cutting, and the most difficult is the non-free oblique cutting.

## 1.2 Chip formation in cutting

From a physical point of view, the process of cutting is a process of deep plastic deformation and fracture, followed by the friction of the chip against the face of the cutting wedge and rubbing of the flank of the tool against the machined surface, which occur under conditions of high pressures and sliding speeds. The mechanical energy is converted into heat, which in turn has a big impact on the mechanics of uncut chip deformation, cutting force, wear and tool life.

The formed during cutting chip is classified into three types: continuous, discontinuous, serrated and segmented.

**Continuous chip** (Fig. 1.9, a) represents a continuous “ribbon”, which, depending on the flow conditions, can be straight, spiral or “comma”-shaped. The shape and dimensions of the chip cross-section are constant along the length, which indicates the stability of the deformation occurring during the chip formation. Continuous chip is produced in cutting ductile metals, generally at a high speed, small and medium feeds and positive rake angles.

**Discontinuous chip** (Fig. 1.9, b) consists of individual elements of metal 1 which are not connected or loosely interconnected by a thin layer. Discontinuous chip is formed in cutting brittle metals (cast iron, bronze, etc.), as well as in cutting ductile metals at low speeds, cutting with thick layer being removed, small rake angles, high hardness of work material and in other conditions that impede plastic deformation.

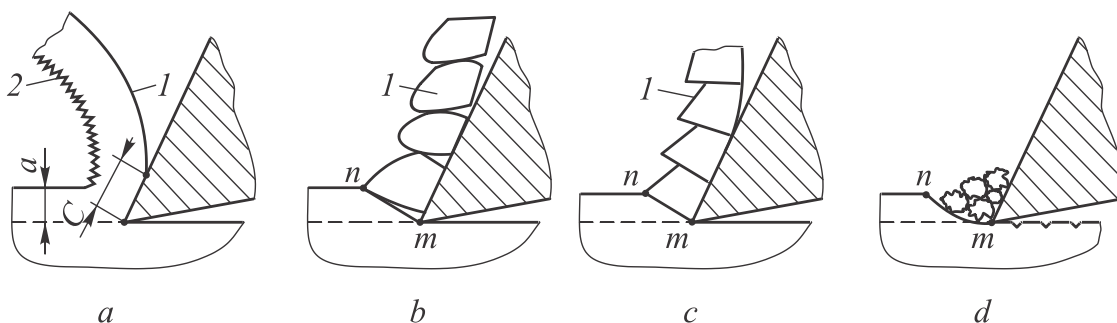
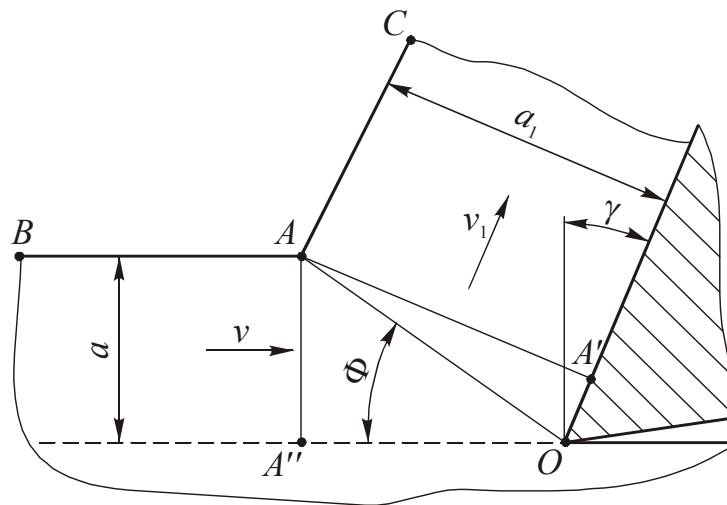


Fig. 1.9 Types of chips:  
(a) continuous; (b) discontinuous; (c) serrated; (d) segmented

**Serrated or sawtooth chip** (Figure 1.9, c) is the transition type between the discontinuous and continuous types of chip. It consists of individual segments, bound to each other with highly deformed material. This type of chip is common in cutting high-alloy steels and titanium alloys.

**Segmented chip** (Fig. 1.9, d) consists of separate not connected pieces of various sizes and shapes. This type of chip is produced in the cutting of very brittle materials or metals with adhesive to the cutter face.

The first model of chip formation in cutting was proposed by I.A. Time (1870), and then it was further developed K.A. Zvorykin (1893). In U.S.A., these models were rediscovered by M.E. Merchant (1945).



*Fig. 1.10 Chip formation with single shear plane model*

According to the I.A. Time model (Figure 1.10) the uncut chip with thickness  $a$  is formed into the chip with thickness  $a_1$  by shearing (sliding) of the thin layers of material in the plane  $OA$ , positioned at the **shear angle**  $\Phi$  to the cutting edge plane. As a result of the deformation of the material during its transition to the chip, the thickness  $a_1$  of the latter is bigger than the thickness of the layer being removed  $a$ , and its length  $l_1$  is shorter than the path  $l$  traveled by the tool. This phenomenon I.A. Time called the **chip shortening** and the ratio of the chip thickness  $a_1$  to the uncut chip thickness  $a$  was called the **chip ratio**.

Further theoretical and experimental researches, carried out in Russia and other countries, have proved the existence of the transition zone (shear zone) between the layer of uncut chip and chip. Thus, for example, was proved the existence of the wedge-shaped zone of chip formation (Fig. 1.11), which has the initial  $OL$  and the final  $OM$  borders.

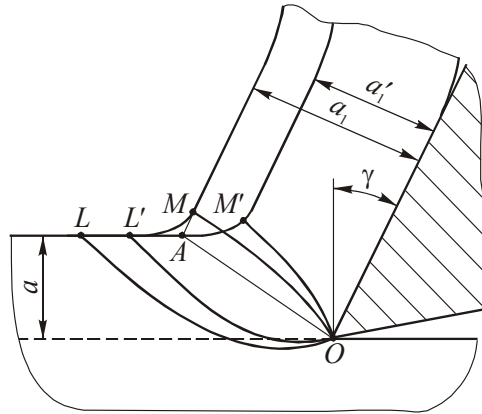


Fig. 1.11 Chip formation

With the cutting speed increasing, the chip ratio reduces and the borders  $OL$  and  $OM$  rotate in the clockwise direction, approaching to each other, and move to the positions  $OL'$  and  $OM'$  respectively.

The ultimate degree of deformation, calculated with the help of the grid distortion, practically matches the deformation, calculated with the use single shear plane (refer to Fig. 1.10) that allows to use the latter as a more convenient and simple for further calculations. However, accounting for the existence of the deformation zone the shear plane and the shear angle, strictly speaking, should be considered as provisional.

The deformation of chip can be calculated, basing on the fact that the fracture of material occurs due to simple shear (Figure 1.12).

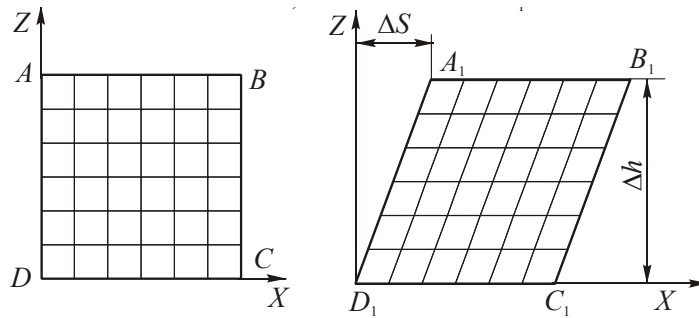


Fig. 1.12 Diagram of a simple shear

In Fig. 1.12 the volume of the undeformed layer of uncut chip is shown in the form of a parallelogram  $OADF$ . During the tool travel from the position I to the position II, the uncut chip undergoes deformation and transforms into chip, with the parallelogram  $OADF$  completely turned into the parallelogram  $OAED$ . In this case, the shear strain:

$$\varepsilon = \frac{\cos \gamma}{\cos(\Phi - \gamma) \sin \Phi} \quad (1.4)$$

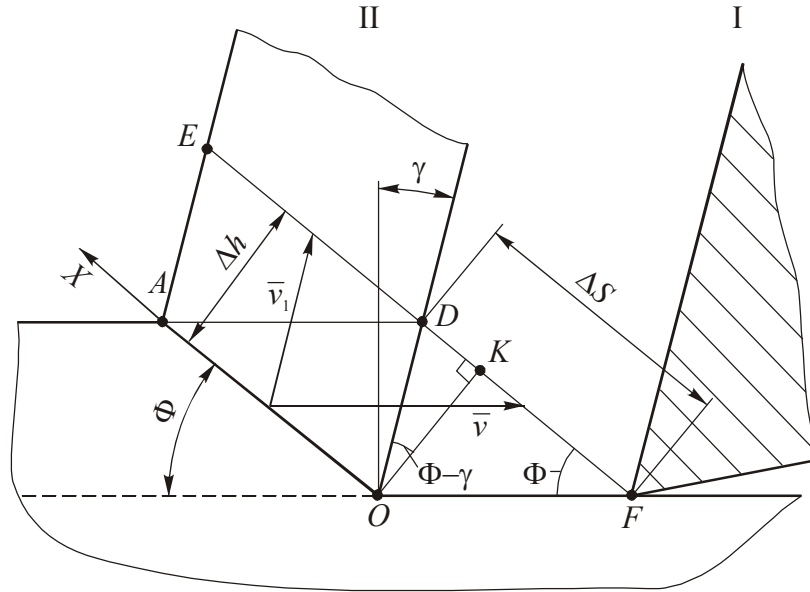


Fig. 1.13 Schematic for calculation of shear strain in metal cutting

### 1.2.1 Stresses and forces in chip formation

Study of the relationship between stresses and strains that occur in the cutting, allows, with the known value of deformation, to determine the cutting force and its components, the load on the machine elements, and most importantly, force and thermal load on the cutter, to establish the mechanisms of tool wear and other important characteristics of the cutting process in relation to the cutting parameters.

Using the scheme with the single shear plane (Fig. 1.10), let's consider the scheme of force interaction of the tool with the work material in a plane perpendicular to the cutting edge (Figure 1.14).

The contact of the tool with the workpiece results in the cutting force  $R$  that is applied to the face of the tool and can be represented as a geometric sum of the normal force  $N$  and friction force  $F$ .

In this case, the angle  $\eta$  between the forces  $N$  and  $F$  is the **angle of friction**, and the  $\text{tg}\eta = F/N = \mu$  is the **coefficient of friction**.

The force  $R$  acting on the chip, initiates stresses in the shear plane  $OA$ . The component of the cutting force  $P\tau$ :

$$P_{\tau} = \tau f_c = \tau \frac{ab}{\sin \Phi}, \quad (1.5)$$

where  $\tau$  is shear stress on the shear plane;  $f_c$  is the area of the shear plane;  $a$  and  $b$  are the thickness and the width of uncut chip respectively.

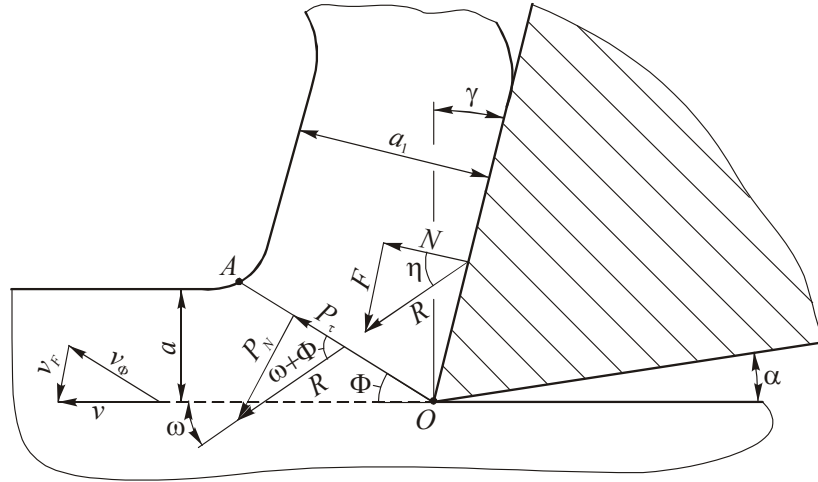


Fig. 1.14 Schematic of the force interaction of the tool with the work material

Force component  $P_N$  is calculated by the following equation:

$$P_N = \sigma_N f_c = \sigma_N \frac{ab}{\sin \Phi}, \quad (1.6)$$

where  $\sigma_N$  – is the normal compressive stress in the shear plane.

Any changes to the conditions of the friction on the face of a tool immediately affect the chip deformation; and any changes in the shear zone influence on the friction at the tool/chip interface. Thus, there is a strong relationship between the shear zone (primary deformation zone) and the zone on the tool/chip interface (secondary deformation zone). The influence of the latter on the values of deformation and force can sometimes be even more significant than the shear stress  $\tau$  influence.

Previously, it was found that the friction angle  $\eta$  with rake angle  $\gamma$  determine the position of the shear plane and the direction of the cutting force  $R$ . With an increase of these angles and rotation of the force vector  $\bar{R}$  in counterclockwise direction, the chip ratio  $K$  and the shear strain increases, and the angle  $\Phi$  with the cutting force component decreases.

Thus, the conditions of friction between the chip and the cutter face have a significant effect on the cutting force  $R$  and its components with the rake values being constant.

### 1.2.2 Tool-chip and tool-workpiece interactions

In the process of cutting, the texture lines in a thin (thickness less than 1 mm) layer adjacent to the rake surface are bent in the direction opposite to the movement of chips (Fig. 1.15). This indicates the presence of secondary plastic deformation of the material, due to the friction force  $F$  that acts on the face of the tool and hinders the movement of chips. Here, the greater is the

friction, the greater is the thickness of the seized layer and the more curved the texture lines are.

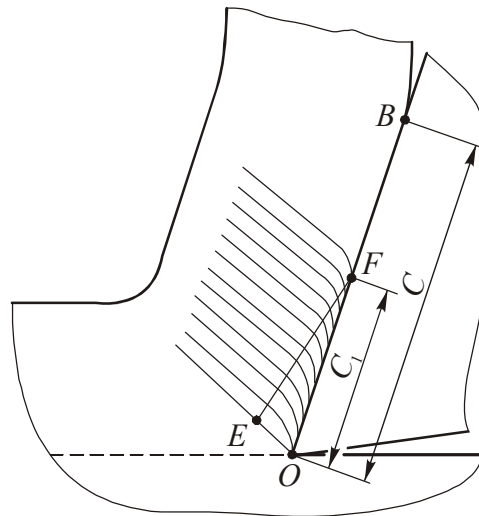


Fig. 1.15 Curved flow lines in a chip due to secondary deformation in seizure zone

Large values of the friction force  $F$  are explained by the high shear stresses  $\tau_F$  caused by friction between the perfectly clean new surface of the chip and oxide-free rake surface of the tool. Here, high normal stresses  $\sigma_N$  are applied to a very small-sized contact area. Under conditions of high cutting temperature and intermolecular action of the seized layer with the rake surface the chip slides not on the tool face, but on the seized layer. Thus, the external friction is replaced by the internal friction.

Metallographic studies of the samples of the chip formation zone, which are also called chip roots, shown that the length of contact of the chip with the rake surface  $C$  (Fig. 1.15) consists of two parts: 1)  $C_1$  – the length of the plastic contact; 2)  $C-C_1$  – the length of external friction. The value of deformation on the contact area  $C$  can be judged by the curved lines of the chip in the seizer zone  $OEF$ .

The work of shearing forces on the rake surface of the tool is not actually work of friction, but the work of plastic deformation of the chip layer adjacent to the face. The average coefficient of friction  $\mu_{mean} = F / N$ , which influences the chip formation process, is dependent on the process. Therefore, with the change of the unit load on the contact area of the chip-tool interface, the mean coefficient of friction  $\mu_{mean}$  also changes. This is the relationship of processes that take place in the chip formation zone and in the chip-tool interface.

Under the action of the components of the cutting force  $R$ : normal  $N$  and tangential (friction)  $F$ , the normal  $\sigma_N$  and shear  $\tau_F$  stresses arise in the chip-tool interface. As a result of steel cutting experiments, were obtained typical

diagrams of the distribution of  $\sigma_N$  and  $\tau_F$  stresses along the tool-chip interface (Figure 1.16)

$$\sigma_N = \frac{N}{Cb}, \quad \tau_F = \frac{F}{Cb},$$

where  $C$  – the length of the contact area of the chip with the tool face;  $b$  – the width of the chip-tool contact.

It was established by [20] that the normal stresses  $\sigma_N$  are highly dependent on the cutting conditions.

These stresses are distributed unevenly along the length of the contact, monotonically increasing towards the cutting edge. In turn, the shear stresses are independent of the cutting conditions and within the length  $C_1$  are approximately constant, decreasing to zero in the section of external friction  $C-C_1$  (Figure 1.16).

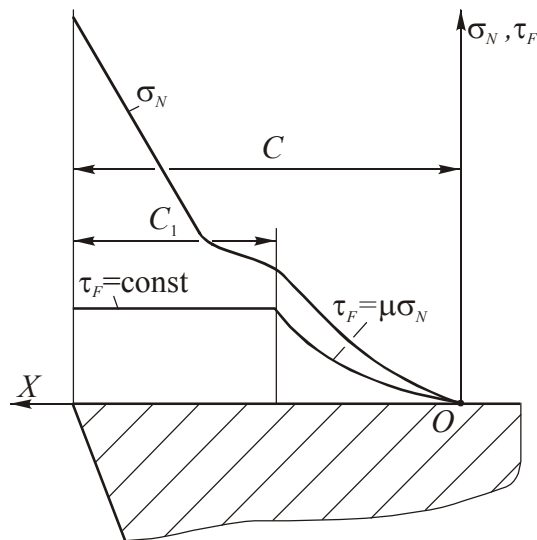


*Fig. 1.16 Distribution of the normal stresses  $\sigma_N$  and shear stresses  $\tau_F$  at the tool/chip interface*

The contact processes on the flank surface of the tool are the subject of discussion below.

In the process of material removing the cutting wedge, despite the presence of the positive clearance angle, interacts with the machined surface by a very small contact area of its flank. This is explained by elastic spring-back of the machined material. The spring-back value  $\Delta$  of the perfectly sharp cutting wedge defines the length of the contact area  $OK$  on the flank of the cutter (Fig. 1.17, a).

Real cutting wedge is always rounded with a radius value within the range  $\rho=0.005\dots0.02$  mm (Fig. 1.17, b). The presence of the radius of such



size has a positive impact on the cutting process, as it prevents the premature failure of the cutting edge.

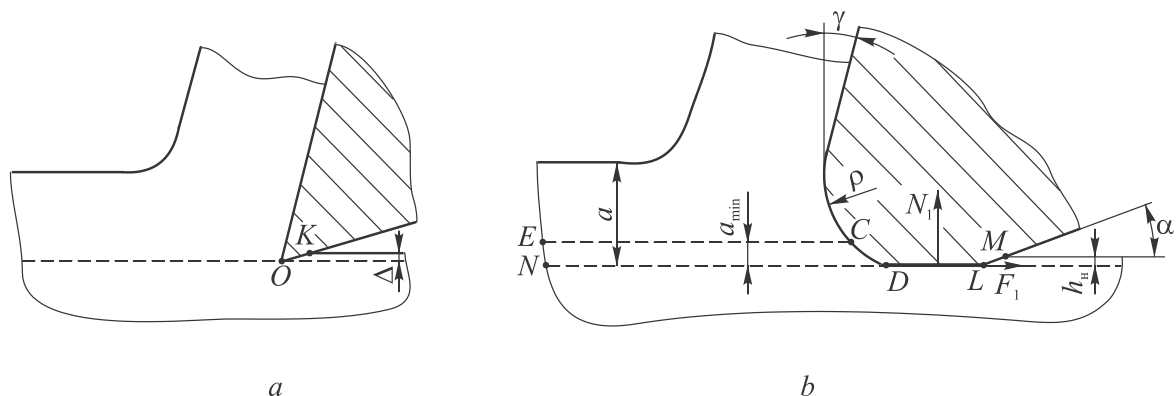


Fig. 1.17 Schematics of the interaction between the tool and work material:  
(a) perfectly sharp tool; (b) tool with a rounded tip

On the other hand, in cutting with a real cutter with the rounded cutting edge (Fig. 1.17, b), work material is divided into two streams at the point C. The upper stream forms the chip and the lower, with thickness  $a_{min}$ , is press down under the flank of the tool. Here, the actual machined surface CE is shifted from the nominal position ND. The volume of metal CEND contacts with the section CD, wear land DL and the flank section LM and undergoes significant deformation. Therefore, thin, strongly deformed (work-hardened) layer with thickness  $h_H$  is formed in the machined surface. The stresses generated in this layer have a great impact on the wear resistance and fatigue strength of parts.

The normal force  $N_1$  and the tangential friction force  $F_1$  applied to the flank of the wedge, and due to small contact area are represented as shown in Fig. 1.18. Here, the force component  $N_1$  is perpendicular to the contact area and the component  $F_1$  is tangent to it. Summing these components, by analogy with the scheme of the forces acting on the rake surface of the tool, the resultant force, applied to the flank of the cutting wedge is obtained

$$\bar{R}_1 = \bar{N}_1 + \bar{F}_1. \quad (1.7)$$

In contrast to the friction process on the face, the forces on the flank of the sharp cutter are much smaller in magnitude. They are practically independent of the uncut chip thickness  $a$  and are the result of the local deformation on the flank.

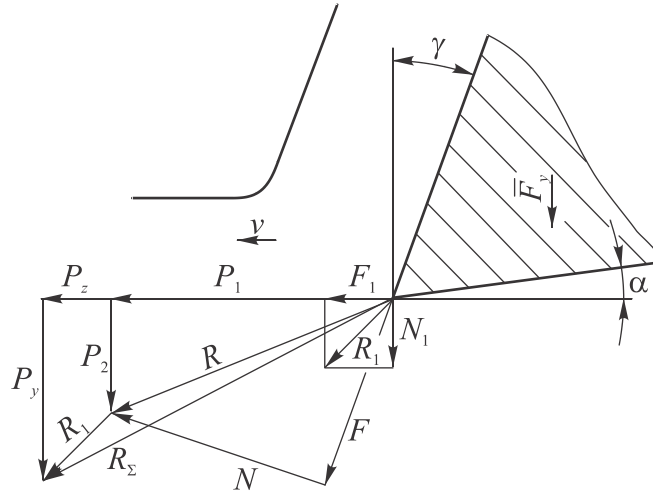


Fig. 1.18 Forces acting on the rake and flank surfaces of a tool

Since the portion of the components  $N_1$  and  $F_1$  of the resultant force  $R_1$ , in the total values of the components  $P_z$  and  $P_y$  is small, they are usually neglected in the calculation of the cutting forces in roughing. In finishing, when the thin chips are cut, as well as in cutting of hardened steels or when the large flank wear is the case, the portion of the flank force components  $N_1$  and  $F_1$  is high and may even exceed the portion of the face cutting force components.

### 1.2.3 Built-up edge

In cutting of certain metals and especially wide range of carbon steels, the certain temperature conditions cause the deposition of the work material of high hardness on the tool face, which is, in fact, a continuation of a cutting edge. This deposited material is called **built-up edge** and it has a significant effect on the characteristics of the cutting process (deformation and forces), as well as on the tool life and surface finish.

Currently, it is assumed that the built-up edge is formed from the seized chip layer at a certain stress state in the cutting zone, when the material is fractured within the chip, which was already deformed in the shear plane.

Study of the polished chip roots showed that the built-up edge has a layered structure and a rounded tip (Fig. 1.19). Moreover, the rake angle  $\gamma$  increases to the actual rake angle  $\gamma_A$  that is  $\gamma_A > \gamma$ .

With the help of high-speed filming technique it was revealed that the built-up edge is not fully stable layer. In cutting, the tip of the built-up edge is below the plane of the cutting and so the layer being removed is thicker than the nominal thickness  $a$  by a certain amount of  $\Delta_a$  (Fig. 1.19).

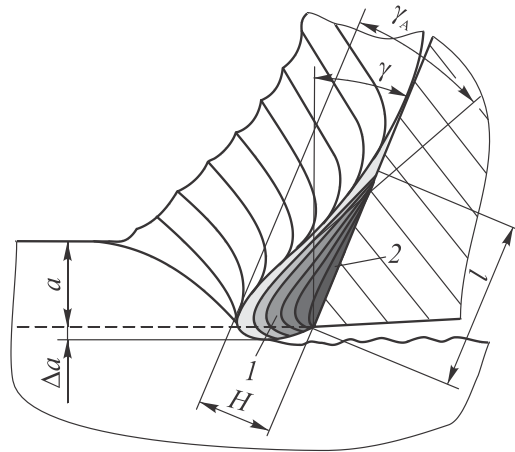


Fig. 1.19 Built-up edge structure

With the destruction of the built-up edge, its debris is embedded in the machined surface, as well as taken away with the flowing chip. Forces of the built-up edge adhesion with the rake surface are quite high and, thus, for carbide cutters the destruction often takes place in the tool material, since carbides have low tensile strength. For this reason, it is recommended to apply sintered carbides only for cutting, with no built-up edge.

The essential effect on the built-up edge size have the mechanical properties of the workpiece material, thickness of the uncut chip  $a$  (feed rate), rake  $\gamma$  and cutting fluid used.

The behavior of the built-up edge and friction coefficient allowed to explain the effect of the cutting speed  $v$  on the basic characteristics of the cutting process: chip length shortening (chip ratio) and cutting force, in the following way (refer to Fig. 1.20).

With the cutting speed rising in the range of  $v_1 \dots v_2$ , the cutting temperature  $\theta$  increases, which is accompanied by an increase in the actual rake angle  $\gamma_A$ . In the range of cutting speeds  $v_2 \dots v_3$  with the temperature increasing, the built-up edge becomes less stable and its height drops to zero at the cutting temperature  $\theta=600^\circ\text{C}$ . The change of the actual rake angle  $\gamma_A$  due to built-up edge formation, determines the behavior of the chip shortening and its deformation – the curve  $K_1$ . The curve  $K_2$  shows the change of the chip ratio for metals that do not form a built-up edge, which also influence on the behavior of the cutting forces.

Cutting in the absence of the built-up edge – at speeds  $v > v_3$  is accompanied by decrease in the mean coefficient of friction  $\mu_{mean}$ . This in turn causes a reduction in cutting force  $R$ .

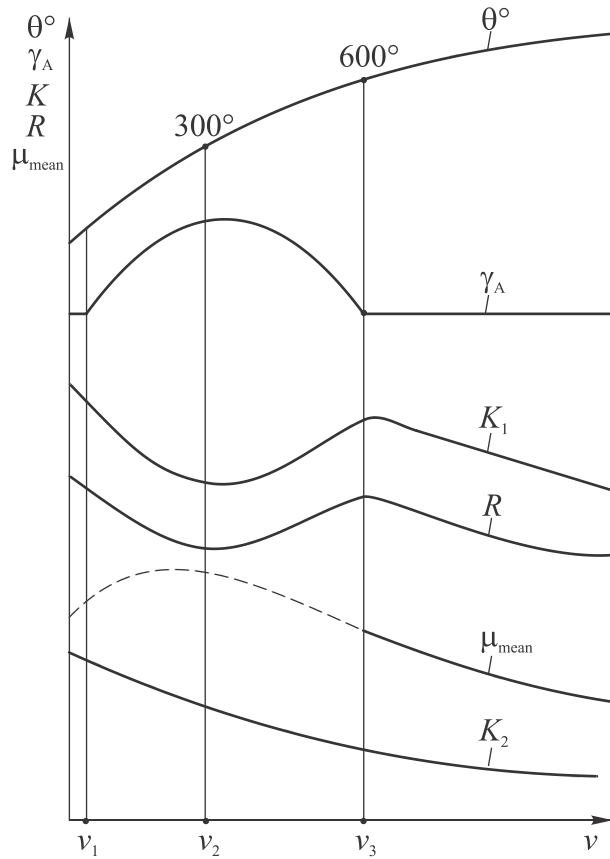


Fig. 1.20 Diagram of the relations between cutting speed  $v$ , temperature  $\theta$ , actual rake angle  $\gamma_A$ , chip ratio  $K$ , cutting force  $R$  and mean coefficient of friction  $\mu_{mean}$

### 1.2.4 Energy and work consumed in the cutting process

Energy consumed in the process of cutting, i.e. effective power without loss is determined by the equation:

$$Ne = P_z v. \quad (1.8)$$

Effective power per unit volume  $W$  of the material being removed, is a specific work:

$$A_W = \frac{Ne}{W} = \frac{P_z v}{abv} = \frac{P_z}{ab}. \quad (1.9)$$

This equation shows that the dimension of the specific work  $A_W$  coincides with that of the stresses, caused by the action of the main component  $P_Z$ , which characterizes the resistance of the work material to cutting. Specific work can be divided into three components:

1)  $A_{W\tau}$  – the specific work of plastic deformation in the chip formation zone (shear zone);

- 2)  $A_{WF}$  – the specific work of friction in the secondary deformation of chips on the chip-tool interface;
- 3)  $A_{WI}$  – the specific work of friction and deformation on the flank of the tool.

### 1.3 Complex schemes of cutting

In practice the free orthogonal cutting is quite rare. The most common are the complex schemes, such as oblique and non-free cutting.

#### 1.3.1 Oblique cutting

Oblique cutting is the process of stock removal, when the cutting edge in contact with the workpiece has an angle of inclination  $\lambda$  between the normal to the cutting edge and the cutting velocity vector  $\bar{v}$  (Fig. 1.21).

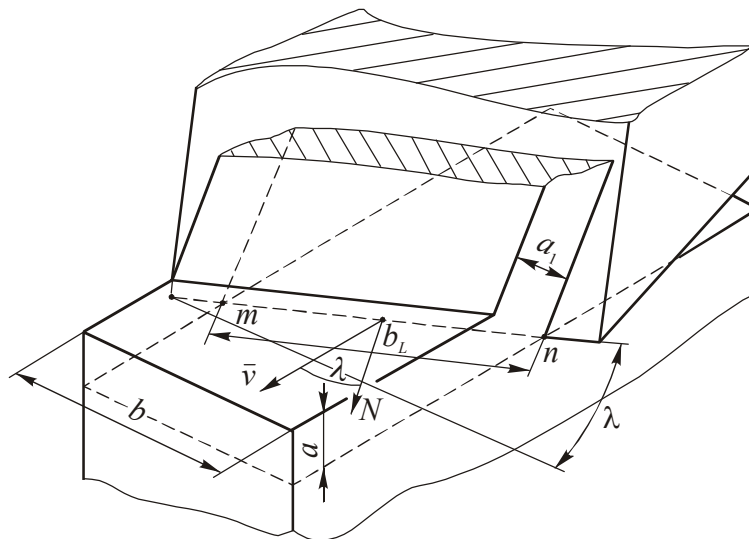


Fig. 1.21 Free oblique cutting ( $\lambda \neq 0$ )

In this case, the material layer of thickness  $a$  and width  $b$  is being cut by the wedge with the cutting edge inclined at an angle  $\lambda$  between the longitudinal velocity vector  $\bar{v}$  and the normal  $N$  to the cutting edge.

The motion of any point on the inclined cutting edge in the direction of the vector  $\bar{v}$  can be represented as a complex one, consisting of two motions: 1) perpendicular to the cutting edge at the velocity  $v_N$ ; 2) parallel (along) the cutting edge at the velocity  $v_L$ . Hence

$$\bar{v} = \bar{v}_N + \bar{v}_L \text{ or } v = \sqrt{v_N^2 + v_L^2} .$$

Shear strain in motion perpendicular to the cutting edge can be calculated in the same way as in orthogonal cutting, by the equation:

$$\varepsilon_N = \text{ctg } \Phi + \text{tg}(\Phi - \gamma). \quad (1.10)$$

Shear strain in motion along the cutting edge:

$$\varepsilon_L = \frac{\Delta L_N \text{tg } \lambda}{\Delta L_{cN} \cos(\Phi - \gamma)} - \frac{\text{tg } \rho}{\cos(\Phi - \gamma)} = \frac{K_{LN} \text{tg } \lambda - \text{tg } \rho}{\cos(\Phi - \gamma)}.$$

Total shear strain in oblique cutting:

$$\varepsilon = \sqrt{\varepsilon_N^2 + \varepsilon_L^2}. \quad (1.11)$$

In oblique cutting, in contrast to the orthogonal cutting, the volume deformation instead of planar deformation takes place. This significantly complicates the scheme of the force components when  $\lambda \neq 0$  (Fig. 1.22).

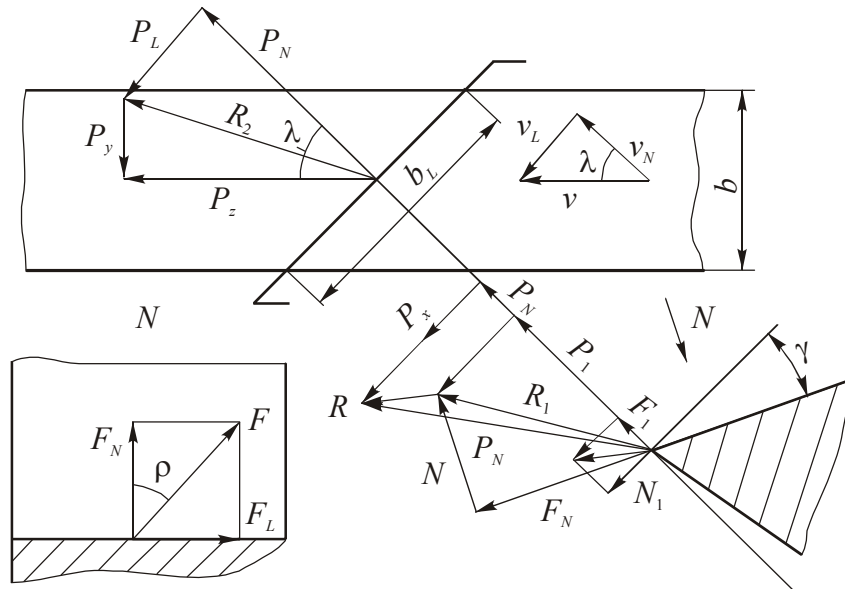


Fig. 1.22 Components of the cutting force  $R$  in oblique cutting

It follows from the Fig. 1.22 that:

$$P_z = P_N \cos \lambda + P_L \sin \lambda; \quad (1.12)$$

$$P_y = P_N \sin \lambda - P_L \cos \lambda; \quad (1.13)$$

$$P_x = P_N \sin(\eta_N - \gamma), \quad (1.14)$$

where  $\eta_N$  is the friction angle in the plane perpendicular to the cutting edge.

Friction coefficient:

$$\mu_N = \text{tg } \eta_N = F_N / N. \quad (1.15)$$

In oblique cutting, with the increase in the inclination angle  $\lambda$ , the normal component  $N$  of the cutting force decreases less intensive than the nor-

mal component of the friction force  $F_N$ . Thus, the friction coefficient  $\mu_N$  and the chip ratio  $K_a$  are greatly reduced.

### 1.3.2 Non-free cutting

In non-free cutting the chip formation involves not one, but two or more cutting edges. Therefore, in contrast to the free cutting, the material deformation is volumetric rather than planar.

The most common example of a non-free cutting is turning, which involves major  $OA$  and minor  $OB$  cutting edges in the formation of chip (Fig. 1.23). Here, the major cutting edge forms transient surface and minor cutting edge forms machined surface.

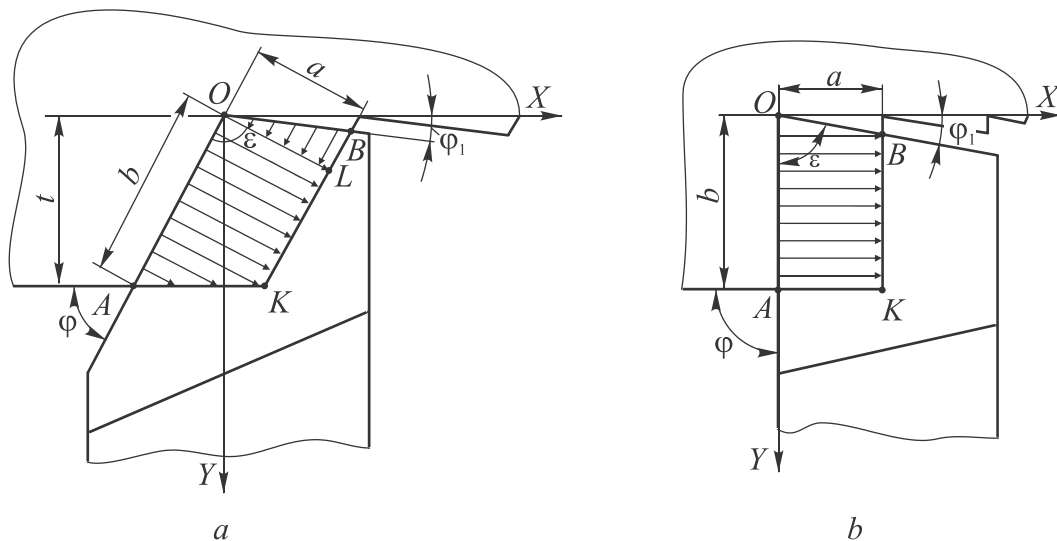


Fig. 1.23 Chip flow direction: (a)  $\varphi < 90^\circ$ ,  $\varepsilon > 90^\circ$ ; (b)  $\varphi = 90^\circ$ ,  $\varepsilon \leq 90^\circ$

Many papers are devoted to the studying of the non-free cutting [10, 14, 28, etc.], but certain issues of non-free cutting are still obscure.

The scheme of chip formation in non-free cutting is shown in Fig. 1.23 and is explained as follows [14]. The metal of cross-section  $AOLK$  ahead of the major cutting edge is deformed in such a way that each of the elementary volumes receives shear deformation in the plane perpendicular to the major cutting edge. The deformation is variable and is the highest on the work surface (point  $A$ ). Here, the shear angle  $\Phi_A$  is the smallest value and the chip ratio  $K_a$  is the largest value. At the top of the tool (point  $O$ ) the deformation is in confined conditions due to the increase of so-called "hydrostatic pressure", which accompanies the deformation. At the point  $O$  the deformation is the minimum and the shear plane angle  $\Phi_O$  is the maximum.

In non-free cutting the three dimensional chip formation zone defines the system of forces, which differs from the free cutting. In turning the resultant cutting force  $R$  can be resolved into technological components:  $P_Z$  – the main component parallel to the cutting velocity;  $P_X$  – axial component parallel to the workpiece axis or to the longitudinal feed;  $P_Y$  – radial component, acts along the workpiece radius.

The technological components of the cutting force are used in the calculation and design of machine tools and equipment, as well as in a number of engineering tasks.

The cutting force  $R$  is basically defined by the value of the main component  $P_Z$ , and the difference between them is little. A set of theoretical equations for the cutting force calculation was suggested. However, in practice they have not received the application since it is impossible a priori (without an experiment) to exactly define some of the parameters of these equations.

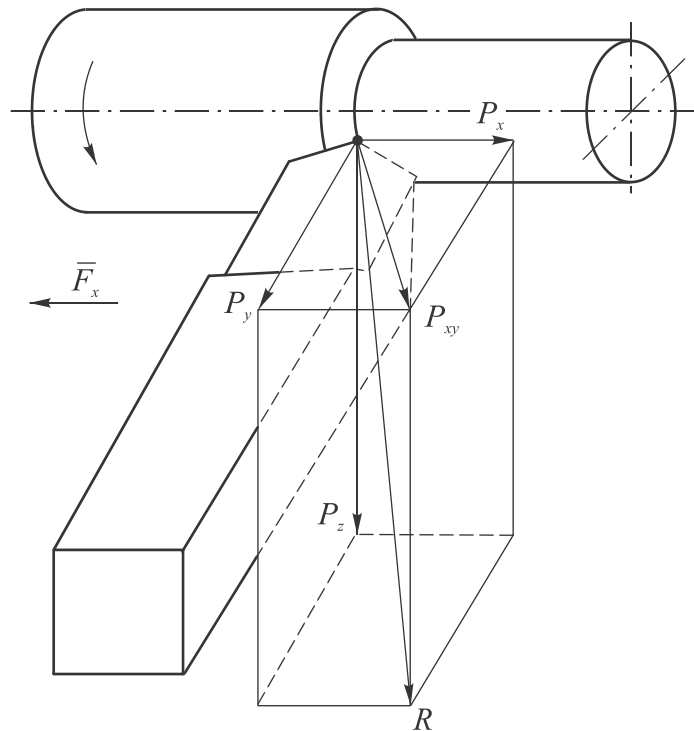


Fig. 1.24 Resolution of the resultant cutting force  $R$  into components  $P_Z$ ,  $P_X$  and  $P_Y$

In practice, cutting forces and their components are calculated by the empirical equations derived from the mathematical treatment of the experimental data. These equations are the power dependencies of the  $y = C_x \cdot x^k$  type and are given in logarithmic scales.



The generalized empirical equations for calculating of the cutting force components account for the main parameters of the cutting parameters and are of the following form:

$$\begin{aligned} P_z &= C_{pz} t^{x_{pz}} f^{y_{pz}} v^{n_{pz}} K_{pz}; \\ P_x &= C_{px} t^{x_{px}} f^{y_{px}} v^{n_{px}} K_{px}; \\ P_y &= C_{py} t^{x_{py}} f^{y_{py}} v^{n_{py}} K_{py}. \end{aligned} \quad (1.16)$$

In these equations, the exponents reflect the influence of the cutting parameters ( $v, f, t$ ) on the components of the cutting force.

The exponent  $y_p$  of the feed  $f$  is smaller than the exponent  $x_p$  of the depth of cut  $t$ . The latter exponent is equal to one, or close to it, and the exponent of the feed, is generally much smaller than one.

The largest share in the value of the cutting force and its components has the coefficients  $C_{Pz}$ ,  $C_{Py}$  and  $C_{Px}$ , which depend on the mechanical properties of the workpiece material, such as strength, hardness and ductility. This influence is quite complex and contradictory or inconsistent and acts via the change of shear stress in the shear plane  $\tau_s$  and the deformation  $\varepsilon$ .

### 1.3.3 Surface finish of the machined surface

Surface finish is specified by the roughness (height of micro-irregularities) and the stress state of the surface layer.

In the free cutting the roughness is the most influenced by a built-up edge. At cutting speeds, where there is a built-up edge, surface roughness parameters are very large and depend on the built-up edge height and stability. When there is no built-up edge, the height of the micro-irregularities is significantly reduced. Effect of the cutting speed on surface finish is schematically shown in Fig. 1.25. Here, the curve for materials that do not form a built-up edge, monotonically decreases with the cutting speed increasing (Fig. 1.25, a). This is related to the decrease in the spring-back of the machined material and decrease of the coefficient of friction on the tool flank. For metals that form a built-up edge the roughness change is related to the change in the built-up edge height (Fig. 1.25, b).

In the non-free cutting the greatest influence on the roughness  $R_z$  of the machined surface has the feed rate  $f$ , cutting edge angles  $\varphi$  and  $\varphi_1$  and the tip radius. In addition, the actual height of the surface micro-irregularities is affected by the workpiece material properties (strength, ductility), the coolant used and the built-up edge.

With the feed rate  $f$ , cutting edge angles  $\varphi$  and  $\varphi_1$  decreasing and the tip radius increasing the micro-irregularities height decreases. With the increase in strength and decrease in ductility of the workpiece material the height of the micro-irregularities decreases due to reduction of the metal deformation.

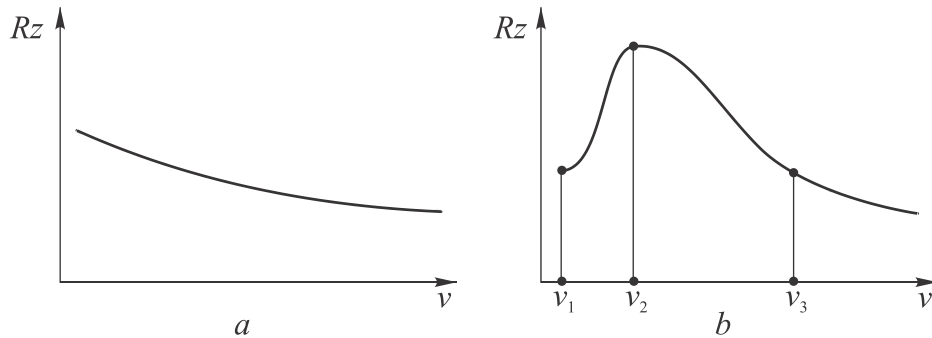


Fig. 1.25 Relation between the machined surface roughness  $Rz$  and cutting speed  $v$  for: (a) non-work-hardening material; (b) work-hardening material

In cutting of brittle materials, which are characterized by the formation of the discontinuous chip, it is difficult to achieve good surface roughness due to the fraction of the particles off the machined surface. If a cutter has minor cutting edge angle  $\varphi_1=0$ , and the length of the minor cutting edge is by 20...30% higher than the feed rate  $f$ , then, theoretically the height of the micro-irregularities will be zero ( $Rz=0$ ). This technique is used in the design of wiper inserts for cutting with high feed rates.

The use of both water-based and oil-based cutting fluids allows to reduce the roughness of the machined surface, especially at the cutting speeds of  $v \leq 50$  m/min. With the further increase in cutting speed the effectiveness of the coolant decreases due to the difficulty of the coolant penetration to the tool-chip interface.

In case of the finishing cutting operations, the stress state of the machined surface layer is determined by the contact processes on the flank of the cutting wedge. The magnitude and sign of the stresses has a significant impact on the performance characteristics of the machined parts. Indicators of the surface layer condition are the stress depth, the degree of work hardening and work-hardened layer depth.

The residual stresses can be of compressive or tensile type. The latter are particularly dangerous, since they reduce fatigue strength of the part material and, consequently, can form cracks on the machined surface. In addition, the residual stresses cause distortion of the parts produced by cutting.

The magnitude and sign of the residual stresses  $\sigma$ , as well as their depth  $\Delta$ , is determined by the influence of the uncut chip thickness  $a$ , cutting speed

$v$ , rake angle  $\gamma$ , the nature and degree of the cutting tool wear. The tensile stresses and their depth  $\Delta$  increase with the uncut chip thickness  $a$ . With the cutting speed increasing the tensile stresses increase, but their depth  $\Delta$  decreases and vice versa. Transition from positive to negative rake angles (up to  $\gamma=-15^\circ$ ) greatly reduces the tensile stresses, but increases their depth  $\Delta$ .

Cutting of brittle materials induces compressive residual stress, while grinding, due to high temperatures, always induces tensile residual stresses [3].

The degree of work-hardening is the ratio:

$$\Delta H_M = \frac{H_{mn} - H_{mc}}{H_{mc}} \cdot 100\%, \quad (1.17)$$

where  $H_{mn}$  is the highest microhardness of the work-hardened layer;  $H_{mc}$  is the microhardness of the non-work-hardened layer.

The degree of work-hardening  $\Delta H_M$  and work-hardened layer depth  $\Delta_H$  depends on the degree of deformation of the material being removed, the forces acting on the cutting wedge, uncut chip thickness  $a$ , rake angle  $\gamma$ , the nature and degree of the cutting tool wear and especially on the material work-hardening characteristics.

#### 1.4 Heat generation in cutting

Plastic deformation and friction on the cutting tool surfaces are accompanied by such extensive heat generation, that the tool and the workpiece are heated to extremely high temperatures. While the warming up of the tool determines the wear rate, permissible cutting parameters and productivity, and the workpiece warm up impacts on the accuracy and level of residual stresses in the machined surface.

Temperature levels in different parts of the cutting area, and in particular, on the working surfaces of the tool depend on the location of heat sources, their shape and intensity of heat generation, as well as on the laws of heat distribution, which in turn are determined by the heat exchange between the workpiece, chip and tool. By defining the sources of heat, their power and heat transfer mechanisms, it is possible to get a picture of the temperature fields in the cutting tool and the workpiece. It will also allow to set cutting materials requirements, select optimum cutting parameters and geometrical parameters of the tool to ensure the highest productivity and identify the ways for the further improvement of the cutting process.

### 1.4.1 Sources of heat and heat balance equation

It was experimentally found that almost all of the mechanical work spent in cutting is converted into thermal energy.

There are three sources of heat formation in the cutting area (Fig. 1.26): 1 – the primary deformation zone (located at the shear plane) with a thermal capacity of  $Q_\phi$ ; 2 – secondary deformation zone due to rubbing of the chips against the tool face, its thermal capacity is  $Q_\gamma$ ; 3 – zone of tool flank rubbing against the workpiece, thermal capacity is  $Q_1$ .

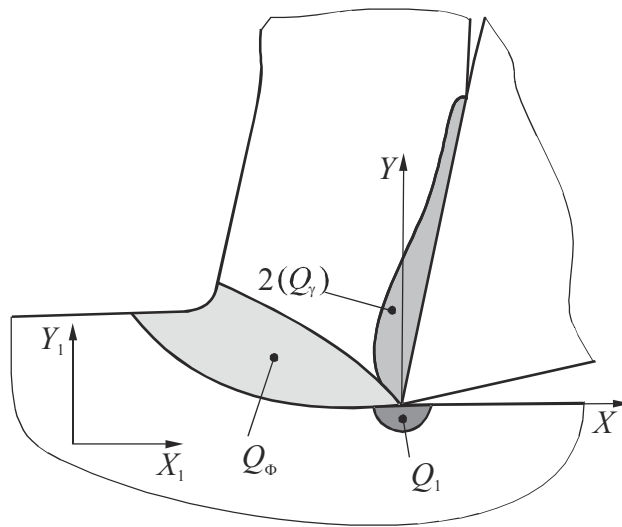


Fig. 1.26 Heat sources in cutting

Thus, the total amount of heat generated in cutting is

$$Q = Q_\phi + Q_\gamma + Q_1.$$

In accordance with the heat exchange laws, the heat generated in the source of heat is dissipated in the direction of less heated parts that are in contact with the source, namely, the workpiece  $Q_W = Q_{\phi_w} + Q_{1w}$ , chips  $Q_C = Q_{\phi_c} + Q_{\gamma_c}$  and the cutting tool  $Q_T = Q_{\gamma_T} + Q_{1T}$  (Figure 1.27). In addition, part of the heat  $Q_{env}$  is dissipated to the environment by the cutting fluid (coolant), for example. However, in dry cutting this heat, due to its small value, is usually neglected.

Considering the aforesaid, the **heat balance equation** is:

$$Q_\phi + Q_\gamma + Q_1 = Q_W + Q_C + Q_T + Q_{env}. \quad (1.18)$$

Analyzing the heat balance in a unit of time, the left side of Eq. (1.18) is the sum of three thermal power sources, which can be found from the equations of the specific work of cutting and friction, using the thermal equivalent of mechanical work  $A_{TE}$ .

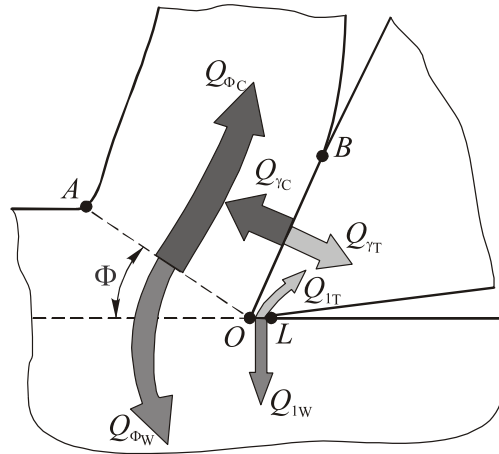


Fig. 1.27 Heat distribution between chip, workpiece and tool

In this case, the thermal power of the three sources can be defined as follows:

$$\begin{aligned}
 Q_{\Phi} &= \frac{\tau \varepsilon a b v}{A_{TE}}; \\
 Q_{\gamma} &= \frac{F v_c}{A_{TE}} = \frac{F v}{A_{TE} K}; \\
 Q_1 &= \frac{F_1 v}{A_{TE}},
 \end{aligned}
 \tag{1.19}$$

where  $\tau$  – the shear stress in the shear plane;  $\varepsilon$  – the shear strain in the deformation zone;  $a$ ,  $b$  – are respectively the thickness and width of the uncut-chip;  $v$  – cutting speed;  $v_c$  – the speed of the chip flow on the face,  $v_c = v/K$ ;  $K$  – chip ratio.

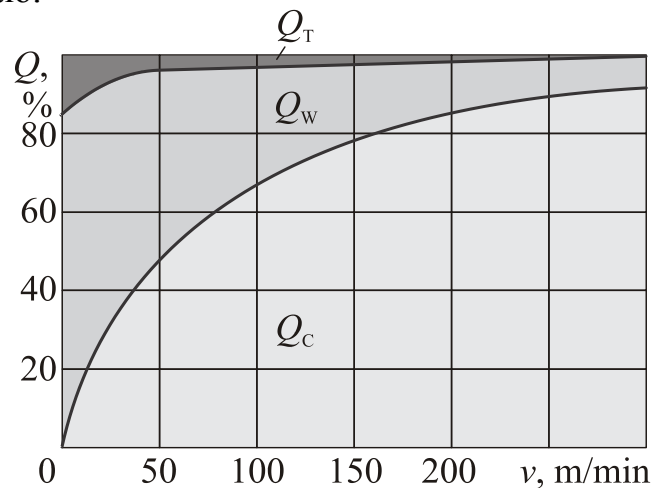


Fig. 1.28 Heat distribution between the chip  $Q_C$ , workpiece  $Q_W$  and tool  $Q_T$  in turning 0.4%C steel with a tungsten carbide cutter ( $t=1,5$  mm,  $F=0,12$  mm/rev)

While the receipt items of the heat balance are determined relatively easily and with high accuracy, the items of expenditure (right side) of the Eq. (1.18) are determined either experimentally or by means of complex thermal-physic calculations.

Generally, the quantity of heat dissipated into chip, workpiece and cutting tool is determined experimentally using calorimeters. According to the carried out researches, the following picture of the heat distribution was established (Figure 1.28).

Here, with the cutting speed increasing, the quantity of heat dissipated into the chip monotonically increases, with the most rapid increase at low speeds of cutting.

Along with the cutting speed, the mechanical and thermal properties of the workpiece material have great influence on the heat distribution. Here, the higher is the thermal conductivity of the workpiece material, the more heat is transferred to the workpiece. The higher is the cutting speed, the less heat is transferred to the cutting tool.

#### 1.4.2 Cutting temperature measurements

The cutting temperature is the mean temperature of the tool-chip interface. It characterizes the level of heating of the cutting tool and has a significant impact on the wear on the face and flank of the tool. The easiest way to determine the cutting temperature is to perform measurement.

Methods of cutting temperature measurements are conventionally divided into direct and indirect. The **direct methods** include measurements with different types of thermocouples, and the **indirect methods** include temperature assessment by the chip temper colors; with the help of thermo-paints which change its color depending on the temperature; by measuring the infrared radiation of the chip surface with photoelectric sensors and radiation pyrometers; by measuring microhardness of the heat-affected zone in the cutting tool; by means of calorimetric method.

Indirect methods of temperature measurement have low accuracy, thus in practice the methods of direct measurement, such as embedded, semi-embedded and tool-work thermocouples, are the most widely used.

The principle of the thermocouple states that if the tight junction 2 of two dissimilar electro-conducting materials 1 is heated and the ends of these electrodes 3 are attached to the recording device 4, the consequent cooling will induce a thermo-electromotive force in the circuit (Fig. 1.29). The value of the thermo-electromotive force recorded by the device 4 increases with the temperature difference between the hot and cold junctions increasing. If there

are additional junctions in the circuit, they must be kept at the same temperature to avoid the influence on the thermo-electromotive force.

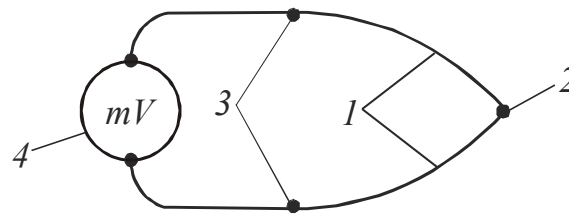


Fig. 1.29 Thermocouple: 1 – thermoelectrodes; 2 – hot junction; 3 – cold junctions; 4 – gauge

The electrodes of the thermocouple can be made of almost any materials with different chemical composition and physical properties.

To measure temperature at different points of the tool the **embedded thermocouples** in the form of thin wires, that are installed in the eroded hole with the hot junction placed as close as possible to the point of measurement, are used (Fig. 1.30, a). In this case the junction is pressed with a force of not less than 50 N, and the wires are securely isolated from each other and from the body of the cutting tool.

It is not always possible to provide reliable junction of the thermocouple and, thus the semi-embedded thermocouples are often used (Fig. 1.30, b). In the latter one an electrode of the pair is welded to the tool surface at the measurement point and the second electrode is a cutting tool itself. Before the application of the semi-embedded thermocouple it is necessary to calibrate it with a standard control thermocouple.

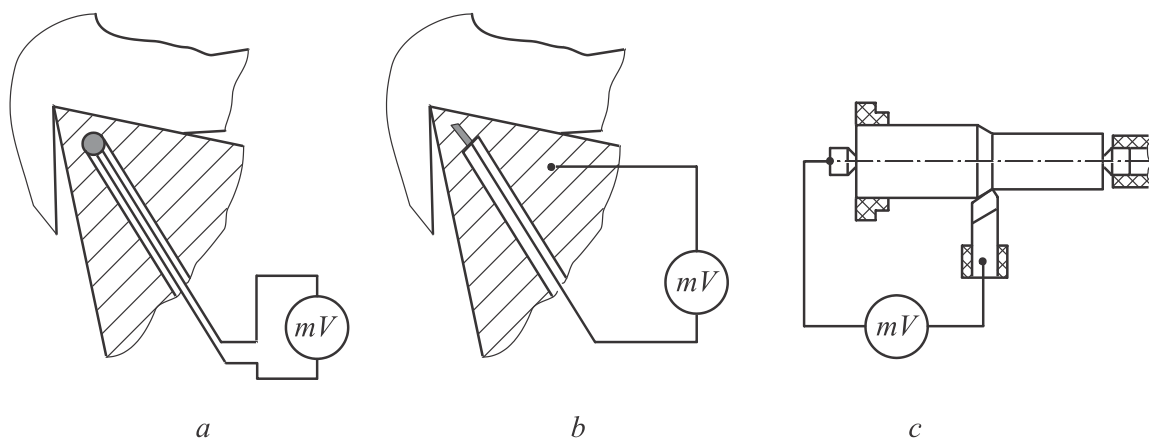


Fig. 1.30 Types of thermocouples for measurements temperature in cutting: (a) embedded; (b) semi-embedded; (c) tool-work

The embedded and semi-embedded thermocouples do not allow to measure the temperature directly on the contact surfaces of the cutting tool, where the temperature is much higher due to the concentration of heat in the finest surface layers and high temperature gradient.

In the experiments for cutting temperature measurement and studying the effect of cutting parameters on it the tool-work thermo-couple is widely used. In this thermocouple, the cutting tool and the workpiece act as electrodes of the thermocouple (refer to Fig. 1.30, c).

It should be noted that the tool-work thermocouple measures not the maximum, but some average temperature on the chip-tool and tool-work interfaces, which, however, according to [8, 26] is sufficiently close to the maximum temperature.

Using the method of single-factor experiment, with the data treated in coordinates with logarithmic scales, the following empirical relationships for the calculation of the cutting temperature were obtained:

$$\theta = C_0 v^m f^n t^q K_T K_F,$$

where  $C_0$  is the temperature coefficient, which characterizes the effect of mechanical and thermal properties of the workpiece and tool materials;  $v, f, t$  are respectively the cutting speed, feed rate and depth of cut;  $m, n, q$  are the exponents characterizing the influence of the cutting parameters on the temperature;  $K_T, K_F$  are the coefficients characterizing the impact on cutting temperature of the, respectively tool geometry and cutting fluid used.

The greatest influence on the cutting temperature has the cutting speed and properties of the workpiece and tool materials, in particular, their thermal conductivity, strength and ductility.

The effect of the feed rate  $f$  and depth of cut  $t$  on the cutting temperature is less noticeable.

The revealed relations between the cutting parameters and cutting temperature allowed to set the following procedure for the cutting parameters selection: 1) the maximum thickness of the layer being removed is specified, based on the allowance for machining and cutting tool strength; 2) the maximum feed rate, permissible by the strength of the tool and insert is specified; 3) the cutting speed is calculated with respect to the given tool life.

The effect of the rake angle  $\gamma$  on the cutting temperature is as follows. With the rake increasing the power of the heat source in the primary deformation zone reduces and the conditions of heat removal to the tool near the major cutting edge worsen. Therefore, the temperature is not much affected by the cutting rake.

The inclination angle  $\lambda$  has even less influence on the cutting temperature value.



## 1.5 Strength and wear of the cutting tools

Due to high contact pressures and temperatures of the cutting process the cutting tool continuously wear, until it is blunt or failed.

The wear of cutting tools is mainly determined by the properties of the tool material and the design of the tool, so the following is a brief look at the types and properties of the major groups of cutting tool materials.

### 1.5.1 Cutting tool materials

The cutting tool materials used for the manufacture of cutting tools, must meet the following requirements: 1) high hardness, more than 3...4 times higher than the hardness of the workpiece material; 2) hot hardness, i.e. the ability to maintain the necessary hardness up to a certain temperature; 3) high wear resistance at elevated temperatures, i.e. the resistance of the cutting wedge to wear; 4) high strength and dimensional stability of the cutting wedge.

All the currently known tool materials can be divided into the following groups: 1) tool steels; 2) high-speed steels; 3) sintered carbides; 4) super-hard materials; 5) abrasives.

Let's consider the basic properties of the tool materials in terms of the requirements stated above.

**Tool steels** – are carbon and low-alloy steels.

After water quenching and tempering the hardness of the carbon steel is *HRC* 61...63. These steels have low cost and high processability, as well as high strength and wear resistance. The main drawback of high carbon steels is their low heat resistance of 200...250°C.

To improve the processability and cutting properties the carbon steels are alloyed in small quantities (1...3%) with the alloying elements (chromium, silicon, manganese, tungsten, molybdenum, vanadium, etc.).

All low-alloy tool steels due to the high carbon content (0.9...1.1%) have hardness of *HRC* 61...63 after the heat-treatment, good through hardenability and a somewhat higher hot hardness (up to 250...300°C).

**High speed steels** (GOST 19265-73) differ from the tool carbon and low alloyed steels by higher content of the alloying elements, such as tungsten, molybdenum, chromium, and vanadium. As a result of the heat treatment the high speed steels (HSS) have high hot hardness (up to 620°C) and hardness (up to *HRC* 63...64) and bending strength ( $\sigma_b=3000...3500$  MPa). Therefore, the high-speed steel allows cutting speeds of 4...6 times higher than the speed of cutting tools made of tool steels.

Due to high toughness the HSS remains one of the most widely used tool materials to present day.

**Carbides** – are a composition of the powders of refractory compounds: tungsten carbides, titanium carbides, tantalum carbides, etc., sintered with binder, mostly cobalt, at high temperatures in a vacuum or controlled atmosphere.

The share of the carbide cutting tools is currently about 55%.

Due to its high heat stability, hardness and wear resistance the cutting speed for the carbide tools is 4...5 times higher compared to the high-speed tools. However, the bending strength of carbides is significantly (2...3 times) inferior to the high speed steel.

The carbides, by its composition and application, are conventionally divided into four main groups: 1) single-component tungsten-cobalt carbide (WC); 2) two- component titanium-tungsten carbide (TC); 3) three-component titanium-tantalum-tungsten carbide (TTC); 4) tungsten-free carbides – titanium carbide and carbonitride based.

Heat stability of tungsten carbide grades is 800...850°C. To improve the wear resistance and strength of carbides, the carbide grain sizes are reduced – from coarse to fine and to ultra-fine. Single-component carbides are used in cutting of cast iron, non-ferrous metals and alloys.

For cutting of steel and other materials (except titanium) the two-component carbides are used. The presence of titanium carbides increases resistance to abrasion on the rake surface of tools. Heat stability of the carbide is 850...950°C.

Even greater heat stability (up to 1000°C), strength and resistance to shock loads showed the three-component carbides, which contain tantalum carbide in addition to titanium carbides.

International designation of carbides is guided by ISO 513, which divides carbides into the six groups, with relation to the workpiece material, type of the chips produced and other factors. Classification adopted in Russia is based on chemical composition of the carbides.

According to ISO all groups of carbides are divided into subgroups, which are indicated by indices: 01, 10, 20,... 50. The lower is the index, the thinner is the uncut chip and the higher is the cutting speed the higher is the wear resistance of the tool material. With the index increasing, the feed and depth of cut, as well as tool material strength increase. For example, P 05 denotes carbide used for finishing machining of steels; M 25 is for machining of stainless steels; P 50 is for roughing machining of steels, etc.

To increase life of the tools made of carbides and high-speed steels, various wear-resistant single and **multilayered coatings** such as titanium carbides, nitrides and carbonitrides, aluminum oxide etc. gained wide applica-

tion recently. The optimum thickness of the coating is 6...10  $\mu\text{m}$  for carbide inserts and 2...6  $\mu\text{m}$  for high-speed tools. Thanks to high hardness and wear resistance, chemical inertness to the material and low thermal conductivity of the coatings, it is possible to increase the tool life in 2...5 times and increase the cutting speed by 20...60% [5, 6].

In most cases, the coating is applied by PVD (physical vapor deposition) coating method. The hardness of these coatings at any temperature is higher than that of the coatings obtained by CVD (chemical vapor deposition) method.

Another common tool material used in industry is the mineral **ceramics**, consisting of aluminum oxide  $\text{Al}_2\text{O}_3$ , and produced by melting alumina (bauxite) in electric furnaces. This type of ceramic is also called the oxide ceramic or white ceramic. It has a very high thermal stability (up to 1400...1500°C) and hardness (*HRA* 90 ... 92), greater than that of carbides, allowing to cut metals at 300...600 m/min or higher.

The main disadvantages of ceramics are its low bending strength ( $\sigma_b=320$  MPa), which is an order of magnitude smaller than the bending strength of high speed steel, and high strength instability.

To increase strength the mineral ceramics are introduced with various refractory compounds: oxides and carbides of tungsten, molybdenum, titanium, etc. Thanks to these additions, as well as reinforcement by filamentary single crystals of silicon carbide (whisker-reinforced), black ceramic compared with white ceramic has higher bending strength ( $\sigma_b=560...700$  MPa), stable properties, but less wear resistance.

Recently, new grades of ceramics based on silicon nitride  $\text{Si}_3\text{N}_4$ , the so-called gray ceramics, which bending strength increased to 800 MPa were created. This allows to apply this ceramic not only for finish turning of high-strength steels and cast irons, but for milling as well, which is characterized by shock loading.

The group of super-hard materials includes diamond (natural and synthetic) and cubic boron nitride (CBN).

**Diamond** is the hardest material in nature (4...5 times harder than tungsten carbide) and has high thermal conductivity, low coefficient of friction, low bending strength ( $\sigma_b=210...480$  MPa) and low ignition point (800°C). At higher temperatures the diamond is oxidized and graphitized to CO and C. The extreme brittleness of the diamond it greatly limits its use in metalworking. One of the major drawbacks of the diamond is its chemical affinity to iron. Therefore, the natural diamond crystals are not use for cutting of steel, and, thus are used only for finish turning of nonferrous metals and alloys at high cutting speeds.

**Cubic boron nitride (CBN)** is a synthetic material with a complex diamond-like crystal lattice; it has no natural counterpart. CBN hardness is close to diamond, but its thermal stability is higher, reaching 1200°C. CBN is chemically inert material and, therefore is suitable for cutting of metals of different composition. Due to the high hardness and wear resistance it is used for cutting very hard materials, hardened steels and even carbides. Polycrystalline cubic boron nitride (PCBN), depending on the composition and manufacturing technology, has bending strength  $\sigma_b = 470 \dots 1200$  MPa.

### 1.5.2 Strength of cutting tools

The cutting tools retain their cutting performance for as long as in the process of cutting their cutting elements keep the geometric and linear parameters. Loss of form of the cutting wedge may occur either because of failure (brittle or plastic), or due to wear of the wedge on the face and flanks.

Brittle failure of cutting wedge occurs in the form of cutting edge chipping and spalling of the tool material in some regions along the cutting edges. Such types of failure are common for the tool materials with low ductility and bending strength, such as, for example, carbides, mineral ceramics and super-hard materials.

Chipping of the cutting edges typically occur beyond the contact area of the tool-chip interface, with micro-cracks, propagating under the external loads and coalescing into the macro-cracks, which leads to the cutting wedge fracture. The macro-chipping of the cutting tools is the most dangerous type of failure, since it leads to large losses of the tool material and defective products.

The chipping is affected by the distribution and sign of stresses induced in the cutting wedge, the wedge angle value, the thickness of the layer being removed, as well as the properties of the tool and the work material.

The brittle failure of the cutting wedge is greatly affected by the number of loading cycles that occur in interrupted cutting, and stress alternation at the engaging and disengaging of the tool with the workpiece. With the number of load cycles increasing the fatigue strength of the tool material decreases and the probability of the brittle failure of the cutting wedge increases.

It should be noted, that in addition to the mentioned reasons, the negative impact on the strength of carbide inserts is provided by the resharpening. Thus, the application of the indexable inserts obviously benefits.

The cutting edge in cutting is sometimes subjected to the plastic failure, which takes the form of the plastic deformation of the tool nose the cutting edge depression. The plastic failure of the HSS cutting tools leads to the

rounding of the cutting edge or even melting when the wear limit is exceeded. The plastic failure of carbide tools develops under high temperatures and chatter. Although the carbides are considered as brittle material, but even in normal conditions they are subjected to creep, which increases with the cutting temperature increasing. Figure 1.31 shows the magnified view of the initial cutting tool form and the same wedge in 80 seconds.

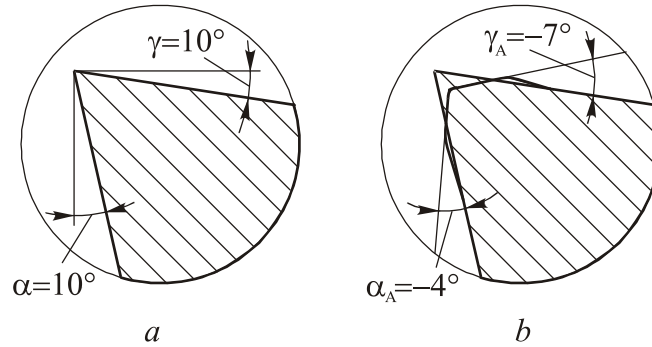


*Fig. 1.31 Plastic deformation of the tungsten carbide cutter after turning titanium alloy ( $v=60$  m/min,  $s=0.47$  mm/rev,  $t=2$  mm)*

### 1.5.3 Physical nature of tool wear

Wear of a cutting tool is a result of rubbing of the rake surface against the chip and rubbing of the flank against the machined surface. In addition, cutting pressures are 300...400 times larger compared to those found between the interacting parts of machines, and the cutting temperatures are 15...20 times higher. Moreover, the cutting wear occurs over a very small area of contact.

Cutting tools wear can be classified into the four basic types: 1) mechanical; 2) adhesive wear; 3) diffusion wear; 4) chemical (oxidation) wear.

**Mechanical (abrasive) wear** occurs due to friction of hard inclusions of the tool material and workpiece material (whisker-reinforce, particle of the built-up edge, carbides, nitrides, etc.) against the face and flanks of the tool. Especially large quantity of inclusions is found in cast irons, as well as in high-alloy steels and alloys. For example, aluminum alloys contain hard silicon particles. In roughing cutting of cast iron, the remains of foundry sand can act as abrasives.

The mechanical wear is the most common for tools made of high-speed steels and is in the form of scratches, grooves and other microscopic irregularities on the face and flanks of the cutting tool.

**Adhesive wear** is the result of action of adhesion forces, i.e. forces of intermolecular interaction of chemically active clean surfaces of chips and workpiece with the tool surfaces during the sliding motion.

In cutting, the sliding surfaces of the tool and the workpiece or chips contact on the points 1...5 (Figure 1.32). These points constitute actual contact area, which is a fraction of the apparent contact area. Under the cutting pressure and temperature the bonding of the contacting points occur, leading to the shearing of the welded points, due to the sliding of one of the surface relative to the other. Afterwards, bonding takes place in other points, which then also broken, etc. Fracture occurs primarily in a workpiece material, which strength is lower than that of the tool material. But sometimes the cutting tool material is fractured. For high-speed steel, the fracture occurs due to fatigue micro-cracks propagating in the thinnest layers of contact, caused by high temperatures.

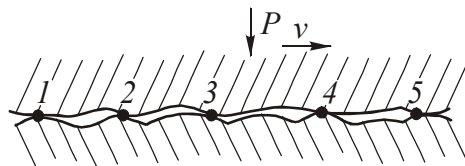


*Fig. 1.32 Contact of two surfaces in adhesion wearing*

Carbides are usually fractured along the carbides grain boundaries, i.e. in the weaker cobalt binder, which content decreases with the cutting temperature increasing.

With the temperature increasing, the strength of adhesive bonds weakens, and the size of wear debris reduces leading to more even wearing surface.

**Diffusion wear** is the result of mutual transfer (diffusion) of atoms of the workpiece and tool materials. The rate of diffusion processes depends on the mobility of the atoms, which, in turn, determined by the cutting temperature. Diffusion becomes significant at cutting temperature of more than 800...900°C, i.e. in the area of application of carbides and super-hard materials.

In cutting ferrous metals with carbide tools, carbon atoms, which have the smallest radius, diffuse rapidly, while the cobalt, tungsten and titanium diffuse significantly slower. As a result, the surface of carbide is decarburized. Such structural changes in the thin surface layers of the tool material make carbides more brittle and reduce its strength to the extent, when these layers are easily destroyed and carried away by the workpiece material and chips.

**Chemical (oxidation) wear** occurs due to oxidation of the sliding surfaces at high temperatures. The oxidation becomes possible due to the penetrating power of oxygen and its accelerated connection with chemically clean surfaces of the chip and the tool. The resulting oxide films are very brittle and are easily fractured, exposing the following layers, which in turn are oxidized and are fractured.

The oxidation wear occurs usually at the cutting temperatures of 700...900°C.

### 1.5.4 Cutting wedge failures

Because of the uneven distribution of stress and temperature on the tool contact surfaces and different nature of wear, the wear rate of different parts of the cutting tools are different and depend on the cutting conditions.

Regardless of the type and purpose of cutting tools, wear usually takes place on the flank surfaces. And the most intense wear occurs on flank surfaces adjacent to the cutting edge, where the contact stresses are particularly high. As a result, the wear land with a zero, and in some cases, slightly negative clearance angle  $\alpha_A$  is produced (Fig. 1.33, a).

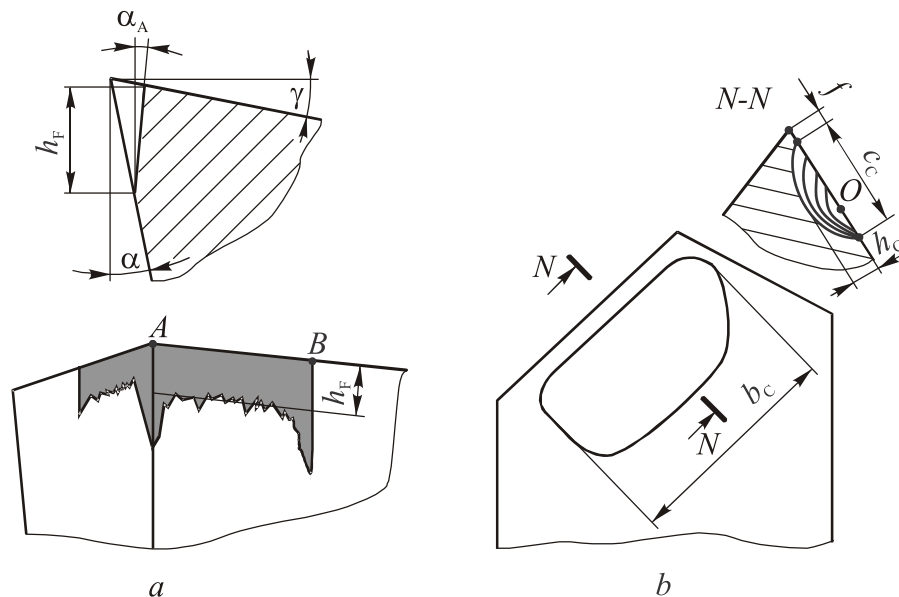


Fig. 1.33 Types of wear: (a) flank wear; (b) crater wear

The wear that develops on the rake surface proceeds with the formation of crater of width  $c_C$ , length  $b_C$  and depth  $h_C$  (Fig. 1.33, b). Here, the point  $O$  of the deepest crater depth  $h_C$  is located approximately at the maximum cutting temperature point at the contact zone of the tool-chip interface. In addition, the edge of the crater spaced a short distance  $f$  from the cutting edge.

The crater is parallel to the cutting edge, a short distance of the minor cutting edge.

The assessment of cutting tool wear is usually carried out in two ways: 1) measuring the width  $h_F$  of the flank wear land or the depth  $h_C$  and width  $c_C$  of the crater on the rake surface; 2) measuring the volume of the worn tool material.

## 1.6 Cutting tool life and machinability of materials

The period of cutting by a new or regrinded cutting tool till its failure, or up to the maximum permissible wear limit, is called a **tool life**.

Except time, tool life can be defined as the area of the machined surface, the number of parts, holes, etc.

Tool life effects on the cutting process productivity. Thus, in theory and practice of cutting, the tool life improvement is of primal concern.

### 1.6.1 Relation between tool life and cutting parameters

Tool life is usually determined with the tool wear curves  $h=f(\tau)$ . But it is required to know the maximum permissible wear limit, i.e. a **tool life criterion**. In practice, as a tool life criterion is taken the permissible width of the flank wear land  $h_F$ . The upper limit of this value is such value, after which a period of catastrophic wear begins (point *B* in Fig. 1.34).

The wear curves for different cutting speeds  $v_3 > v_2 > v_1$  show that with the cutting speed increasing, the curves become steeper and the point *B* displaces to the higher permissible values (Figure 1.34), i.e. in this case the optimal wear limit  $h_F$ , strictly speaking, is different for each curve. However, in practice, the flank wear limit is the same value for the entire family of the wear curves, and it is called the **criterion of equal wear**.

Values of the wear criteria are determined experimentally. The criteria depend on a variety of cutting conditions and, mainly, on the combination of the tool and workpiece material properties.

The following technological criteria can be used to define the moment when the cutting tool is dull: a) increasing roughness of the machined surface; b) the loss of dimensional accuracy in finishing; c) noise; d) vibrations or chatter; e) catastrophic failure of small-sized tools, etc. Usually, the actual tool wear value, when using these criteria, is smaller than the specified permissible wear limit, thus the maximum tool life is not reached.

As it was shown above, the greatest influence on the tool wear has a temperature-velocity factor. Therefore, in the earliest works on improving



cutting tools F.W. Taylor offered to assess their performance by finding the dependence of the "life-speed" ( $T-v$ ). This technique has not lost its relevance today.

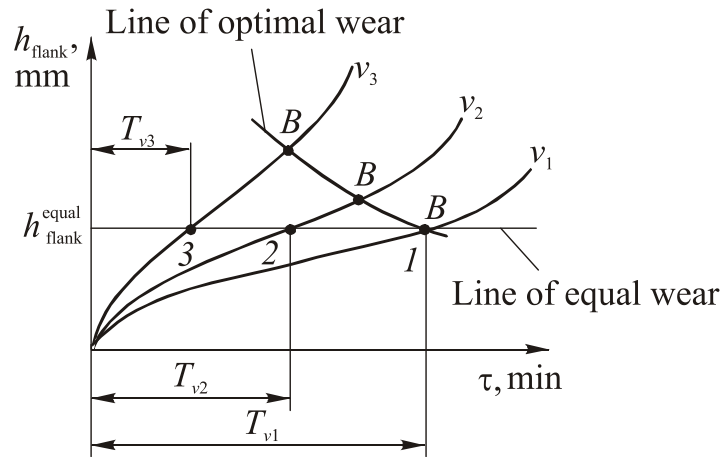


Fig. 1.34 Criteria of equal and optimal wear

For the convenience of technological calculations, these curves are plotted in coordinates with logarithmic scales (Figure 1.35), thus the relationship  $T-v$  is approximated by exponential empirical functions:

$$T = \frac{C_1}{v^{m_1}} \tag{1.20}$$

For the cutting speed calculations Eq. (1.20) is converted to the equation

$$v = \frac{C}{T^m} \tag{1.21}$$

where  $C$  - a constant;  $m$  - the index of relative tool life.

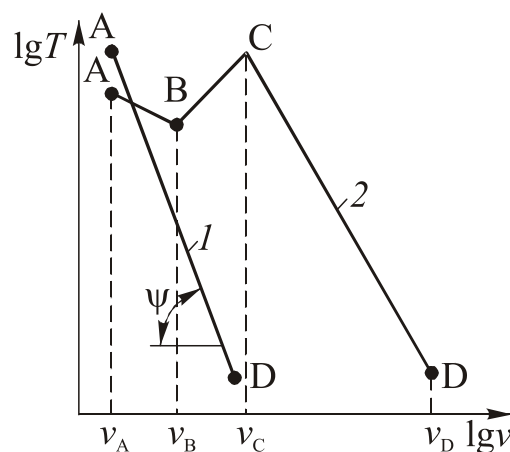


Fig. 1.35 Relation between cutting speed and tool life given in logarithmical scales

Drop in tool life in the region  $A-B$  is attributed to the influence of adhesive wear, which increases when the cutting speed within the  $v_A...v_B$  increasing. The increase in tool life in the region  $B-C$  is associated with a decrease in the strength of adhesive (intermolecular) interaction due to growth of the cutting temperature. With further increase in speed within the  $v_B...v_D$ , when the cutting temperature is higher than  $800...900^\circ\text{C}$ , the diffusion wear prevails. It is evident, that the use of carbide tools at speeds less than the  $v_B$  is unpractical.

Effect of feed and depth of cut on the tool life is defined by the same method as the effect of the cutting speed. Based on the three partial dependencies  $T = \frac{C_1}{v^{m_1}}$ ,  $T = \frac{C_2}{t^q}$ ,  $T = \frac{C_3}{f^p}$ , the general dependence is found:

$$T = \frac{C_4}{v^{m_1} f^p t^q}. \quad (1.22)$$

Here, because according to the effect of the cutting parameters on the cutting temperature the exponents in Eq. (1.22) are arranged in descending order, i.e.  $m_1 > p > q$ .

Resolving the equation (1.22) for cutting speed calculation [3] the following equation is obtained:

$$v = \frac{C_v}{T^m t^{x_v} f^{y_v}}. \quad (1.23)$$

It follows from equation (1.23) that with the given tool life, it is needed to work with the highest  $t/f$  ratio, to achieve higher cutting speeds, and therefore higher productivity.

During the development of the standards for cutting parameters, it was found that the exponents  $x_v$  and  $y_v$  are not constant but depend on the type of a cutting tool, properties of tool materials, as well as feed and depth of cut.

Properties of the workpiece material have the greatest impact on the cutting speed. For example, when cutting hardened steels or high-strength cast irons the cutting speed is 200 times lower than that in cutting of aluminum. Next, in descending order of influence, comes cutting tool material; the change in tool material can cause the cutting speed to vary up to 75 times, and with change of the tool geometry, depth and width of cut cutting speed can vary up to 3...5 times.

## 1.6.2 Machinability of materials

**Machinability of materials** is the property of a material to be machined freely or easily, in other words it is a combination of the material properties, which permit the achievement of the following parameters: 1) cutting speed  $v_T$  for a given tool life  $T$ ; 2) good surface finish (roughness, work-hardening, residual stresses); 3) low cutting force and power consumption; 4) form and size of chip, its transportability, etc.

Machinability depends on the chemical composition of the workpiece material, its mechanical and thermal properties, type of machining operation, tool design and tool material, cutting conditions, coolant type and other factors.

Under production conditions, of the above criteria of machinability the most often used criterion is the cutting speed  $v_T$  for a specified tool life. This criterion is used to determine the productivity of the given material cutting, and costs necessary for the cutting process.

To compare machinability of different materials the **machinability index** is often used, which is the following ratio:

$$K_M = \frac{v_{60}^A}{v_{60}^B},$$

where  $v_{60}^A$  is the cutting speed at  $T=60$  min, which define machinability of the investigated material A;  $v_{60}^B$  is the cutting speed at  $T=60$  min, which define machinability of the reference material B.

Usually, the steel grade 45 (0.45% C,  $\sigma=650$  MPa,  $HB\ 180$ ) is taken as the standard, and its machinability coefficient  $K_M=1$ . The higher is the value of the machinability coefficient, the better is the machinability.

If the machinability index for the given material is unknown, it is necessary to experimentally determine "life-speed" ( $T-v$ ) relation for its calculation.

To save time and costs of the experimental findings of this relation, various methods of rapid assessment of machinability were developed. Let's consider the simplest of them – a method of machinability assessment by the wear intensity, which was proposed by A.S. Kondratov. The method consists in the fact that the material is test with only one cutter at a constant depth of cut  $t$  and feed rate  $f$ , but at different cutting speeds  $v_1, v_2, v_3, \dots, v_i$ . For each speed at specified time intervals  $T_i$  the increments of the tool flank wear  $\Delta h_{Fi}$  are measured and the wear rate  $U$  is calculated by the following equation:

$$U_i = \frac{\Delta h_{Fi}}{T_i}.$$

In the coordinates with double logarithmic scales the relationship  $U=f(v)$ , which is a straight line, is plotted, the slope of the line about the  $U$  axis is taken equal to the index of relative tool life of the equation

$$v = \frac{C}{T^m}.$$

The method gives good accuracy in cutting with carbide cutters and, in comparison with the classical method  $T-v$  described above, in 6...10 times reduces the time of testing.

### 1.6.3 Application of cutting fluids in cutting

Lubricating-cooling agents (LCA) are widely used in machining in order to improve the machinability of materials and are used in the form of liquids, gases, greases (consistent) and solid lubricants. Of these, the greatest application received liquid coolants, which are called **cutting fluids** (coolant).

The function of the cutting fluids in cutting process is mainly consist in lubrication, cooling and detergency.

The lubricating effect of the cutting fluid should be preceded by the penetration of the lubricating medium to the zones of the tool and workpiece contact.

According to recent studies, the coolant penetration to the cutting area can occur in the following ways (Figure 1.36): (a) via capillary network between the workpiece, tool and chip surfaces; (b) via the cavities, generated by the repetitive built-up edge destruction; (c) due to decrease in tool-work contact intensity; (d) by diffusion through cracks and other defects that occur during the formation of the chips in the process of plastic deformation.

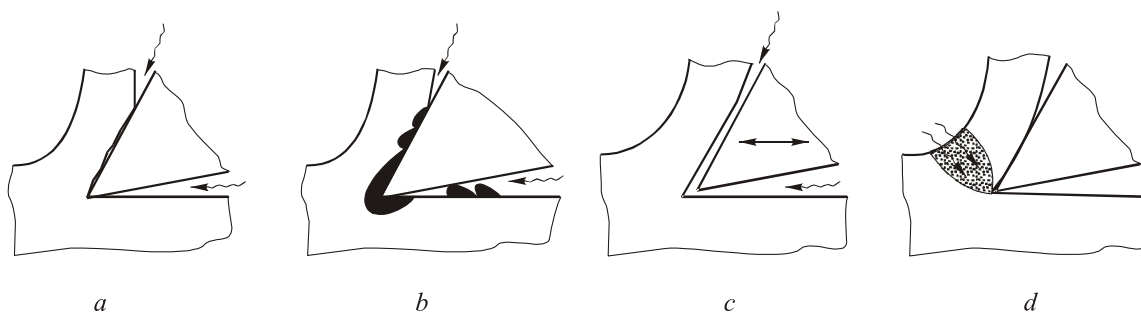


*Fig. 1.36 Penetration of cutting fluid to the cutting zone (V.N. Latyshev): (a) via capillary network between the workpiece, tool and chip surfaces; (b) via the cavities, generated by the repetitive built-up edge destruction; (c) due to decrease in tool-work contact intensity; (d) by means of diffusion via the surface cracks and defects*

Despite the small size of the capillaries (1...4 mm), especially at low and medium cutting speeds, a constant supply of ions and molecules and vapor of cutting fluid to the cutting zone is ensured. At high speeds and high feed rates the conditions for cutting fluid penetration deteriorate due to a sharp growth of contact pressure and temperature.

**Lubricating effect** of cutting fluid is fulfilled by the formation of films on rubbing surfaces. These films by their nature can be physical, i.e. created by the molecular adsorption or chemical – due to chemical reactions with the newly formed surfaces of the chip and the workpiece.

Lubricating effect of the cutting fluid decreases the roughness of the machined surface. Therefore, the fluids with increased lubricating effect are used in finishing operations, in cutting at low and high cutting speeds, for example, in burnishing by the tools with burnishing elements.

**Cooling effect** of cutting fluid consists in removing heat from the most heated areas of the tool and the workpiece by convective heat transfer, i.e. heat-transfer related to the movement of the liquid and its thermal conductivity. Here, the higher is the thermal conductivity, specific heat capacity, cutting fluid wettability and speed of cutting fluid movement through the cutting area, the more effective is the heat removal.

**Detergency of the cutting fluid** consists in removing the wear debris of the tool and the workpiece from the cutting zone. The debris can be in the form of hard carbide particles, small chips, etc. that facilitates the abrasive wear of the tool and deteriorates surface finish. Detergency improves with the introduction of emulsifiers – surface-active agents (surfactants) into the cutting fluid, which reduce the surface tension of the liquid.

In addition to these three basic properties, cutting fluid must also: 1) be stable during storage and operation; 2) cause no corrosion of machine parts, cutting tool and workpiece; 3) non-degradable by bacteria; 4) have no harmful impacts on the environment and health of workers. For these purposes, cutting fluids are supplied with anti-corrosion, anti-wear, anticoring, anti-foam, bactericidal and other additives and agents.

All the cutting fluids on the physicochemical characteristics are divided into water-based and oil-based.

Water-based cutting fluids have the best cooling effect; however their lubricating effect is weak. In addition, these cutting fluids can cause severe corrosion of machine parts, tools and workpieces. Water-based cutting fluids are used in machining of metals at high cutting speeds and with high contact pressures, that is, where the cooling is primary (turning, drilling, grinding, etc.).

Water-based cutting fluids are divided into four groups: 1) electrolyte solutions; 2) oil emulsions; 3) synthetic cutting fluids; 4) semi-synthetic cutting fluids.

Oil (hydrocarbon) emulsions are composed of mineral oil and special additives of different purposes.

The advantages of oil emulsion are good lubricity and corrosion protection, among shortcomings there are low (5...8 times lower than that of water coolant) cooling capacity, thermal conductivity and heat capacity, high cost, and increased flammability. Therefore, oil-based cutting fluids are used mainly in operations characterized by high contact pressure and low heat generation, operations that require a lubricant (threading, broaching, gear cutting, deep drilling).

The effectiveness of coolant is also greatly influenced by the method of its delivery to the cutting area. There three most frequently used ways of coolant delivery (Fig. 1.37): 1) flooding; 2) high pressure jet applied to the clearance surface; 3) through the tool.

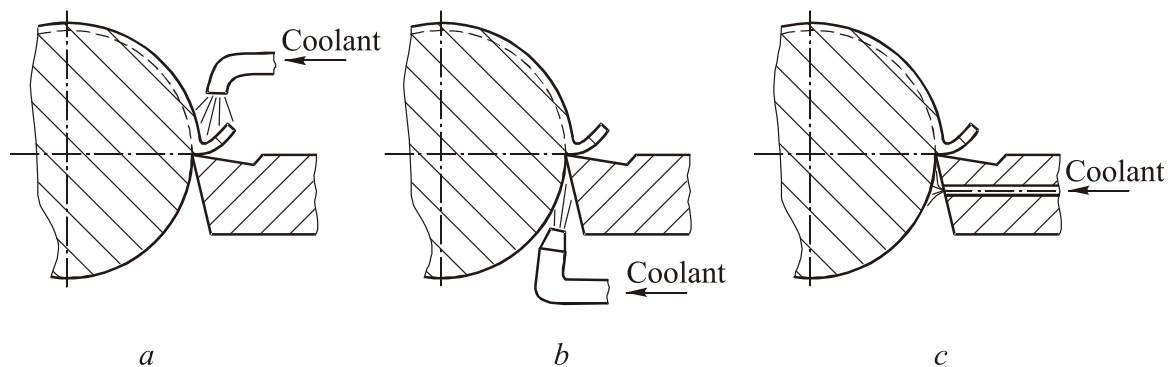


*Fig. 1.37 Methods of cutting fluid delivery to the cutting zone: (a) flooding; (b) high pressure jet applied to the clearance surface; (c) coolant-fed tool*

Flooding is the simplest but also the least effective method of cutting fluid delivery. It is characterized by high consumption, spattering and heating of the cutting fluid.

Cutting fluid deliver by high-pressure jet is more efficient as compared to flood method. The disadvantages of the pressure jet cooling are: the need for special devices for cutting fluid delivery and fine filtering, and a high level of noise.

The delivery of cutting fluids through the cutting tool body is commonly used in deep-hole drilling, particularly in gun drilling and high-speed machining. In addition to a good penetration of cutting fluid, it also provides a reliable evacuation of chips that carry the most part of the heat. However, in this case, the cost of cutting tool manufacture, as well as cutting fluid spatter-

ing increases. To limit the spattering it is required to enclose the cutting area. In addition, special pump stations are needed for the coolant delivery.

A brief look at other types of coolants is given below.

**Gaseous coolants** compared with liquids are highly penetrating and therefore are used for cutting at high speeds and feeds.

**Consistent coolants** are used in the form of plastic or viscous lubricants. They consist of two components: a liquid base (oil) and thickener (5...30%), which hold the oil in its cells. Plastic lubricants are applied in forming operations.

**Solid coolants** (talc, graphite, molybdenum disulfide, wax, paraffin, etc.) are rarely used in pure form. Solid coolants ensure low coefficient of friction (graphite –  $f_F=0.04$ , molybdenum disulfide –  $f_F=0.03$ ) and withstand high temperature and pressure.

High cost of cutting fluids along with the cost for recycling and chip cleaning from the fluids evoked tendency to decrease and even eliminate (dry cutting) the use of cutting fluids wherever it is possible.

## 2. Basic Types of Machining

The term **machining** embraces a wide range of various techniques and processes of controlled material removal used to form a workpiece into a finished part of desired shape and size.

Although machining refers to a broad range of process involved in manufacture, the current chapter is devoted to the most common machining operations found in mechanical engineering. These operations are often called “traditional” or “conventional” and include the following processes: turning, shaping, planing, slotting, drilling, core-drilling, reaming, boring, milling, sawing, broaching and threading (some of these operations are shown in Fig. 4.1 of the Section 4.1).

Turning processes are dealt with in the following Section 2.1. Drilling and associated hole machining processes, such as core-drilling and reaming, along with the tools used are discussed in Section 2.2 and Chapter 5. Grinding operations are examined in Chapter 3. The aspects of broaching are examined in Section 4.2.

Non-traditional machining embraces such advanced machining processes as: Laser cutting, plasma cutting, water jet cutting, abrasive jet machining, ultrasonic machining, electro-chemical machining, electrical discharge machining, etc. These processes are based on non-mechanical material-removal methods, and are not considered here.

### 2.1 Turning Operations

Turning is the most common of all types of machining operations found in metal cutting industry. It is the basic machining process since, in addition to the relatively simple single-point cutters, it can also include application of the multiple-point cutting tools as well.

Operations related to turning include: straight turning, taper turning, facing, profiling, grooving, face grooving, cutting off, threading, cutting with a form cutter, knurling, boring, drilling, core-drilling and reaming.

Since the machining aspects examined in the first chapter of the book were considered on an example of turning, the most part of turning issues are already discussed. Thus let's sum it up, let's see what we have. The elements of a turning cutter, as well as its geometrical parameters were introduced in Section 1.1. Calculation of cutting force and power consumption in turning was considered in Sections 1.2 and 1.3. Considerations on surface finish were made in Section 1.3.3. Impact of the cutting parameters on the turning pro-



cess as well as the procedure of the parameters selection was scoped in Section 1.4.2. As for types of cutters, the basic types and designs, as well as calculation of a form cutter, will be presented in Section 4.1.

## 2.2 Drilling operations

The process of drilling is implemented by the drills of various types; with the HSS twist drill that is one of the most complex designs of the multiple tools, being the uppermost and the most important. Twist drills have variable rake and clearance angles along the cutting edges, helical rake and profiled clearance surfaces, unfavorable geometry of cutting wedges and in the center of the drill especially, a small radial stiffness due to considerable overhang, and difficult conditions of chip removal that altogether have the greatest influence on the patterns of the drilling operation.

Thus, the chip formation conditions, heat and power loads that affect the wear and tool life are different at each point along the drill cutting edges. Because of the low radial stiffness of twist drills and high loads that occur due to large width of the chips, the use of carbide faces certain difficulties. This greatly impedes productivity of drilling, especially drilling of high-strength materials.

### 2.2.1 Cutting force components in drilling

In contrast to turning the drilling involves not one, but three cutting edges (two lips and one chisel edge), which together determine the power load on a drill. In addition, the torque needed for drilling is affected by the friction between drill margins and walls of the hole being drilled.

The resultant cutting force applied at the drill lip can be resolved, as in turning, into three mutually perpendicular components: 1)  $P_Z$  – tangential, acts in the direction of the cutting velocity; 2)  $P_X$  – the thrust force parallel to the drill axis, 3)  $P_Y$  – radial to the drill axis (Figure 2.1).

The radial components  $P_Y$  at the lips are directed in opposite directions and in theory should be balanced. However, in practice due to errors of sharpening and mounting of the drill, uneven cutting load caused by, for example, hard spots in a work or other reasons, the balance of the radial components  $P_Y$  is disturbed. In this case, because of the appearance of unbalanced force  $\Delta P_Y$  the transverse vibrations of the drill arise. These vibrations cause the hole oversize (undesirable increase of drilled hole diameter), drill wandering, which increase, with depth of drilling increasing.

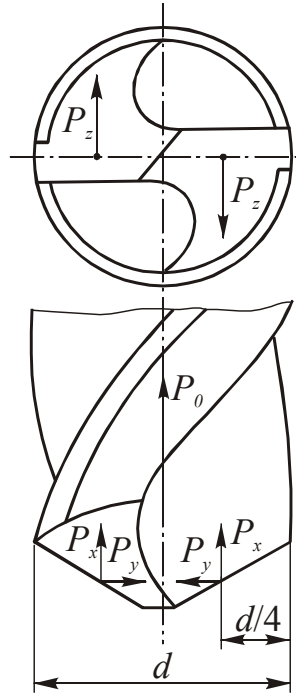


Fig. 2.1 System of forces acting on a twist drill

In practice, the axial force and torque are calculated, respectively, by the following equations

$$P_O = C_P d^{x_p} f^{y_p} K_P, \quad (2.1)$$

$$M_T = C_W d^{x_T} s^{y_T} K_T, \quad (2.2)$$

where  $C_P, C_W$  - coefficients characterizing drilling conditions and properties of the reference workpiece material;  $K_P, K_T$  - factors that characterize the drilling conditions (method of sharpening, web thinning, cutting fluid, etc.).

Hence the power consumed in drilling is

$$Ne = 1.6 \cdot 10^{-3} M_T n, \text{ (kW)}. \quad (2.3)$$

### 2.2.2 Wear and life of drills. Calculation of drilling parameters

In drilling the cutting speeds and friction travel are variable along the cutting lips. The chips are wide and thin, thus the twist drills wear mostly on the clearance surfaces adjacent to the cutting lips. The wear takes the form of wear lands  $h_F$ , which are variable along the cutting edges. In drilling brittle materials the drill wear occurs on the lip corners. In drilling ductile materials at high speeds the wear take place on the rake surfaces in the form of craters and on the margins in the form of wear land  $h_C$  (Figure 2.2).

The most dangerous is the wear on the lip corners and margins, as in this case, heavy wear will need a significant amount of the tool material to be ground off. Therefore, in drilling the catastrophic wear, as the lip corner melting and margins failure, should not be allowed.

Chisel edge due to low friction velocities in the center of the drill wear much slower. The heavy wear of the chisel edge is sharply increases thrust pressure, and the wear on the margins significantly increases the torque. Intensive wear of the chisel edge indicates that the heat treatment parameters were violated during the manufacturing process.

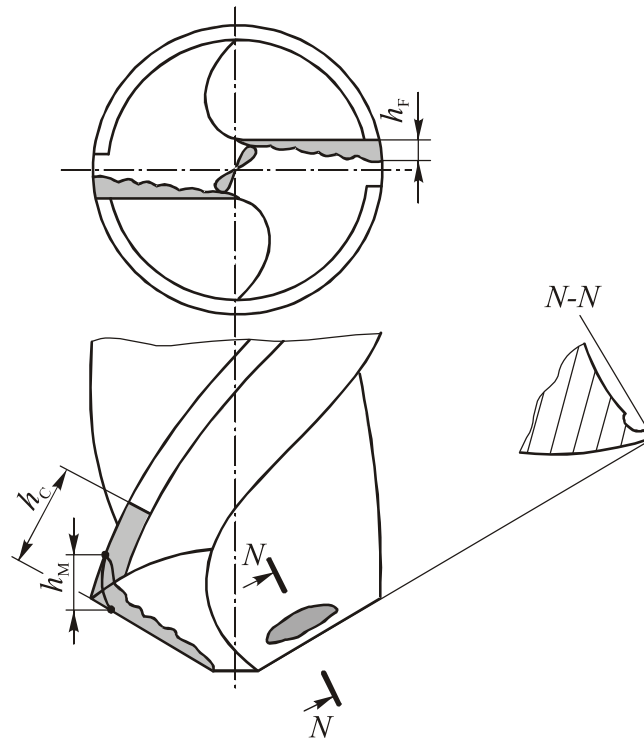


Fig. 2.2 Wear on the rake and clearance surfaces of a twist drill

The impact of various factors on the drill flank wear in cutting structural steels can be expressed by the following empirical equation [34]:

$$h_F = C v^{4.85} f^{2.35} T^{1.42} \quad (2.4)$$

It follows from Equation that the greatest influence on the drill wear has the cutting speed and a much smaller effect – feed rate. For this reason, in terms of drill life, it is preferable to work with a greater feed rate and lower cutting speed, as for a given tool life  $T$  it provides higher productivity of the drilling process.

The cutting speed for drilling is calculated as:

$$v = \frac{C_v d^{x_v}}{T^m f^{y_v}} K_v \quad (2.5)$$

where  $C_V$  is the coefficient of the workpiece material properties, for structural steels ( $C > 0.6\%$  and  $\sigma = 750$  MPa) and feed rate  $f < 0.2$  mm/rev –  $C_V = 89$ , and for feed rate  $f > 0.2$  mm/rev –  $C_V = 12.4$ ; for cast iron ( $HB 190$ ) –  $C_V = 20.6$ ;  $m$  – exponent for these materials, respectively,  $m = 0.2$  and  $m = 0.125$ ;  $x_V = 0.4$  and  $x_V = 0.25$ ; and  $y_V = 0.6$  and  $y_V = 0.5$  [8, 31];  $K_V$  – the coefficient for cutting fluid used, drilling depth, method of sharpening etc.,  $K_V = K_{fluid} \times K_L \times K_{sharp}$ .

The main weaknesses of twist drills that reduce the drill life include: 1) high positive rake angles on the drill periphery; 2) unfavorable geometry of the chisel edge; 3) the lack of clearance on the minor cutting edges (margins).

The aspects on the correction of these shortcomings and drill point enhancement are presented in Section 5.1.4.

The cutting parameters for drilling operation are assigned in the following order:

1. In order to achieve maximum performance, the maximum permissible feed rate  $f$  with respect to the drill strength and stiffness is assigned [3]:

- for steel drilling  $f_{\max} = 4.46 \frac{d^{0.8}}{\sigma^{0.94}}$ , (mm/rev);

- for cast-iron drilling  $f_{\max} = 7.34 \frac{d^{0.81}}{(HB)^{0.75}}$ , (mm/rev).

2. Further, according to the depth and type (blind or through) of holes, the calculated feed rate values are refined.

3. With respect to the given values of the hole diameter  $d$ , feed rate  $f$  and accepted tool life, the cutting speed is calculated by Equation (2.5). Afterwards, the drill RPM is adjusted according to the machine PRM settings, so that the  $n_{drill} \leq n_{calculated}$  is met.

4. Drilling forces and power are calculated by Equations (2.1), (2.2) and (2.3), and checked in terms of main drive power and strength of the machine feed-drive mechanism.

## 2.3 Milling Operations

Milling in contrast to turning or planing is accomplished with the help of the multiple-point cutting tools and is therefore a very productive method to machine flats, faces, shoulders, grooves, slots, and various shaped surfaces (gears, splines, threads, etc.). The following are the details of the cutting mechanics of milling.

### 2.3.1 Fundamentals of milling processes

The primary motion in milling is a rotation motion of a milling cutter around its axis, and feed motion is implemented either by the cutter or by the workpiece mounted to a milling machine table. Unlike turning, in milling these two motions are not kinematically interlocked and are executed independently. If these motions are opposite in direction, the milling is called conventional milling (up milling), and if the motions are unidirectional that is the climb milling (down milling).

Since the position of the milling cutter axis with respect to the workpiece can be different, influencing on dimensions and shape of the produced chips and other parameters of the cutting accordingly, the aspects of milling are examined on the examples of peripheral and face milling only.

**Plain milling cutter or slab mill** (Figure 2.3) is a cylinder of a length  $L$  greater than the diameter of the cutter  $d$ . On the mill periphery straight or helical teeth, mostly for a smooth entry into a workpiece, are cut (side milling cutters as opposed to plain cutters have  $L \ll d$ ).

Dimensions of the layer being removed during slab milling are (Figure 2.3):  $B$  – width of cut;  $t$  – depth of cut;  $\psi_m$  – angle of contact of a cutter with a workpiece. Since the length of the slab mill is greater than its diameter, and minor cutting edges are missing, slab mills, unlike other types of mills, work in conditions of free cutting. Provided that the teeth of a slab mill are helical ( $\omega \neq 0$ ), the milling is the free oblique cutting.

Depending on the length of the arc of engagement it can incorporate a number of teeth:  $m = \psi_m / \varepsilon$ , where  $\varepsilon$  – tooth pitch angle (there is also peripheral pitch  $t_p = \pi d / z$  and axial pitch  $t_a = \pi d / z \operatorname{tg} \omega$ ).

The trajectory of the cutter edges is a composition of rotational motion and translational motion in the direction of feed. The thickness of the chip cut by a single tooth rotated on an angle  $\psi_i$  is defined as the distance along the normal to the two successive positions of the tooth trajectory, i.e. in radius and is equal to  $a_i = f_z \sin \psi_i$ , where  $f_z$  – feed per tooth (Fig. 2.4). Thus, during the

cutter motion along the length of engagement, the chip thickness changes from zero to  $a_{max}=f_z \sin \psi_m$ .

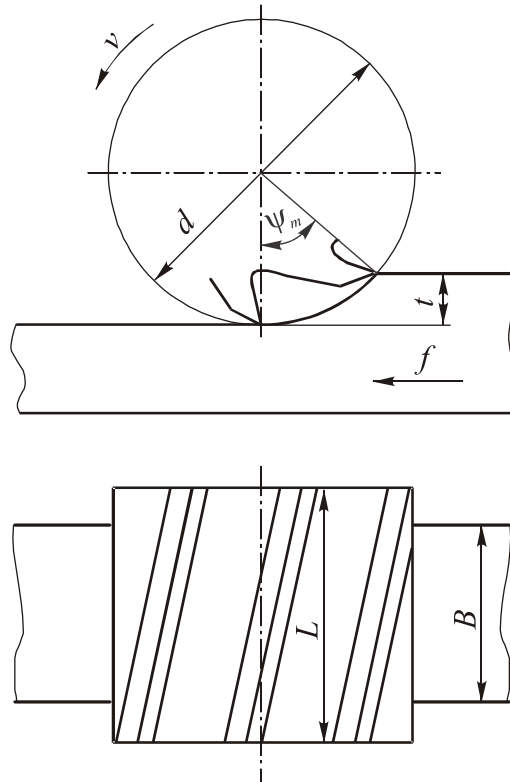


Fig. 2.3 Dimensions of a layer being removed in slab milling

In further calculations the median chip thickness  $a_m=f_z \sin(\psi_m/2)$ , which is measured in the middle of the arc of engagement, will also be used.

Full contact angle  $\psi_m$  can be found by the following equations:

$$\cos \psi_m = 1 - \frac{2t}{d} \text{ and } \sin \psi_m = 2\sqrt{\frac{t}{d} - \frac{t^2}{d^2}} \approx 2\sqrt{\frac{t}{d}}$$

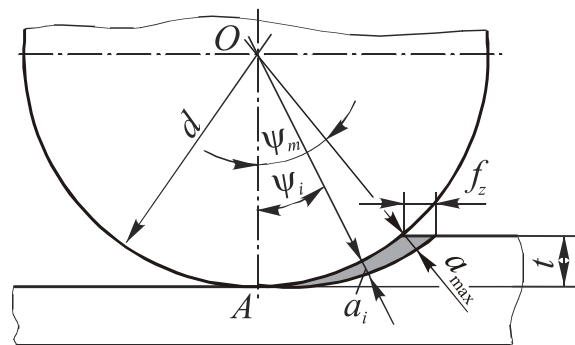


Fig. 2.4 Schematic for chip thickness in slab milling

In milling the following types of feed are used: feed per revolution  $f_o=f_zz$  (mm/rev) and feed per minute or just feed rate  $f_M=f_o n=f_zzn$  (mm/min), where  $z$  – number of teeth;  $n$  – cutter rpm (rev/min).

The area of the layer being cut by a single straight tooth as it moves along the arc of engagement is  $F_z = Bf_z \sin \psi_m$ , and the area of the chip cut with all the teeth within the arc of engagement is

$F_{total} = Bf_z (\sin \psi_1 + \sin \psi_2 + \dots + \sin \psi_i)$ , i.e.  $F_{total} = Bs_z \sum_{i=1}^{i=m} \sin \psi_i$ , where  $m$  – number of teeth of the cutter that are within the arc of engagement.

For the cutters with helical teeth the chip thickness along the length of helical teeth is variable.

**Face mills** unlike the slab mills work with the scheme of non-free cutting, since in addition to the major cutting edges located on the cutter periphery, the minor cutting edges are also involved in cutting process.

Fig. 2.5 shows the parameters of the layer being removed in face milling:  $t$  – depth of cut;  $B$  – milling width.

Comparison with the plain milling cutters shows that with the transition from the slab milling to the face milling, the positions of  $t$  and  $B$  parameters are swapped over. In addition, face milling is characterized by large angles of contact, which are up to  $\psi_m=180^\circ$ .

Thickness of the chip being removed by each tooth of the face mills at any given time is determined by the same equation as for the slab milling:  $a_i=f_z \sin \psi_i$ . The thickness of the chip is variable and varies from zero to a maximum value  $a_{max}=f_z$  at an angle  $= 90^\circ$ , and then reduces back to zero.

The chip cross-section has a rectangular shape with an area  $F_z=f_z \sin \psi_i t$ , and the area of the chips that are cut by all the teeth on arc of engagement:

$$F_{total} = tf_z \sum_{i=1}^m \sin \psi_i. \quad (2.6)$$

The contact angle  $\psi_m$  depends on the position of a milling cutter (in the reference plane) with respect to the workpiece, and on the ratio  $B/d$ . In a full-width milling  $B=d$  (Fig. 2.5, a), contact angle  $\psi_m=180^\circ$ ; in partial milling  $B<d$  (Fig. 2.5, b),  $\sin \psi_m = 2\sqrt{B(d-B)}/d$ ; in a central symmetrical milling  $B<d$  (Fig. 2.5, c),  $\sin \psi_m / 2 = B/d$ ; in a central asymmetrical milling with the cutter offset with respect to the workpiece by the value  $B_0$  (Fig. 2.5, d),

$$\psi_m = \arcsin\left(1 - \frac{2B_0}{d}\right) + \arcsin\left[\frac{2(B+B_0)}{d} - 1\right].$$

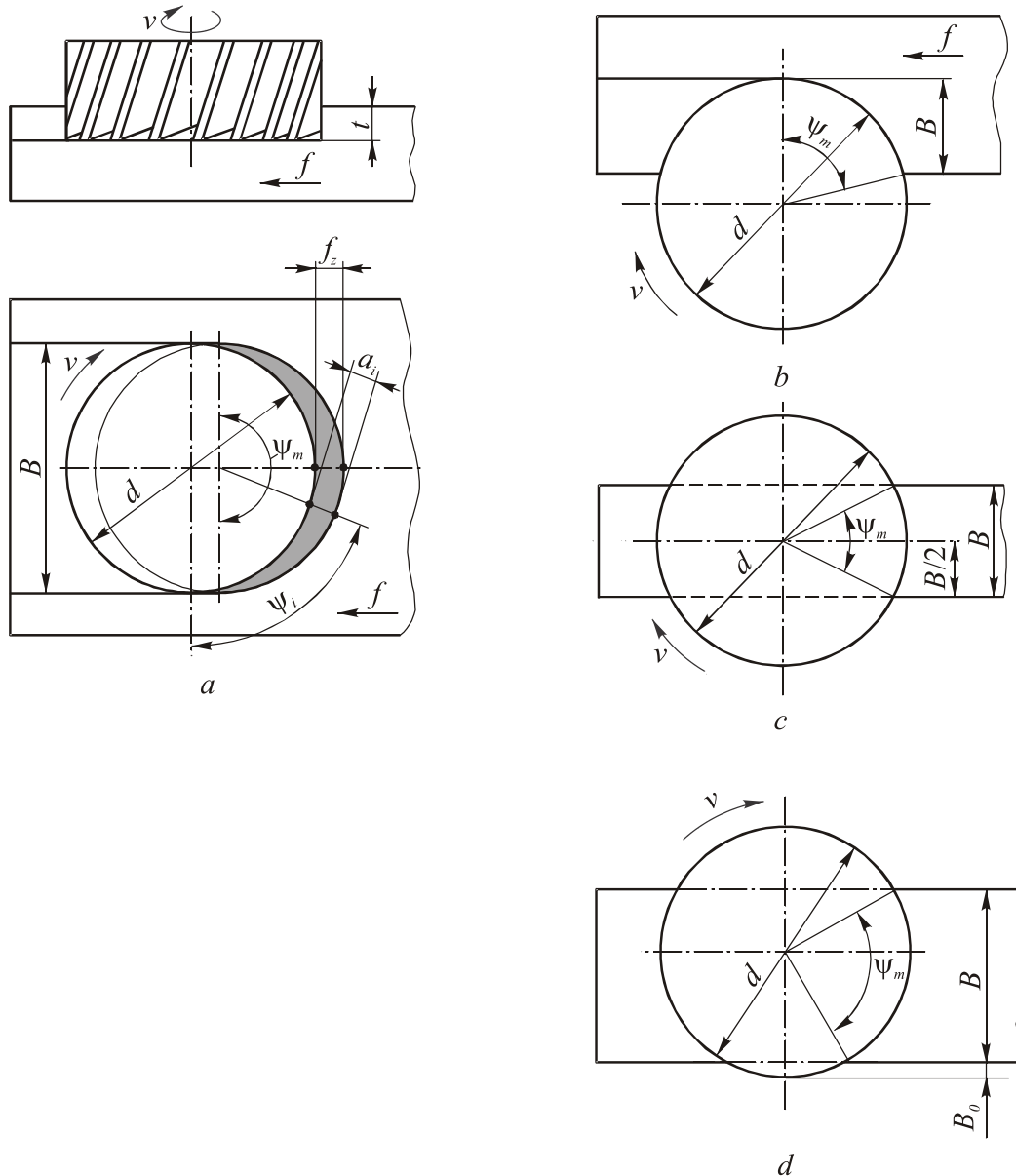


*Fig. 2.5 Schematics of face milling with respect to the cutter position relative to the workpiece: (a) full-width; (b) partial and shifted; (c) central symmetrical; (d) central asymmetrical*

### 2.3.2 Thickness of uncut chip for helical plain cutter. Uniform milling condition

Fig. 2.6 shows the unfolded flat patterns of the transient surface ( $m, n, q, p$ ) and the helical tooth of a plain cutter, which extreme points 1 and 2 within the actual working area are positioned at different angles of contact  $\psi_1$  and  $\psi_2$  at any instantaneous position of a cutter tooth. The thickness  $a$  of the layer being removed along the cutting edge is variable.



The area of the layer being removed by a single tooth can be defined as:

$$F_z = \frac{f_z d}{2 \sin \omega} (\cos \psi_1 - \cos \psi_2). \quad (2.7)$$

It follows from this equation that as the tooth moves along the transient surface, the area of the chip cross-section is variable. Then, when the  $m$  teeth are engaged with the workpiece within the contact angle  $\psi_m$ , the total cross-sectional area of the layer being cut is:

$$F_{total} = \frac{f_z d}{2 \sin \omega} \sum_1^m (\cos \psi_1 - \cos \psi_2). \quad (2.8)$$

It is possible to make such conditions in milling with a helical plain cutter, when the  $F_{total}$  is constant for a cutter to be rotated at any angle. In this case, power load on the cutter is also constant and the cutting process is performed uniformly, without pulses in force and vibrations, leading to increased tool life and productivity.

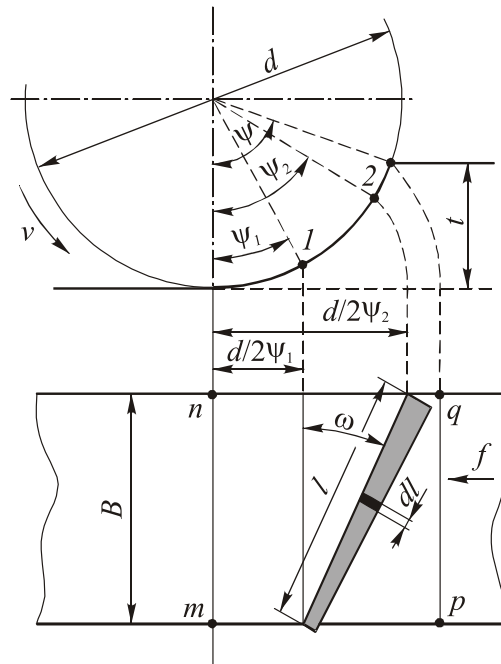


Fig. 2.6 Thickness of the layer being removed by a helical tooth of a slab mill

The condition of the uniform milling is ensured if the following ratio is maintained:

$$C = \frac{B}{t_o} = \frac{Bz \operatorname{tg} \omega}{\pi d}, \quad (2.9)$$

where  $C$  is integer;  $B$  is the milling width;  $t_{axial}$  is the axis tooth pitch;  $\omega$  is the helix angle of the cutter teeth.

The condition of uniform milling (2.9) should guide the design of milling operations, especially in medium and large production runs.

### 2.3.3 Forces, work and power in plain milling

Fig. 2.7 shows the schemes of resolution into components of the resultant cutting force  $R$  acting on the helical tooth of a plain cutter for conventional and climb milling. These schemes have much in common with oblique free turning and shaping. Here, the resultant cutting force  $R$  is the geometric sum of two components:  $P_Z$  and  $P_Y$ .

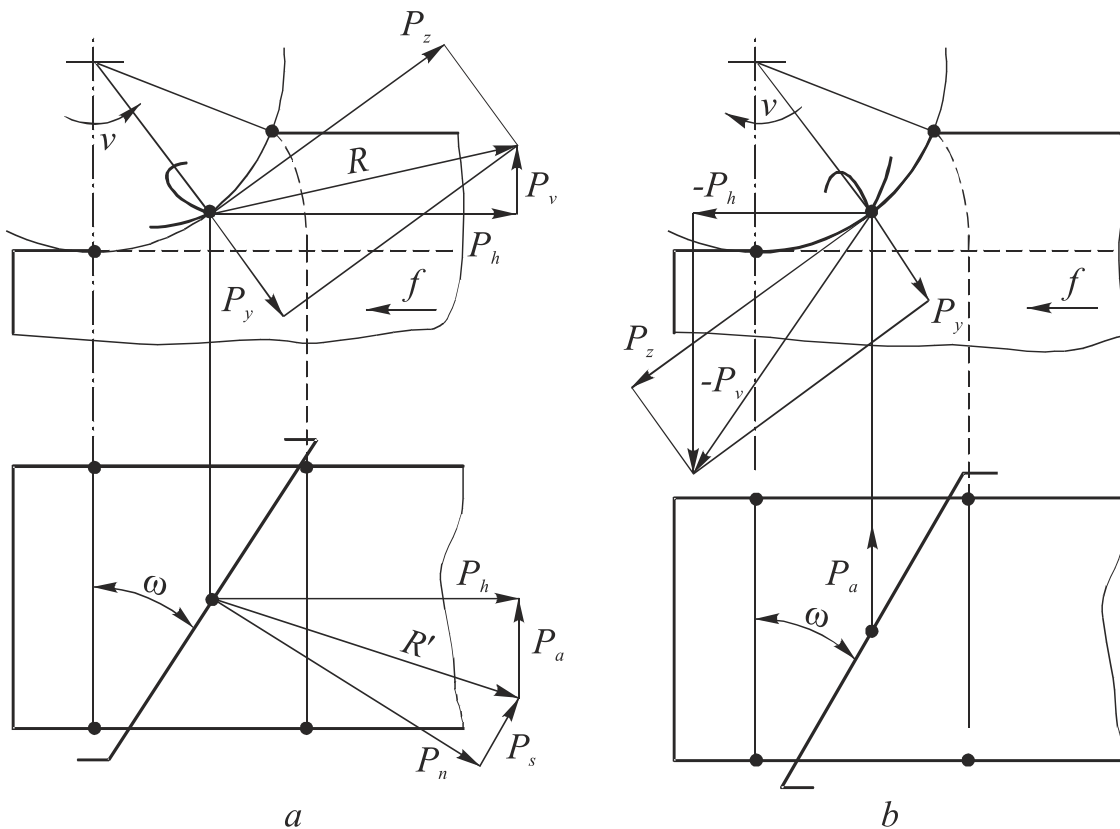


Fig. 2.7 Components of the cutting force  $R$  on a helical tooth of a plain milling cutter: (a) conventional milling; (b) climb milling

The resultant cutting force  $R$  can also be resolved into a horizontal component  $P_h$  that is directed against the feed direction (Fig. 2.7, a) and loads machine feed drive, as well as vertical component  $P_v$ , which causes deflection of the tool in conventional milling and forces the workpiece down to the machine table in climb milling.

Total peripheral component of the cutting force:

$$P_{ztotal} = C_p \frac{Bz}{\pi} \frac{2^{K+1}}{K+2} f_z^{K+1} \left( \frac{t}{d} \right)^{\frac{K+2}{2}}, \quad (2.10)$$

where  $K$  is the exponent.

Effective power in milling can be found:

$$Ne = \left( \frac{2^{K+1}}{K-2} \cdot \frac{C_p}{6000 \cdot 1000} \right) B d^{-\frac{K}{2}} t^{\frac{K+2}{2}} zn, \text{ (kWt)}. \quad (2.11)$$

In practice, the effective power is calculated by the following empirical equation:

$$Ne = C_N B t^x f_z^y z n d^q. \quad (2.12)$$

### 2.3.4 Forces and power in face milling

For the full-width milling, when  $B=d$ , contact angle  $\psi_m=180^\circ$ ,  $\varphi=0^\circ$  and  $\omega=0^\circ$ , Fig. 2.8 shows a diagram of the resultant force resolution into the components acting on the tooth of a face mill. Other schemes of the cutting force resolution in face milling are particular cases of this diagram.

Resultant cutting force  $R$  applied on the cutter tooth can be resolved into the peripheral component  $P_z$  and a radial component  $P_y$ , or into the horizontal component  $P_h$  (feed power) and a vertical component  $P_v$ .

Teeth of a face mill located on the first (lower) half of the arc of engagement work in up-milling conditions, and teeth in the second half work in climb-milling conditions. At the same time with the milling cutter rotating, the components  $P_z$  and  $P_h$  change not only in magnitude but also in the direction (Figure 2.8).

In the non-free cutting conditions, the peripheral component  $P_z$  acting on the cutter tooth can be represented as:

$$P_z = C_p f_z^{K+1} t^{l+1} \sin^{K+1} \psi. \quad (2.13)$$

To determine the power consumption in face milling, the methodology adopted for slab milling can be applied.

Work performed by a single tooth of a face mill, can be expressed as:

$$A_z = 2^{-\frac{K}{2}} C_p d s_z^{K+1} t^{l+1}. \quad (2.14)$$

Hence the effective power in face milling is:

$$Ne = \frac{A_z zn}{6000 \cdot 1000} = \frac{2^{-\frac{K}{2}} C_p f_z^{K+1} t^{l+1}}{6000 \cdot 1000} d zn, \text{ (kWt)}, \quad (2.15)$$

where  $C_P$  is the specific cutting force,  $\text{N}/\text{mm}^2$ ;  $f_z$  is the feed per tooth,  $\text{mm}/\text{tooth}$ ,  $t$ ,  $d$  are respectively, the depth of the layer being removed and the cutter diameter,  $\text{mm}$ ;  $n$  is the cutter speed,  $\text{rev}/\text{min}$ .

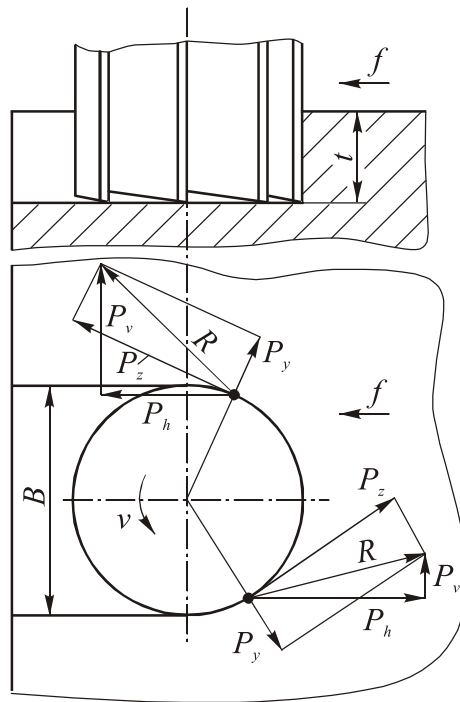


*Fig. 2.8 Components of the resultant cutting force  $R$  in face milling*

### 2.3.5 Milling parameters calculation

Calculation of cutting parameters in milling, as with other types of machining, starts with the selection of the cutter design with respect to the sizes and material of the workpiece and the requirements given in the part drawing. It is essential to choose size and geometric parameters of the cutter so that to ensure the uniform milling conditions, or at least ensure the least variation of cutting force.

For finishing operations the feed per revolution  $f_o=f_zz$  is selected with respect to the surface finish requirements. For roughing operations the maximum feed per tooth  $f_z$  is selected based on the conditions of strength of cutter teeth and machine feed drive. The maximum depth of cut is assigned based on the amount of allowance for machining. In roughing milling the allowance is usually removed in one pass, provided that the limitations mentioned above are met.

### 3. Grinding Operations

Grinding is the abrasive machining performed with grinding wheels and is mainly applied for finishing operations. Grinding is sometimes used instead of cutting in roughing operations to remove large allowances, for instance in rolling mill. This is due to its high productivity, achieved by a very long total active length of the cutting edges of the wheel grains and high cutting speeds ( $V=30\text{...}60$  m/s and more), which are due to high heat stability and wear resistance of abrasives. Grinding provides minimum roughness and high accuracy in machining of various materials, including hard-to-machine materials and materials which cannot be machined by cutting tools.

The disadvantages of grinding are as follows: 1) high level of energy required to remove a unit volume allowance (about 10 times larger than in cutting) because of unfavourable geometry of the cutting grains, removing very thin chips, and 2) high instantaneous temperature ( $1000\text{...}1600$  °C), leading to the appearance of burn marks on the machined surface, and 3) indentation of grains debris into the workpiece surface, which accelerates wear of the mating part.

#### 3.1 Types of Grinding Operations

The basic types of grinding operations are as follows:

1. **Traverse external cylindrical grinding** (refer to Fig. 3.1, a). Workpiece and grinding wheel are rotating about parallel axes. The diameter of the wheel  $d_{wh}$  is much larger than the diameter of the workpiece  $d_w$ . The wheel (or workpiece) is fed at the longitudinal feed  $F_L$  (mm/rev) along the axis of the workpiece. The feed value is set as a fraction of the grinding wheel width  $B$ . The peripheral speed  $V_{wh}$  (m/s) of the grinding wheel is much higher than the peripheral speed of the workpiece  $V_w$  (m/min). The width  $t$  (mm) of the stock that is being removed depends on the infeed value  $F_{cr}$  (mm/double stroke). In plunge grinding (Fig. 3.1, b) the traverse feed is not active and the grinding wheel has only infeed (mm/rev).

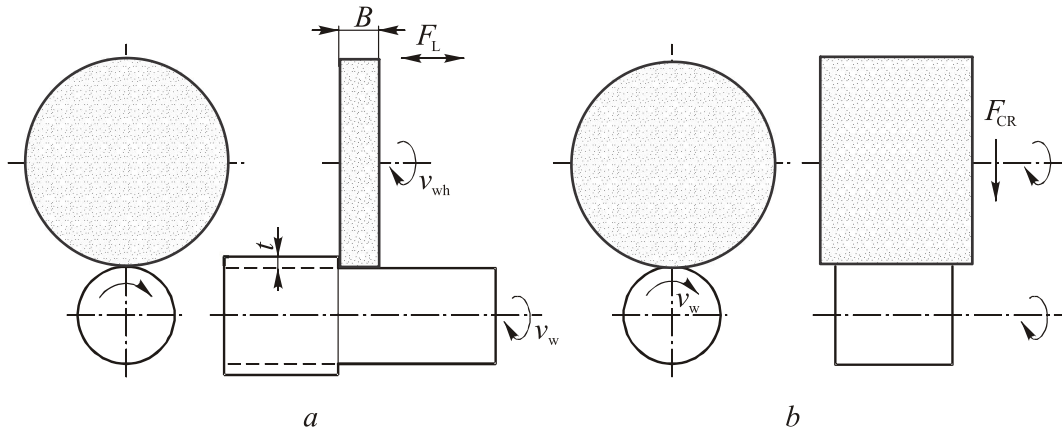


Fig. 3.1 External cylindrical grinding: (a) traverse; (b) plunge

2. In **internal cylindrical grinding** (Fig. 3.2), the workpiece and grinding wheel are rotating about parallel axes, as in external grinding, but the diameter of the grinding wheel is smaller than the hole diameter. Traverse feed is specified the same way as for external grinding. Internal grinding can be performed as the plunge grinding with infeed. Grinding machines are equipped with a special drive for high rotational speeds of the grinding wheel in internal grinding.

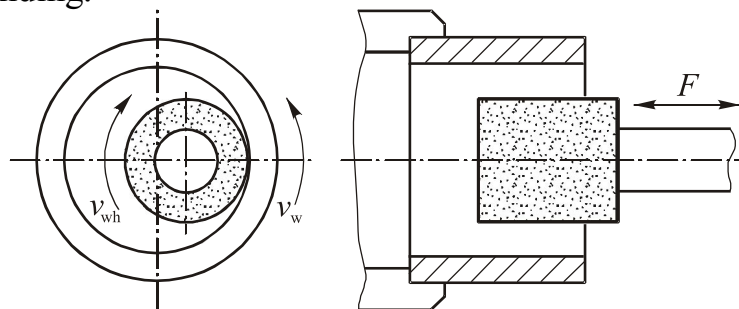


Fig. 3.2 Internal cylindrical grinding

3. **Surface grinding** is used to produce flat surfaces. The kinematics of this process is similar to a milling operation kinematics. Two types of surface grinding are commonly used. Depending on the position of the grinding wheel axis relative to the workpiece surface, the grinding can be performed by the periphery of the grinding wheel (Fig. 3.3, a) or by the face of the grinding wheel (Fig. 9.3, b). The linear reciprocating motion of the workpiece  $F_{work}$  (m/min) is usually executed by the magnetic table of the surface grinding machine, on which the workpiece is fixed. In case of a surface grinding machine equipped with a round table rotating at the speed  $V_{work}$ , a few workpieces can be clamped for continuous grinding.

Other schemes of grinding are also possible.

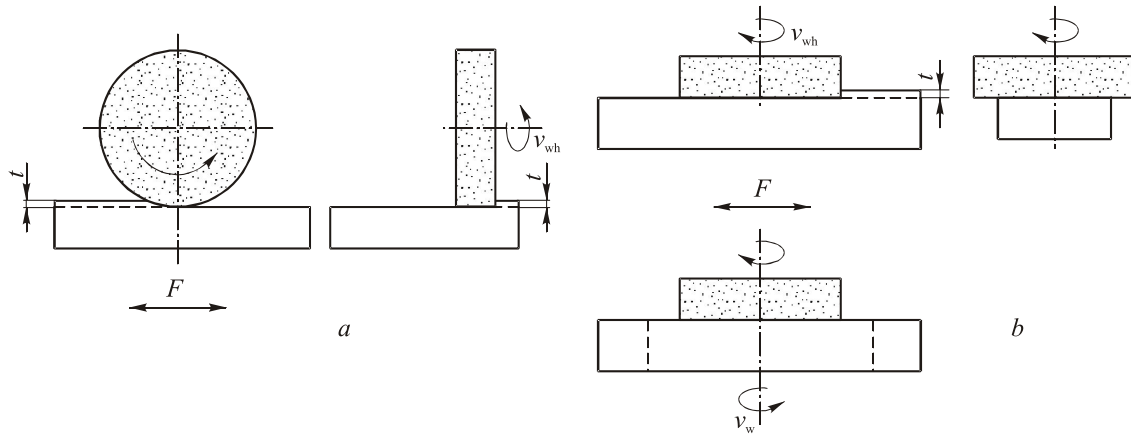


Fig. 3.3 Surface grinding: (a) by wheel periphery; (b) by wheel face

### 3.2 Types of Abrasives

**Abrasive grains** commonly used in grinding wheels are single crystals, poly-crystals and crystal fragments of irregular geometric forms with high hardness, heat stability and durability. Abrasive grains are chemically inert to most of the workpiece materials.

Two types of abrasives are used in grinding wheels: natural and manufactured, with the manufactured abrasives being the most common.

1. *Aluminum oxide or corundum* – crystals of aluminum oxide ( $\text{Al}_2\text{O}_3$ ) are obtained by melting alumina (bauxite) in electric furnaces with subsequent crushing and sorting of grains by size. Depending on the degree of purity aluminum oxide have a different color, structure and properties. Three basic types are available: normal or general purpose, white and monocrystalline alumina. Depending on their properties and application, these in turn are divided into groups with special markings, for example, general purpose aluminum oxide is indicated as 12A ... 16A, and white aluminum oxide is indicated as 22A ... 25A. Here, the higher is the number, the higher is the degree of purity and the higher are the physical and cutting properties.

Heat stability of aluminum oxide is  $1700\text{...}1800^\circ\text{C}$ .

Monocrystalline alumina or monokorund (43A, 44A, 45A) contains up to 99% of aluminum oxide crystals and is manufactured by a special process by melting bauxite with iron sulfide and reducing agent. Monokorund grains are freed from sulfides, undergo enrichment and screening. Monokorund has high cutting ability and is used for machining of difficult-to-machine steels and alloys.

Alloyed aluminum oxides: chromium, titanium, zirconium, which have better cutting properties and high durability are used in recent years.

2. *Silicon carbide (carborundum)* – chemical compound of silicon and carbon (SiC), obtained by melting a mixture of quartz sand, petroleum coke and anthracite in an electric furnace at a high temperature (2100...2200°C). Depending on the degree of purity, the silicon carbides are available of two types: black and green. Green silicon carbide has fewer impurities, thus it has higher cutting capacity and is used for sharpening the carbide cutting tools. Black silicon carbide is used for grinding metals with low tensile strength, such as, for example, cast iron, copper, brass, bronze and aluminum. In general, due to the higher microhardness the cutting properties of silicon carbide are higher compared to corundum, but the heat resistance is slightly lower (1300...1400°C).

3. *Synthetic diamonds* are produced by the synthesis of carbon with a cubic lattice from graphite with a hexagonal lattice at very high pressure (1000...2000 MN/m<sup>2</sup>) and temperature (1500...2500°C). They have a complex diamond-like lattice and the highest hardness. The relatively small crystals, weighing 0.2...0.8 carats and smaller than 1.0 mm are formed in the process. By changing the mode of synthesis, several grades of abrasive powders, differing mainly in mechanical properties, shape and surface roughness, and, consequently, different abrasive ability are produced.

4. *Cubic Boron Nitride or CBN (Borazon etc.)* – artificial superhard material obtained from hexagonal boron nitride ("white" graphite) and catalysts on special presses under pressure of 300...980 MN/m<sup>2</sup> and temperature of about 2000°C. CBN has the same cubic crystal structure as diamond, but a slightly lower hardness. Unlike diamond, CBN is neutral to iron, does not interact with iron chemically and has higher heat stability (up to 1200°C). These properties have made CBN very promising material for the machining of high-strength and high-alloy steels. With the use of crystalline and polycrystalline cubic boron nitride all kinds of tools are produced.

### **3.3 Features of a Grinding Wheel as a Cutting Tool**

Design of the abrasive tools is more complex compared to the cutting tools. Abrasive tools consist of a large number of the cutting elements – abrasive grains held together by a bond.

Abrasive tools are produced in the form of wheels of various sizes and configurations, bars, segments, as well as belts, abrasive papers, powders and pastes.

Specifications of grinding wheels manufactured on a rigid base include: abrasive type, grain size, bonding material, structure and grade of a grinding wheel. For diamond and CBN grinding tools is the concentration of grains.



These characteristics are marked on the working surfaces of tools in the form of labeling. The marking also indicate the operational cutting speed allowed by the strength of the grinding wheel.

Dimensions of the abrasive grains of grinding tools are defined by the **grain size**, which can vary from 200 to 16. Number 200 stands for the very coarse grains with sizes from 2.0 to 2.5 mm, and number 16, respectively – for grain sizes from 0.6 to 0.2 mm. The range of grain size variation corresponds to the size of the screen opening, which the abrasive grains pass.

**Bond** in the grinding wheel may be of inorganic or organic origin. Up to 90% of abrasive tools are made with inorganic vitrified binder consisting of many components: white clay, feldspar, chalk, quartz, liquid glass and etc. Vitrified bond have high moisture resistance and thermal stability, and keeps the shape of a grinding wheel well. However, vitrified bond is fragile and therefore is not suitable for interrupted cutting with shock loading, such as cutting or cutting-off narrow slots.

Organic bonding materials include resinoid (bakelite resine) and rubber bonds that ensure greater strength and elasticity. Organic bonded wheels are used for high grinding speeds and are of thinner thickness.

Diamond and CBN wheels are also produced with metal bonds, obtained by sintering powders of copper and aluminum alloys, or with electro-plated nickel-based bond, which is obtained by galvanic fixing of grains onto a metal wheel in a form of a layer.

**Wheel hardness** or **grade** – is not actually the hardness of the abrasive, it is a value that characterizes the ability of bonding material to hold the grains in a wheel as the grains become dull. Standards implement 12 grades of hardness that vary from soft to medium hard and extremely hard.

The **structure of the wheel** refers to the volume ratio of grains, bond and air gaps (pores) per unit volume of the wheel. There are 13 numbers of structure, combined in three groups: dense or closed-structure (№ 0...4), medium-structure (№ 5...8) and open-structure (№ 9...12). For example, the closed-structure №1 (dense) contents 60% of grains by volume, and the open-structure №12 – only 38%. The rest of the wheel is occupied by bonding material and air gaps, which are necessary to accommodate the chips. The air gaps can also be used to deliver the coolant directly to the cutting area. Highly porous wheels with an open structure, with pore sizes up to 2...3 mm are used for grinding soft and ductile materials.

Another important characteristic of the diamond and CBN wheels is the **concentration** of grains. A 100% concentration is equivalent to 0.88 g (4.4 carats) per 1 cm<sup>3</sup> of the abrasive layer. Diamond and CBN wheels are produced with diamond concentrations from 25 to 250%.

### 3.4 Work of a Single Grain

The cutting process in grinding, unlike the process of cutting with cutting tools, is performed with a large number of abrasive grains, which cutting edges are very small in size and remove very thin chips. This results in massive microcutting that is close to scratching. Therefore, the ground surface is a combination of many scratches.

Grains have irregular shape with rounded corners radius equal to  $8 \dots 12 \mu\text{m}$  (Fig. 3.4). Such form of grains provides dynamic strength and resistance to breakage.

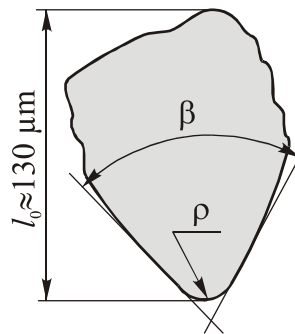


*Fig. 3.4 Shape of a sharp aluminum oxide abrasive grain*

It should be noted that the geometry of the grain depends not only on their shape, but also on the spatial position in the wheel. Depending on the position of the grain relative to the cutting velocity vector, the rake angles of the grain can vary from negative values to positive values (Fig. 3.5, a). Since the rake and clearance angles are of random nature, depending not only on their spatial orientation, but also on the shape of the grains themselves, statistical analysis was performed to determine relative frequency  $m$  for the angles values. The curves of rake and clearance angles distribution show that the value of the relative frequency  $m$  is the greatest for the rake angles equal to  $-75^\circ$ , and for clearance angles equal to  $12^\circ$  (Fig. 3.5, b). Therefore, abrasive grains of the grinding wheels work mostly with large negative rake angles, causing large cutting forces and work hardening of the machined surface. At the same time, only 10% of the total number of abrasive grains is involved in cutting action.

Some of the grains (near 12%) that exert from the wheel periphery do not form chips but rub and plough due to unfavorable orientation and low height of the protrusion, and the remaining 78% of the grains, that are below the periphery and do not cut (Figure 3.5), are revealed and brought to the cutting action only after the dulled grains are removed during or after the self-sharpening or dressing of the wheel.

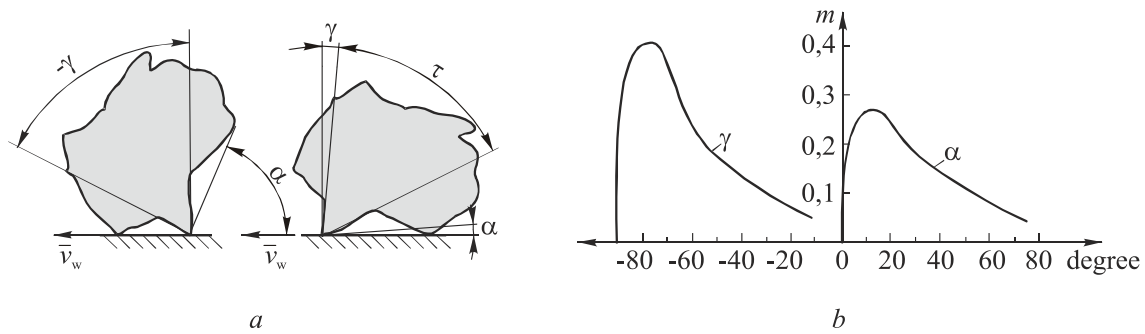


Fig. 3.5 Geometry aspects: (a) geometry affected by the grain orientation in a wheel; (b) relative frequencies  $m$  of the rake and clearance angles

Using custom techniques to orient the grains during the production of grinding wheels it is possible to increase the number of active grains to 45...60%.

The grinding process is performed at high speeds and low depth of cut due to high hardness, heat stability and sharpness of the grains. Grinding can be considered as a process of a mass, very fine high-speed machining. Chips are removed by individual grains in  $10^{-4} \dots 10^{-5}$  s, that is almost instantly (at  $V_{wh}=30$  m/s). The total number of chips, cut in unit time is large thus very high instantaneous temperature may occur, often approaching the melting point of the workpiece material.

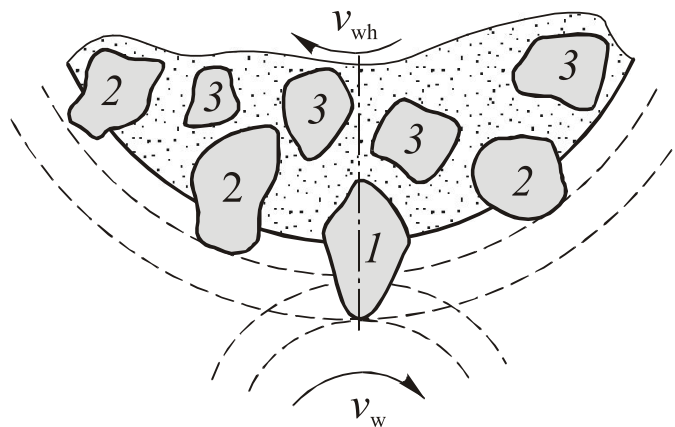


Fig. 3.6 Position of abrasive grains in a wheel: (1) cutting grains; (2) rubbing grains; (3) idle grains

To determine chip thickness in cylindrical external grinding, let's roughly compare a grinding wheel to a milling cutter, which has a large number of teeth randomly located along the periphery. Figure 3.7a schematically shows the "comma"-shaped cross sections of the chips, where the normal distance between the trajectories of the two adjacent grains is the thickness of the uncut chips. The chip thickness is variable, because the feed per grain

$S_{z1} \neq S_{z2} \dots \neq S_{zn}$  is also variable, since the teeth spacing and orientation is not definite. The thickness of uncut chip will be variable, provided that the each successive grain gets into the groove left by the previous grain. However, some of the grains will engage uncut sections of microprofile of the surface and cut the layers in the form of segments (Fig. 3.7, b).

In the real process of grinding, the majority of layers being removed will have different shapes ranging in form between the forms given on Figure 3.7.

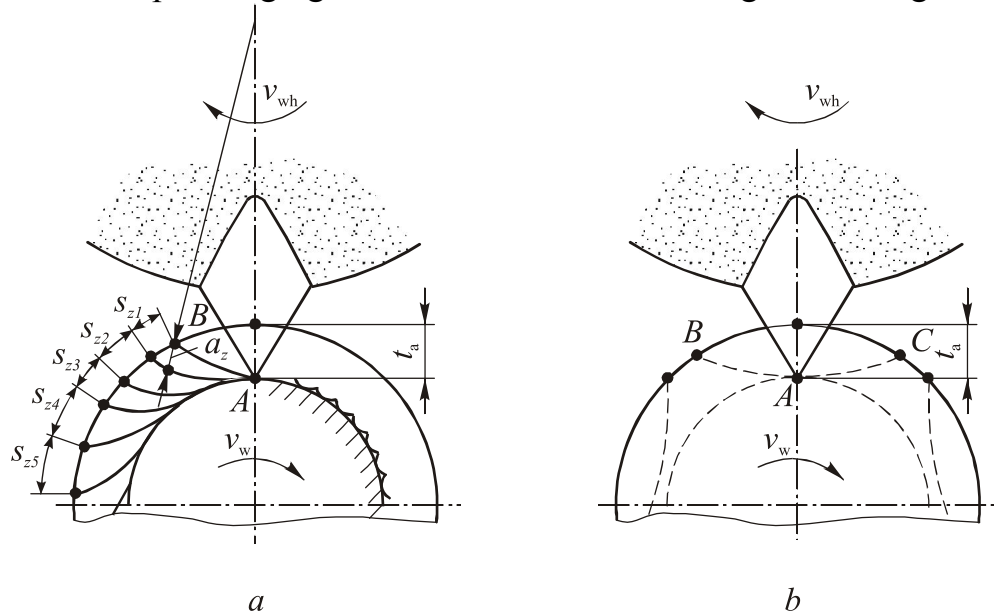


Fig. 3.7 Chip shapes in cylindrical external grinding:  
(a) “comma”-shaped; (b) segmental

The feed per grain that determines the thickness of the chip in severing “comma”-shaped layers is:

$$F_z = \frac{v_w}{60n_{wh}z} = \frac{v_w}{60n_{wh} \frac{\pi d_{wh}}{l_a}} = \frac{v_w}{60v_{wh}} l_a, \quad (3.1)$$

where  $V_w$  – is the workpiece peripheral speed, m/min;  $n_{wh}$  – is rotational speed of the grinding wheel, rps;  $z$  – is the number of grains on the outer perimeter of the wheel;  $l_a$  – is actual grain spacing;  $V_{wh}$  – is the grinding wheel peripheral speed, m/s.

It follows from the equation (3.1) that the feed per grain depends on the  $V_w/V_{wh}$  ratio, and for a given wheel peripheral speed the feed per grain increases with the increasing workpiece peripheral speed.

The theoretical and experimental studies, performed by E.N. Maslov, established generalized formula for determining the average thickness of the

uncut chip being removed by a single abrasive grain for various grinding schemes is as follows:

$$a_z^{\text{mean}} = \frac{v_w}{60v_{wh}} l_a \sqrt{t_a} \sqrt{\frac{1}{d_{wh}} + \frac{\alpha}{d_w}} \cdot \frac{F_l}{B}, \quad (\text{mm}), \quad (3.2)$$

Where  $V_w$  and  $V_{wh}$  – is the speed of the workpiece and the wheel respectively, m/min and m/s;  $l_a$  – is actual grain spacing, mm;  $t_a$  – is the actual depth of cut of a grain, mm;  $F_l$  – is longitudinal table feed, mm/rev;  $B$  – is width (height) of a grinding wheel, mm  $\alpha$  – factor,  $\alpha=1$  – external cylindrical grinding,  $\alpha=(-1)$  – internal grinding ( $d_{wh} < d_w$ ),  $\alpha=0$  – surface grinding.

Minimum thickness of the uncut chip depends on the  $a_z / \rho$  ratio, that is, the sharpness of the grain and the mechanical properties of the workpiece material.

The values of  $t_a$  and  $l_a$  in equation (3.2) are variable, and depend on a number of grinding parameters, including grain size, grain protrusion distribution, degree of grains bluntness, etc. The actual depth of cut of a grain can be represented as:

$$t_a = n \cdot l_a,$$

where  $t$  – is the nominal depth of cut, equal to the infeed;  $n$  – is the number of passes needed to obtain a firm repetitive microprofile on the machined surface.

Usually, depending on the grain size, grain protrusion distribution and the degree of bluntness  $n= 1...12$ . The number of passes is determined experimentally. So, for example, for the grain size 25,  $n$  is equal to 8, and for grain size 80,  $n$  is equal to 12. The actual grain spacing is  $l_a \approx 3.5l_0$ , where  $l_0$  is the most likely average grain size in cross section.

Analysis of the Eq. (3.2) shows that the greatest influence on the  $a_z$  value the speed of workpiece rotation has. When the  $V_{wh}$  is constant, the uncut chip thickness and, consequently, the cutting force increases.

The  $a_z$  increases proportionally with the increase of longitudinal feed. The increase of infeed ( $t_a = F_{cr}$ ) in two times causes  $a_z$  to increase only in  $\sqrt{2} = 1.4$  times.

With the wheel speed increasing, the  $a_z$  decreases, and the  $a_z$  remains unchanged when both the workpiece and wheel speeds increase.

The  $a_z$  value is also affected by the type of grinding. Thus, for example, for cylindrical external and internal grinding, as well as for surface grinding, as it follows from the eq. (3.2), the  $a$  is calculated in the following way:

$$a_{z_{\text{internal}}} : a_{z_{\text{surface}}} : a_{z_{\text{external}}} = \sqrt{\frac{d_w - d_{wh}}{d_{wh} d_w}} : \sqrt{\frac{1}{d_{wh}}} : \sqrt{\frac{d_{wh} - d_w}{d_{wh} d_w}}.$$

Therefore, with other conditions being equal  $a_{z_{\text{ext}}} > a_{z_{\text{surf}}} > a_{z_{\text{int}}}$ . This means that the same wheel will wear faster in external grinding compared to the surface grinding and, especially, internal grinding.

Effect of workpiece and grinding wheel diameters on the thickness of the uncut chip is quite complex. Thus, for example, when the  $V_{wh} = \text{const}$ , the decrease in  $d_{wh}$  has a limited effect on  $a_z$ . But when the  $n_{wh} = \text{const}$ , the decrease in  $d_{wh}$  leads to a dramatic increase of the  $a_z$ , especially when  $d_{wh} \leq 250$  mm, as the  $V_{wh}$  and radicant of the Eq. (3.2) will decrease.

The calculations made by the equation (3.2) show that, depending on the conditions of grinding the medium thickness  $a_z$  can vary significantly, although being a very small value within the range of tenths of a micron to 100 microns (for an infeed).

### 3.5 Phenomenon of Self-sharpening

An important property of grinding tools is the ability to **self-sharpen** in the cutting process, which is in the automatic replacement of blunt grains by new grains. To ensure the normal course of self-sharpening process for all workpiece materials and cutting parameters it is essential to choose the right wheel grade correctly. Here, the harder is the workpiece material and the bigger is the depth of cut and feed rate (which increase load on grains and intensity wear), the softer should be a wheel. The hard wheel in these conditions will become **glazed**, which means that cutting of chips stops and the dull grains start to slide on the work surface. This gives rise to high temperatures, resulting in burn marks and cracks on the ground surface.

### 3.6 Principles for the Selection of a Grinding Wheel

Grinding wheels are characterized by form, dimensions, abrasive material, grain size, bond, hardness, accuracy grade and imbalance. For diamond and CBN wheels the concentration of grains in the working layer is also applied.

**Wheel shapes and size.** The geometrical parameters of grinding wheels are defined by the machine tool intend to use, by form and dimensions of the workpiece surface and the nature of the wheel motions.

*Grinding wheels* (refer to Fig. 3.8 a) are applied when the primary motion is rotational. Therefore, they are different axisymmetric forms.

Straight shape is used for centerless, external and internal cylindrical grinding, surface grinding with the wheel periphery and for cutting tools sharpening. Straight tapered shape (2II) is used for screw thread and gear teeth grinding. Straight shape with one side recessed (IIB) and two sides re-

cessed (ПВД) allow clamping flanges to be placed in the recesses, and thus perform cylindrical grinding combined with face grinding. These wheels are also used as a regulating wheel in centerless grinding.

Straight cup (ЦК) and flaring cup (ЧК) wheels are used for sharpening cutting tools and for surface grinding by the wheel face.

Dish shaped wheels (Т) are used for grinding and fine grinding of the milling cutter faces, gear shaping cutters and other cutting tools.

**Diamond wheels** (Fig. 3.8, b) are available of straight shape, straight cup, flaring cup, dish shape and etc., and are used for grinding and finish grinding of carbide tools, as well as grinding and parting-off of hard-to-machine nonmetallic materials.

**CBN wheels** have the same shapes as diamond wheels. They are applied for grinding of hardened steels ( $HRC \geq 60$ ), finishing sharpening of HSS cutting tools, for fine grinding of threads, as well as for the grinding of heat-resistant and corrosion-resistant steels.

Dimensions of grinding wheels should be as large as possible, as in this case grinding conditions improve and the cost of grinding reduces. The upper limit of the size range is limited by the design and dimensions of a grinder, and, in some cases, by the sizes and shape of the workpiece. For example, the wheel for internal grinding should be no more than 0.7...0.9 of the hole diameter.

**Grinding heads** (Fig. 3.8, c) are small diameter (3...40 mm) grinding wheels. These wheels are glued to a steel shank and are applied for internal grinding and for manual cleaning of workpieces with grinding machines.

**Grinding bricks** (Fig. 3.8, d) are used for benchwork, honing and superfinishing. In the latter cases, the bricks are fixed in a special steel heads.

**Grinding segments** (Fig. 3.8, e) are applied for surface grinding. In this case, the grinding wheel is composed of several segments clamped in a head or cartridge.

**Abrasive papers** – are abrasive tools available on flexible backing (paper, cloth, metal tape) or on a combined backing (paper and cloth) with the layer of bond and abrasive material glued on. Papers are produced in the form of sheets and strips, and are used for hand and machine finishing of parts.

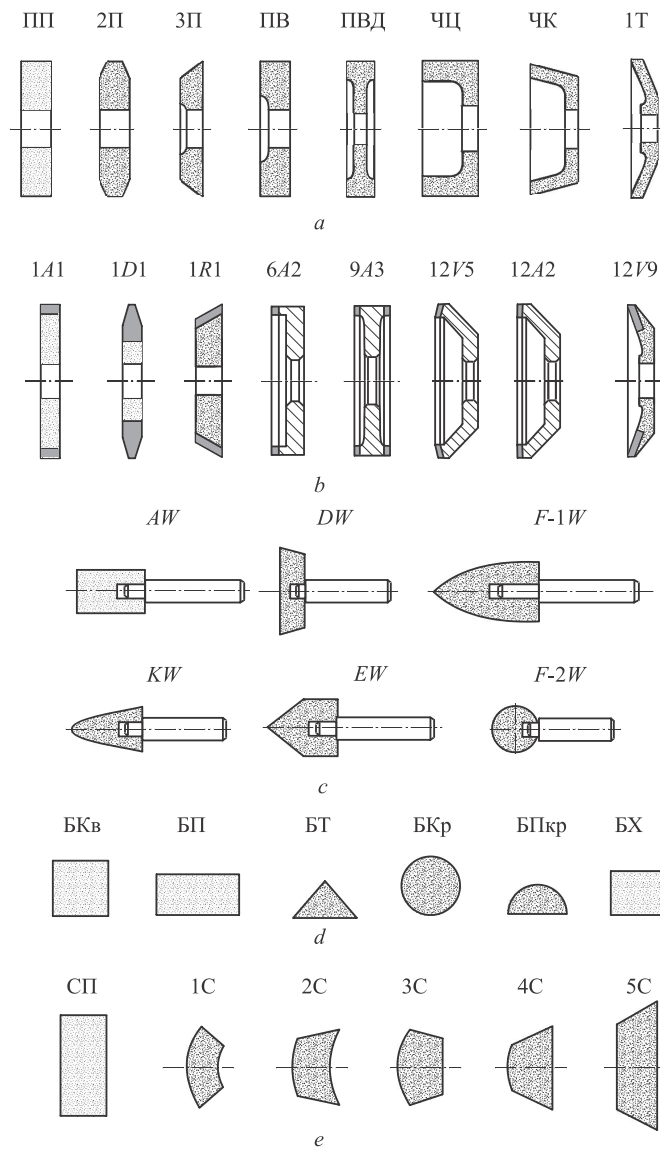


Fig. 3.8 Abrasive tools: (a) grinding wheels; (b) diamond and CBN wheels; (c) grinding heads; (d) grinding bricks; (e) grinding segments

### 3.7 Grinding Wheel Life

The most typical kinds of grinding wheel wear are: 1) rounding of the protruding grains tops and their splitting with increasing load; 2) pulling out of grains from the bonding material and consequent self-sharpening; 3) abrasion of the bonding material in the surface layer of the wheel; 4) wheel glazing by chips and wear products.

All kinds of wear typical for cutting tools: abrasive, adhesive, diffusion and chemical can be found in abrasion wear of grains. The wear rate of grains and bonding material is affected by grinding parameters and temperature,



which reaches high values (1000...1600°C). However, with the temperature increasing, the microhardness of abrasive reduces. For example, at 1200°C micro-hardness of SiC grains is reduced by 3 times compared to the microhardness measured at room temperature. The strength of grains bonding weakens as well.

During the adhesive wear abrasive material seizure with the workpiece material, which leads to the destruction of grain by breaking them apart.

At high temperatures (over 900...1000°C) diffusion wear of abrasive grains becomes possible. It was established, for example, that during the titanium alloys grinding at high temperatures the chemical compounds of titanium with carbon, silicon and aluminum are produced. This leads to a sharp increase in the wear rate of the wheels. To reduce the reactivity of titanium, the special coolants that not only increase heat dissipation, but also form a protective film, are applied. The greater effect is achieved when the coolant is supplied through the pores of the grinding wheel.

It is known that almost all the mechanical power of grinding, as with any type of cutting, is converted into heat and is distributed between the workpiece, wheel, chips and coolant. Only a small part of the heat goes into radiation.

By calculations and experiments it was found that, depending on the grinding parameters the 60...80% of the heat goes to the workpiece, 1...30% – to the chips, and 10...13% – to the grinding wheel.

The types of temperature found in grinding are as follows: 1) instantaneous temperature, formed immediately in the microcutting area, this one is high and short-duration; 2) contact temperature, found in the workpiece-wheel interface; 3) average temperature, found on the ground surface of the workpiece.

Experimentally measure the instantaneous temperature at high cutting speeds is rather difficult. However, it can be determined by indirect means, for example, by structural transformations in thin surface layers of the ground surface. In grinding very hard materials (such as hardened steels) the instantaneous temperature is in the range from 1000°C to the melting point of the material. This is demonstrated by the flow of sparks flying out of the cutting area, even with abundant cooling.

Contact temperature is much lower than instantaneous temperature (especially when using a water-based emulsion) due to the intense heat removal from the wheel-workpiece interface to the workpiece, which usually has large mass compared to a very small volume of the heated layer. Contact temperature affects the residual stresses value and determines the probability of burn marks on the surface layers of the workpiece. Depending on the grinding

conditions and thermal conductivity of the workpiece material the contact temperature is in the range of 200...1000°C.

Average temperature of the workpiece varies between 20...350°C and influences on accuracy, as it causes thermal deformations of the workpiece.

The all three types of temperature in diamond grinding are much lower than in abrasive grinding, because of the high hardness, high thermal conductivity and a low coefficient of friction of the diamond grains. This also applies to the CBN wheels, which, although slightly inferior to diamond in hardness, but due to the absence of chemical affinity to iron, with other things being equal, causes temperatures of 1.5...2 times smaller than in diamond grinding.

Coolant has great impact on the contact temperature, and, therefore, on the wheel wear rate. For example, the application of a 3% aqueous solution of baking soda as a coolant, allows to reduce contact temperature in 1.5...2.0 times compared to the dry grinding. The coolant delivery through the pores of a wheel provides a particularly high effect of preventing burn marks, in this case special high-porous wheels are used.

As the abrasive grains become dull the grinding wheel surfaces gradually lose their shape and size. The most intense wear areas are angular sections and protruding parts of the wheels. For example, straight shaped wheels (type 1), used in external cylindrical grinding and surface grinding, wear unevenly across the width. This can lead to the form errors and dimension deviations of the part, which is especially vital in grinding of profiled surfaces.

To restore the wheel cutting ability after glazing or wear of abrasive grains, and to reshape the working surface of a wheel, dressing processes with the help of dressing sticks, carbide wheels and diamond dressing tools are carried out.

CBN grinding wheels life is about 50 times higher than the life of aluminum oxide wheels in grinding of steels. Moreover, CBN wheels with vitrified bond do not glaze and don't require dressing.

The experimental investigations of grinding wheels life provided generalized equations for determining tool life. For example, the wheel life for a cylindrical external traverse grinding is calculated by the following equation:

$$T = \frac{C_T d_w^{0,6}}{v_w^{1,8} t^{1,1} F^{1,8}}, \quad (3.3)$$

where  $C_T$  – is the workpiece material coefficient,  $C_T=2260$  for hardened steel,  $C_T=2550$  for mild steel,  $C_T=2870$  for cast iron.

The equation (3.3) is obtained for the case of grinding with aluminum oxide wheels at 60 m/s. It is found from the equation that the wheel life is affected by the grain load, which depends on dimensions of the layer being re-

moved. It should be remembered that the formula (3.3) does not take into account such characteristics of the wheel, as grain size, wheel grade and structure, and therefore this equation is inaccurate.

The grinding wheels wear criteria are external and indirect signs of decreasing cutting ability, increasing grinding power, vibration, noise, or appearance of chatter marks on the machined surface and etc.

The glazing of a wheel leads to great friction forces between the wheel and the workpiece surface, dramatic decrease in metal removal rate and increase in contact temperature, which may cause formation of cracks and structural change in surface layer. Here the process of self-sharpening of the wheel fails and the grinding process is stopped.

With wrong wheel hardness selected its intense wear and loss of form, so called "shedding", is observed, here wheel prematurely loses sharp grains. The problem of shedding is solved by the proper selection of the grinding parameters, wheel grade, cutting fluid and methods of its supply, as well as by the use of segmented wheels with discrete work surface, etc.

### **3.8 Grinding Wheels, Specification and Application**

The composition of grinding wheels is described with the help of marking, which is applied to a wheel face with waterproof paint.

Example of abrasive wheel marking, according to Russian standard, is given below.

PP 500×50×305 24A 10-P C2 7 K5 35m/s A 1 grade GOST 2424-83

PP – is the shape of the wheel; 500 × 50 × 305 – OD×height×hole diameter; 24A – abrasive; 10-P – grain size; C2 – hardness; 7 – number of structure; K5 – bonding material; 35m/s – working circumferential speed; A – wheel accuracy grade; 1 class – is the imbalance class.

Example of diamond grinding wheel marking:

1 A 1300×40×76×5 AC4 100/80 100 BP2 2720-0139 GOST 16167-80

1 – is the wheel shape; A – is the form of the diamond layer cross-section; 1 – is diamond layer location on the wheel; 300×40×76×5 – is OD×height×hole diameter×diamond layer thickness; AC4 – is diamond powder grade; 100/80 – is diamond grain size, 100 – is diamond concentration; BP2 – bond; 2720-0139 – is the wheel size code.

### 3.9 The Procedure of Selection and Calculation of Cutting Parameters and Required Power in Grinding

Cutting parameters for grinding are selected in the following order:

1. Depending on the grinding process conditions, required accuracy and surface finish the characteristics of a grinding wheel, such as size, shape, grain size, bond and etc. are selected.
2. The depth of cut, infeed, traverse feed and speed of workpiece rotation are selected.

Allowance for grinding depends on the type of grinding. Usually the allowance is removed in 3 steps: 1) preliminary (0.5...0.6 of allowance is removed); 2) finishing (0.30...0.35 of allowance); 3) final (0.05...0.10 of allowance). To improve surface finish, the final step is often accomplished with sparking-out, that is a few additional passes with zero infeed.

For example, for a preliminary step of the cylindrical external grinding it is recommend to assign the allowance up to 1 mm, traverse feed equal to 10...30 m/min, infeed equal to 0.01...0.025 mm per double pass, and for finish step: allowance equal to 0.05...0.20 mm, traverse feed equal to 5 ... 20 m/min, infeed equal to 0.005...0.02 mm per double pass.

To maximize the performance the feed rate and workpiece peripheral speed are assigned small with respect to the surface finish and required accuracy.

3. Next, the cutting speed, which relates to the wheel peripheral speed, is assigned in m/s. Here, the influence of the wheel speed on surface finish, accuracy, grain load  $a_z$  (Eq. (3.2)) is taken into account. The wheel speed shouldn't exceed the maximum permissible speed, which is labeled on the wheel. So, for example, the maximum permissible speed for vitrified aluminum oxide wheels is equal to 20...35 m/s, for high-speed grinding wheels it is 40 m/s, and for the cut-off wheels with rubber bond it is equal to 60 m/s.

When selecting the cutting speed, it should be noted that with the wheel peripheral speed increasing the surface finish improves, cutting temperature increases and danger of burn marks arises. To maintain the load per grain constant the workpiece speed should be increased in proportion to the wheel speed. This provides the increasing material removal rate in cylindrical grinding  $w = \pi \cdot d_w \cdot n_w \cdot t \cdot F$ , mm<sup>3</sup>/min.

4. Then the grinding parameters are corrected in accordance with the grinder kinematics parameters.
5. Then the cutting force components  $P_z$  and  $P_y$  as well as power consumption are calculated using the equations (3.4) and (3.5), which are given below.

Empirical equation for calculation of power consumption in external cylindrical grinding is:

$$Ne = 0,208(v_w F_{\text{traverse}} F_{\text{cross}})^{0,7} d_{\text{wh}}^{0,25} B^{0,25} K_1 K_2, \quad (3.4)$$

where  $K_1$  – is the coefficient for the wheel grade,  $K_1=0.9$  (soft wheel with... M2...M3 hardness),  $K_1=1.58$  (superhard wheels with T1...CT3 hardness);  $K_2$  – workpiece material coefficient,  $K_2=0.9$  for cast-iron,  $K_2=1$  for non-hardened steels,  $K_2=1.1$  for hardened steels,  $K_2=1.2$  for heat-resistant steels.

Using the equation (3.4), the equation for the calculation of the tangential component of the cutting force can be obtained. For example, for an external cylindrical grinding with aluminum oxide wheel of 500 mm in diameter, width  $B= 40$  mm and a wheel speed  $V_w= 30$  m/s:

$$P_z = C_{Pz} v_w^{0,7} F_{\text{traverse}}^{0,7} F_{\text{cross}}^{0,6} K_1 K_2. \quad (3.5)$$

## 4. Design and Calculation of Cutters and Broaches

This chapter is devoted to the aspects of design and calculation of turning cutters and broaches.

The first part deals with cutters of various constructions, including special-design form cutters. Special features of indexable cutters with insets made of sintered carbides, ceramic, diamond and CBN are also examined.

Design and calculation of internal and external broaches, broaching patterns and applications are covered in the second section of the chapter.

### 4.1 Lathe Cutters

The sections below are devoted to design and construction of cutters.

#### 4.1.1 Constructions of turning cutters

Turning cutters are the most common of all types of cutting tools. They are designed for turning outer surfaces, facing, threading, grooving, cutoff, boring, etc.

Facing cutters (Fig. 4.1, a, b) are made with curved and straight holders.

Boring cutters (Fig. 4.1, c, d) are used for enlarging through and blind holes and cutting internal grooves.

Cut-off cutters (Fig. 4.1, e) are used for cutting outer grooves and face grooves, as well as for parting operations.

Since the operation conditions are heavy (considerable overhang, difficult conditions for chip formation, cutter low rigidity, low chatter stability) cutting cutters are often made of high speed steel. Major cutting edge is usually positioned at an angle  $\varphi=90^\circ$  and two minor cutting edges are at angles  $\varphi_1=1^\circ30' \dots 3^\circ$ .

To increase the rigidity of the cutter point it is usually thickened, and to eliminate the tearing off of brazed carbide insert the cutting edge is positioned below the axis of rotation by 0.5...1.0 mm.

Rake angle  $\gamma$  has a big impact on the chatter stability of the cutter, which decreases with the rake decreasing. Thus, it is recommended to sharpen the angle  $\gamma = 15 \dots 20^\circ$  with reinforcing chamfer with width  $f=0.2 \dots 0.3$  mm and an angle  $\gamma_p=0 \dots -5^\circ$ , clearance angle  $\alpha=10 \dots 12^\circ$ .

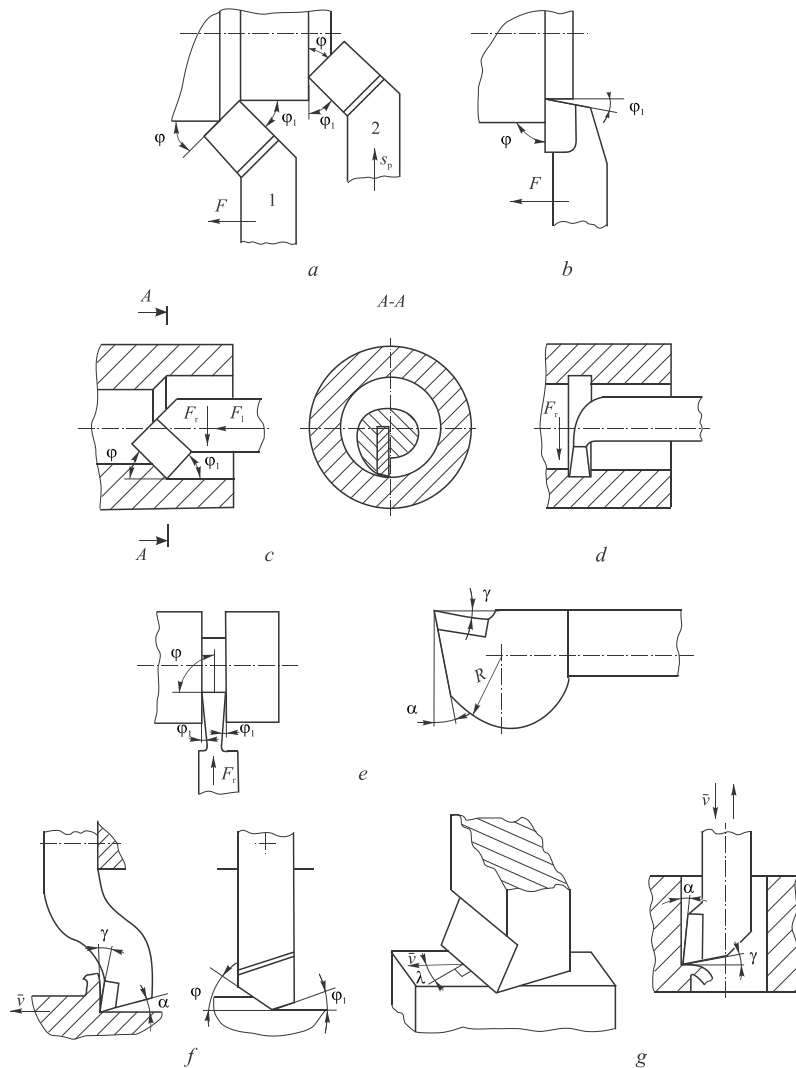


Fig. 4.1 Cutters: (a) and (b) turning and facing; (c) boring; (d) internal grooving; (e) cut-off; (f) planing; (g) slotting

**Planing and slotting cutters** (Fig. 4.1, f, g) are subjected to shock loading during interrupted-cutting. Due to overhung mounting, the holders of these cutters are subjected to elastic deformation and chatter. The cutting speeds are limited due to large inertial masses and larger chip cross-sections compared to turning. For these reasons, the cutting conditions are unfavorable for the use of carbide inserts. Therefore, most of these cutters are manufactured from high-speed steels.

To prevent the indentation of the planer cutter flank into the machined surface of the workpiece due to elastic deformation of the cutter, face of the cutter must be positioned in the same plane as the cutter base, thus the holder is of a curved shape.

Figure 4.1, e shows geometric parameters of planning cutters in non-free and free cutting (no auxiliary edges), and Figure 4.1, g shows  $\gamma$  and  $\alpha$  angles for slotting cutters.

**Carbide-inserted cutters** are cutters equipped with sintered carbide tips or inserts. These cutters provide high performance and are the most widespread in practice.

The inserts can be held in tool holder by brazing, soldering, welding or mechanically. Solid carbide cutting tools are made only of small sizes.

Brazing or soldering of standard carbide inserts of various shapes provides compact sizes of cutters. The cutters after sharpening have optimal values of geometric parameters and have considerable number of sharpening permitted.

However, brazing give rise to internal thermal stresses in the carbide-holder interface, which is due to big difference (approximately 2-fold) between the linear expansion coefficients of carbide and steel holder. Cooling that follows soldering leads to the formation of micro-cracks in the insert, which are revealed during grinding or cutting process. Micro cracks cause chipping and even breakage of inserts. The stresses caused by soldering can be eliminated by mechanical clamping of the indexable inserts. The blunt cutting edges are changed by indexing the insert to the next cutting edge position, thus making the toolchange quick and eliminating the process of re-grinding.

#### 4.1.2 Cutters with indexable inserts

Indexable cutters compared to brazed ones have the following advantages:

- 1) high strength, reliability and durability;
- 2) less cost of tool change and disposal;
- 3) less downtime for the tool replacement and adjustment of the tool size, which is particularly important for the operation of modern CNC machine tools and flexible manufacturing systems;
- 4) improved conditions for applying wear-resistant coatings, which significantly (up to 4...5 times) increase insert hardness and hence the performance of the cutting process;
- 5) limited waste of highly deficit materials (tungsten, cobalt, tantalum, etc.) due to higher recycling.

Disadvantages of the indexable cutters include:

- 1) high cost, due to high accuracy, and therefore, high cost of manufacture of inserts and of the tools in general;



- 2) the increased size of the tool body to contain the elements of fastening plates;
- 3) non-optimal geometry of the cutting tool due to the definite shape of inserts and conditions of clamping.

Inserts are differed by the number of cutting edges and shape. Some of the types are shown in Fig. 4.2, a.

The geometrical parameters of indexable tools are determined by the insert geometry in statics and are corrected by the insert position in the tool holder, with respect to kinematics of the machine tool and cutting conditions.

According to geometry, indexable inserts are divided to: a) negative ( $\gamma=0^\circ$ ,  $\alpha = 0^\circ$ ); b) positive ( $\gamma=0^\circ$ ,  $\alpha > 0^\circ$ ); c) negative-positive ( $\gamma>0^\circ$ ,  $\alpha = 0^\circ$ ) (Fig. 4.2, b).

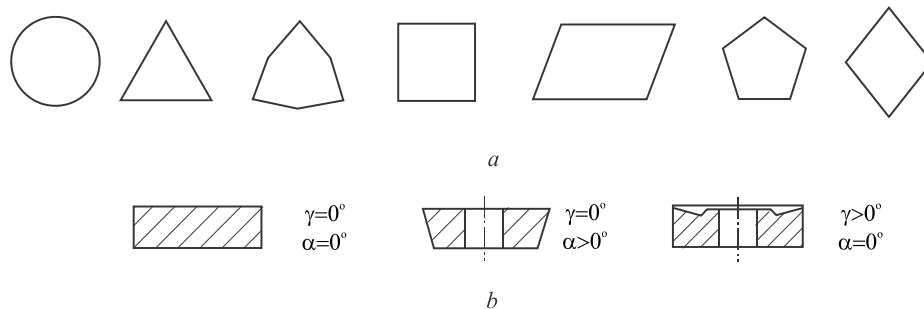
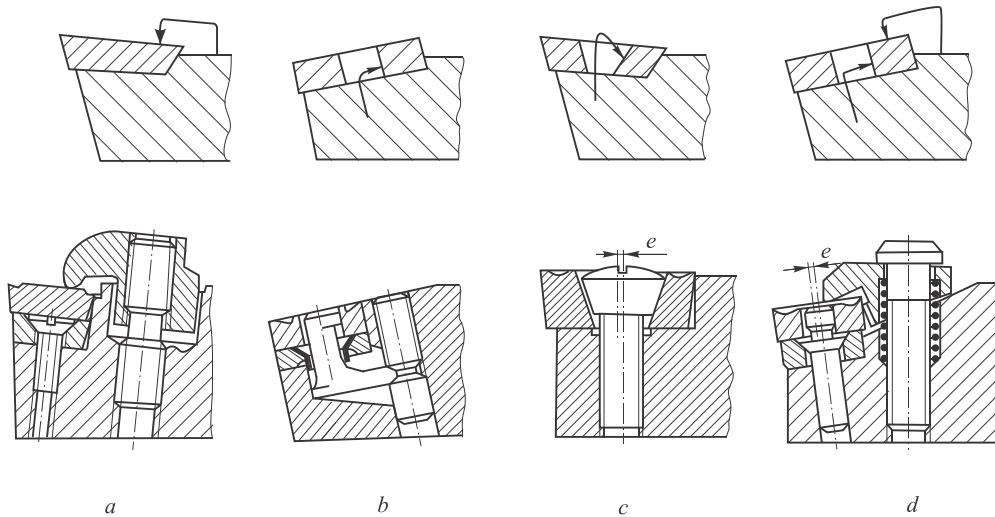


Fig. 4.2 Indexable carbide inserts: (a) inserts shapes; (b) geometric parameters (negative, positive, negative-positive)

Clearance angle of the negative and negative-positive inserts is created by their inclination in a tool holder. Thus the rake angle of negative inserts become negative, i.e.  $-\gamma=\alpha$ , and for negative-positive inserts the rake angle  $\gamma$  is reduced by the clearance angle value.

There are a variety of clamping methods for indexable inserts. For the purpose of convenience some inserts are made with mounting holes. The analysis of numerous methods of insert clamping allowed to bring them to the following scheme (for ISO): a) top clamp; b) center cam; c) a screw with a conical head; d) a center pin and top clamp. Constructional examples of these methods are shown in Fig. 4.3.

Inserts with a hole are the most widely used. This ensures free chip flow on the rake surface and provides significantly smaller sizes of clamping elements that are placed in the holder.



*Fig. 4.3 Indexable insert clamping: (a) top clamp; (b) center cam; (c) conical head screw; (d) center pin and clamp*

Cutters with inserts made of ceramic and synthetic superhard materials are of high performance, precision and tool life due to high hardness, wear-resistance and heat stability. Their disadvantage is the low strength of the cutting wedge, which limits their application. They exhibit the greatest performance in finish turning of steel, especially hardened, cast irons with different hardness and even carbides with cobalt content above 25%. In this case, the machining should be carried out on high-precision, rigid, high-speed and powerful CNC machines.

As for ceramic indexable inserts, they are available of various sizes and shapes, such as round, square, triangular, diamond etc. Negative ceramic plates are used with the same holders as carbide inserts with top clamp (Fig. 4.3, a).

The group of super-hard materials include diamonds (natural and synthetic) and composites based on polycrystalline cubic boron nitride (PCBN).

Since diamonds are very small in size, they are usually held by soldering or mechanical clamping. Diamonds can be brazed either directly to the tool-holder (Fig. 4.4, b), or with the use of intermediate tips (Fig. 4.4, c). The latter version the tip is pressed and sintered together with the diamond by powder metallurgy. Mechanical clamping is shown in Fig. 2.6, e.

The geometrical parameters of diamond tools:  $\gamma=0\dots-5^\circ$ ,  $\alpha=8\dots12^\circ$ ,  $\varphi=15\dots45^\circ$ . The cutter nose is rounded with  $r=0.2\dots0.8$  mm or with multiple lands (facets) (Fig. 4.4, e). The cutting edge rounding radius measured in the section normal to the cutting edge has values  $\rho < 1$   $\mu\text{m}$ . Due to this fact the diamond turning can reduce surface finish to  $R_a 0.08\dots0.32$   $\mu\text{m}$  and raise the accuracy to IT 5...7.

The diamond tool life in turning and boring non-ferrous metals, plastics and composite materials is much higher than the carbide cutting tools life. Diamond cutters can machine over 200...300 h without additional size adjustment and tool change, which is especially important for automated production. Diamonds weighing 0.5...0.6 carats allow 6...10 regrinding.

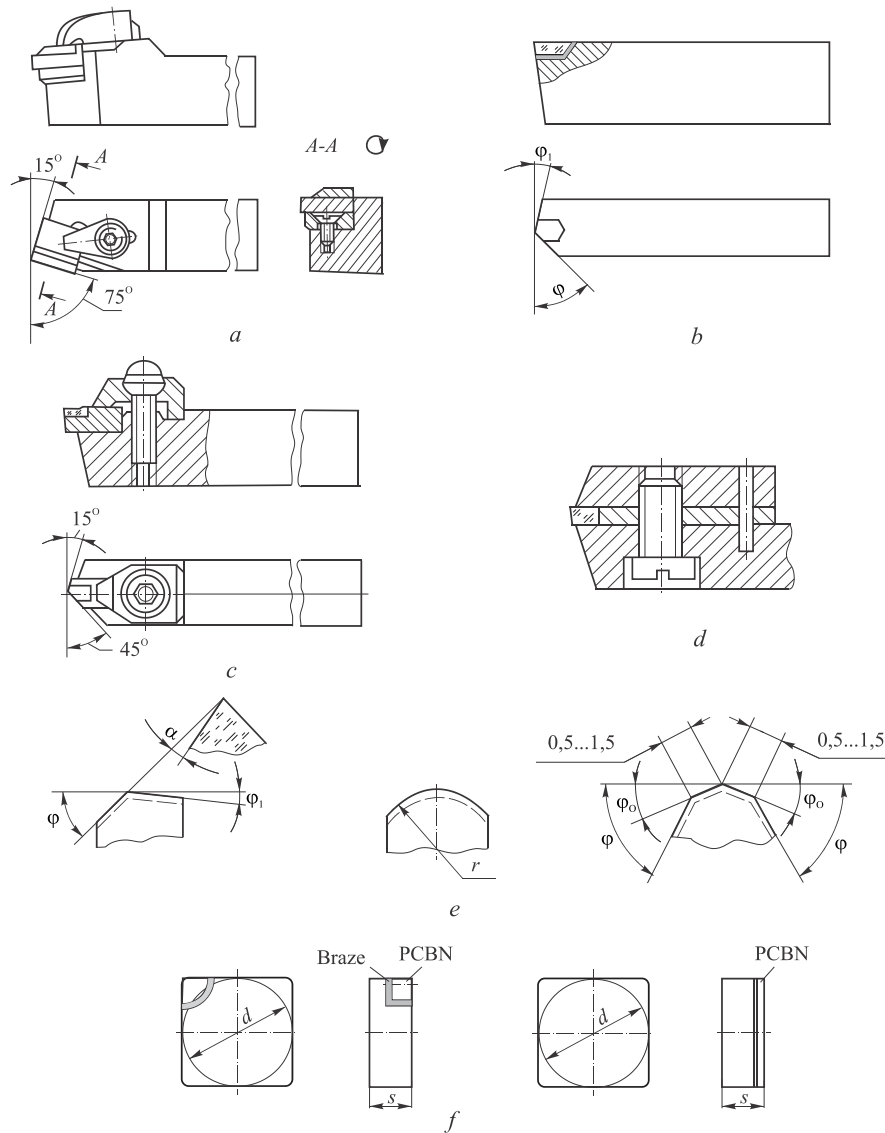


*Fig. 4.4 Indexable cutters: (a) mechanical clamping of ceramic inserts; (b) brazed diamond; (c) tipped diamond; (d) mechanical clamping of a diamond crystal; (e) diamond cutting edge shapes (linear, round, faceted); (f) – inserts with brazed super-hard material*

In turning of parts made of hardened carbon steels, stainless and heat resistant steels and alloys as well as high-strength cast irons the cutters equipped with CBN are used. Currently, triangular, round, square and diamond shaped PCBN inserts are available. The inscribed circle diameter of the

inserts  $d=4\text{...}12.7$  mm, thickness is  $3\text{...}5$  mm ( $\gamma=0$ ,  $\alpha=0\text{...}11^\circ$ ). PCBN inserts are held by a top clamp.

In recent years, two-layered inserts, with PCBN layer applied to the carbide substrate, or with PCBN tipped in the carbide insert corners are applied (Fig.2.6, e). These inserts are larger and can be mechanically clamped to the holders.

#### 4.1.3 Form cutters

Form cutters are applied for cutting of circular parts with profiled external or internal surfaces. The form cutters are usually used in automatic machines and turret machines in medium run production or mass production. Calibrated rolled bars are most often used as blanks for the form cutting.

Compared with other types of cutters, the form cutters have the following advantages: 1) identity of the part shapes and high dimensional accuracy independent of the qualification of the worker; 2) high productivity due to great length of the active cutting edge; 3) large number of allowable regrindings; 4) simple regrinding along the face surface; 5) do not require time-consuming set-up and configuration of the machine tools.

The disadvantages of form cutters include: 1) complicated manufacture and high cost; 2) special design, as they are suitable for the manufacture of parts only of the specified profile; 3) large radial forces caused by radial feed, result in chatter and elastic deformation of non-rigid workpieces, thus requiring feed rate reduction, which in its turn decrease the productivity; 4) working rake and clearance angles of the form cutters vary considerably along the cutting edges from the optimal values.

The main types of form cutters are radial (Fig. 4.5, a), circular (Fig. 4.5, b), radial prismatic (Fig. 4.5, c), tangential prismatic (Fig. 4.5, d). The **circular** and **prismatic cutters**, working with radial feed, are the most common of all the other types of form cutters.

**Radial cutters** are similar to prismatic, but allow a smaller number of regrindings. They are mainly used for relieving milling cutters, as well as for threading. These cutters are clamped in a machine tool post the same way as common turning tools.

**Tangential prismatic cutters** can handle parts of low stiffness or rigidity, but require special machine tools and thus, are rarely used in practice. Another disadvantage of this type is the variability of the rake and clearance angles during stock removal.

Analysis of radially fed circular and prismatic cutters design shows that the circular cutters are easier to manufacture and thus, can be made of higher

precision. However, the number of regrindings and mounting rigidity is limited, since the cutter bore diameter depends on the outer diameter of the cutter. The latter is recommended to assign of smaller than 100 mm in diameter, since the quality of high-speed steel used for the manufacture of cutters of such size is deteriorated. Prismatic cutters have greater stiffness and clamped with help of dovetail shank, they have a large number of permissible regrinding and, as it will be shown below, provide higher accuracy of machining.

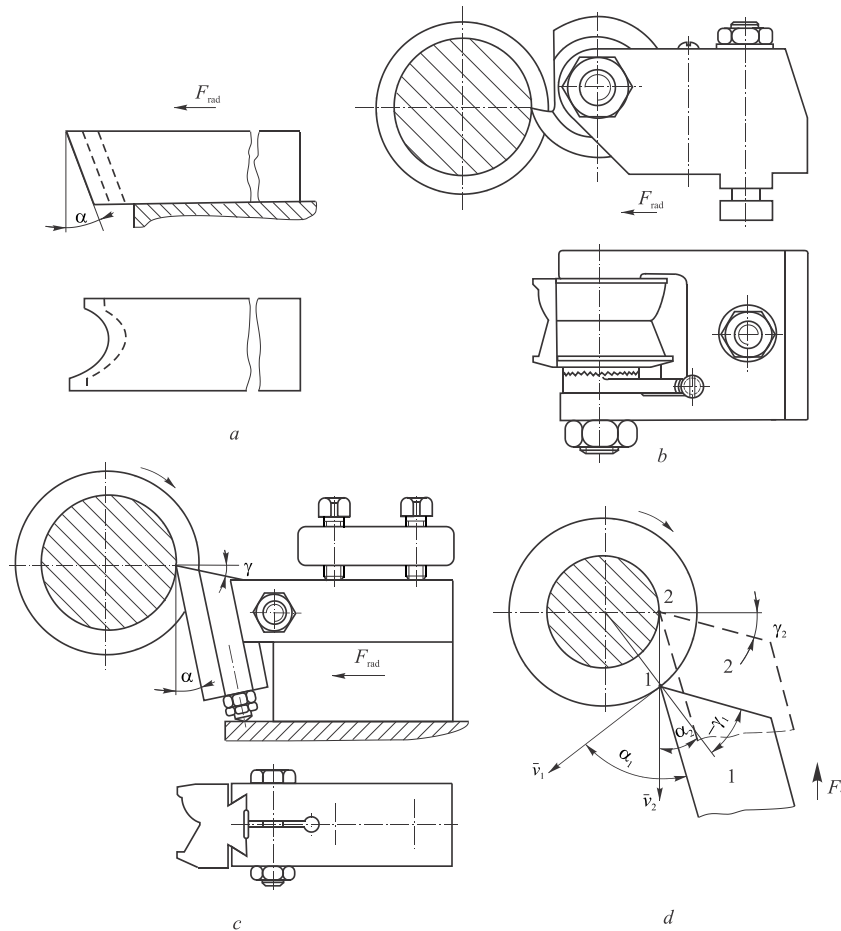


*Fig. 4.5 Form cutters:  
(a) radial; (b) circular; (c) prismatic; (d) tangential prismatic*

For cutting internal form surfaces only circular shank-type form cutters are used.

The specific feature of the form cutters working with radial feed is variable values of rake and clearance angles along the cutting edge.

The clearance angle  $\alpha$  of the circular form cutters is created by positioning the center of the tool  $O_C$  above the center of the workpiece  $O_W$  by the height  $h$ , and the rake angle  $\gamma$  is created by grinding the rake surface at the

distance  $H$  from the center  $O_C$  (Fig. 4.6). In the example the points located on the outer diameter of the cutter (points 1 and 3) lie on the center line of a machine:

$$\sin \alpha = h / R, \quad \sin(\alpha + \gamma) = \sin \psi = H / R,$$

where  $R$  – is the radius of the cutter outer diameter.

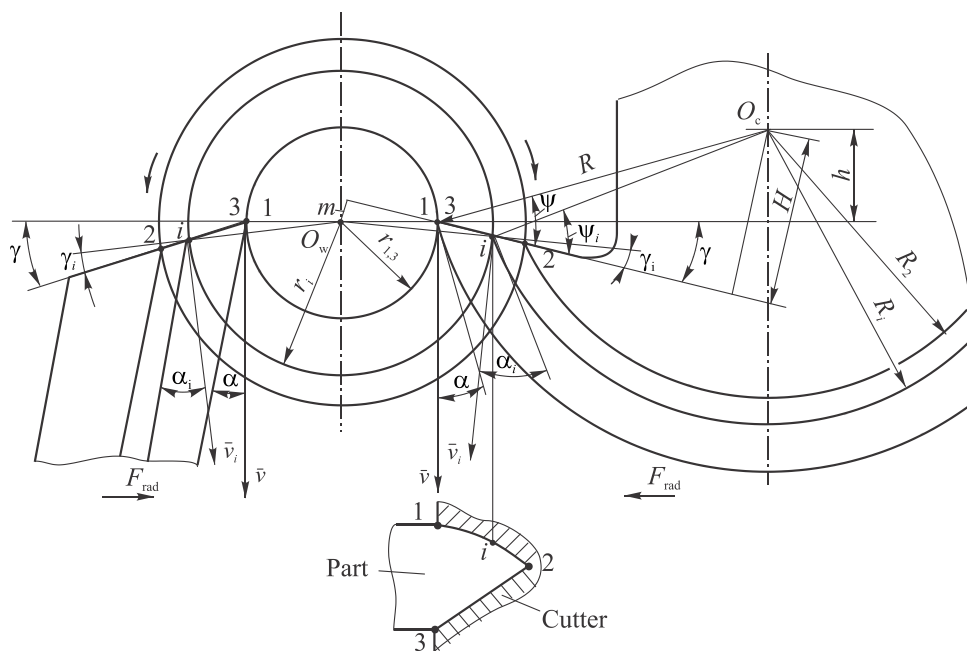


Fig. 4.6 Geometric parameters of a circular (right) and a prismatic (left) form cutters with the feed directed radially

At other points of the cutting edge the angles  $\alpha$  and  $\gamma$ , measured in a section perpendicular to the axis of the cutter, depend on the position of the reference planes (reference plane and cutting edge plane) and tangents to the face and flank surfaces of the cutter. Tangent to the flank surface drawn at different points along the cutting edge – is a normal to the radius, drawn from the cutter center  $O_C$ .

For the calculation of rake angle at any  $i^{\text{th}}$  point of the cutting edge of the cutter it is required to drop a perpendicular  $m$  from the workpiece center  $O_W$  to the continuation of the face line, having this done, it will be found that:

$$m = r_1 \sin \gamma = r_i \sin \gamma_i, \quad \text{i.e.} \quad \sin \gamma_i = \frac{r_i}{r_1} \sin \gamma, \quad (4.1)$$

where  $r_i, r_1$  – are radii of the part profile points.

Position of the prismatic cutter during the cutting process is shown on the left side of Fig. 4.6. During the manufacture of these cutters the face is cut at an angle  $\gamma + \alpha$ , and the actual clearance angle  $\alpha$  in the working position

is created by tilting the tool relative to the part. The Equation (4.1), obtained for a circular cutter, is valid for prismatic cutter as well. Clearance angles ( $\alpha_N$ ) on inclined cutting edges are generally measured in sections normal to these edges.

To avoid rubbing of cutter side flanks against the surface of the workpiece the cutting edges that perpendicular to the axis of the workpiece are either undercut at an angle  $\varphi_1=1^\circ30' \dots 3^\circ$ , or cut away with only the narrow ribbon of width  $f=0.5 \dots 1.0$  mm left (Fig. 4.7, b). It is also possible to manufacture cutters with cutting profile inclined at an angle relative to the axis of the workpiece (Fig. 4.7, c), in order to create more desirable clearance angles on such cutting edges.

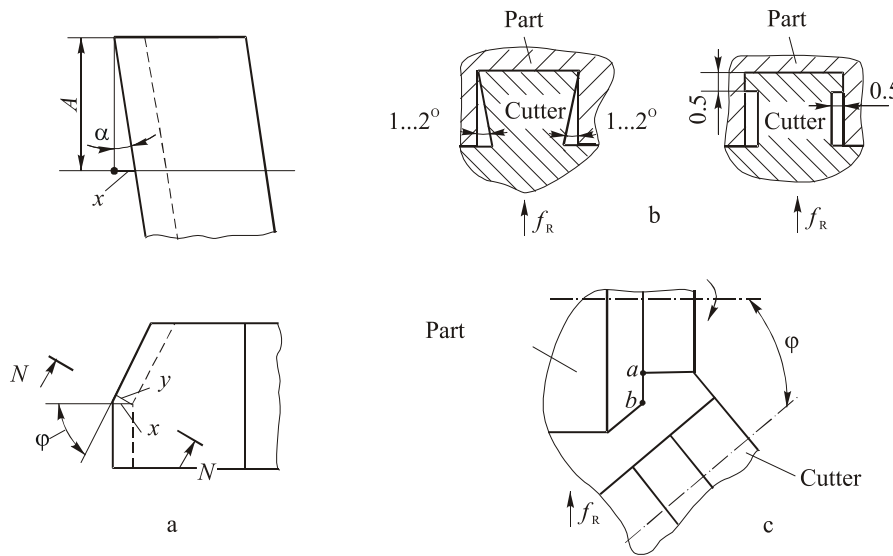


Fig. 4.7 Elements of the form cutters: (a) clearance angles on inclined cutting edges; (b) undercut on the cutting edges perpendicular to the workpiece axis; (c) cutter with inclined profile

**Profiling of form cutters** (analytical calculation of the profile) is necessary for the manufacture and design of cutting tools of the second order, as well as templates and counter-templates, used to check profiles of cutters and templates respectively.

Circular cutters are calculated in the radial (axial) section, and prismatic cutters are calculated in a section normal to the flank surface.

Because of the variable angles  $\alpha$  and  $\gamma$  the depth (height) of the cutter profile points in these sections does not match the profile depth of the workpiece in its axial section. Calculations consist in determining the heights of the profile points, measured from the reference point, for which the highest profile point (cutter tip) is chosen. Axial dimensions of the profile are transferred from parts without distortion.

**Profiling of the circular form cutters** starts by specifying the initial data for the calculation of the profile of the tool, such as workpiece material, part profile defined by the radii of circles  $r_1, r_2, \dots, r_i$  passing through the nodal points, and axial dimensions  $a_1, a_2, \dots, a_i$ . On the recommendations of [23, etc.] the angles  $\gamma$  and  $\alpha$  for the reference point and the radius  $R$  of the outer circle of the cutter are selected. Then the radii of the circles of the cutter points, that relate to the corresponding points of the workpiece profile with  $R_1, R_2, \dots, R_i$  are calculated, further the height coordinates  $\Delta R_i = R - R_i$  of the tool profile in the axial cross-section are calculated (Figure 4.8, a).

The parameters of the cutter tip (point 1, which lie on the machine center line) are preliminary defined according to the specified initial data. The parameters include:  $h_1 = R \sin \alpha$ ;  $m = r_1 \sin \gamma$ ;  $\psi_1 = \alpha + \gamma$ ;  $A_1 = r_1 \cos \gamma$ ;  $H = R \sin \psi_1$ ;  $B_1 = R \cos \psi_1$ .

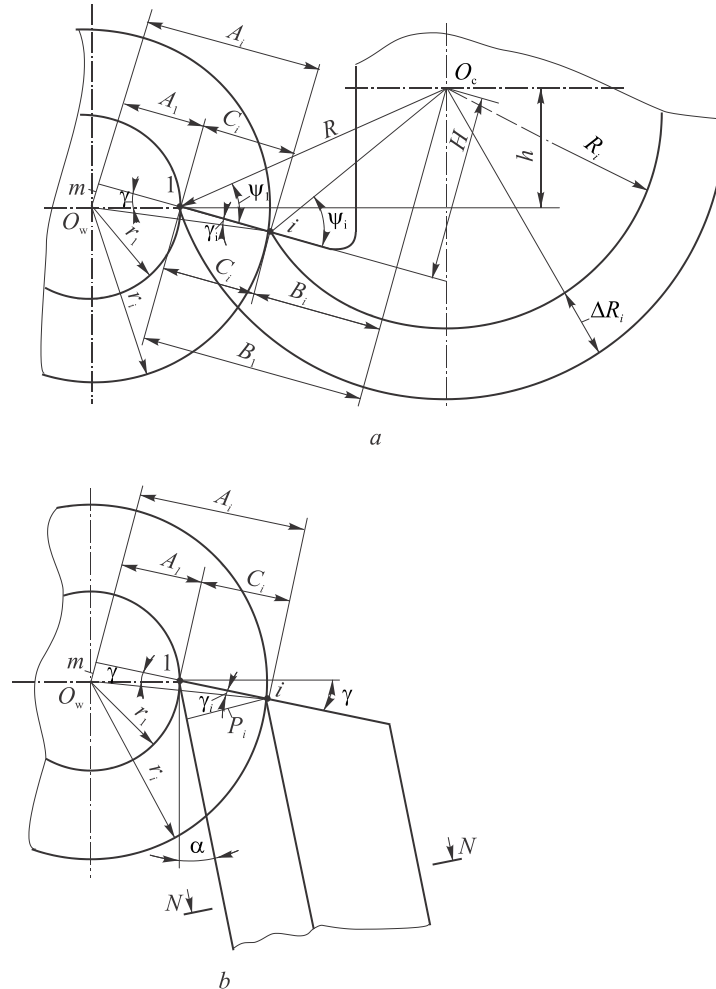


Fig. 4.8 Analytical diagram for a form cutter profiling:  
(a) circular cutter; (b) prismatic cutter



Further, using these parameters, for any  $i^{\text{th}}$  point of the profile the following parameters are found in the given order:

$$\sin \gamma_i = m / r_i; \quad (4.2)$$

$$C_i = r_i \cos \gamma_i - A_1; \quad (4.3)$$

$$B_i = B_1 - C_i; \quad (4.4)$$

$$\text{tg } \psi_i = H / B_i; \quad (4.5)$$

$$R_i = H / \sin \psi_i; \quad (4.6)$$

$$\Delta R_i = R - R_i. \quad (4.7)$$

Here, the parameters  $A_i$ ,  $B_i$  and  $C_i$  are variable and are measured along the cutter face, and the angular parameter  $\psi_i = \alpha_i + \gamma_i$  is defined using their values.

**Profiling of the prismatic form cutters** is based on the same initial data and is to identify height coordinates  $P_i$  of the cutter profile nodes in a section perpendicular to the flank surface of the tool. It follows from the analytical diagram shown in Figure 4.8, b that it is enough to have three equations:

$$\sin \gamma_i = m / r_i; \quad (4.8)$$

$$C_i = r_i \cos \gamma_i - A_1; \quad (4.9)$$

$$P_i = C_i \cos(\alpha + \gamma). \quad (4.10)$$

By analogy with the circular cutters, the values of the parameters  $m$  and  $A_1$  are roughly found. The axial coordinates of the nodal points of part profile are transferred to the tool without distortion.

With the found coordinates of the nodal points located in the specified sections, a profile, usually on a larger scale, is drawn on a cutter drawing. The straight sections of profile are built as straight line that links two points, and curved sections are drawn as a line that connects at least three or four points of the section of a profile.

## 4.2 Broaches

Broaches are multiple-point high productive cutting tools, widely used in the medium run production and especially in mass production. Broaches have inherent feed motion, since the machine performs only the pulling motion without feed available.

The allowance distribution between the teeth of a broach is implemented by the progressive increase of height or width of each subsequent tooth relative to the previous one. The increase in height, which specifies thickness of chip  $a_z$ , is called **feed per tooth** or **rise per tooth**.

Broaches used for machining holes of different shapes are called **internal broaches**. Broaches for external surfaces, i.e. surfaces with open non-closed contour, are called as **external broaches**.

The primary motion of broaching, that performs process of cutting, is often straight-line linear motion. Less common types of broaches involve rotational or spiral primary motion.

The process of broaching is carried out in special horizontal or vertical broaching machines.

### 4.2.1 Common types and application of broaches

A few types of broaching are shown in Figure 4.9. Other schemes of broaching are also possible, as the broaching, and the broaching tool itself, is constantly developing and improving.

First broaches appeared in the 30's of the XX century and spread widely due to the following advantages of the broaching process:

- 1) high productivity. The active length of the cutting edges is very large, although the cutting speed is low (6...12 m/min). In general the productivity of broaching is in 3...12 times higher than for other types of machining;
- 2) high accuracy (*IT7...IT8*) and surface finish ( $Ra$  0.32...2.5  $\mu\text{m}$ ) of the machined surface, due to broach design with separate roughing, finishing and sizing teeth, and in some cases even with burnishing buttons;
- 3) high tool life, which is up to several thousands of parts. This is achieved by the optimal cutting conditions and large stock for re-grinding;
- 4) simple design of broaching machines, since there is no need for feed motion, so the machines do not have feed gearboxes, and the primary motion is performed by hydraulic rams.

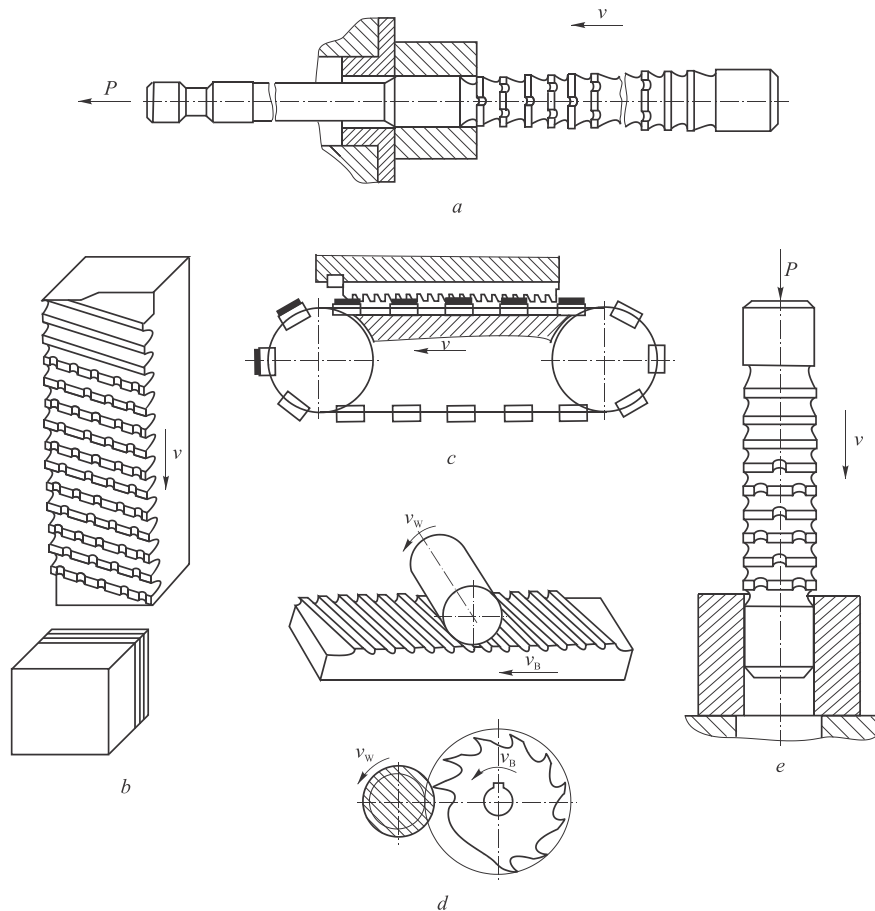


*Fig. 4.9 Broaching: (a) internal; (b) flat surface broaching; (c) continuous surface broaching; (d) broaching of a cylinder with external flat and rotary broaches; (e) internal push broaching*

The disadvantages of broaches include:

- 1) high labor and cost of a broach due to complex design and high accuracy requirements;
- 2) broaches are special-purpose tools, designed for manufacture of parts of only one size and given shape;
- 3) the high cost of regrinding, caused by the complexity of the broach design.

Therefore, cost-effectiveness of applications of broaches is achieved only in medium-production and mass production.

During the design of broaches the following peculiarities of the broaching process should be considered:

- 1) broaches experience large tensile loads, and therefore internal broaches should be checked for strength of the weakest cross-sections;
- 2) the entire chip produced by a broaching must be freely contained in the gullets for the whole period of broaching, and should be easily

leave the gullets after the broaching process is finished. Therefore, issues of chip breaking and accommodation require a lot of attention. So, for example, the ring-shaped chips are not allowed in broaching round holes, since it would be quite time-consuming to release broaches from them;

- 3) the length of broaches is limited by the broaching machine stroke and technological capabilities of machines and equipment used for machining and heat-treatment of the broaches. Moreover, broaches must be stiff and rigid enough for the manufacture and operation, so rests and other supporting devices are sometimes used in broaching.

The broaches for round holes are the most widespread (60%) of all internal broaches. Therefore, the design principles of the round internal broaches will be discussed in the following sections. For the other types of broaches (irregular shape, spline, external) only the distinctive features of the calculation of the cutting part will be considered.

#### 4.2.2 Calculation of the round internal pull broaches

Broaches consist of the following main parts: pull end, neck, front and rear pilots, cutting and sizing parts, retriever (Fig. 4.10).

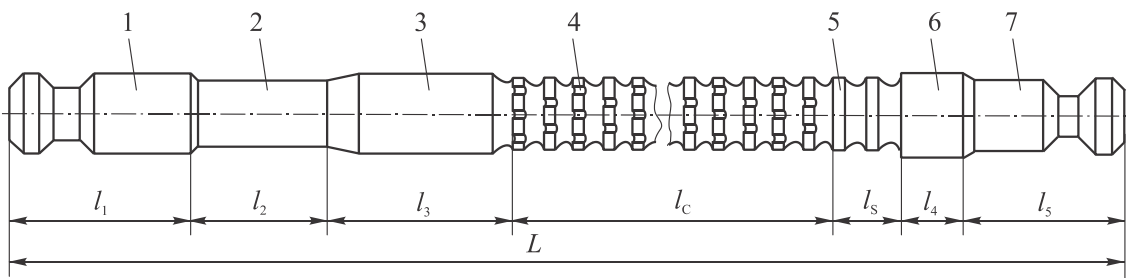


Fig. 4.10 Construction of an internal broach: (1) pull-end; (2) neck; (3) front pilot; (4) cutting part; (5) sizing part; (6) rear pilot; (7) retriever

The **pull end** is used to couple the broach to the puller of the broaching machine. Basic types and sizes of a pull end are standardized (GOST 4044-70). The diameter of the pull end should be smaller by 1...2 mm than the diameter of the starter hole for broaching.

The **neck** and the following **transition cone** play a supplementary role. Their length should ensure broach coupling with the machine puller before the broaching has started. Transition cone provides free entry of the front pi-

lot to the starter hole. Neck diameter is taken smaller than the shank diameter by 0.3...1.0 mm.

**Front pilot** aligns the axis of the workpiece relative to the axis of the broach before pulling. The length of the front guide relates to the workpiece hole length. Tolerance of the front pilot diameter is  $e8$ .

**Rear pilot** ensures broach alignment as the final teeth exit the workpiece hole. The length of the rear pilot is slightly smaller than the front pilot length, and its diameter is machined with  $f7$  tolerance zone.

A **retriever** is used to return the broach to starting position automatically after the broaching, especially if a broach of large length and diameter is used.

**Cutting part** of a broach contains roughing and finishing teeth, with intermediate teeth added for the rotor-cut broach, which are located on a step-conical surface. The length of the cutting part is the result of the number of teeth multiplied by their pitch, which, in turn, depends on the required accuracy and surface finish of the hole, as well as on the volume of material to be cut.

**Sizing part** contains 4...10 teeth of the same diameter, i.e. with zero rise per tooth. It is used to size or calibrate the hole, reduce the hole size distribution, and is a reserve for finishing teeth regrinding, thereby increasing the broach overall life.

The design of the cutting part is determined by the **cutting pattern** adopted, which refers to the procedure for successive allowance removal.

There are the following cutting patterns: a) by the method of dividing the thickness and width of the allowance – there are standard and rotor-cut patterns; b) by the method of a hole profile forming – there are full-form, generating and combination patterns.

The **standard cutting pattern** is characterized by the fact that each tooth of a broach cuts allowance of a certain thickness around the whole perimeter of the hole, with the diameter of each subsequent tooth being larger than the diameter of the previous by the value  $2a_z$ , where  $a_z$  is the rise or feed per tooth ( $a_z=f_z$ ).

Since the ring-shaped chip is unacceptable, the chips are to be divided by its width with the help of the V-shaped notches (Fig. 4.11, a), which are arranged in a staggered fashion on the adjacent teeth.

Thus the chips removed by the tooth are separate segments with an incorporated stiffening rib with thickness  $2a_z$  due to the fact that the notch of the previous tooth leaves this part of the chip uncut. The ribs impair chips curling in the gullets between the teeth, thus the rise per tooth (RPT) is considerably reduced, which in its turn leads to an undesirable increase in the length of a broach.

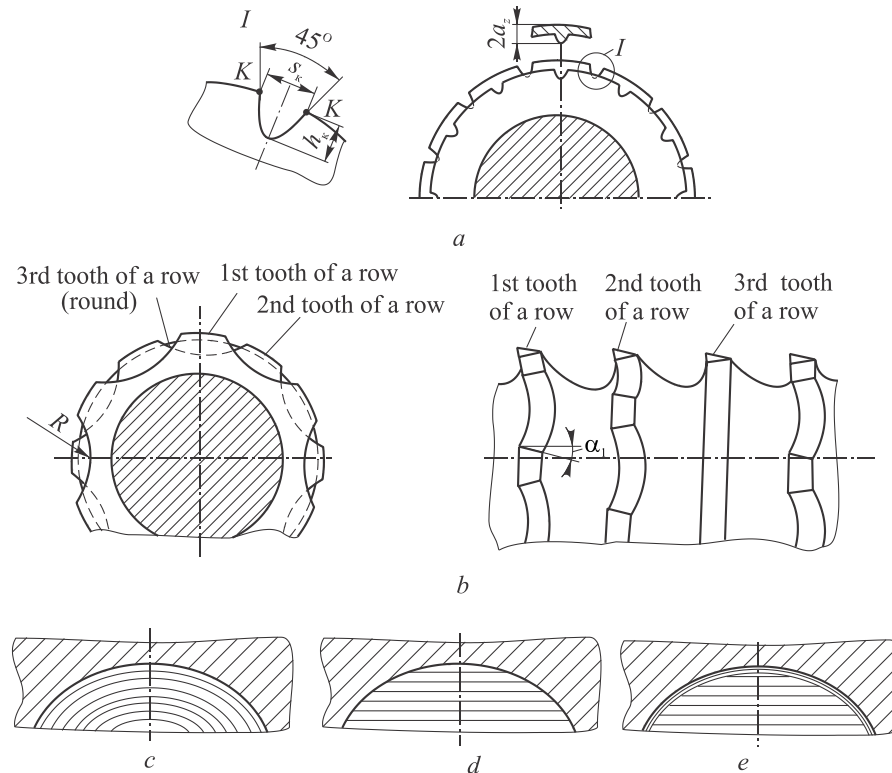


Fig. 4.11 Cutting patterns of broaching: (a) standard; (b) rotor-cut; (c) full-form; (d) generating; (e) combination

The **rotor-cut pattern** (also known as rotary-cut, rotor-kut, jump-cut) differs from the above by the fact that all cutters are divided into groups or rows, consisting of 2...5 teeth, within the limits of which the teeth have the same diameter (Fig. 4.11, b). The allowances thickness is divided between the rows of teeth, and the width of chip is divided between the teeth of a row with the help of chip breaking notches or slots, which are deeper and wider compared to the notches of a standard broach, and a positioned in a staggered fashion. Each tooth removes segments of chip by its cutting edges. The rotor-cut broaches are significantly shorter compared to the standard ones.

The last tooth in a row is a cleaning tooth with no slots and 0.02...0.04 mm reduce in diameter relative to the other teeth of a row. This is necessary to avoid the formation of ring-shaped chip, which is the result of elastic spring back of the machined surface after the passage of slotted teeth.

The disadvantage of the rotor-cut pattern is the increased complexity of the broach manufacture compared to the standard pattern.

In the **full-form pattern** (Fig. 4.11, c) the profile of the cutting edges is similar to the profile of the hole being broached. Here the final formation of the surface is performed only by the last tooth, and the rest serve to remove the stock. The application of the full-form pattern for complex shapes of the workpiece hole is impractical, since it complicates the manufacture of the

broach. Full-form pattern is generally used for surfaces of simple form, such as round or flat.

In **generating (or nibbling) pattern** of broaching (Fig. 4.11, d) the form of the cutting edges is not identical with the workpiece hole profile, which is formed as the envelope of a series of all teeth cutting edges. In this case, the production of a broach is simplified, since all the teeth are shaped by the same grinding wheel of a single profile. However, the broached surface may incorporate scratches (steps) due to the errors of teeth grinding, which degrades the finish of the machined surface.

In case of high requirements for surface finish it is recommended to apply a **combination broach** (Fig. 4.11, e), which two or three last cutting and sizing teeth are full-form, and the rest are generating.

Teeth of a broach must meet the following basic requirements:

- 1) the size of the teeth should provide the greatest possible number of regrindings;
- 2) the tooth must have a certain margin of safety, and thus resist the acting forces;
- 3) the shape and size of gullets should provide chip curling into a tight coil, and the volume of the gullets must provide sufficient room for chips cut during tooth contact with the workpiece;
- 4) have a geometry with the greatest broach life provided.

The size of teeth and gullets is limited by the permissible values of the broach length and strength.

**Rake angle**  $\gamma$  of a broach is chosen according to the workpiece material. So, for steels of different machinability the  $\gamma=10...20^\circ$ , for cast-irons with various hardness  $\gamma=4...10^\circ$ , for aluminum and copper  $\gamma=12...15^\circ$ .

Considering that the teeth of the internal broaches are reground only along the face and resharpening decreases their diameter, the roughing teeth clearance angle  $\alpha=3^\circ$ , for finishing teeth  $\alpha=2^\circ$ , and for sizing teeth  $\alpha=0...1^\circ$ . These values of the clearance angles are much smaller than optimal, resulting in reduced tool life.

Another important consideration of the internal broach design is the gullet sizes in terms of **chip accommodation** (Figure 4.12). This is due to the fact that the chips produced in the process of broaching have no free evacuation.

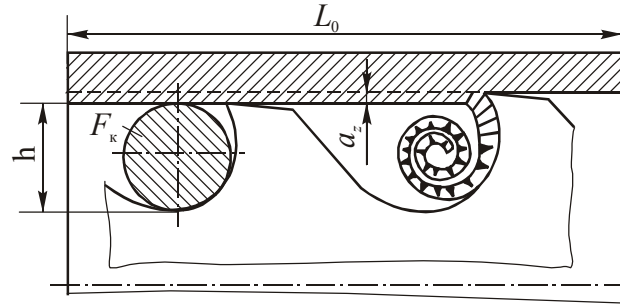


Fig. 4.12 Chip accommodation in a gullet

Accounting to high tensile stresses found in broaching, the **internal broaches are checked for strength**

$$\sigma = P_z / F_{OP} \leq [\sigma], \quad (4.11)$$

where  $P_z$  is the tensile force;  $F_{OP}$  is the area of the weakest section;  $[\sigma]$  is the permissible tensile stress (for solid HSS broaches  $[\sigma]=350\text{...}400$  MPa, for constructional steels  $[\sigma]=250$  MPa).

Broach weakest sections include two sections with minimum areas: 1)  $F_1$  – area of the section that runs through the notched pull-end; 2)  $F_2$  – area of the root diameter, measured in a gullet between teeth.

$F_1$  is found in the tables of GOST 4044-70, and  $F_2$  is calculated as:

$$F_2 = \pi(d_1 - 2h)^2 / 4,$$

where  $d_1$  – is a diameter of the first tooth of a broach.

In case Equation (4.11) is violated, the cutting pattern should be changed or the factors that determine the cutting force  $P_z$  value reduced, which, for example, for round broaches with standard cutting pattern is calculated by the following equation

$$P_z = C_p a_z^x \pi d z_p K_\gamma K_{CF} K_W, \quad (4.12)$$

where  $C_p$  – is workpiece material coefficient;  $x$  – is the exponent of the chip thickness  $a_z$ ;  $\pi d$  – is the chip width;  $z_p$  – is the number of simultaneously working teeth;  $K_\gamma$ ,  $K_{CF}$ ,  $K_W$  – are correction factors for the rake angle, cutting fluid and wear respectively.

The calculation starts with the selection of material for the cutting part of the broach. The best material is high-speed steel. In the short-run and single-part productions the tool steels, that are cheaper than HSS, are applied. To save high-speed steel the broaches with diameter of 15...40 mm are modular with welded or threaded (for diameter greater than 40 mm) pull ends made of hardened structural steels.

Before the calculation of the cutting part of the broach, the allowance for broaching, with respect to the workpiece hole diameter, length, accuracy and surface finish requirements, as well as starter hole parameters, should be assigned.



The allowance (diametric) for the standard cutting pattern is assigned from the experimental data or calculated by the following empirical equations:

1) for drilled starter hole

$$A_0 = 0,005d_0 + (0,1...0,2)\sqrt{L_0} + (0,7...1,0)\delta; \quad (4.13)$$

2) for core-drilled, reamed or bored starter hole

$$A_0 = 0,005d_0 + (0,05...0,1)\sqrt{L_0} + (0,7...1,0)\delta, \quad (4.14)$$

where  $d_0$  – is the minimum diameter of the broached hole;  $L_0$  – is the length of the hole;  $\delta$  - is the tolerance of the hole diameter.

The finishing part allowance  $A_F$  is assigned with respect to the accuracy requirements of the broached hole. 2...4 finishing tooth with RPT  $a_z=0.025...0.005$  mm, decreasing from the first to the last tooth, are usually chosen.

The number of roughing teeth is determined by the equation

$$z_0 = (A_0 - A_F) / 2a_z. \quad (4.15)$$

Preliminary RPT for roughing teeth is chosen with regard to the work-piece material on the recommendations [27].

The diameter of the first tooth is usually equal to the diameter of the starter hole. The diameters of the subsequent teeth are calculated by adding double RPT ( $2a_z$ ) value to the previous tooth diameter.

The pre-determined teeth pitch is corrected for the conditions of chip accommodation and with respect to the number of teeth in cut  $z_p$ .

The cutting force  $P_z$  is calculated with accordance to Equation (4.12) and the broach is checked for strength by Equation (4.11).

The diameters of the last finishing tooth and sizing teeth are taken equal to the maximum limit of size of the broached hole, with the hole oversize, which is typically 0.005...0.010 mm for thick workpieces, considered.

The number of sizing teeth is taken from 4 to 10, depending on the required accuracy of broaching.

Maximum length of a broach is limited by certain conditions: the stroke of the broaching machine, warping due to heat treatment, technological capabilities of the broach manufacture. If the broach length is greater than the allowable, the broach is divided into 2 or 3 shorter broaches that make a set.

The method of calculation of rotor-cut broaches is described in detail in [18]. Only fundamental differences in calculation of the broaches, compared to the standard cutting pattern broaches are mentioned below.

1. The cutting part of the rotor-cut broaches is supplemented with two or three sections of intermediate teeth with two times smaller RPT compared to roughing teeth, placed between roughing and finishing sections. Intermediate teeth help to avoid sharp decrease in cutting

force when the roughing teeth leave the broached hole and also serve to semi-finish the hole.

2. The calculation begins with the selection of RPT for roughing teeth provided that the roughing teeth life is equal to the finishing teeth life for a given cutting speed value.
3. Then the depth  $h$  of the tooth gullet and tooth pitch is determined. Broaches with diameters less than 40 mm are checked for strength, and, if needed, the gullet depth is corrected.
4. The permissible cutting force  $P_z$  is selected from three values: 1) machine pulling capacity,  $P_M$ ; 2) strength of the pull end weakest section  $P_{PE}$ ; 3) strength of the weakest section of the first tooth gullet of the cutting part,  $P_{CP}$ . In further calculations, the smallest of these values is taken as the maximum permissible,  $P_{zmax}$ .
5. The number of roughing teeth in a row is calculated.
6. Broaching allowance  $A$  is divided between roughing  $A_0$ , intermediate  $A_I$  and finishing  $A_F$  teeth. The values of  $A_I$  and  $A_F$  are taken from tables [18], depending on the required surface finish of the machined holes. Thus, the allowance for roughing teeth

$$A_0 = A - (A_I + A_F).$$

7. Then the number of roughing teeth rows is determined
 
$$i_0 = A_0 / 2s_{z0}.$$
8. The number of finishing and sizing teeth, as well as RPT for finishing teeth is selected from the tables [18], depending on the requirements for accuracy and surface finish. Pitches for these teeth are assigned variable. There are three pitch values, related to the pitch of roughing teeth  $t_0$  as increased or decreased by 0.5...1.0 mm. The smallest pitch is used to define tooth profile and size of the tooth gullets. Finishing teeth, as well as intermediate teeth, are divided into two teeth rows.
9. Further, the number and size of fillets or slots on the teeth periphery is calculated or appointed according the table [18].

#### 4.2.3 Internal broaches for holes of irregular shape

The broaches of this type are intended for cutting multi-faceted shapes, such as, for example, triangle, square, rectangular, hexagonal, etc.

Design and calculation of the broaches for irregular-shaped holes are examined for the process of square hole broaching. The use of full-form cutting pattern is impractical in this case, since the square cutting edges (Figure 4.13, a) near the corners have clearance angles close to zero.

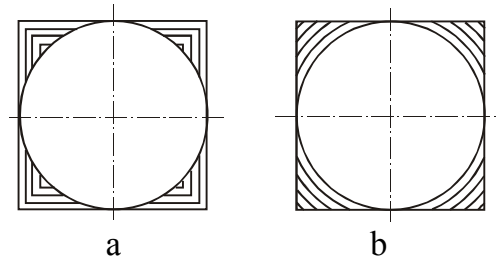


Fig. 4.13 Broaching patterns for square holes: (a) full-form; (b) generating

It is possible to avoid these undesirable clearance angle values with the help of generating broaching, as in this case, the major cutting edges of the teeth are circular, the radius of which varies with relation to the RPT values. Minor cutting edges have a profile similar to the hole profile.

Making the major cutting edges of circular shape provides good centering of the broach in the hole and better conditions for cutting and chip removal.

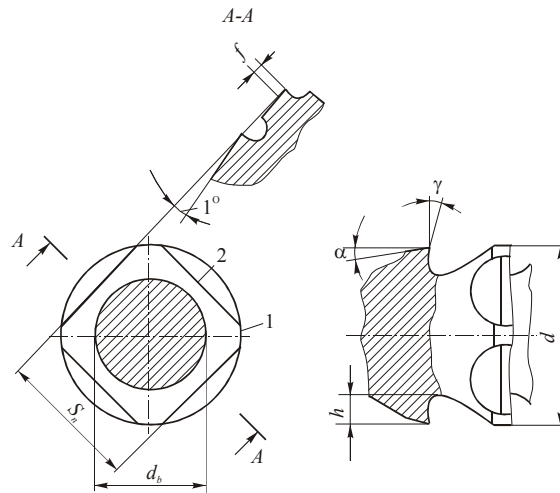


Fig. 4.14 Teeth of a square broach in normal and axial sections

Fig. 4.14 shows normal and longitudinal sections of the broach, shapes of the tooth and gullets, geometrical parameters of the major and minor cutting edges.

In order to maintain a pulling force constant within the whole hole length, the RPT should evenly increase from the first tooth to the last tooth. This would ensure not only the uniformity of a pulling force, but even the most important, would reduce the length of the broach. However, due to small values of RPT, individual values of RPT ( $a_z$ ) for each tooth would complicate the process of broach manufacture. Therefore, it was suggested [27] to divide all the cutting teeth to 3 or 4 steps, depending on the width of the face  $S_n$  and to assign value  $a_{zm}$  for the each step.

The check for strength in weakest sections is similar to standard round broaches. The pulling force is calculated by Equation (4.12) for the condi-

tions in which the width of cut is maximum and equal to  $b = \pi d_1$ , where  $d_1$  – is a diameter of the first tooth equal to the starter hole diameter.

Design of **spline cutting broaches** is discussed below.

Spline slot shapes include: a) straight-sided (Fig. 4.15, a); b) involute; c) trapezoid; d) triangular, etc.

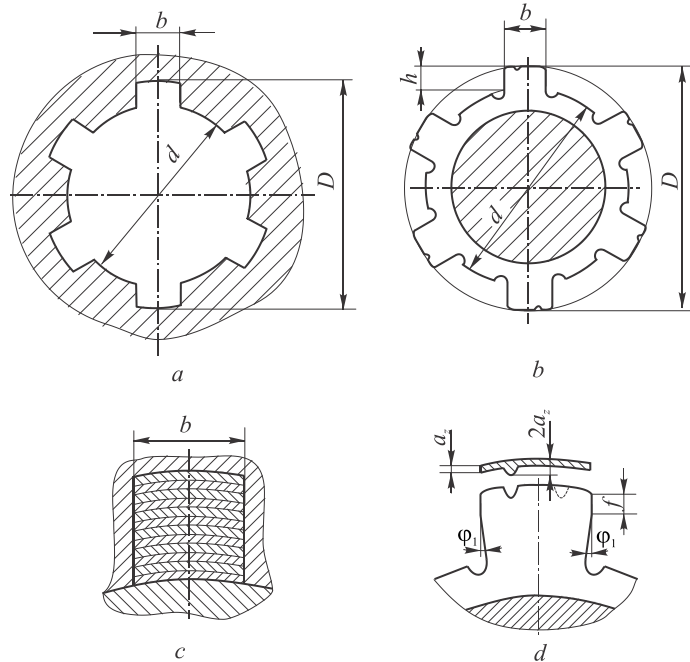


*Fig. 4.15 Shapes of a splined hole and broach: (a) splined hole; (b) spline cutting broach; (c) standard broaching; (d) tooth of a spline cutting broach*

Spline-cutting broaches resemble splined shafts, with splines turned into teeth by cutting flutes and, thus creating rake and clearance angles. Tooth height  $h$  is variable.

Let's examine features of the spline-cutting broach design by the example of a broach for cutting straight-sided splines.

The Fig. 4.15, b shows cross-sections of a splined hole and a broach, and the Fig. 4.15, d shows allowance distribution for standard cutting pattern and form of a broach tooth.

The major diameter of spline slots is formed by the full-form cutting, and sides of the spline slot are cut by generating pattern. When the width of the spline slot is bigger than 6 mm, one or two staggered notches are applied to the major cutting edges. Unlike the round broaches, spline broaches have chip breaking notches applied to all the cutting teeth and even to the sizing teeth.

The rotor-cut spline broach has rows consisting of two teeth (Fig. 4.16): the first tooth is notched in corners and is cutting, and the second tooth is cleaning. In addition, the second tooth is decreased in diameter by 0.03...0.04 mm.

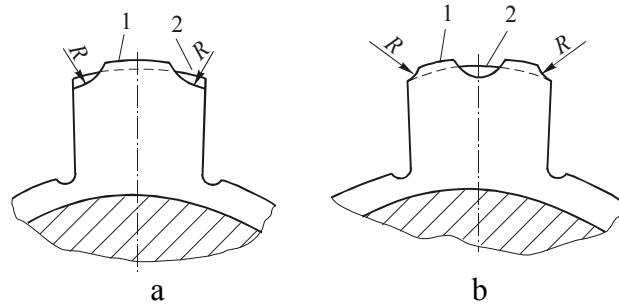


Fig. 4.16 Row of roughing teeth of a spline rotor-cut cutting broach: (a) tooth width  $b \leq 18$  mm; (b) tooth width  $b > 18$  mm (1 is the first tooth of a row, 2 is the second tooth of a row)

To improve the accuracy and surface finish of the splined holes and to reduce the number of broaches in a set, the combination broaches, with the cutting part consisting of round, chamfer and spline teeth, are used. The allowance severed by the teeth is shown in Fig. 4.17.

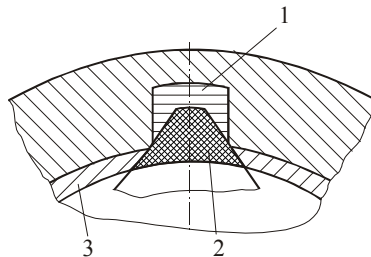


Fig. 4.17 Allowance or stock for broaching by a spline-cutting combination broach: 1 – for splined teeth; 2 – for chamfer teeth; 3 – for round teeth

Most often the first teeth are chamfer-teeth. They remove the most of the allowance from the splined slot, and form a chamfer on the minor diameter. In addition, they act as cutting or preliminary teeth for round teeth. The latter have no notches and have one continuous cutting edge.

#### 4.2.4 Surface broaches

External broaching is applied for different surfaces with open non-closed contour, such as planes, shoulders, slots, concave, convex, cylindrical,

complex contours, etc. Thus, there are a variety of designs of the external broaches.

In contrast to the internal, the external broaches usually have no pull ends and pilots, and have only cutting and sizing teeth. External surfaces allow specifying larger sizes of structural elements and cross-sectional area for the surface broaches. Therefore external broaches usually are not checked for strength. Conditions for chip flow are more favorable and conditions of chip accommodation in teeth gullets are checked only for the broaching of narrow slots.

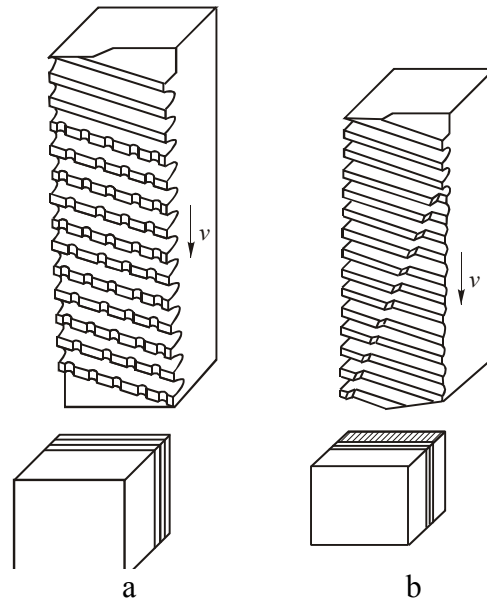


*Fig. 4.18 Broaching patterns for external surfaces: (a) full-form; (b) generating with full-form finishing teeth*

The special features of the external broaches include the possibility to assign much larger, close to optimal, clearance angles ( $\alpha=8\dots10^\circ$ ), since the regrinding doesn't affect the height of a broach in terms of the part size deterioration. Thus the total life of surface broaches much larger compared to internal broaches.

The same cutting patterns are applied in surface broaching as in internal broaching. Fig. 4.18 shows full-form and generating cutting patterns used in surface broaching of flats. To improve surface finish, the last teeth of a broach (Fig. 4.18, b) are full-form.

By the method of cutting layer thickness dividing the standard cutting pattern is most often used.

Sharpening of the teeth with straight cutting edges can be done either along the flank or along the face, while the cutting edges of complex shape are reground only along the face.

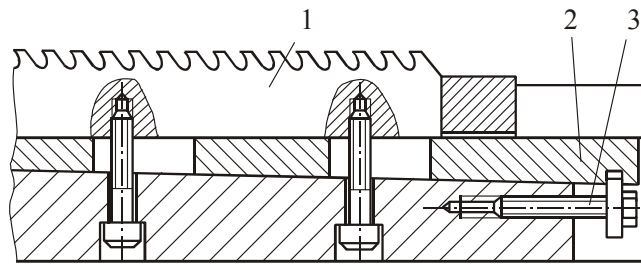


Fig. 4.19 Height adjustment of sections of a surface broach performed with a wedge: 1 – broach section; 2 – wedge; 3 – adjustment screw

Surface broaches can be solid or modular, consisting of several sections of the relatively short length (300 mm). Sections are attached to the body with screws, wedges and strips from the top, bottom or side (Fig. 4.19 and 4.20). Sections secured with bottom screws are more compact and simple. However, for regrinding and adjustment of these sections it is required to remove the whole broach from the machine. This can be avoided by fixing sections by screws from the top.

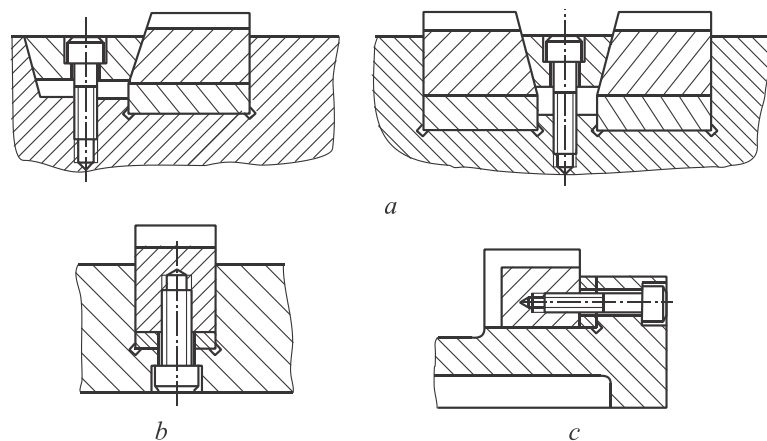


Fig. 4.20 Common types of clamping sections in a surface broach: (a) by a top screw and a wedge; (b) by a bottom screw; (c) by a side screw

To provide continuous removal of the chips from the cutting area during broaching of long surfaces, the teeth of a broach are placed at a shear angle  $\beta=70\text{...}80^\circ$ . This technique also ensures uniform process of broaching.

In broaching with teeth inclined at a shear angle the additional lateral component of the cutting force  $P_N$ , which is normal to the direction of pulling, arises. For accommodation of the  $P_N$  force as well as the main force component  $P_Z$ , the broach body is provided with additional slots or stop bars, which are used when the broach is clamped on the machine carriage.

## 5. Design and Calculation of Drills, Core-Drills and Reamers

The following sections discuss various tools applied in manufacturing for making and enlarging holes.

### 5.1 Drills

Drills are the cutting tools intended for making holes in solid parts, as well as for enlarging holes that were previously made by forging, stamping, casting or drilling. They are widely used in mechanical engineering, ranking the second place after cutters on this basis.

Kinematics of drilling consists of two movements: the primary one is rotation of the tool or workpiece and linear motion that is feeding along the tool axis.

Drills are mainly distinguished by design, according to which the following basic types are found: 1) spade drills; 2) twist drills (with helical flutes); 3) special type (for drilling deep holes, trepanning drills, combination drills, etc.).

The cutting part is usually made of high-speed steel. In recent years, the carbide drills of various designs have spread.

#### 5.1.1 Spade drills

Spade drills have been known since ancient times. For example, their prototypes in the form of hard material spades pointed at the end and designed for manual drilling holes in softer materials were found in the archaeological excavations. Spade drills have been constantly improved since the emergence of metalworking. Modern constructions of spade drills are shown in Fig. 5.1, a, b, c.

Solid spade drills (Fig. 5.1, a) are made of a bar with forged or milled plate-shaped head, which is sharpened to a cone angle of  $2\varphi=118^\circ$ . This process forms two major and two minor cutting edges. Grinding of two flat flanks creates clearance angle  $\alpha=10\dots12^\circ$ . At the intersection of these surfaces the chisel edge is formed. If the rake surfaces are flat, the rake angles on the major cutting edges have negative values, which is undesirable due to the increase of power load on the drill and the appearance of chatter.



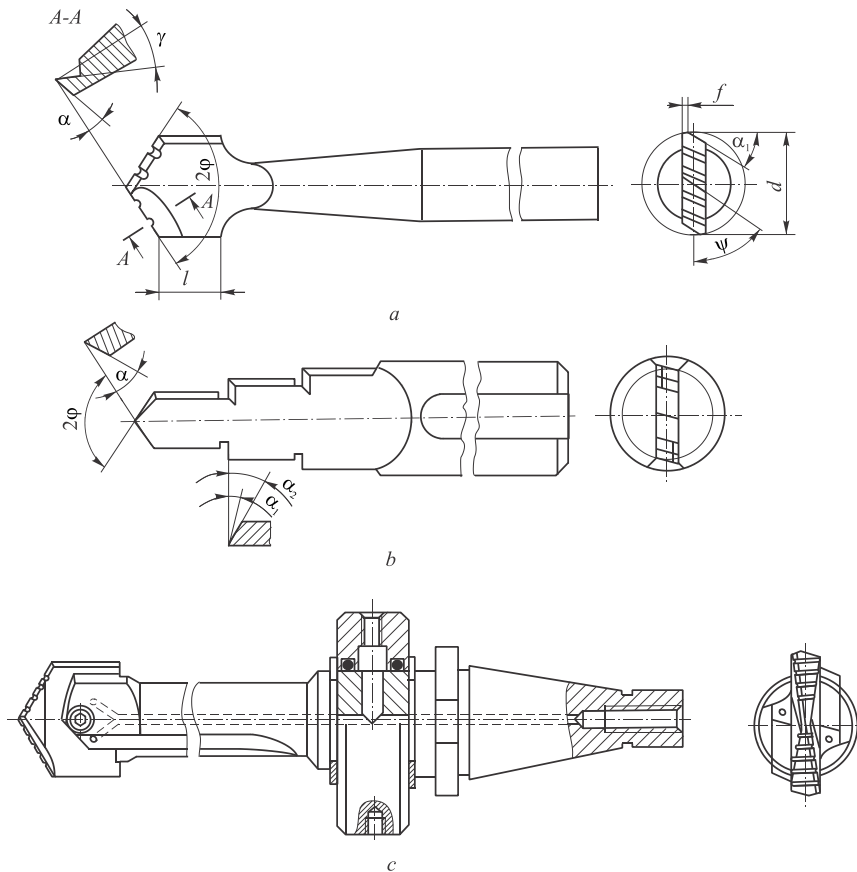


Fig. 5.1 Flat drills: (a) solid; (b) for stepped holes drilling; (c) indexable; (d) coolant fed

The advantages of spade drills are a simple design, and the possibility to manufacture drills of different diameter and length even in the repair workshops.

Disadvantages of spade drills include: 1) difficult conditions of chip removal; 2) tendency to chatter due to low stiffness of the cutting part; 3) low number of permissible resharpenings; 4) low performance of the drilling process due to small values of feed and the necessity of drill withdrawal out of the hole for chip removal.

### 5.1.2 Twist drills

Twist drills have the most widespread application among the other well-known types of drills due to the following advantages: 1) a good chip evacuation out of the hole due to helical flutes; 2) positive rake angles along the greater length of the lips; 3) a large stock for resharpening, which is done on the flanks and can be carried manually or on special grinding machine tools, including automatic machine tools; 4) a good guiding of a drill in a hole because of the margins on the periphery of the drill body.

Basic elements and geometric parameters of a twist drill are shown in Fig. 5.2. Two major cutting edges, called lips, are located on the tapered cutting part with a point angle  $2\phi$ . The lips are the lines of intersection of helical face and flank. The shape of the flank surface is defined by sharpening. A chisel edge is appeared as the result of intersection of two flank surfaces. The chisel edge is inclined with respect to the major cutting edge at an angle  $\psi$ . This edge is located on the drill web with a nominal diameter  $d_0=(0.15\dots0.25)d$ , where  $d$  is the diameter of the drill. Two minor cutting edges lie on the intersection of the rake surfaces and cylindrical margins that guide a drill in the hole and form a sizing part of the drill. The angle between the minor edges and the drill axis is helix angle  $\omega$ , which primarily determines the value of the rake angles  $\gamma$  on the major cutting edges. The rakes, as will be shown below, are variable in size at different points along the lips.

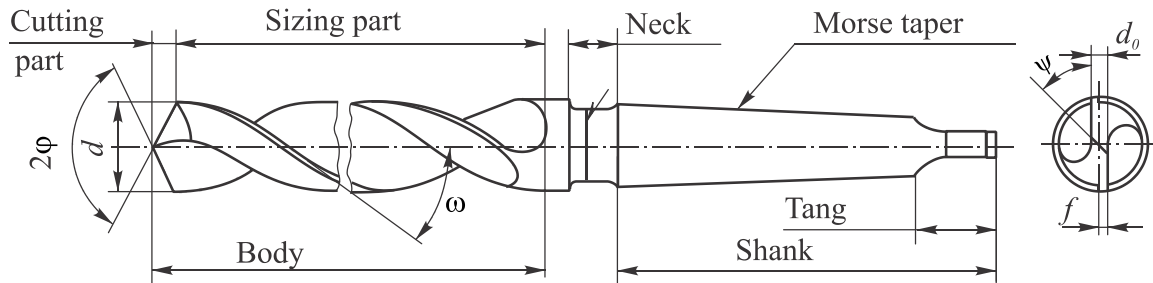


Fig. 5.2 Twist drill nomenclature

To reduce friction between margins and walls of the hole, the margins width, depending on the diameter of the drill, is taken equal to  $f=(0.32\dots0.45)\sqrt{d}$ , and the height is  $\Delta=0.1\dots0.3$  mm. The reduction in drill diameter from the point to the shank is applied to avoid the jamming of the drill in a hole. This reduction is called back taper and is equal to 0.03...0.12 mm per 100 mm of length. To increasing strength and rigidity of the drill web, it is tapered, i.e. the diameter of the web increases in the direction to the shank by 1.4...1.7 mm per 100 mm of length.

The cutting and sizing parts of the drill constitute its working part, the length of which is divided into short, medium and long series. Standard twist drills are manufactured of 0.1...80 mm in diameter with tolerances h8...h9.

There is a portion of decreased diameter between the drill body and the shank, which is called neck. It is used for purposes of drill marking, which can include: diameter, material of the cutting part, trademark of the manufacturer.

Shanks can be of two types: tapered (Morse taper) with a tang at the end, for drills  $d=6\dots80$  mm and cylindrical – for drills  $d=0.1\dots20$  mm. Shanks for drills with  $d>8$  mm are made of structural steel grades 45 or 40X, welded

with a working part. To increase friction force during clamping and provide possibility for drill calibration, the drill shanks aren't hardened. Drill tangs are hardened, as they are used to knock the drill out of the spindle or adapter sleeve hole.

Further the **geometrical parameters of twist drills** are considered. Twist drills have a complex geometry of the cutting part, due to the presence of a large number of edges and a complex configuration of rake and flank surfaces.

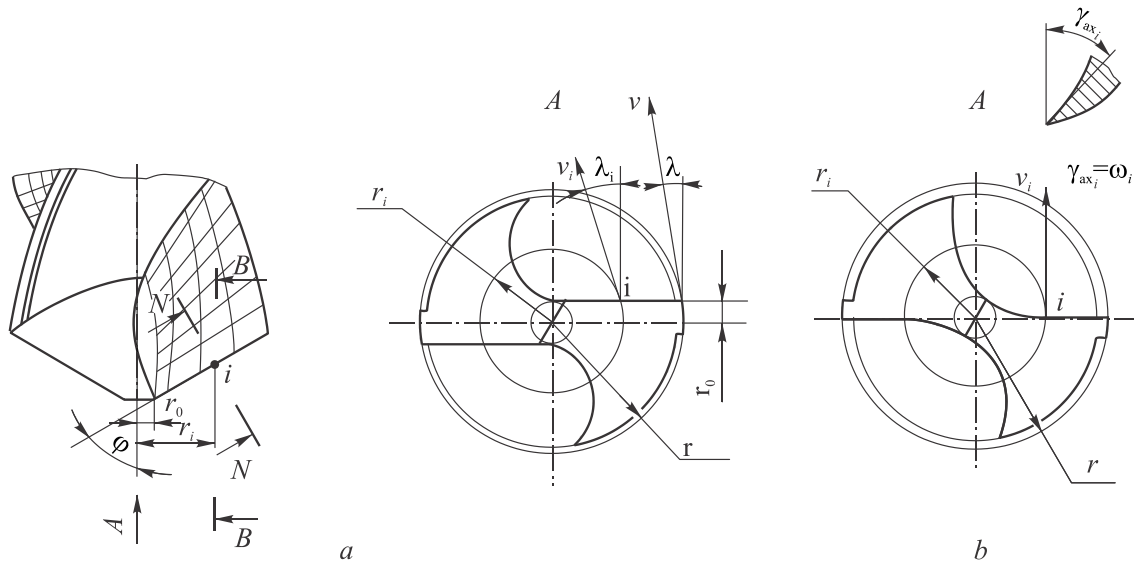


Fig. 5.3 Twist drill geometry: (a) standard drill; (b) drill with lips in axial plane

**Point angle**  $2\varphi$  is a double cutting edge angle measured in the reference plane. Standard drills have  $2\varphi=116\dots120^\circ$ . Here, the major cutting edges are linear and match the generating line of the helical rake surface.

According to the manufacturing experience the optimum value of the  $2\varphi$  angle is recommended to select with respect to the workpiece material, for example, in cutting of structural steels  $2\varphi=116\dots120^\circ$ , for stainless and high-strength steels  $2\varphi=125\dots150^\circ$ , for cast iron and bronze  $2\varphi=90\dots100^\circ$ , for cast iron of high hardness  $2\varphi=120\dots125^\circ$ , for non-ferrous metals (aluminum alloys, brass, copper)  $2\varphi=125\dots140^\circ$ .

Angle of the helical flutes that is **helix angle**  $\omega$  is measured on the periphery of the drill and is one of the most important drill parameters.

During designing new types of drills for cutting definite materials, the ISO recommends to apply the following values for the helix angle  $\omega$ : for steel cutting –  $25\dots35^\circ$ , for cast iron and other brittle materials –  $10\dots15^\circ$ , for aluminum, copper, and other free-cutting materials –  $35\dots45^\circ$ .

The helix angle of special twist drills is increased up to  $40 \dots 60^\circ$  because this angle has a major impact on chip removal from the cutting zone. However, as the angle  $\omega$  decreases the transverse drill stiffness and the rake angle increase, especially on the peripheral parts of the cutting edges, which can greatly decrease the strength of the cutting wedge and reduce drill life.

**Rake angle**  $\gamma$  of twist drills has a variable value along the length of the major cutting edges. This is due to the fact that the rake surface of the drill is helical linear convolute, as it is formed by helical motion of a line segment, inclined to the axis of the tool.

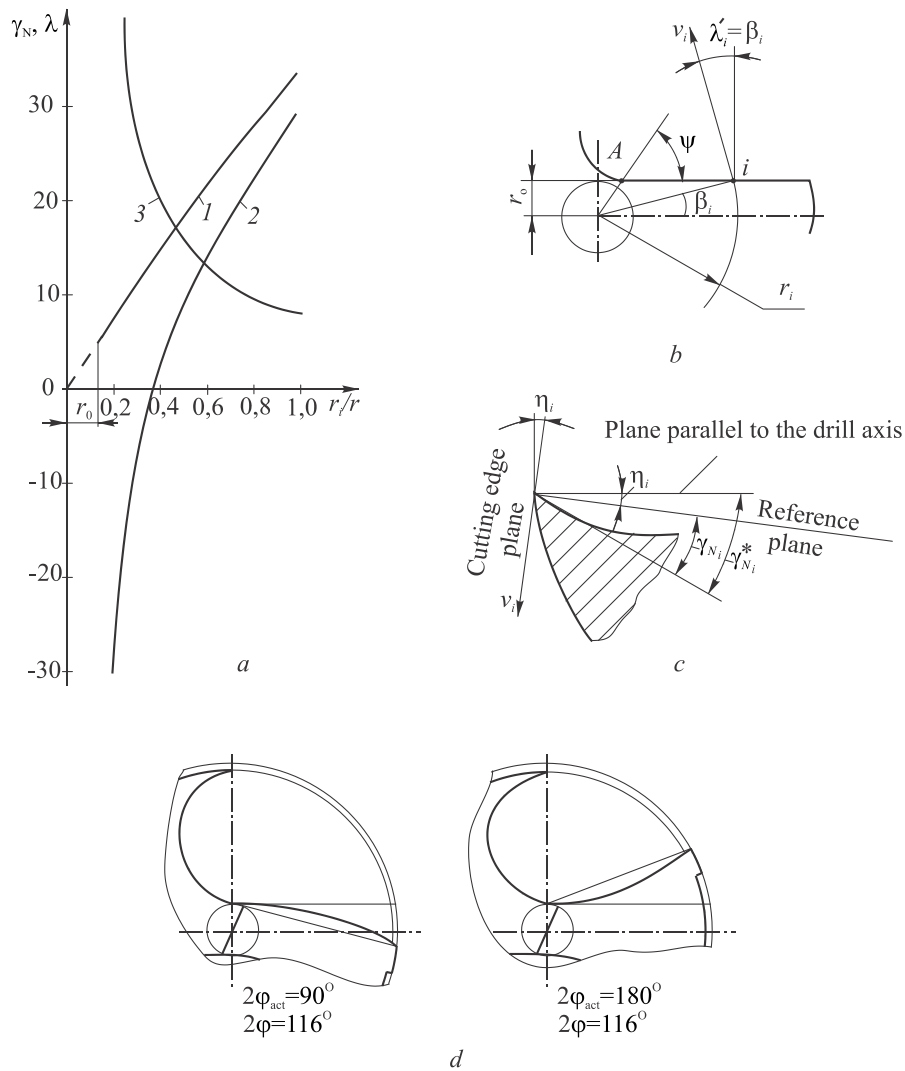


Fig. 5.4 Values of rake angle  $\gamma_{Ni}$  and inclination angle  $\lambda_i$  along the lips of a twist drill: (a) 1 –  $\gamma_{Ni}$  for axial-planed lips, 2 and 3 are standard drill  $\gamma_{Ni}$  and  $\lambda_i$  respectively; (b) cutting speed vector direction along the lips; (c) working rake angle diagram; (d) lip shape with respect to the actual value of the point angle  $2\phi$

The equation for the angle  $\gamma_{Ni}$  of a standard drill with  $\omega=30^\circ$ ,  $\phi=60^\circ$  and  $c=0.16$  is presented below:

$$\gamma_{N_i} = \arctg\left(0,7\sqrt{(r_i/r)^2 - 0,0256}\right) - \arctg\left(\frac{0,08}{\sqrt{(r_i/r)^2 - 0,0256}}\right). \quad (5.1)$$

The distribution of the angle  $\gamma_{N_i}$  calculated by Equation (5.1) is represented by curve 2 in Fig. 5.4, a. In this case, starting with  $r_i/r < 0.37$ , the rake angles on a section adjacent to the chisel edge are less than zero, reaching large negative values near the web, which is a significant drawback of the standard geometry of the twist drills.

Standard drills with the lips shifted over the axial plane of symmetry have an **inclination angle**  $\lambda_i$  due to the rotation of the cutting velocity vector at each point of the cutting edge. This angle is between the velocity vector and the normal to the cutting edge. As can be seen from Fig. 5.5, b the angle  $\lambda_i$  is variable. From Fig. 4.5, b:

$$\sin \lambda_i = \frac{r_o}{r_i} \sin \varphi. \quad (5.2)$$

The inclination angle  $\lambda_i$  variation along the length of the major cutting edge, calculated from Eq. (5.2) with  $r_o = 0.16d$ ,  $\varphi = 60^\circ$  is shown in Fig. 5.4, a (curve 3). It follows from the Fig. 5.4 that the largest values of  $\lambda_i$  are on the section of the lip edge, adjacent to the drill web.

**Clearance angle**  $\alpha$  on the lips is created by grinding the drill heels, which are the flank surfaces and can be shaped as a part of the flat, conical or helical surfaces.

The clearance angle of a twist drill is usually measured in the cylindrical section, which is coaxial with the drill, as the angle between the cutting edge plane and a tangent to the flank surface. The former is a plane that passes through the lip perpendicular to the axial plane of a drill (Fig. 5.5, a).

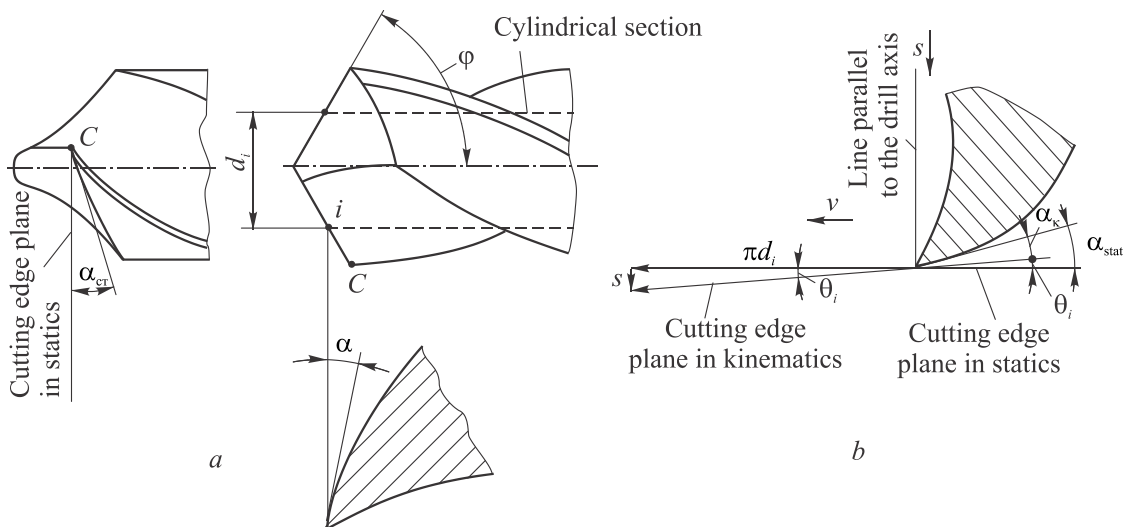


Fig. 5.5 Clearance angles of a twist drill: (a) tool-in-hand; (b) working

The pattern of the clearance angle variation along the lip is determined by the method of sharpening, which should provide some increase in  $\alpha_i$  with the approach of the  $i^{th}$  point to the axis of the drill. Such requirement is explained by the influence of feed  $f$  on the value of the working clearance angle  $\alpha_k$ , which becomes more pronounced at points of cutting edges, located closer to the web.

It follows from Fig. 5.5, b that the angle  $\alpha_k$  is an angle between the development of the helical trajectory of the lip point and a tangent to the flank of the drill. In addition,

$$\alpha_{\kappa_i} = \alpha_{st_i} - \theta_i, \quad (5.3)$$

where  $\alpha_{st_i}$  is the clearance angle, measured in static between a plane perpendicular to the drill axis and a tangent to the flank;  $\theta_i$  is the helix angle of the  $i^{th}$  point of the lip, depending on the diameter of the cylinder, passing through the  $i^{th}$  point and on the drill feed  $f$ , mm/rev.

From Fig. 5.5, it follows that

$$\operatorname{tg} \theta_i = s / \pi d_i. \quad (5.4)$$

The common methods of drill grinding provide peripheral angle  $\alpha_{ST}=8\dots14^\circ$  and clearance angle at the web  $\alpha_{ST}=15\dots20^\circ$ .

### 5.1.3 Methods of twist drill sharpening

Technologically, the simplest method of sharpening is a plane or double plane sharpening. However, during a **single plane sharpening** (Fig. 5.6, a), in order to eliminate rubbing of the drill heels against the machined surface, it is necessary to take large values of clearance angles  $\alpha=20\dots25^\circ$ , which dramatically weakens the cutting wedge. Therefore, this method is applied only for sharpening small diameter drills with  $d < 3$  mm, when the width of the heels is small.

**Double plane sharpening**, used to make four faceted drill point (Fig. 5.6, b), provide sharpening of the flank surface, adjacent to the lip, with the optimal clearance angles, and rest of the heel sharpened at much larger clearance angles (secondary clearance). This provides greater strength of cutting wedges, more favorable variation of the rake angles along the chisel edge, formed by the intersection of the plane flanks, and the best conditions of hole starting.

A very common method of sharpening of the high-speed steel drills, especially of large diameter, is a **conical sharpening** (Figure 5.6, c), which is performed on a special grinding machines or universal grinders equipped with special devices (Fig. 5.7, d). Though this method of sharpening is simple

to perform and provides a favorable variation of the clearance angle  $\alpha$  along the lips, its main drawbacks are interrupted grinding process and a highly negative rake angles on the chisel edge. The value of the clearance angle  $\alpha$  is controlled by the displacement value  $k$  of the drill axis relative to the cone axis. The apex of the cone can be positioned either above or below the drill point, resulting in different clearance angle variation along the lips. In the first case the clearance angles increase from the drill periphery to the chisel edge. And in the second case vice versa.

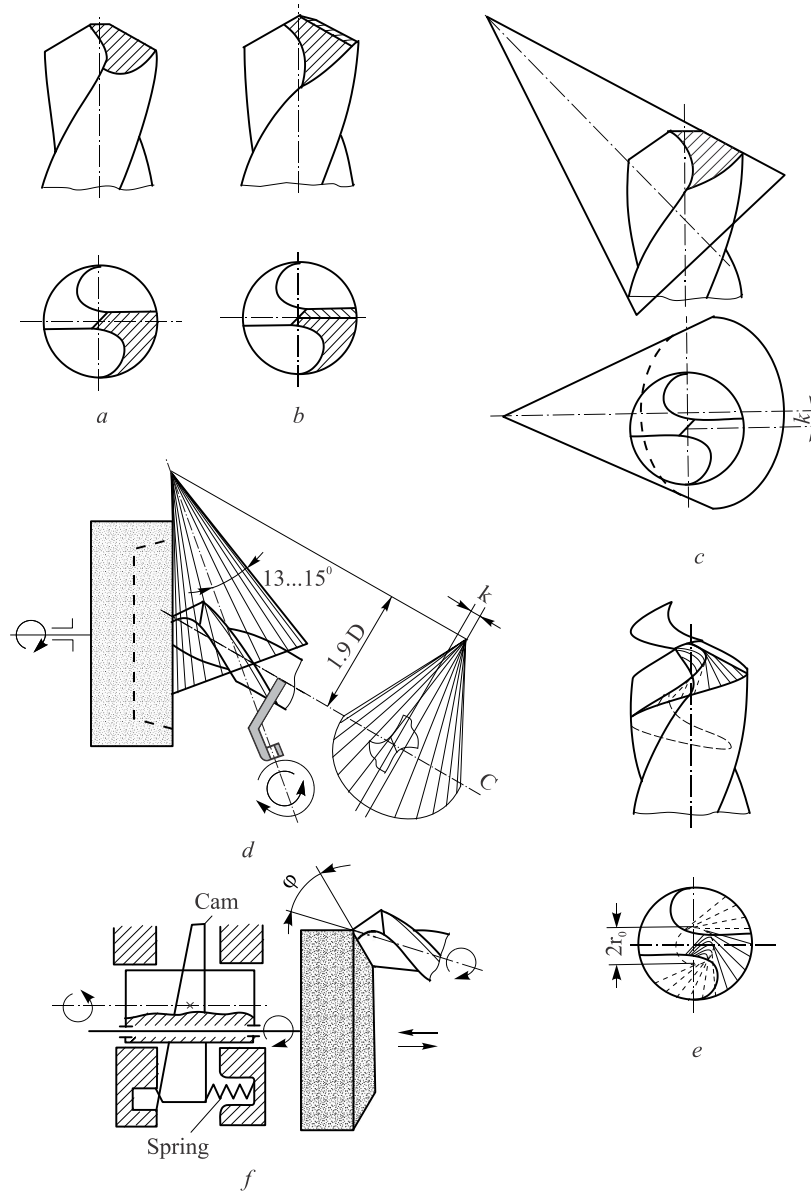


Fig. 5.6 Methods of twist drill sharpening: (a) single-planed; (b) double-planed; (c) and (d) conical; (e) and (f) spiral

**Sharpening of helical surface** is found to be the most widely used method in large production runs (Fig. 5.6, d). It is performed on special au-

automatic or semi-automatic grinding machines. Due to special kinematics of the grinding wheel (Fig. 5.6, e), the grinding is implemented with continuous rotation of the drill and provides the best symmetry and geometry of the lips, leading to improved drill performance.

### 5.1.4 Disadvantages and correction of twist drill geometry

The main drawbacks of geometry of standard twist drills, which reduce drill life and productivity, include: 1) a zero clearance angles on the minor cutting edges that are margins; 2) negative rake angles on the lips; 3) large rake angles on the peripheral part of the lips.

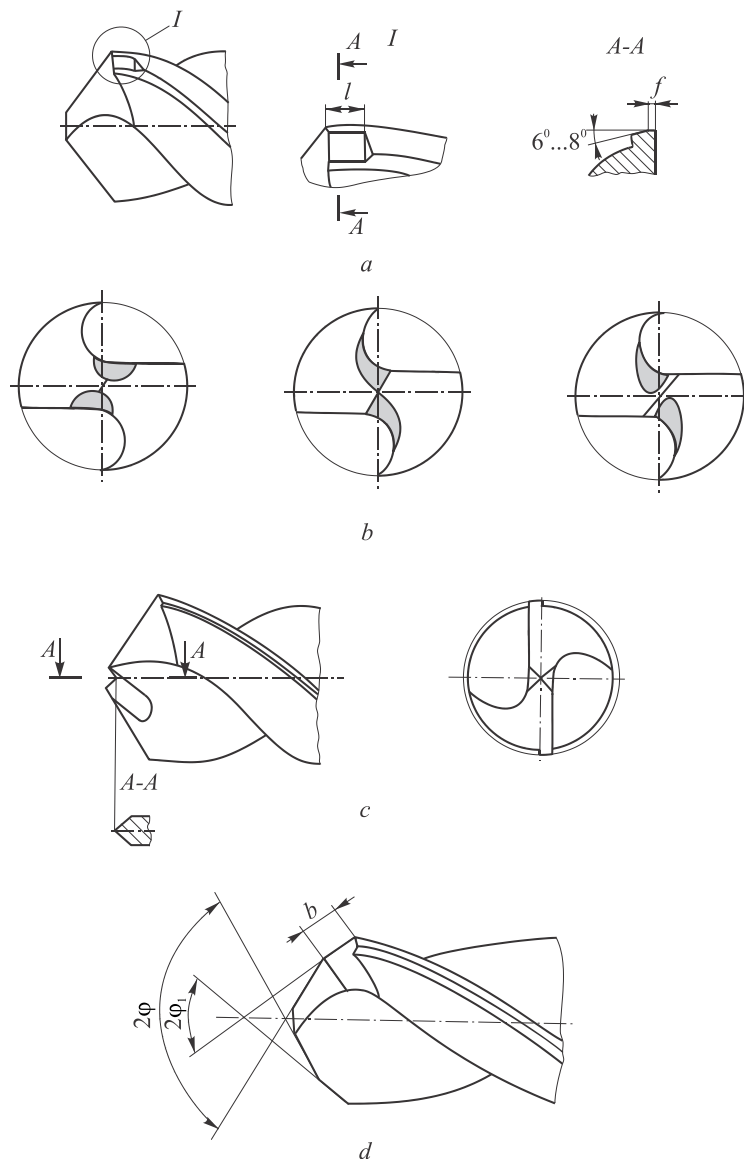


Fig. 5.7 Correction of the twist drill geometry: (a) margin grinding; (b) and (c) web thinning; (d) double point angle



The following ways are widely used to reduce the effect of these shortcomings in practice:

1. Sharpening of the margin with clearance angles  $\alpha_1=6\dots8^\circ$  and a small land left uncut (Fig. 5.7, a). This reduces the friction forces on margins, and eliminates adhesion of fine chips in drilling of steels, resulting in increased tool life.
2. Various methods of web thinning are applied, reducing the thrust force, improving the conditions of hole starting and increasing the drilling performance by allowing to increase the feed rate. Some methods of web thinning are shown in Fig. 5.7, b and c.
3. Double cone point sharpening of the drill is used (Fig. 5.7, d). Here  $2\varphi=116^\circ$ ,  $2\varphi_1=70\dots90^\circ$ . This reduces the wear on the most vulnerable sections of the peripheral cutting edges of the drill, where the cutting speed is the greatest, and the rake angles are less than  $7\dots8^\circ$ .

In practice, other ways of the drill point sharpening are used to increase drill life and improve drill performance.

### 5.1.5 Deep hole drills

The term “deep holes” is usually related to the holes, the depth of which exceeds  $5d$ . However, even with the  $h>3d$  there are some difficulties with a coolant supply to the cutting zone and chip removal out of the hole using twist drills, which leads to a reduction of tool life. Therefore, in practice, the application of deep hole drilling tools usually starts with a hole depth larger than  $3d$ .

The main difficulties of drilling deep holes are: 1) difficult conditions of coolant supply to the cutting area and chip removal; 2) axial hole deviation; 3) dimensional errors and from errors of the holes in the radial and longitudinal sections.

In practice, the drilling of deep holes with depths up to  $20d$  is performed on universal drilling machines with help of twist drills of long series, which have longer shank and body of standard length (Fig. 5.8, a). In this case, automatic pecking of the tool is used to release a drill from the chip during drilling.

To reduce axial hole deviation it is recommended to grind four margins on the drill periphery and increase the web thickness as much as possible (Fig. 5.8, a).

To improve chip evacuation the special high-helix drills or **auger drills** are implemented (Fig. 5.8, b), which are mostly used for drilling holes with depths up to  $(30\dots40)d$  in the cast iron and other brittle metals. Unlike stand-

ard twist drills, they have greater helix angle of the helical flutes  $\omega = 60^\circ$  and increased web diameter  $d_0 = (0.30 \dots 0.35)d$ .

To ensure effective chip breaking without pecking and raise the drill life, the HSS coolant-fed twist drills are used (Fig. 5.8, c). Their drawback is high manufacturing complexity, the necessity to have special internal coolant chucks and pump stations, as well as protection from chips and coolant spray.

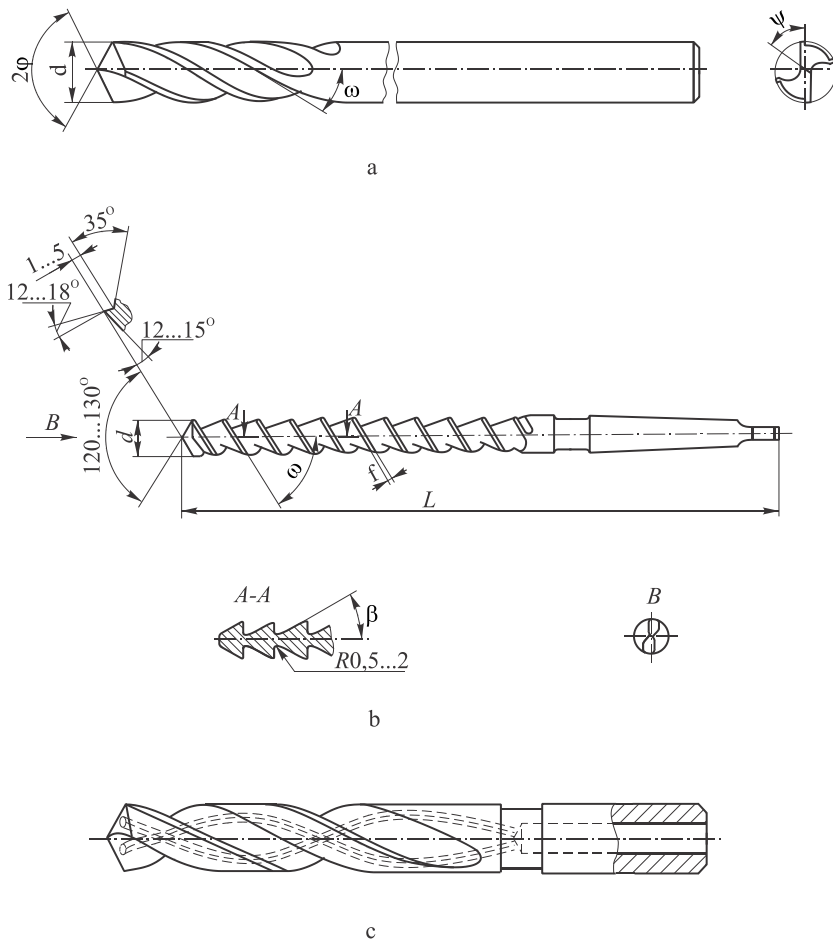


*Fig. 5.8 Deep hole twist drills:  
(a) four-margined with extended shank; (b) auger drill; (c) coolant fed*

Drill wandering with two symmetrically positioned lips occurs due to low stiffness of end mounting of the drills, inevitable errors of sharpening of the cutting edges, evidence of hard spots in workpiece material, etc.

The most effective way to minimize drill wandering and increase the accuracy of the holes is an application of self-piloting cutting tools that are supported and guided by the machined surface. For this purpose, the cutting edges are positioned so that the deliberately unbalanced radial component of

the cutting force arises and presses guide pads against the hole surface, which is machined by the cutting edges positioned ahead these pads (Figure 5.9).

Tools working on this basis are called **self-piloting tools** or tools of single-sided cutting [7, 9]. These tools include half-round drills, gun drills, BTA drills and ejector drills. They can have one or more cutting edges, but in any case the total radial component  $R$  of the cutting and friction forces should be directed straight to the supporting surface and be located between the guide pads, to implement the self-piloting principle.

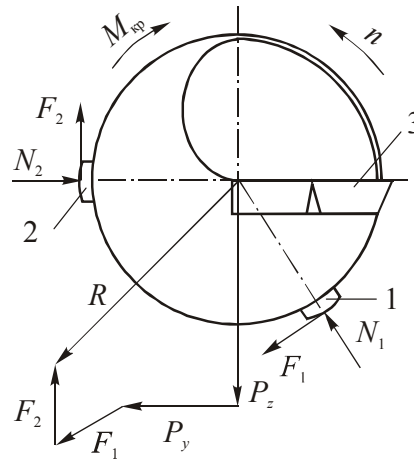


Fig. 5.9 Forces acting in a transverse plane of a self-piloted drill: (1) and (2) carbide guide pads; (3) carbide cutting insert

### 5.1.5.1 Half round drills

Historically, the first and the simplest design of the deep hole drill is a **half-round drill** or **cannon drill**. The half-round drill (Fig. 5.10, a) is a rod with its length equal to the depth of the hole, with the working part cut to about half of the diameter and sharpened at the end with the clearance angle  $\alpha$ . Half-round drill has rake angle  $\gamma=0^\circ$ , and the clearance angle  $\alpha=8\dots10^\circ$ . To reduce the axial component of the cutting force the rake surface of the half-round drill is curved with the radius  $R$  and has a very slight depression near the tool axis. During the drilling the radial unidirectional load is taken by the cylindrical surface of the drill, supported by the wall of the machined hole.

Half-round drills work under difficult conditions. Continuous chip removal isn't provided; therefore the drill has to be repeatedly withdrawn from the hole. Because of the low transverse rigidity and large width of the chip, it is prone to chatter, and works with small feed rates. These drills now are rarely used, only for single-part and medium-run production.

### 5.1.5.2 Gun drills

**Gun drills** (Fig. 5.10, b) in contrast to half-round drills, have internal channel for coolant supply and straight (sometimes helical) flute for the external evacuation of mixture of chip with coolant. Gun drills are used for drilling holes with depths equal to  $(5...100)d$  and a diameter of  $1...30$  mm. Originally gun drills were used for drilling gun barrels. Nowadays gun drills are widely used in all branches of engineering, mainly for drilling deep holes on special machines in mass production. Equipped with carbide inserts and internal coolant supply, they provide high productivity for drilling holes with high straightness and high dimensional accuracy (H8 ... H9) and good surface finish of the machined holes ( $Ra\ 0.32...1.25\ \mu m$ ).

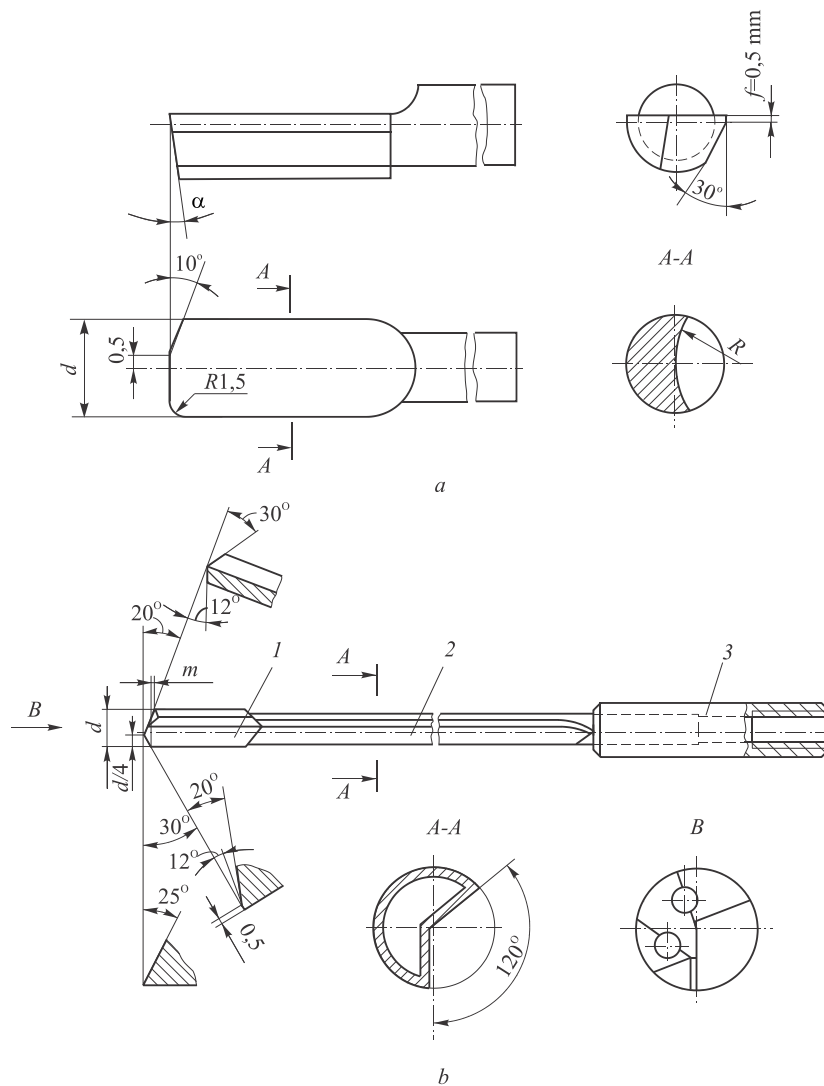


Fig. 5.10 Deep hole drills:  
 (a) half round drill ( $d=3...36$  mm); (b) gun drill ( $d=1...30$  mm)

The geometrical parameters of the cutting part of a gun drill are shown in Fig. 5.10, b.

Pressure and coolant flow rate depends on the diameter of the drill. For example, the coolant pressure for small diameter drills is 9...10 MPa.

The disadvantages of gun drills include small lateral and torsional stiffness due to tubular shank weakened by a flute. For this reason, the feed rates are reduced, and hence the productivity of the drilling operation.

### 5.1.5.3 BTA drills

**BTA drills** are produced in various designs: single-edged (Fig. 5.11, b, c), multiple-edged (Fig. 5.11, d, e), brazed or indexable ( $d \geq 20$  mm).

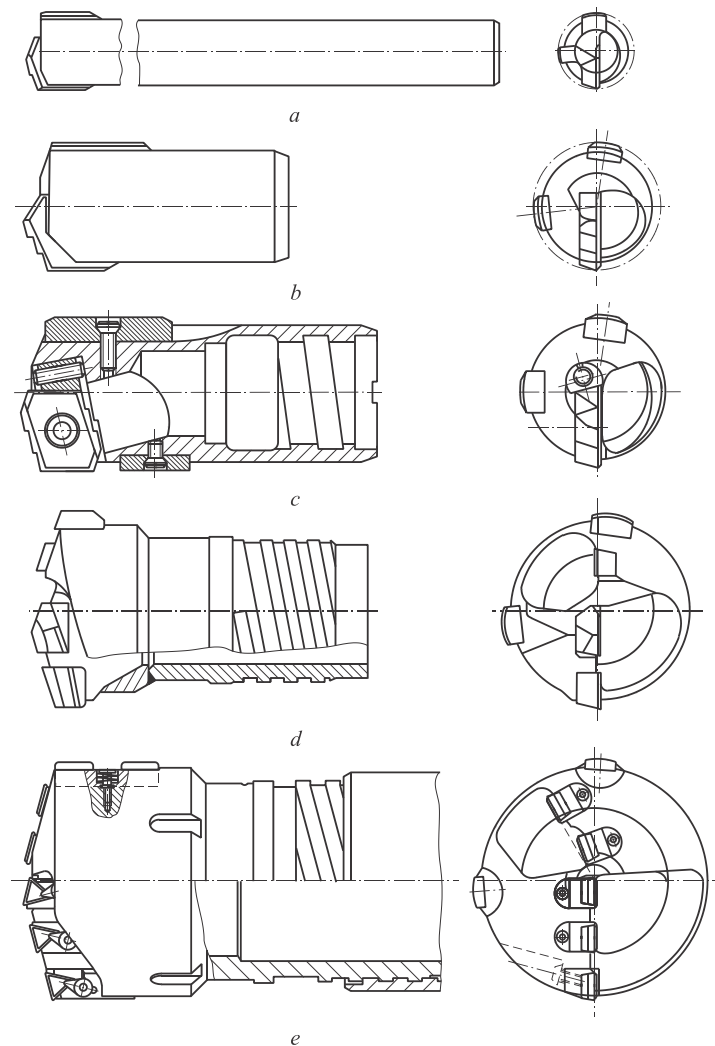


*Fig. 5.11 BTA drills: (a) with a single brazed T-shaped insert ( $d=6...18$  mm); (b) brazed head with a single insert ( $d=18...30$  mm); (c) head with a single indexable insert ( $d=18...65$  mm); (d) brazed head with a set of inserts ( $d=18...65$  mm); (e) head with a set of indexable inserts ( $d > 65$  mm)*

Unlike gun drills, the BTA drills and heads have thick-walled tubular shank of ring cross-section. BTA drills work with external coolant supply (between the walls of the shank and machined hole), internal coolant evacuation and chip removal.

Advantages of BTA drills include 2...4 times higher feed rates due to the high rigidity of the tubular shank as compared to gun drills, and improved surface finish of the machined surface due to internal chip evacuation.

Disadvantages of BTA drills include difficulties with reliable chip removal through a relatively small cross-section hole of a tubular shank.

The common depths of horizontal BTA drilling are up to  $100d$ , and in vertical drilling are up to  $50d$ .

### 5.1.5.4 Ejector drills

**Ejector drills** are similar to BTA drills in design (Fig. 5.12). Differences between these two drills consist in coolant supply and evacuation of chip with coolant mixture. The coolant is supplied between the inner 6 and outer 7 tubes, and then through the holes in the head to the cutting area. Ejector nozzles 5 are C-shaped and are positioned in the back part of the thin-walled tube 6.

The maximum depth of the holes obtained by ejector drilling is up to 4000 mm.

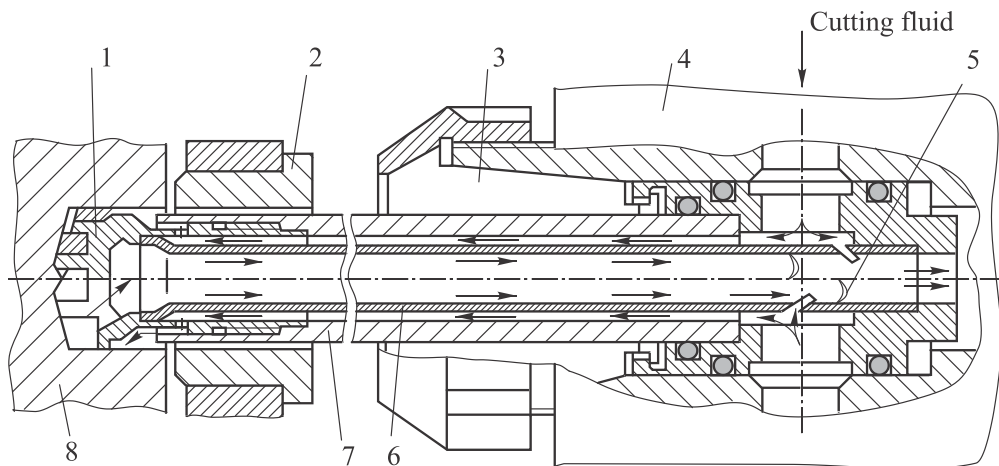


Fig. 5.12 Ejector drill operation: (1) cutting head; (2) guide bushing; (3) collet; (4) chuck; (5) orifices; (6) thin-walled tube; (7) tubular shank; (8) workpiece

### 5.1.5.5 Trepanning drills

A large amount of chips that are produced in drilling of the holes with diameter greater than 50 mm leads to considerable power consumption and higher cost of tools due to increased use of tool materials. Moreover, cutting forces are also sharply increased. During **trepanning** the annular groove is cut in the workpiece and a center core is left uncut, allowing for its further use as a workpiece or test sample. Due to lower horsepower, the feed rate can be significantly increased and hence the productivity of the drilling operation is also increased.

The simplest design of a trepan drill is shown in Fig. 5.13, a. Cutting fluid is supplied through the holes in the tool body and is removed along with chips through the gap between the drill periphery and the workpiece.

There are other designs of trepan drills, including those with carbide indexable inserts screwed to the drill body. These drills are applied for short (Fig. 5.13, b) and deep (Figure 5.13, c) holes. In the latter case, self-piloting trepan designs are used to reduce the tool deflection and produce straight holes.

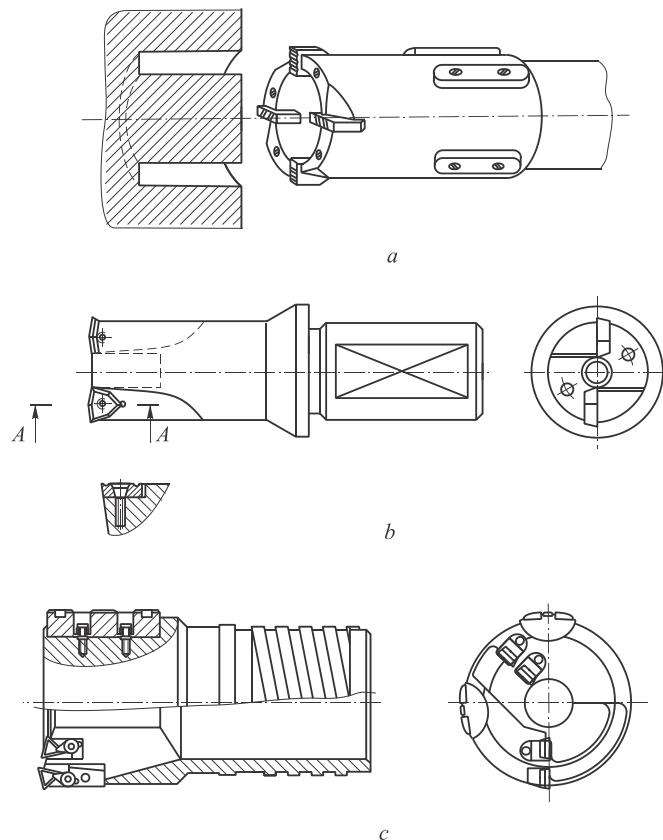


*Fig. 5.13 Trepanning drills: (a) with mechanically clamped inserts and guide pads; (b) indexable drill for short holes; (c) deep hole self-pivoted indexable heads with internal chip evacuation*

## 5.2 Core drills

Core-drills are the multiple point axial cutting tools, which are used for semifinishing or finishing holes, created by drilling, casting, forging or stamping. Core-drilling is used to improve hole accuracy to IT11...IT10 and improve surface finish to Ra 40...10  $\mu\text{m}$ .

Kinematics of core-drilling is similar to drilling. However, core-drills provide greater productivity and accuracy, compared to drills, since the allowance removed is smaller ( $t=1.5...4.0$  mm,  $d=18...80$  mm), core-drills have a greater number of cutting edges ( $z=3...4$ ) and margins. Due to shallow flutes, core-drills have higher rigidity as compared to drills, and the lack of chisel edge allows higher feed rates.

Core-drills are classified according to:

a) type of cutting: cylindrical **core-drill** is used to increase the diameter of the holes (Fig. 5.14, a), **counter bore** is used to provide a step of enlarged diameter in a hole (Fig. 5.14, b), **countersink** produces chamfer or conical entry to the hole to allow the head of a screw to be seated beneath the part surface (Fig. 5.14, c), **spot facer** creates a flat adjacent to the hole on bosses and pads of the parts (Fig. 5.14, d);

b) method of core-drill mounting: shank-type core drill (with either straight or tapered shank and  $d=10...40$  mm and  $z=3$ ) and shell core-drill ( $d=32...80$  mm,  $z=4$ );

c) core-drill design: solid, assembled or indexable (with inserted blades,  $d=40...120$  mm) and adjustable;

d) type of cutting material: high-speed steel and carbide.

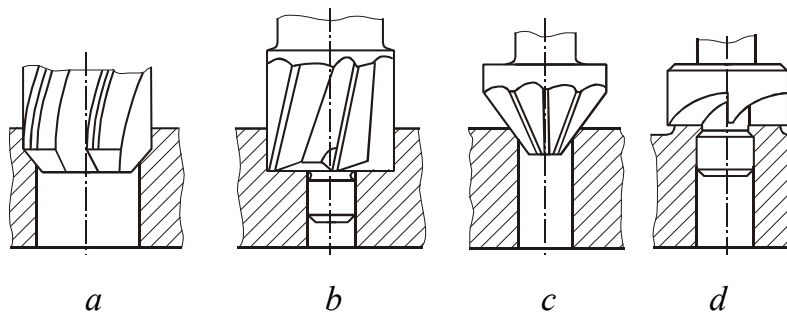


*Fig. 5.14 Core drills:  
(a) straight core drill; (b) counter bore; (c) countersink; (d) spot facer*

### 5.2.1 Cylindrical core drills

Cylindrical core-drills can be of shank-type (Fig. 5.15, a), and shell-type (Fig. 5.15, b). The main **structural elements** of a core-drill are: the cutting



part (starting taper), the sizing part, number of flutes (teeth), the shape of flutes, and type of mounting part. The **geometric parameters** include: point angle  $2\varphi$ , rake  $\gamma$  and clearance angle  $\alpha$ , helix angle  $\omega$  and major cutting edge angle  $\lambda$ .

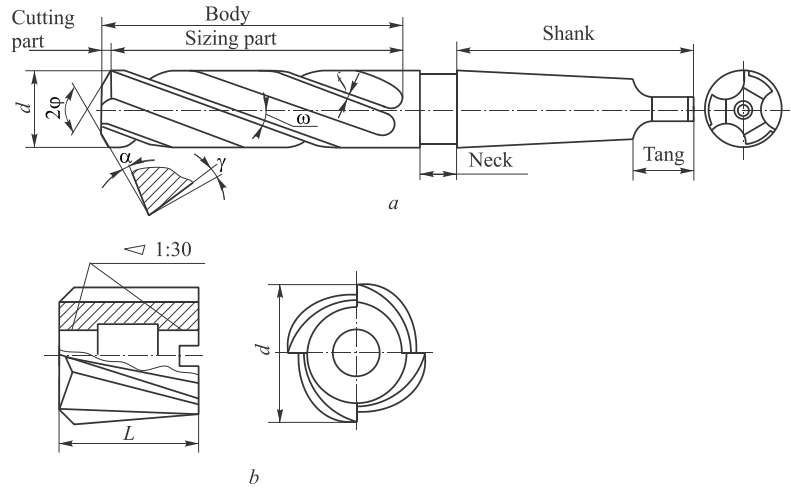


Fig. 5.15 Straight core drills: (a) shank-type; (b) arbour-type

**Sizing part** of a core-drill provides the required accuracy of the machined hole, guides the core-drill in the hole and serves as a reserve for re-grinding. Sizing part includes cylindrical margins of width  $f=0.8...2.0$  mm for  $d=10...80$  mm. Radial run-out of the margin should be smaller than  $0.04...0.06$  mm.

Back taper of margins is used to reduce friction and to eliminate core-drill jamming in the hole, and is equal to  $0.04...0.10$  mm per 100 mm depending on the diameter of the tool.

Increase of the margin width of carbide core-drills is not appropriate, as it is accompanied by adhering of small chips, and leads to a decrease in tool life. The increase in back taper causes chatter and accelerated decrease of core-drill diameter after the regrinding.

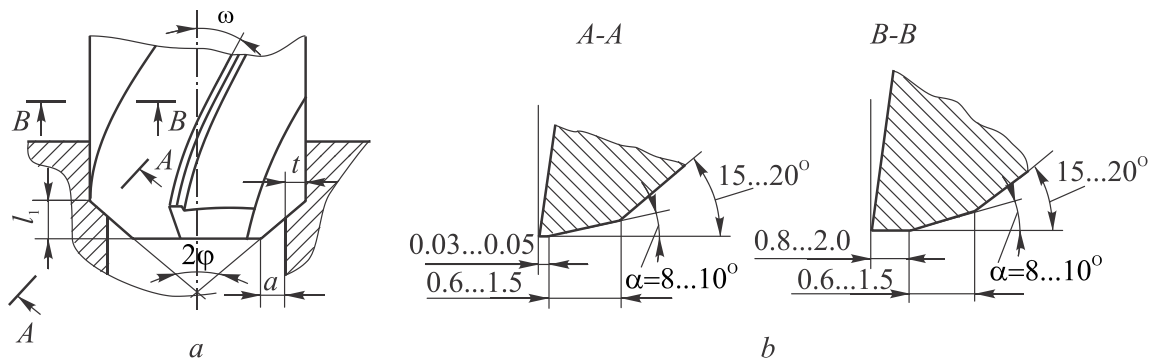


Fig. 5.16 Cutting part of a core drill: (a) elements; (b) types of sharpening

In terms of **number of flutes**, core drills are made with three (shank-type) or four (shell-type) flutes. Shell core-drills of larger size ( $d > 58$  mm) have six or more flutes. Core-drill flutes are generally helical, but they may be straight, such as carbide core drills for cutting steel and hardened cast iron. Assembled core-drills with clamped or brazed inserts have flutes inclined to the core-drill axis.

In cutting of steel the **cutting edge angle** is  $\varphi = 60^\circ$ . In cutting of cast-iron the cutting edge angle is  $\varphi = 60^\circ$  or  $45^\circ$ .

**Rake angle**  $\gamma_N$  can be determined by Equation (5.1) that was used for the twist drill calculation, but without taking the radius of points on the edge taken into account, since the lips have small length and are positioned in the diameter plane, i.e.

$$\operatorname{tg} \gamma_N = \operatorname{tg} \gamma_{ax} / \sin \varphi = \operatorname{tg} \omega / \sin \varphi$$

Hence, for a given value  $\gamma_N$  a helix angle of flutes is  $\operatorname{tg} \omega = \operatorname{tg} \gamma_N \sin \varphi$ .

When designing the new core drills the following values of these angles are recommended: cutting of steels  $\gamma_N = 8 \dots 12^\circ$ , cast-iron  $\gamma_N = 6 \dots 10^\circ$ , non-ferrous metals  $\gamma_N = 25 \dots 30^\circ$ , hardened steels and cast irons  $\gamma_N = 0 \dots 5^\circ$ .

To increase the strength of the cutting edges of core-drills with brazed carbide inserts the **inclination angle** of the major cutting edge is  $+\lambda$  (Figure 5.17), protecting the insert nose from chipping. It is recommended to adopt angle  $\lambda = 12 \dots 15^\circ$ .

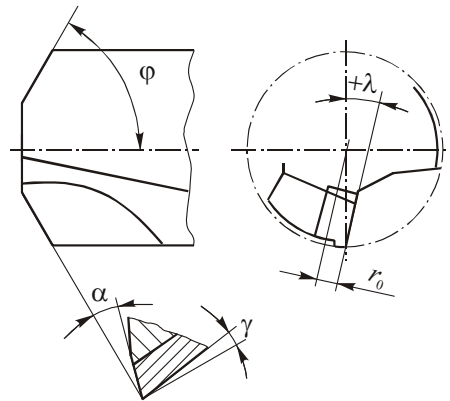


Fig. 5.17 Inclination angle  $\lambda$  of a core drill major cutting edge

**Clearance angle**  $\alpha$  of core drills, the same as for twist drills, is created by grinding the flanks as a part of plane, conical or helical surfaces. To control the axial run-out of cutting edges during the grinding or lapping the flank surface adjacent to the cutting edge is provided with a narrow margin with the width of  $0.03 \dots 0.05$  mm (Fig. 5.16, b). The run-out of the cutting edge should be within  $0.05 \dots 0.06$  mm.

**Diameter tolerance** of core-drills depends on the purpose of the core-drill and allowance for core-drilling. According to the purpose, size and location of the diameter tolerance the core-drills are distinguished as follows: core-drill number 1 - for drilling holes for subsequent reaming and core-drill number 2 - for finishing holes.

**Assembled core-drills** are provided with blades or inserts to save tool materials. The inserts are clamped in tool body that is made of structural steel. Assembled core-drills are typically mounted on the arbor with the hole taper 1:30 and end key (Fig. 5.18, b).

Core-drill cutting inserts are made of high speed steel or with brazed carbide inserts.

Core-drill body is provided with wedge-shaped flutes with angles  $5...7^\circ$ , in which the serrated inserts are set (Fig. 5.18, a). When a core-drill is worn it is possible to adjust its diameter with the help of the serrations. The disadvantage of this design is the inability to control the axial position of the inserts. To overcome this shortcoming, core-drills are supplied with wedges (Fig. 5.18, b). Here the inserts and wedges are inserted into the flat flutes so that it is possible to adjust both the diameter of a core-drill and axial position of the inserts.

Solid carbide core-drills are used for small diameter holes ( $d=8...20$  mm).

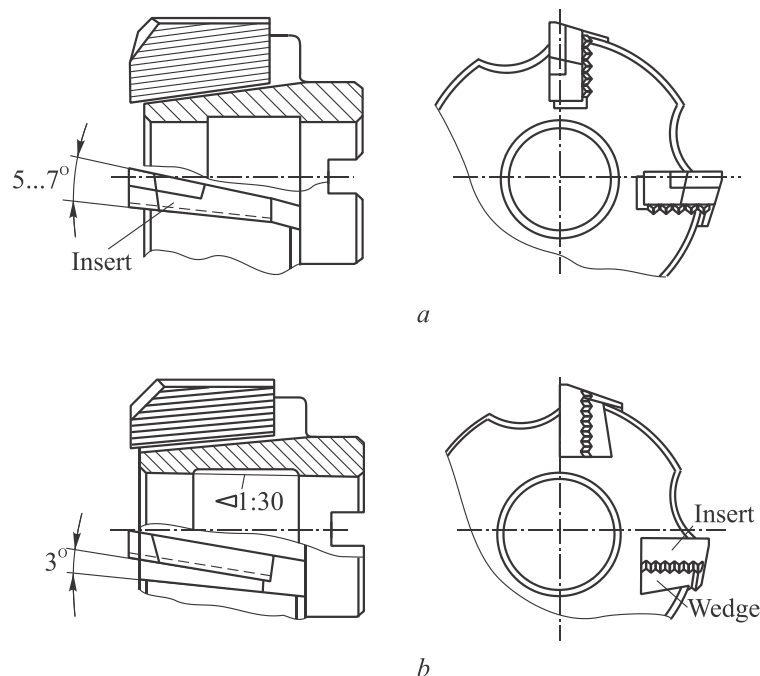


Fig. 5.18 Inserts clamping: (a) wedged serrated inserts; (b) flat inserts with wedges

### 5.2.2 Counter bore, countersink and spot facer

Countersinks and counter bores, in contrast to standard core-drills, cut chips of greater width and have a less stable position in the radial direction during the entering the hole, especially in the case when the cutting edges lie perpendicular to the axis of the tool. Thus, the counter boring is often accompanied by chatter and, as a consequence, by chipping of cutting edges. Therefore, to guide the counter bore in a hole the pilot is used, which is made either as a part of the body of small diameter counter bores, or as an inserted-type for indexable large diameter counter bores, which is more preferable. During the counter boring, a pilot enters the pre-drilled hole, and then the cutting edges start to cut the hole to the desired shape.

Counter bores are made of high speed steels, and sometimes are equipped with brazed carbide inserts. Shanks are welded with the cutting part and may be of straight or tapered.

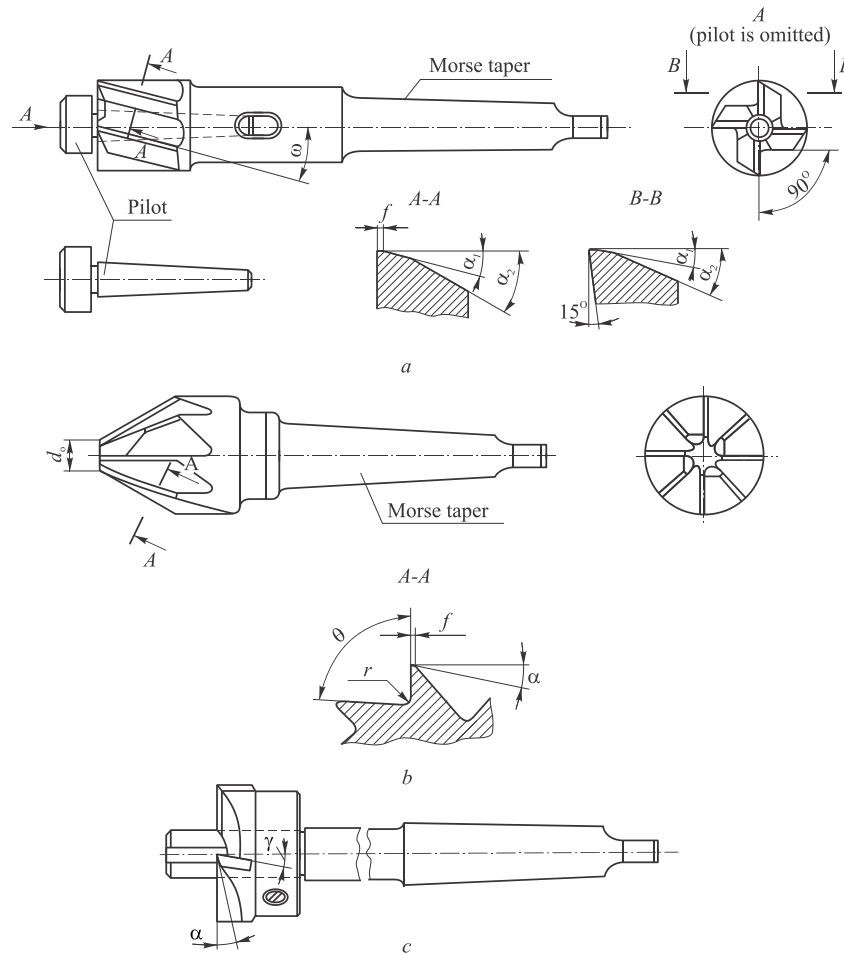


Fig. 5.19 Core drills: (a) counter bore; (b) countersink; (c) spot facer

Fig. 5.19 shows a counter bore with a replaceable pilot and helical flutes ( $z=4$ ) that is used for producing cylindrical holes. The major cutting edges are located at the end, and minor cutting edges on the periphery of the tool. The flank surfaces are double-planed with primary and secondary clearance angles  $\alpha_1=8^\circ$ ,  $\alpha_2=30^\circ$ , and rake angle  $\gamma=\omega=15^\circ$ . Teeth are sharpened with the smallest edge radius possible. Margins are produced on the minor cutting edges with width  $f=0.3$  mm and double clearance angles  $\alpha_1=8^\circ$ ,  $\alpha_2=30^\circ$ .

Countersinks used for conical holes have major cutting edges located on the conical surface (Figure 5.19, b) with flat rake surfaces located at an angle  $\gamma=0^\circ$ . According to the diameter ( $d=12\text{...}60$  mm) the number of teeth is  $z=4\text{...}12$ , and the point angle is chosen respectively according to the shape of the hole and more often is equal to  $2\varphi=60^\circ, 75^\circ, 90^\circ, 120^\circ$ . The diameter of the countersink at the point is  $d_0=(0.15\text{...}0.18)d$ , the angle of the flute gash is  $\theta=90\text{...}75^\circ$ . The cutting edge is sharpened very sharply or a narrow margin is left with width of  $f=0.03\text{...}0.05$  mm and the clearance angle  $\alpha=12^\circ$ .

Spot facers used for cutting flat surfaces have cutting edges only at the end. Minor cutting edges are absent (Fig. 5.19, c). Spot facers are manufactured as shank-type or shell-type. Spot facers are equipped with brazed carbide inserts for cast-iron cutting. The guide pilots are made either assembled or integral with the body of the tool. The spot facer diameter is  $d=14\text{...}40$  mm. Number of teeth is even and equal to 2 or 4 because of the hard work conditions. To improve work conditions of a spot facer, which cut with long cutting edges, it is recommended to cut the staggered chip breaking notches on the cutting edges.

### 5.3 Reamers

Reamers are axial multiple point cutting tools used for finishing of the holes. The dimensional accuracy after reaming is IT8...IT6 and surface finish  $Ra1.25\text{...}0.32$  microns. The best results are obtained by double reaming, when the first reaming removes two thirds of the allowance, and the second one removes the remaining 1/3.

Kinematics of reaming is similar to drilling and core-drilling. In contrast to core-drills, reamers have more teeth ( $z=6\text{...}14$ ) and, as a consequence, the best guiding in the hole. They removes significantly less allowance ( $t=0.15\text{...}0.50$  mm) than by countersinking. To achieve the minimum surface finish the reamers work at low cutting speeds ( $v=4\text{...}12$  m/min), i.e. when there is no built-up edge. Nevertheless, productivity of reaming is quite high due to large number of teeth, thus the working time is reduced:

$$t_M = L_o / s_z z n,$$

where  $L_0$  is the length of the machined hole, mm;  $f_z$  is the feed per tooth, mm;  $z$  is the number of teeth;  $n$  is the rotational speed of the reamer or workpiece,  $\text{min}^{-1}$ .

To reach high accuracy of the holes the reamers are manufactured with tolerances narrower as compared to core-drills and the holes for reaming are either drilled, core drilled or bored. The reaming directly after the drilling is used only in the machining of small diameter holes (less than 3 mm).

Reamers are classified according to:

- drive type – hand and machine;
- method of mounting – shank-type or shell-type;
- type of the hole – cylindrical and tapered;
- tool material – high-speed steel, carbide and diamond;
- design – solid, assembled and indexable.

Hand reamers (Fig. 5.20, a) machine the hole by the rotation of the tool manually by a tap-wrench. These reamers ( $d=3\text{...}40$  mm) are usually made of tool steel grades. A starting taper of greater length and a sizing part of the reamer are designed to get better reamer guidance in the hole. The rest part of the hand reamers doesn't differ from the machine reamers.

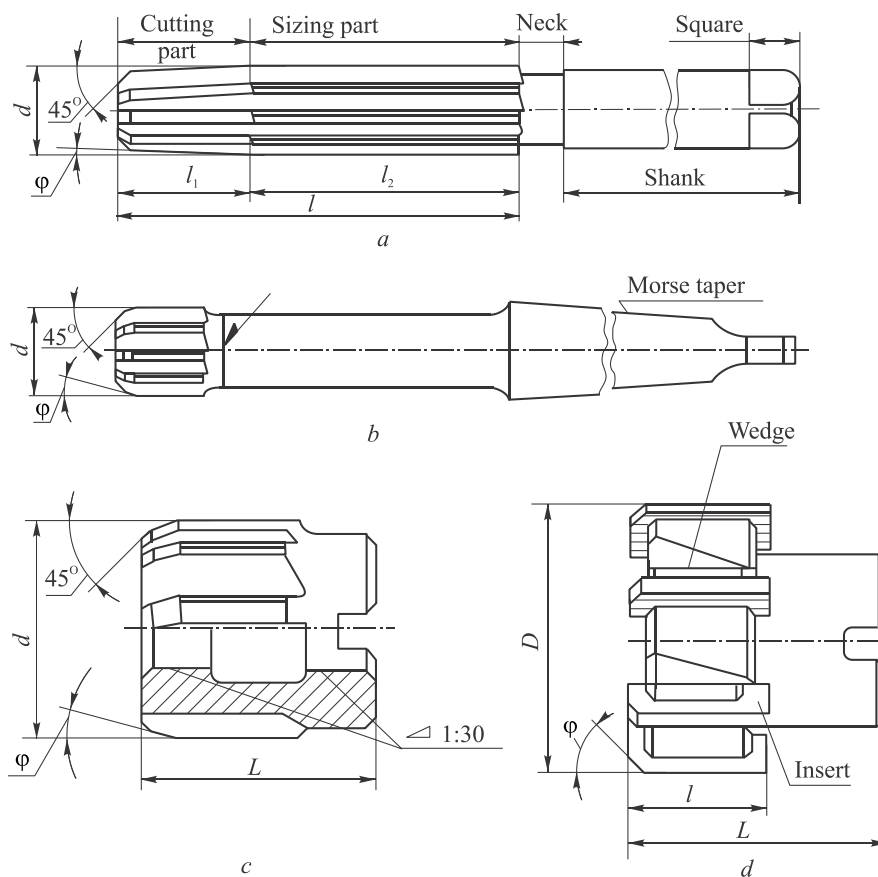


Fig. 5.20 Reamers: (a) hand-type; (b) machine-type; (c) shell-type; (d) inserted

Machine reamers of end-type and shell-type either solid and inserted (Fig. 5.20, b, c, d) are used for machining holes on drilling and turning machines, turret lathes, coordinate boring machines and other machine tools. Shanks of the machine reamers can be either straight ( $d=1\text{...}9$  mm) or tapered ( $d=10\text{...}32$  mm) with a relatively long neck and a Morse taper. Shell-type reamers are mounted on the arbour. The tapered hole of the spindle (taper 1:30) ensures high accuracy concentricity. Key slot is cut on the face of the reamer for torque transmission.

### 5.3.1 Straight reamers

**Working part** of straight reamers (Figure 5.20) consists of cutting and sizing parts. The chamfer cut at an angle  $\varphi=45^\circ$  facilitates entry of the tool into the hole and protects the cutting edges from damage. Chamfer is followed by the **starting taper** with a cutting edge angle  $\varphi$ , where teeth remove reaming allowance. The chamfer and starting taper constitute the **cutting part** of the reamer.

**Cutting edge angle**  $\varphi$  of the starting taper has a great influence on the working conditions of the reamer, as it defines the relationship between the width  $b$  and thickness  $t$  of the layer that is being cut with each tooth of a reamer. Angle  $\varphi$  also defines the thrust force for the process. With decreasing angle  $\varphi$  the thrust force is decreases and a smooth entry and exit of the reamer out of the hole is provided. For these reasons, hand reamers have the angle  $\varphi$  equal to  $1\text{...}2^\circ$ . Machine reamers for cutting of steels have the angle  $\varphi=12\text{...}15^\circ$ , for cutting of cast-iron  $\varphi=3\text{...}5^\circ$  and for blind holes  $\varphi=45^\circ$ .

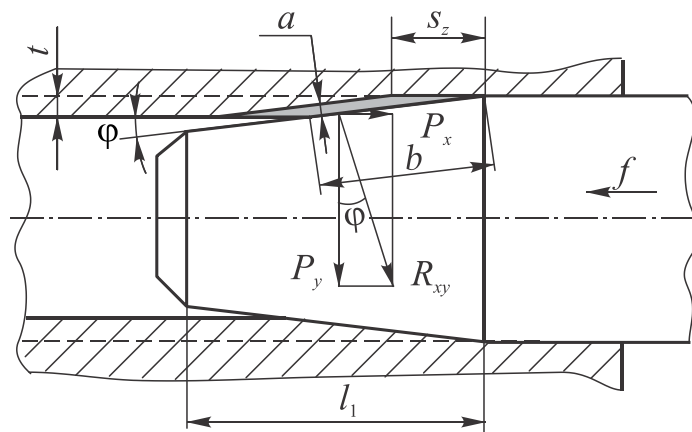


Fig. 5.21 Radial  $P_y$  and axial  $P_x$  cutting force components, and dimensions of the uncut chip in reaming

**Sizing part** of the reamer is cylindrical approximately up to the half of the length  $l_2$ . The rest of the sizing part is sharpened with a small back taper. Back taper is needed to reduce the oversizing of the hole during reamer exiting the hole. Since the oversize of the reamed hole is small, the back taper for short sizing part is sometimes done immediately after the starting taper, without leaving the cylindrical portion.

In reaming high precision holes it is necessary to consider the radial run-out of the reamer teeth, which should not exceed 0.01...0.02 mm.

Number of reamer teeth is adopted depending on the diameter  $d$  of the reamer. So for example:

$$z = 1,5\sqrt{d} + (2..4) \text{ for a solid reamer;}$$

$$z = 1,2\sqrt{d} \text{ for an assembled reamer.}$$

Calculated teeth number  $z$  is rounded up to the nearest whole even number to facilitate the measurement of the reamer diameter. And a number of teeth of assembled reamers are decreased due to the necessity to use auxiliary elements for the blades clamping.

The spacing of teeth on the outer circumference of the reamer is recommended to make irregular to reduce the faceting and improve surface finish of the reamed hole (Figure 5.22). The diametrical located angles are taken equal for convenient measurement of the reamer diameter.

In addition to the values of the angular pitches, outlined in Fig. 5.22, other values are also possible, depending on the diameter and a number of teeth of the reamer.

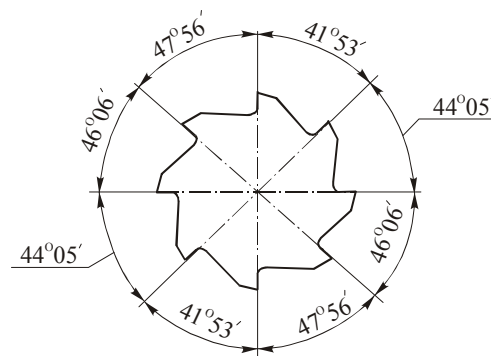


Fig. 5.22 Reamer teeth spacing,  $z=8$  (GOST 7722-77)

**Flutes** of a reamer are usually straight with teeth ground at a rake angle  $\gamma=0$ . In reaming ductile materials the teeth are sharpened with positive angles  $\gamma=5...10^\circ$  in order to avoid the adhesion of chips and scuffing of the machined surface.



Clearance angle equal to  $\alpha=5...12^\circ$ , is obtained by plane sharpening of the flank surfaces. Moreover, in contrast to other types of tools, the smaller value of this angle is recommended for finishing, and greater values – for roughing.

The teeth on the starting taper are sharpened very sharply and narrow cylindrical margins with width of 0.08 ... 0.40 mm for reamers  $d=3...50$  mm are left on the sizing part. They are carefully honed, which ensures smoothing of asperities of the machined surface and prevents the adhesion of small chips that worsen the surface finish of the holes and reduce life of reamers.

A negative value of the thrust force can be appeared due to the thin thickness of the layers being removed in reaming. The hand of helical flutes of the reamer should be reversed to the hand of the reamer rotation, to avoid self-pulling and jamming of the reamer in the hole, i.e. left handed flutes for right-handed reamer and vice versa. In this case, the roughness of the machined surface improves and the feed thrust increases. Hand reamers are allowed to have the same handedness of the helical flutes and the rotation, as they work with smaller feed rates.

**Mounting of the reamers** on the machine tools should provide matching of the reamer axis, guide bushing and a hole being machined. The errors induced by rotational motion (run-out, oversizing, etc.) would be transferred to the workpiece in case the reamer is rigidly mounted directly in the spindle of the machine tool. Best results are gained by mounting of the reamers into the floating chucks. There are many constructions of such chucks. The best accuracy is provided by chucks that provide not only rocking of the reamer in two planes, but the displacement, parallel to the axis of rotation of the workpiece as well. The values of the reamer displacement must be small, since in the opposite case, the reamer exiting out of the hole increases the oversize of the latter.

Forced guiding of the reamers with the help of the cylindrical guides mounted before or behind the working part is used to ream precise holes with high straightness.

**Tolerances of the reamer diameter** must be very small, about 3 times smaller than the tolerances of the machined hole due to the fact that the reamer is a finishing tool that provides high dimensional accuracy (IT8...IT6).

The upper and lower deviations of a new and lower deviation of a worn reamer are determined accounting to the possibility of occurrence of positive or negative hole oversizing in reaming.

Diameter of the reamed hole with a positive over-size is greater than a reamer diameter. The main reasons of this oversize: 1) misalignment of the

reamer axis and machined hole axis; 2) run-out of the cutting edges; 3) built-up edge and small chips adhered to the margins, etc.

Negative oversizing is a reduction of the hole diameter after the reaming. It is less common and occurred in reaming of the thin-walled workpieces, reaming of ferrous metals due to elastic deformation of the part material, as well as in reaming with carbide reamer of the hardened steels due to high cutting temperature and thermal deformation of the part.

### 5.3.2 Reamers of other types

In repair shops the adjustable cylindrical hand reamers are commonly applied. One design of the reamer is shown in Fig. 5.23, a. The body of the reamer has a hole 3 consisting of conical and cylindrical parts, in which the ball 2 is placed. The ball is moved by the adjustment screw 1 along the reamer axis. Long slots between the teeth are cut to permit the elastic deformation of the teeth. Due to the elastic deformation of the reamer walls, the diameter of the reamer sizing part increases with the ball being displaced by the screw. The value  $\Delta$  of diameter adjustment is small and is adopted according to the diameter of the reamer, for example,  $d=10...20$  mm  $\Delta=0.25$  mm,  $d=20...30$  mm  $\Delta=0.4$ ,  $d=30...50$  mm  $\Delta=0.5$  mm.

The diameter of the shell assembled machine reamers (Fig. 5.23, b) can be adjusted by shifting the position of the blades in the serrations.

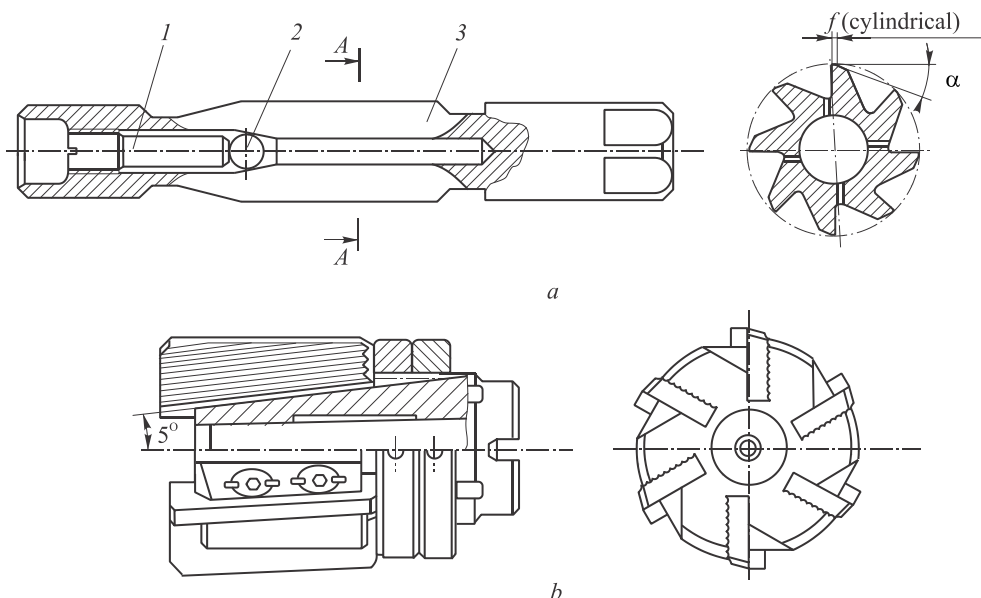


Fig. 5.23 Adjustable reamers: (a) hand-type; (b) shell indexable machine reamer

There are other designs of assembled reamers. It should be noted that the grinding and finishing of the reamer teeth are needed after each adjustment, as reamer accuracy can't be provided only by adjustment.

**Rivet hole reamer** (Figure 5.24) is used for machining holes for riveting two or more sheets together. They are widely used in boiler, ship and aircraft manufacture, as well as in manufacturing of bridge structures.

Rivet hole reamers work under heavy conditions. A large allowance - up to 1...2 mm per radius is needed to be removed due to unavoidable misalignment of holes axes in the sandwiches. Moreover the materials being machined are usually ductile and gummy.

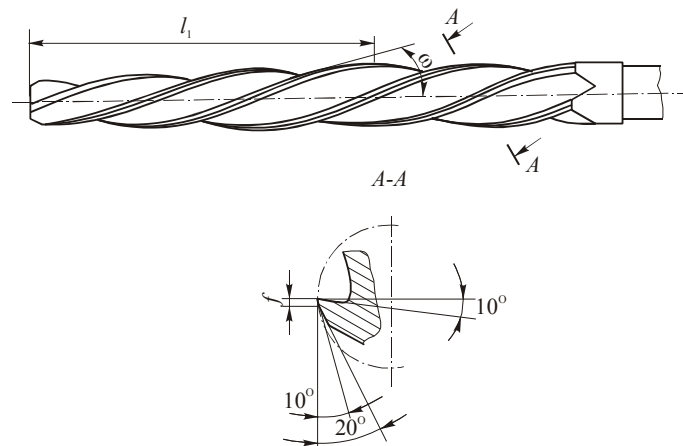


Fig. 5.24 Rivet hole reamer

Helical teeth with a helix angle  $\omega=25...30^\circ$  and handedness opposite to the rotation of the tool are used for a better guiding of reamers in the hole, as well as to reduce the axial thrust and improve surface finish of the machined hole. Rivet hole reamers have a low angle of the starting taper equal to  $2\varphi=3...5^\circ 30'$  and, therefore, a greater length of the cutting part equal to  $1/3...1/2$  of the working part length of the reamer. Number of teeth is  $z=4...6$  for the reamer diameter of  $d=6...40$  mm. Rake angle of the teeth in a section perpendicular to the helix is  $\gamma=12...15^\circ$ , clearance angle is  $\alpha=10^\circ$ . The teeth on the sizing part have a narrow margins of width  $f=0.2...0.3$  mm with the back taper of  $0.05...0.07$  mm per 100 mm of length.

Rivet hole reamers are made either a hand-type with a straight shank and machine-type with a tapered shank that is used to mount the reamer on radial drilling machines or in pneumatic drills.

**Taper reamer** is used to obtain exact tapered pin holes (taper 1:50), Morse tapers and metric tool mounting holes of shell core-drills and reamers (taper 1:30) and others. Taper holes are formed either from cylindrical holes, made by drilling or from taper holes, created by boring of very steep tapers, such as taper 7:24.

Working conditions of such reamers are very heavy, i.e. length of cutting edges, removing the allowance is large and equal to the length of the taper, and the thickness of the layer being removed is determined by the difference in cone diameters.

In contrast to cylindrical, the taper reamers have no division of the cutting and the sizing parts, as the teeth located on the conical surface are both cutting and sizing.

Reaming of the holes with taper larger than 1:20 is possible only with the help of a set of reamers (Figure 5.25), since the amount of allowance being removed is considerable.

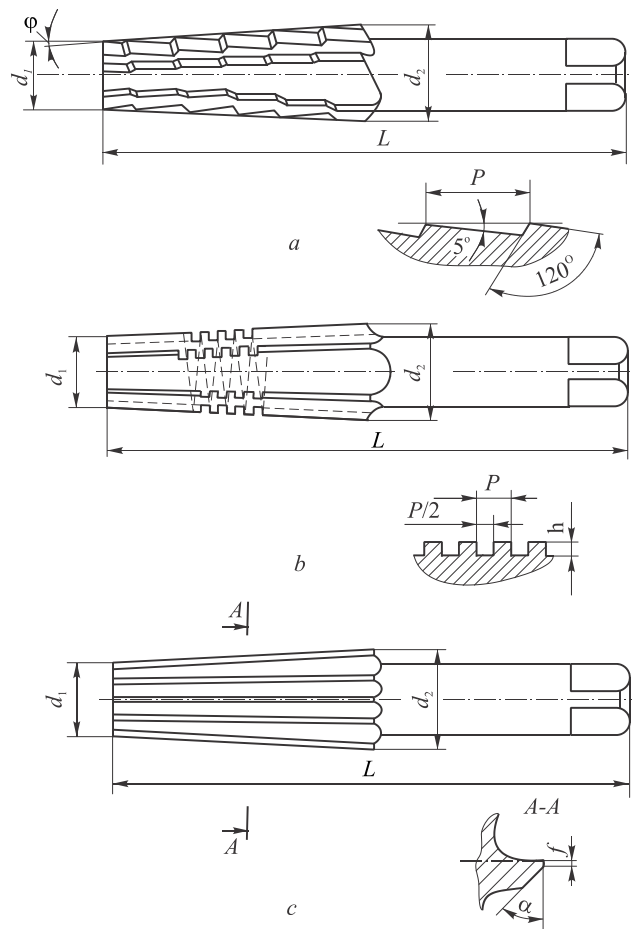


Fig. 5.25 A set of taper reamers:  
 (a) roughing (№1); (b) semi-finishing (№2); (c) finishing (№3)

Reamer №1 is roughing and has stepped shape of the teeth, located along the helical surface, which has the same hand as the hand of the tool rotation. Allowance is removed with cutting edges located on the faces of the teeth, the same as in core-drilling. Cylindrical hole is turned into stepped hole after the roughing reaming.

Reamer №2 that is intermediate or semifinish has the shape of the machined hole. Its cutting edges are supplied with small notches cut as rectangular thread with handedness opposite to the rotation of the tool.

Reamer №3 is finishing and has straight teeth along the length of the cutting part. Margins with the width of 0.05 mm are used for better alignment of the reamer in the hole. This reamer ensures cutting of the residual part of allowance and sizes the hole.

Taper reamers have straight flutes and rake angle of the cutting edges is  $\gamma=0^\circ$ . Flank surfaces of the reamer №1 teeth are form-relieved, flanks of reamers №2 and 3 are sharpened at an angle  $\alpha=5^\circ$ .

Self-piloting reamers are made with one or more cutting edges and guide pads. Due to the smoothing action of carbide guide pads, which withstand the radial component of the cutting and friction force and guide the single blade reamer, the high accuracy and low roughness of the machined surface is achieved. One example of such reamers is shown in Fig. 5.26.

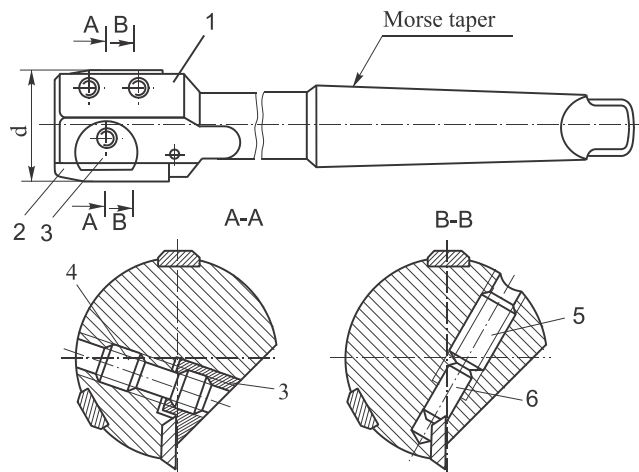


Fig. 5.26 Self-piloting carbide gun reamer

## 6. Design and Calculation of Milling Cutters

Milling cutters – are multiple point cutting tools used to machine planes, slots, special shaped surfaces, circular parts, as well as to cut-off parts.

In the process of milling, several teeth are engaged with the workpiece, removing chips of variable thickness. High performance of milling process is provided due to the large total active length of the cutting edges. Higher speeds in milling help to increase productivity, due to periodic exit of the teeth from the cutting area, providing cooling and removal of thermal stress in the cutting wedge.

Kinematics of milling is simple: a milling cutter is rotated by the main drive, and a workpiece, mounted on the machine table is fed by the individual drive of machine tool, which isn't kinematically connected with the rotation of the milling cutter. Feed movement can be linear, rotary or helical and mill cutting edges can be straight, inclined to the axis, helical or of special form. This causes a huge variety of milling cutter designs and a wide range of their applications.

Milling cutters can be classified according to the following criteria:

- 1) design of the cutting teeth and the method of their sharpening: cutters with chisel-shaped (common) teeth, which are reground on the flank surface, and cutters with form-relieved teeth, which are reground on the face;
- 2) shape and location of the cutting edges relatively to the axis of revolution of the tool: plain, side, face, end, angle and form milling cutters (Fig. 6.1);
- 3) teeth position relatively to the axis of the milling cutter: straight, helical and inclined teeth;
- 4) method of mounting on the machine tool: shell mills with a hole for the arbor, and end-mills with a straight or tapered shank;
- 5) mill design: solid, assembled and indexable with inserted teeth, including soldered, welded or mechanically clamped cutting inserts from carbide or super hard materials.

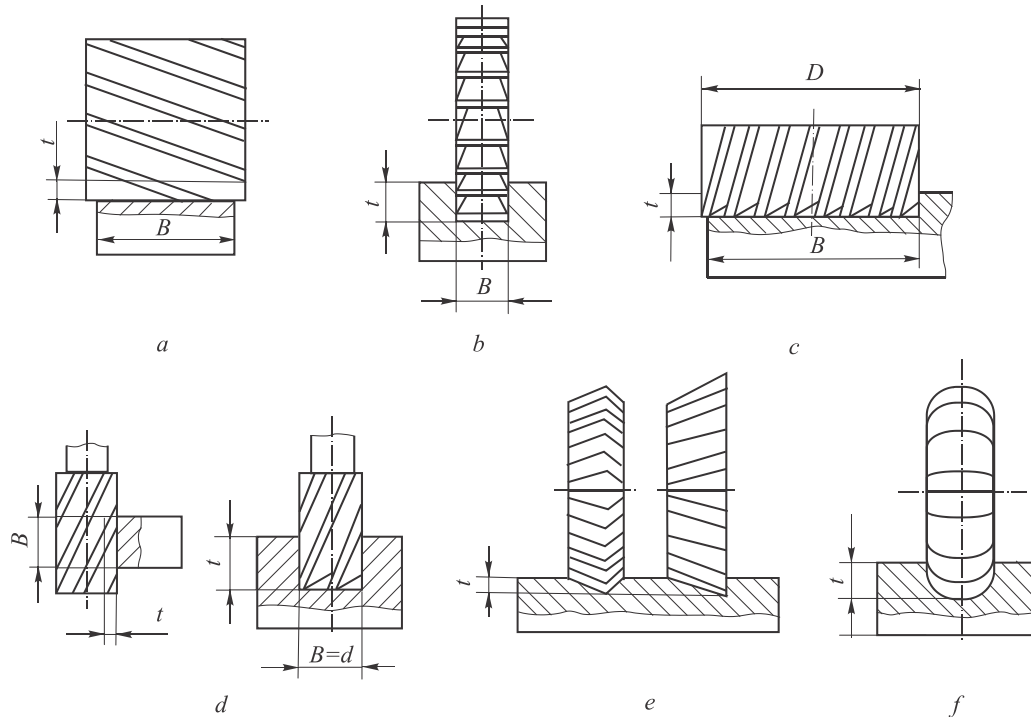


*Fig. 6.1 Milling cutters: (a) plain cutter; (b) side cutter; (c) face mill; (d) endmills; (e) angle cutters; (f) form milling cutter*

### 6.1 Milling cutters with pointed teeth and form-relieved teeth

It has been mentioned that according to the teeth design the cutters are divided into two groups: pointed (or common) teeth and form-relieved teeth (Fig. 6.2). The principal differences of these mills are in the process of sharpening, number of teeth, its shape, complexity of manufacturing, durability, performance and surface finish.

Milling process is characterized by the removal of thin chips of variable thickness. The chip thickness of the plain milling cutters starts from zero thickness. Regrinding of the pointed teeth by the flank surface, on which the wear occurs more often in milling, helps to reduce the allowance for regrinding, extend the life of milling cutters, reduce the sizes of teeth and, the most important – to increase the teeth number  $z$ , which impacts on the productivity of the milling process proportionally.

With the number of teeth increasing the surface finish and uniformity of the milling process improves.

The shape of the milling cutter teeth should be as: 1) to provide the necessary strength of the teeth; 2) to provide higher number of permissible regrinding; 3) to provide enough volume of the flutes between the teeth to accommodate the chips.

Three forms of pointed teeth became widespread in practice: 1) trapezoid; 2) parabolic; 3) reinforced.

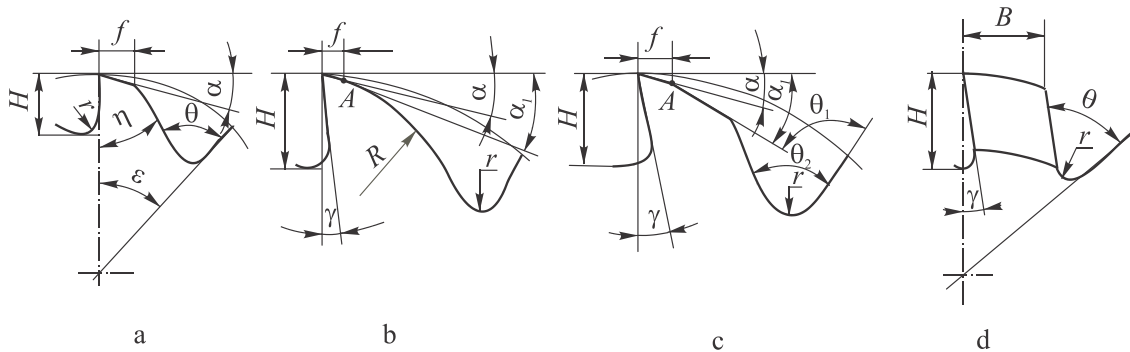


Fig. 6.2 Shapes of the milling cutters teeth: (a) trapezoid; (b) parabolic; (c) reinforced; (d) from-relieved

**The trapezoid shape** (Fig. 6.2, a) is the simplest to be manufactured, but the tooth is weakened a little, and therefore has a low height and low volume of chip gash. Resharpener of the tooth on the clearance surface, that is in the form of the land with width  $f=1...2$  mm, reduces the height of the tooth and, thus make it stronger. However, this form of teeth allows a small number of regrinding and is used for the finishing cutters. Moreover, the number of teeth due to their small size can be as large as possible. The gashes in such milling cutters are machined by milling or grinding with PCBN or diamond wheels from a solid blanket on CNC machines.

Tooth height is reduced during the regrinding, so the total life of these mills is low as they allow only 6...8 regrindings. Tooth root radius or fillet is taken equal to 0.5...2.0 mm.

**Parabolic shape of the tooth** (Fig. 6.2, b) has the highest bending strength, as the tooth back, made as a parabola, provides uniform strength in all sections at the height of the tooth. The disadvantage of this shape is the necessity for each tooth height to have its complex form milling cutter to cut the flute. Therefore, a parabola is often replaced by the arc of a circle with a radius  $R=(0.3...0.4)d$  to simplify the shape of the tooth back.

A straight line portion of the rake surface defines the number of permissible regrinding. Regrinding is allowed only on the flank surface (land  $f$ ). The clearance angle  $\alpha$  must be less than the angle  $\alpha_1$  by 10...15° ( $\alpha_1$  – an angle between the tangent to the parabola at point A and cutting edge plane). Failure to comply with this condition during resharpener leads to great variation in the width of the margins.

**Reinforced shape of the tooth** (Fig. 6.2, c) is used for heavy-duty milling instead of a parabolic shape. This tooth has a faceted back, and an increased thickness and height. These teeth are shaped by double milling with



angle cutters, which have angles  $\theta_1=28\dots30^\circ$  and  $\theta_2$ . Although the number of operations is doubled, such teeth are easier to make than parabolic. They have a greater number of regrindings and higher strength. A standard flute milling cutters are used, which cutting edges are straight. During the regrinding the teeth are sharpened on the flank surface at an angle  $\alpha$  and with obligatory sparking-out in order to avoid run-out of the cutting edges. Sometimes small cylindrical margins with width  $f_M=0.02\dots0.03$  mm are left, which simplify the control of run-out of cutter teeth.

**Form-relieved tooth** (Fig. 6.2, d) differs by having a greater thickness, and mainly by the different shape of the flank surface, which is performed on a special operation called **relieving**, which is used to create clearance angles in all points of the cutting edges. This is achieved by the fact that the radial section of the tooth with profiled section during its rotation is shifted towards the center by the relieving cutter or a grinding wheel. Due to relieving the profile of the cutting edge after the resharpening on the face will be same in all radial sections regardless of its complexity. These are the main advantages of such mills, along with a very simple operation of resharpening. Moreover, the teeth of this form have high strength, and during the process of resharpening the amount of flutes for chips location are increased, which is beneficial to the work of the cutter. At the same time, the cutters with form-relieved teeth have a number of drawbacks, the most important of which are:

- 1) the number of teeth of the form-relieved cutters are significantly less compared to cutters with pointed teeth. Form-relieved teeth are considered to have a greater thickness, since regrinding the rake surface a big allowance is cut in order to get rid of wear, which is focused on the flank surface of the tooth;
- 2) after regrinding, a large radial run-out of the teeth is observed, which leads to worse surface finish and reduced milling cutter life;
- 3) decarbonized areas on the flank surfaces are left after heat treatment of the cutters with unground tooth profile, i.e. reducing their life;
- 4) residual thermal stresses can cause distortion of the profile of the cutting edges.

Because of these disadvantages the cutters with form-relieved teeth are inferior by productivity and surface finish to cutters with pointed teeth. However, due to the ease in resharpening they are widely used in the milling of curved or form surfaces.

The process of relieving is used to create the clearance angles on the cutting edges of form cutters, carried out on special machines according to the scheme (Fig. 6.3). The milling cutter rotates around the axis and a relieving cutter performs reciprocating movements. A cutter approaches the center

of the milling cutter while it revolves at  $1/z$  of the complete revolution, and then instantly moves away from the milling cutter after cutting of a tooth flank, and then approaches to the next tooth. This creates clearance angles at all points of the cutting edges, and when resharpenering on the rake surface their shape will remain unchanged in radial section.

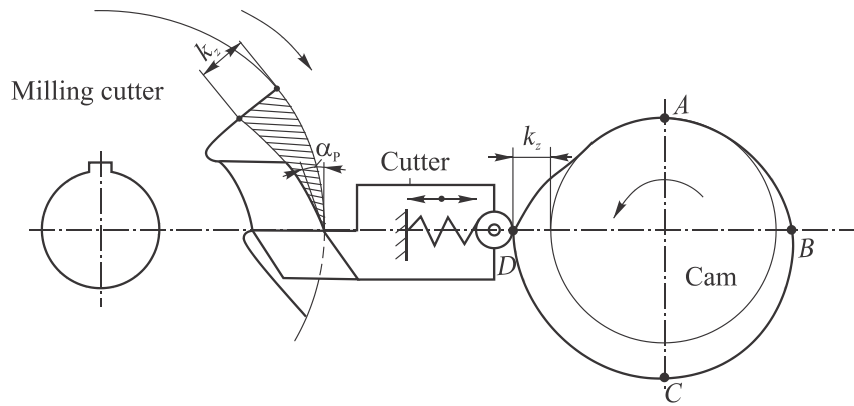


Fig. 6.3 Form-relieving (relieving cutter is at the end of relieving motion)

The curve of the relief is defined by the shape of the cam (refer to Fig. 6.3), which controls the movement of the tool as the milling cutter rotates. A part of the cam ABCD determines the working stroke of the relieving cutter, and the part DA defines an idle stroke, when the cutter departs from a tooth of the mill. The resulting curve of relieving defines the picture of changes of the clearance angles during the process of regrinding and their value at different points on the cutting edge along the tooth height.

Among well-known curves applied for relieving (logarithmic and Archimedean helixes, etc.), Archimedean spiral meets these requirements the best, thus it is the most frequently used in practice.

An important parameter of the relieving curve is the radial relief value  $k_z$ , which depends on the value of the clearance angle on the top of the tooth  $\alpha_p$ , cutter diameter and the number of teeth.

As can be seen from Fig. 6.3, the value  $k_z$  is measured on the face of the next tooth from the point of intersection with the relieving curve up to the corner of the tooth, which lies on the cutter periphery. Hatched area (Figure 6.3) is the amount of metal that is removed at the top of the tooth by relieving.

The radial relief value can be expressed as:

$$k_z = \frac{\pi d}{z} \operatorname{tg} \alpha_p. \quad (6.1)$$

## 6.2 Types of milling cutters

The design features of **plain milling cutters** and **side milling cutters** are the location of the major cutting edges on a cylinder which axis coincides with the axis of rotation of the tool that is parallel to the workpiece surface. Plain milling cutters do not have minor cutting edges, and they work in free cutting conditions. The teeth of side milling cutters, on the contrary, have minor cutting edges positioned on one or both faces. Moreover, in contrast to the plain milling cutters, their diameter is much larger than the cutter length. Both types of milling cutters, as a rule, are shell or arbor-type cutter, with a hole and keyways for mounting on an arbor.

Teeth of the plain milling cutters are often made helical to reduce variation of cutting forces and vibrations. This gives a rise to unwanted axial component of the cutting force. However, the conditions of chip removal from the cutting area are much better when the helical teeth instead of straight ones are used.

Plain milling cutters with coarse teeth are designed to remove large allowances and particularly effective in the machining of extended surfaces. In order to save high-speed steel the milling cutters of larger diameter are assembled with inserted cutting teeth, and milling cutter bodies are made of structural steel.

Side milling cutters, in contrast to the plain milling cutters, are designed to machine narrow surfaces, shoulders, to cut slots, cut off the part, etc. Milling cutters work under difficult conditions of non-free cutting, often accompanied by chatter due to low transverse rigidity of the cutter bodies and unfavorable chip removal from the cutting zone.

The following types of side milling cutters are distinguished: half-side cutter, side cutter, slotting cutter, slitting cutter and cut-off cutters (saws).

Cutting edges of the teeth of half-side milling cutters are located on the periphery and on a single side (Fig. 6.4, a). The side milling cutter has teeth on the periphery and on the both sides as well (Fig. 6.4, b). These cutters can machine, respectively, two or three surfaces of slots or shoulders. They are made with fine teeth for finishing and coarse teeth for roughing. The latter are characterized by removal of large amounts of metal from the deep slots, so they have bigger flutes. The teeth of the mills with small width of cutting edges are straight, or inclined to the axis. The latter provides a more uniform milling, have favorable geometry of the teeth and better chip removal.

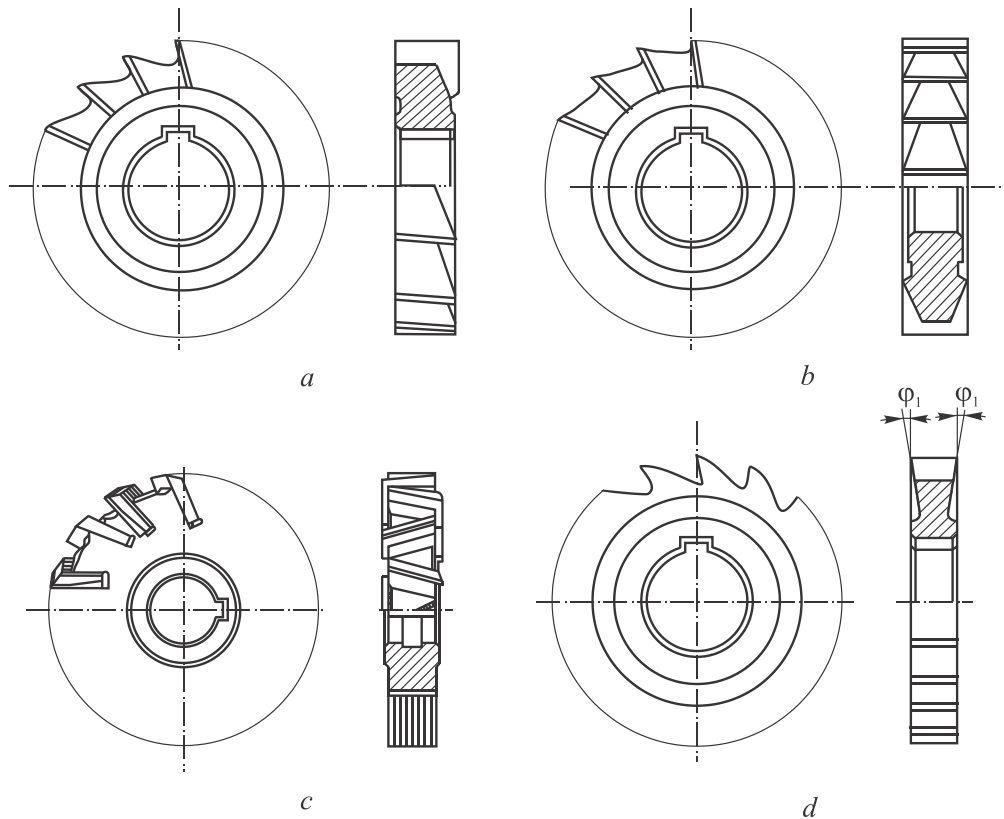


Fig. 6.4 Side milling cutters: (a) half-side cutter; (b) side cutter; (c) side cutter with staggered inserts; (d) slotting cutter

Side milling cutters are made with staggered teeth, which allows to create positive rake angles  $\gamma > 0$  on the side edges (Fig. 6.4, c). Regrinding of the cutter decreases its width, thus to avoid this drawback the dual cutters consisting of two halves with a spacing bush between them are also used. Solid milling cutters are manufactured with diameters  $d = 63 \dots 125$  mm and widths of  $B = 6 \dots 28$  mm. Assembled cutters with inserted blades have  $d = 75 \dots 200$  mm and  $B = 12 \dots 60$  mm. These blades are made of high speed steel and mounted in wedge-shaped flutes with serrations (Fig. 6.5, b).

**Slotting cutters** (Fig. 8.4, d) are used for milling slots of precise width. Slotting cutters are similar to side milling cutters in design, but have a shorter length of major cutting edges with  $\gamma = 10 \dots 15^\circ$  and  $\alpha = 20^\circ$ . Minor cutting edges that are located on the sides are sharpened with the minor cutting edge angle  $\varphi_1 = 1 \dots 2^\circ$ . Flutes are cut only on the periphery of the cutter. Slotting cutters are manufactured with a diameter of  $50 \dots 100$  mm and a width of  $3 \dots 16$  mm. Sometimes, they are made with relieved teeth to maintain consistency of the slot width  $B$  after the cutter regrinding.

**Slitting cutters and cut-off cutters (saws)** are similar to the slotting cutters in the shape of a tooth and are used for cutting shallow and narrow

slots, such as spline slots with width  $B=0.2\text{...}6.0$  mm as well as for cutting off parts of any profile and thickness. The sides of these cutters are provided with flutes with depth of 0.5 mm, to reduce friction and improve the penetration of coolant to the cutting area. Unlike other designs of slitting saws, the tooth back of the segment saw is a circular arc in shape, and regrinding is made on the rake surface with the help of special semi-automatic grinding machines. Here, the rake angle according to the hardness of the treated material is taken equal to  $\gamma=0\text{...}25^\circ$ . The worn segments of the saw are possible to replace with the new ones.

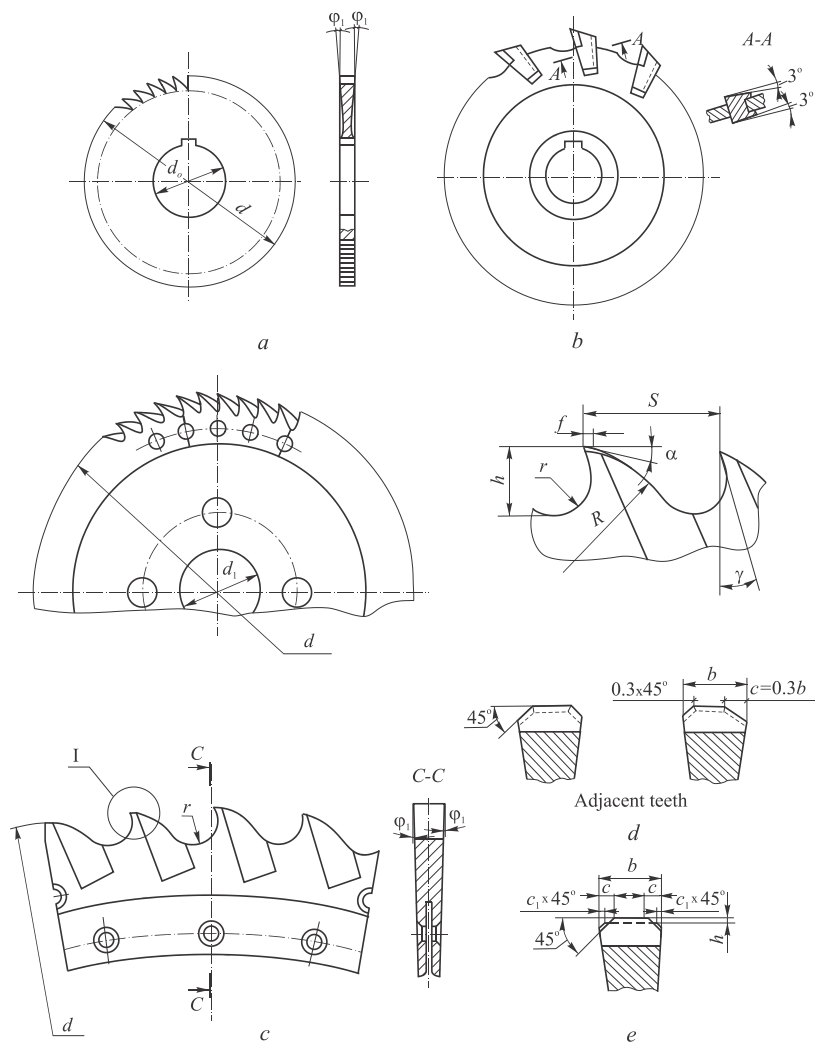


Fig. 6.5 Slot and cut-off cutters: (a) solid slot cutter (slitting) and cut-off cutter; (b) inserted slot cutter; (c) segmented cutter; (d) and (e) teeth form

**Face mills and end mills** (Fig. 6.1, c, d) have the axis of rotation perpendicular to the working surface. These cutters, in addition to the major cutting edges located on the periphery, have minor cutting edges located on the end of the cutter at an angle  $\phi_1$ . The face mills are usually manufactured as

shell-type cutters. When the cutter diameter is much smaller than the length, then the cutter is considered to be an end mill. Face mills are widely used in the machining of flat surfaces, including the stepped surfaces that can't be machined with plain milling cutters. Compared to the latter they provide the following advantages:

- 1) face mills can accommodate more teeth along the arc of engagement with the workpiece, resulting in greater productivity and more uniform cutting;
- 2) face mills can be made with rigid, massive bodies, with a reliable mechanical mounting of cutting elements, for example, in the form of carbide indexable inserts;
- 3) in milling the planes it is possible to achieve a lower roughness due to the large number of minor cutting edges on the face of the mill, which also can be made as wiper teeth with  $\phi_1=0$ .

Face mills are the most frequently used in metalworking due to these advantages.

The major cutting edge angle of face mills can vary widely, from  $90^\circ$  and lower. To improve the tool life and productivity the  $\phi$  angle can be reduced to  $45^\circ \dots 60^\circ$  and even up to  $10^\circ \dots 20^\circ$ . These mills are called face-conical, as the major cutting edges are on the conical face surface (Fig. 6.6).

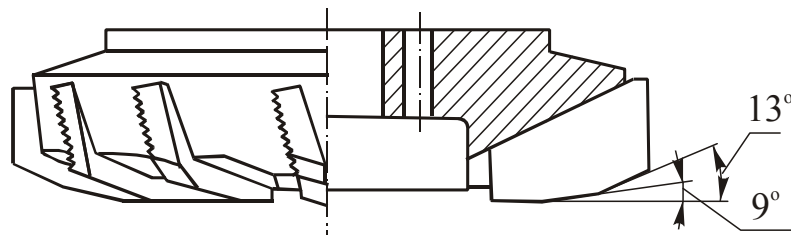


Fig. 6.6 face-conical inserted milling cutter

**End mills** are used for milling slots, shoulders and for contour machining. The major cutting edges that remove the allowance are located on the periphery, and the minor on the end. The teeth are usually made helical, with a helix angle reaching up to  $\omega=30 \dots 45^\circ$ . Such large angle value  $\omega$  along with large-volume flutes ensures a reliable chip removal out of the cutting zone, even under very restricted conditions of cutting. For this reason, the number of cutting teeth of the end mills is much smaller than that of face mills. However, the decrease in productivity is compensated by increasing the feed per tooth.

Fig. 6.7 shows a standard three-fluted end mill and its geometrical parameters. Shanks of such cutters are straight ( $d=3 \dots 20$  mm) or tapered with Morse taper ( $d=14 \dots 63$  mm). Shanks with 7:24 taper are used for mills of

larger diameters. Mounting of cutters with straight shank in the machine spindle is made with the collet chucks, tapered shank cutters with an internal thread are mounted with the help of tamper (pull bar) passing through the hollow spindle of the machine tool.

A **keyway end mill** and a **t-slot cutter** is a variety of end milling cutters, which are widely used in machining of work tables and bodies of the machine tools.

Keyway cutters (Fig. 6.7, b, c) have two teeth with deep flat or inclined ( $\omega=12\dots15^\circ$ ) flutes and the working length equal approximately to three cutter diameters. One of the cutting edges runs to the center of the cutter to provide axial feed in the milling. The diameter of the cutter web is increased to  $0.35d$ , which ensures the maximum rigidity of the cutter.

The special feature of the keyway cutter work is that the keyway is cut in several passes. At the end of each pass the keyway endmill plunges to a certain depth with the vertical feed. During plunging the cutting is done by cutting edges located on the end of the cutter, which are sharpened at an cutting edge angle  $\varphi_1=5^\circ$  and relief angle  $\alpha_1=20^\circ$ . Sharpening of the center edge of the HSS keyway mill is made to avoid a significant increase of the axial component of the cutting force. As for carbide brazed keyway end mills (Fig. 6.7, c), one of the edges reaches the center, and the other one is shorter and is separated from the center by a distance. This greatly simplifies the technology of manufacture and improves the cutting process.

Regrinding of keyway end mills is performed on the flank surfaces of the end cutting edges. The diameter of the cutter after regrinding doesn't change, which is necessary to maintain width of the milled slots constant.

Mills used for cutting T-slots (Fig. 6.7, d) work under difficult conditions and often failure because of chip jamming. To improve chip removal the mills are provided with staggered teeth positioned at an angle  $\varphi_1=1\dots2^\circ$ .

**Angle cutters and form milling cutters** with pointed teeth are similar to side milling cutters in the way of operation. These cutters are manufactured, as a rule, solid or of a shell-type and small-diameter mills are sometimes of a shank-type.

The major cutting edges of single-angle cutters are located on the surface of a truncated cone, while double-angle cutters have cutting edges on the surfaces of two adjacent cones. These cutters are mainly used as a second-order tools applied for cutting flutes in multiple-point cutting tools such as milling cutters, reamers, etc., and also for the milling different flutes, slots and inclined surfaces.

Form milling cutters have teeth with different in shape cutting edges that are located on the form milling cutter periphery. They work as side cutters or

angle cutters, and are designed for milling convex or concave surfaces, straight or helical flutes and various profiled surfaces.

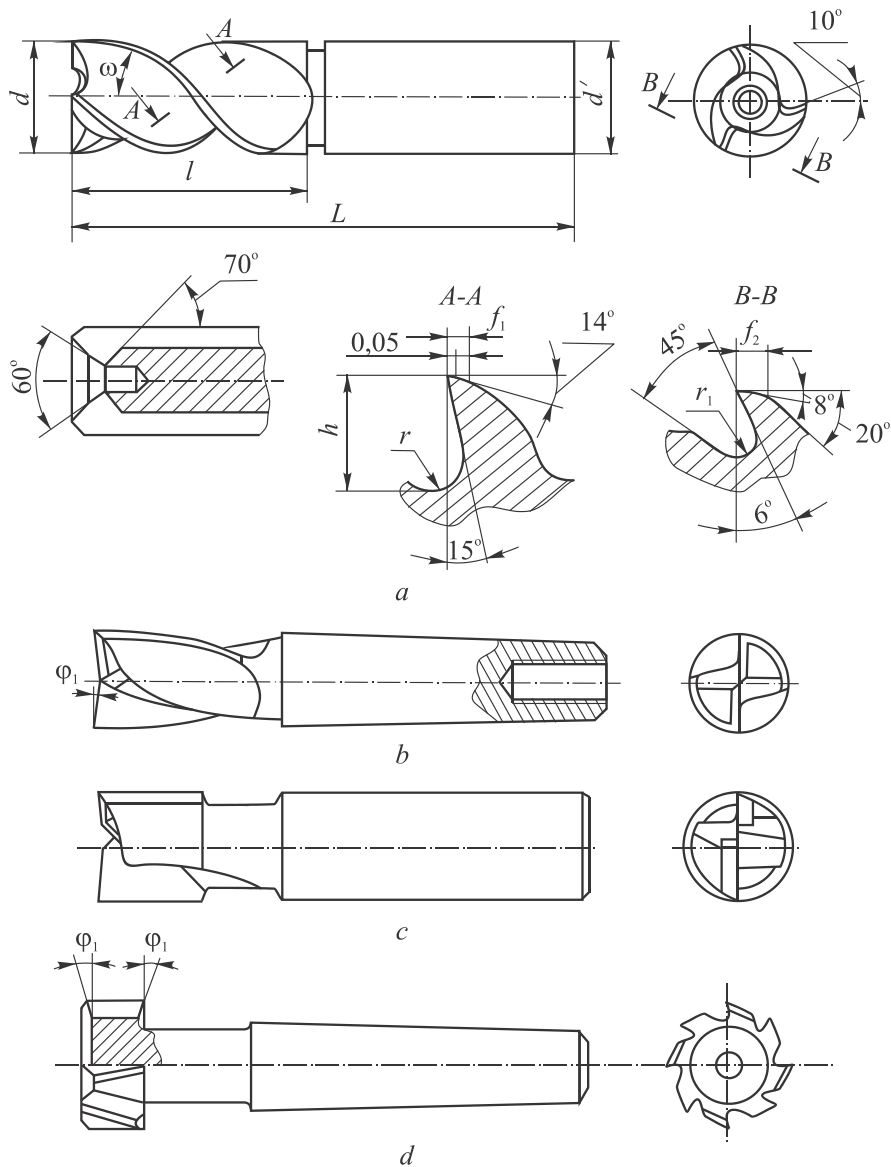


Fig. 6.7 End mills: (a) general purpose end mil; (b) HSS keyway end mill; (c) end mill with brazed carbide inserts; (d) T-slot cutter

When the regrinding of the form milling cutters with common chisel-shaped teeth is performed on flanks, it is difficult to ensure the identity of the cutting edge profile. Thus, the grinding process requires special templates, copiers or tracing devices that provide the necessary path of the grinding wheel during the resahrpening. This sharpening is very labor-intensive, therefore form milling cutters are usually made with form-relieved teeth.



## 7. Design and Calculation of Thread Cutting Tools

Almost half of all parts used in modern engineering are threaded. Commonly thread is used for fastening, as well as for the transmission of motion (lead screws and nuts). Thread is of complex helical nature with high requirements on accuracy, surface finish and strength.

Tools used for threading are very diverse in design. They can be divided into three groups: 1) cutting tools that cut thread by removing the allowance with cutting edges; 2) fluteless tools that form thread by cold plastic deformation; 3) abrasives tools, used for thread profile grinding.

In practice, the most widely used threading tools are the first two groups. These include: cutters, chasers, thread milling cutter, taps, threading dies, die heads. Analysis of these tools is the main subject of this section.

The tools of the second group, which includes plates, thread rollers and thread rolling heads are not discussed. Abrasive tools for the thread grinding are not considered due to the simple construction, and significantly less applicability.

### 7.1 Threading cutters and chasers

Thread cutters are used for cutting all kinds of threads and have the following advantages: simple design, production-friendly construction and versatility. The latter advantage is that the same cutter can cut both the cylindrical and tapered threads of different diameter and pitch.

In thread cutting by a cutter, a form-copying (profiling) method is usually used. Thus the cutter edges profile must be of the same shape as the thread profile. In order to raise performance, a generating cutting is used.

Stock removal in threading is performed in non-free cutting conditions with a large degree of deformation of the workpiece material. The thread is formed, as a rule, in a few passes with small chip cross-sections. Due to this fact, the process productivity is low, thus the screw cutters are primarily used in single-part or small-batch production.

Screw cutters can be of three types: straight-shank, prismatic and round (circular).

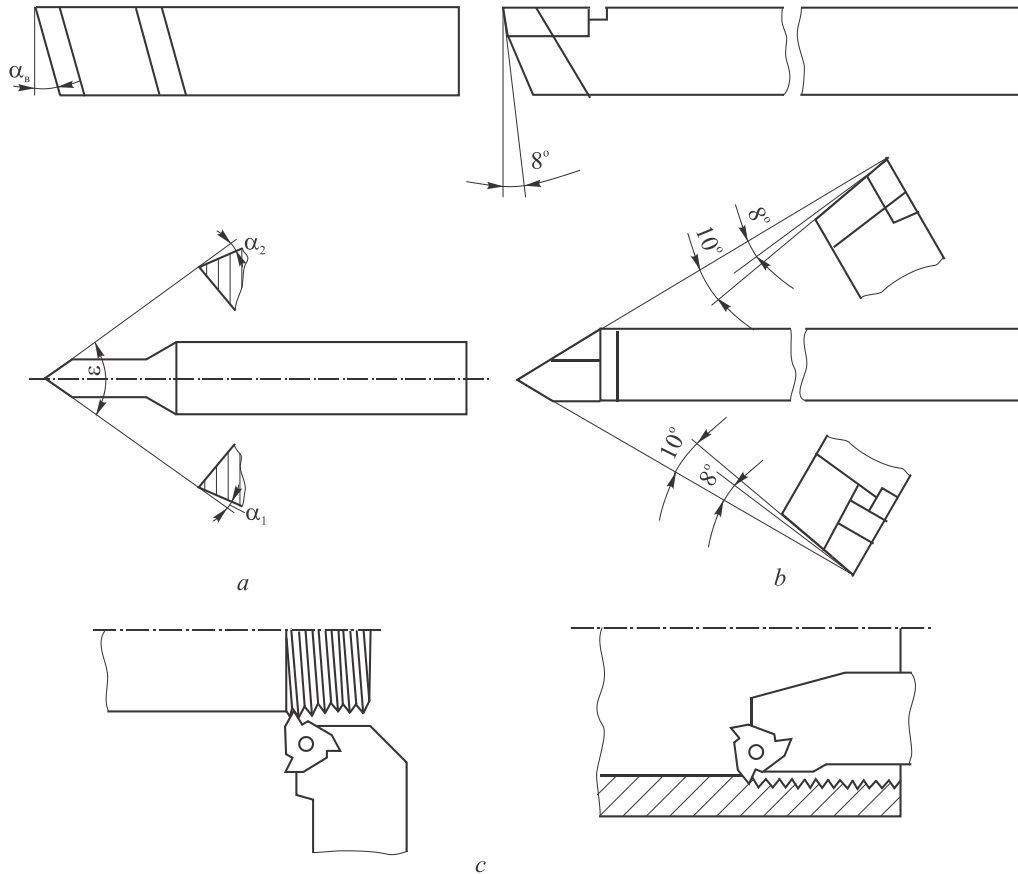


Fig. 7.1 Radial thread cutters: (a) HSS; (b) carbide inserted; (c) indexable carbide

The typical designs of straight-shank thread cutters are shown in Fig. 7.1.

The thread cutters differ from conventional turning tools in the head shape and cutting edges profile. Rake angle  $\gamma$  is commonly equal to 0, for easy resharpening. Clearance angles on the both cutting edges are equal in statics. In roughing threading clearance angles are 4...6°, and for finishing threading – 8...10°. Clearance angle at the top of a cutter are equal to 15...20°.

For small diameter threads with great profile height or multiple-start threads with a high helix angles ( $\tau > 3...4^\circ$ ) it is needed to take into account the effect of the helix angle on the value of the actual rake and clearance angles.

As it can be seen from Fig. 7.2 in cutting right-hand threads with face positioned in the axial plane of the workpiece, the rake and clearance angles are affected by the angle  $\tau$ :

$$\gamma_1 = +\tau; \gamma_2 = -\tau; \alpha_1 = \alpha_{st} - \tau; \alpha_2 = \alpha_{st} + \tau; \tau = P / \pi d,$$

where  $\alpha_{st}$  – is the clearance angles of the cutting edges in static;  $P$  – is the thread pitch;  $d$  – is the nominal diameter of the thread.

Due to negative value of rake angle, the cutting conditions on the right cutting edge worsen, and wedge weakens. The reduced clearance angle on the left cutting edge leads to tool life reduction.

When the tool face is installed in the plane perpendicular to the threads (Figure 7.2, b),

$$\gamma_1 = \gamma_2 = 0 \text{ and } \alpha_1 = \alpha_2 = \alpha_{st},$$

i.e. the cutting conditions are the same on the both cutting edges, but the thread profile distorts, since the Archimedean screw surface turns into convolute helical surface and their axial sections do not match. So the first method, with clearance angles adjusted for high  $\tau$  angles, is used for finishing operations, and the second one is used for roughing operations.

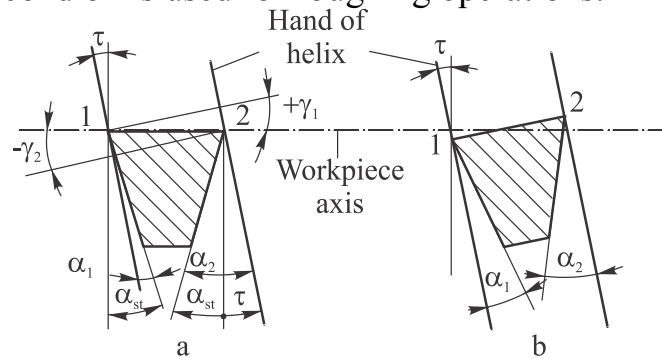


Fig. 7.2 Radial thread cutter setup for high-helix threads: (a) face is in axial plane; (b) with inclined face normal to the thread coils

In multipass cutting of triangular shaped threads, the thread profile can be formed with the help of three methods (refer to Figure 7.3): a) profile – with radial cutter feed; b) generating – with cutter fed at an angle to the workpiece axis; c) a combination of flank feed for roughing and radial feed for finishing (final) pass.

The advantage of the generating scheme is doubled chip thickness, which provides a corresponding reduction of passes. In this case, the right cutting edge works as a minor cutting edge and leaves a step on the machined surface. This drawback is eliminated with the combination method.

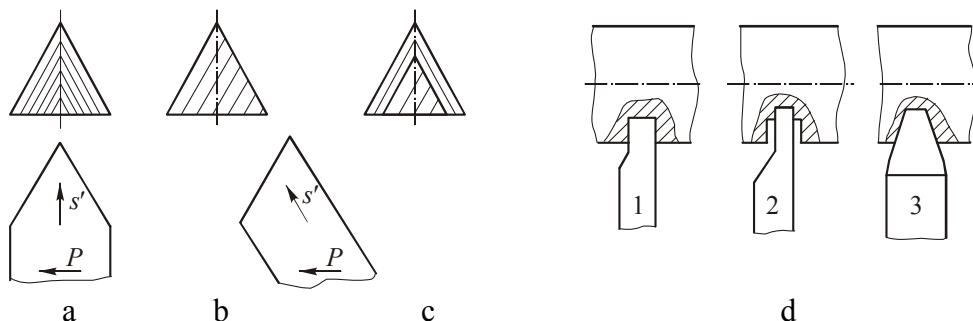


Fig. 7.3 Thread cutting methods: (a) profile; (b) generating; (c) combination; (d) for acme thread

Preliminary operations for deep profiled threads cutting, ACME thread, for example, are carried out with cutters of different profile (shown in Fig. 7.3 d).

**Straight-shank cutters** (Fig. 7.4, a) are attached to the tool holder in tilted at the angle  $\alpha$  position. In order to reduce the cutting force the rake  $\gamma$  is selected with respect to the properties of the workpiece material.

**Circular cutters** (Fig. 7.4, b) have more production-friendly construction compared to straight-shank cutters, but have a smaller stock for regrinding and less rigid clamping. To create clearance angles the cutter is installed above the center of the workpiece.

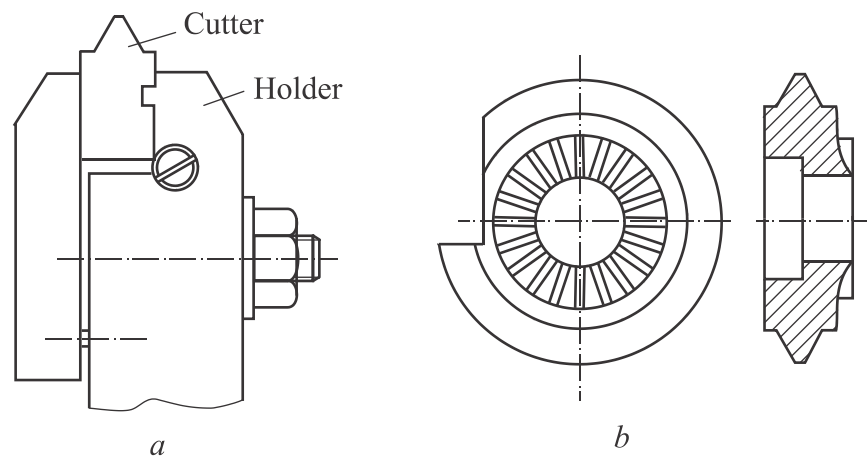


Fig. 7.4 Form thread cutters: (a) prismatic; (b) circular

**Chasers** (Figure 7.5) are the multiple-flute cutters, which can be of straight-shank, prismatic or circular shape. They are usually used for cutting threads with fine pitch, i.e. threads with shallow profile.

As it is shown in Fig. 7.5, d, the cutting part of a chaser consists of a leading chamfer of  $l_1$  length, sharpened at an angle  $\varphi$  and the sizing part  $l_2$ :

$$l_1 = (1,5 \dots 2,0)P, \quad l_2 = (3 \dots 6)P,$$

where  $P$  – is the thread pitch.

The chamfer angle  $\varphi = 25 \dots 30^\circ$ , so that the load is distributed between several cutting edges of a flute. Therefore, the number of passes for tapping is decreased in 2...3 times compared to cutters. When thread is cut in a single pass, the length of chamfer is increased to

$$l_1 = (3 \dots 4)P.$$

Chaser has radial infeed in the beginning of thread cutting and then moves along the axis of a rotating workpiece with feed per revolution equal to the thread pitch.

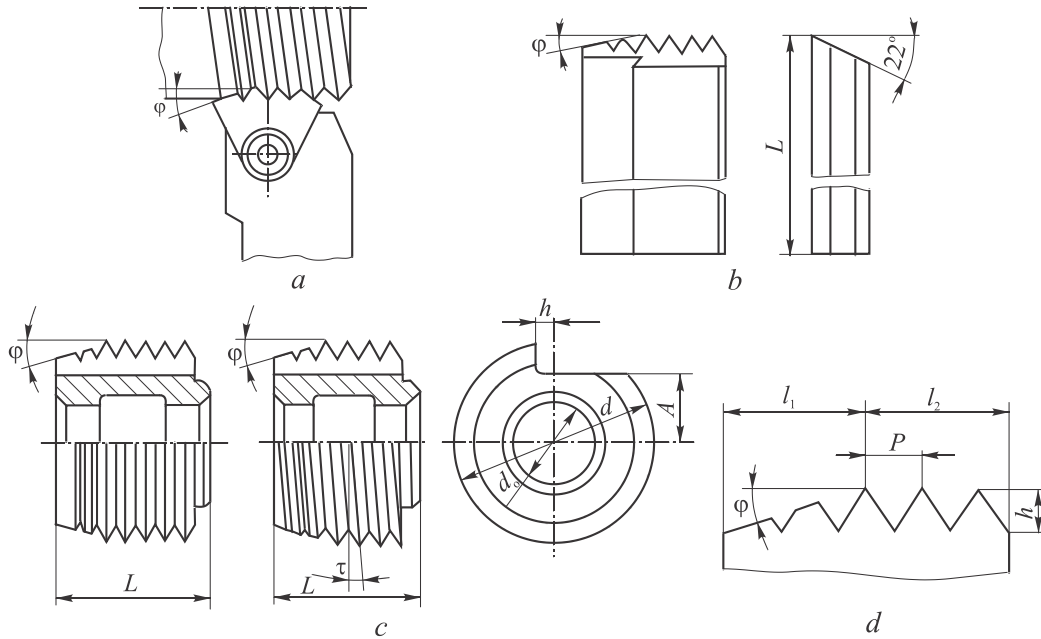


Fig. 7.5 Thread chasers:  
 (a) indexable insert; (b) prismatic; (c) circular; (d) chaser cutting edges

## 7.2 Taps

Taps are widely used for tapping holes and are very diverse in design and geometrical parameters.

**Tap** – is a screw turned into a cutting tool by machining flutes and creating cutting edges, rake, clearance and other angles. For mounting in the machine or in the tap wrench, a tap is equipped with a shank. The cutting part of a tap is usually made of high speed steel, while carbide taps are not so common.

Thread cutting conditions are very heavy, due to non-free cutting, high cutting forces and friction, as well as poor chip evacuation. In addition, taps have low strength due to weakened cross-section. The latter is particularly critical for cutting small diameter threads in gummy ductile materials, since taps are easily fail due to damage caused by chip jamming.

Advantages of a tap are simplicity and production-friendly design, the possibility of self-feeding threading, high accuracy of the machined thread related to the tap thread accuracy.

The main parts of a tap (Fig. 7.6) are cutting part (chamfer), sizing part, flutes, number of teeth and shank with clamping elements. Geometrical parameters include:  $\varphi$  – cutting edge angle (chamfer angle),  $\gamma$  and  $\alpha$  – rake and clearance angles of the cutting edges;  $\omega$  - helix angle;  $\lambda$  – spiral-point angle (cutting edge inclination angle).

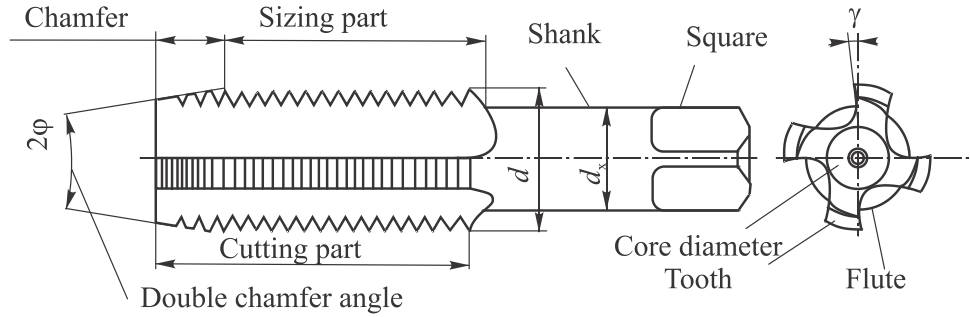


Fig. 7.6 Tap nomenclature

Cutting part of the tap, that is chamfer, does most of the work on cutting off the allowance, forming the thread profile and removal of chip from the cutting zone. Chamfer determines thread accuracy and taps life.

The cutting part of a tap is tapered at an angle  $\varphi$  to distribute the cutting allowance over several teeth. Since the cutting part is tapered, the height of teeth is variable.

With a thread profile height  $h=l_1 \text{tg} \varphi$ , the allowance per tooth is equal to:

$$a_z = \frac{h}{z_F n} = \frac{l_1 \text{tg} \varphi}{z_F n} = \frac{l_1 \text{tg} \varphi P}{z_F l_1} = \frac{P}{z_F} \text{tg} \varphi. \quad (7.1)$$

It follows from the Equation (7.1) that the smaller is the number of flutes  $z_F$ , with other things being equal, the greater is the allowance per tooth  $a_z$ , and, consequently, the smaller is the specific cutting force. By reducing the total volume of flutes the tap has a greater safety factor. However, the surface finish and accuracy of the machined thread decreases. Therefore, smaller number of flutes  $z_F$  is used for small diameter taps only, since the main requirement here is the tap strength.

Limit values for  $a_z$  are equal to 0.015 and 0.15 mm. For  $a_z < 0.015$  mm the cutting becomes difficult, if not impossible, since the chip thickness  $a_z$  value in this case is close to the cutting edge radius, which leads to rubbing and scraping of the thread surface. When  $a_z > 0.15$  mm the thread surface roughness deteriorates and increase in cutting force value leads to decrease in thread accuracy.

Usually, it is difficult to remove the entire stock in one pass in hand tapping. Therefore the total allowance is distributed between several taps of a set, which may consist of two or three taps. Thus  $l_1$ ,  $\varphi$ ,  $d$  and  $d_2$  of the thread are different (Figure 7.7).

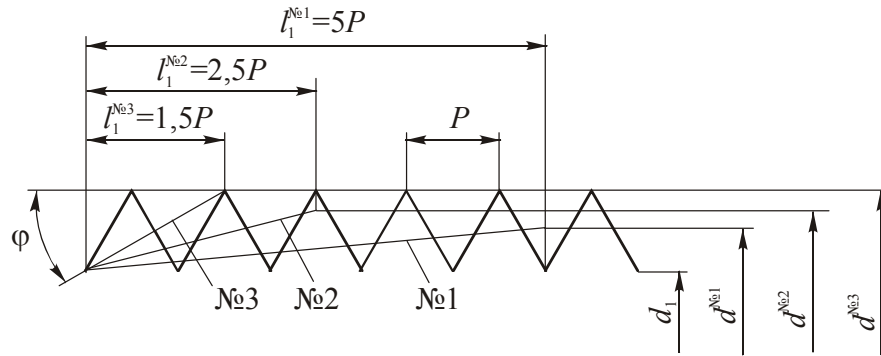


Fig. 7.7 Allowance distribution between taps of a set

The allowance distribution guidelines [13], as well as angle  $\varphi$  values, length of a chamfer  $l_1$  and load percentage per tap, are given in the Table. 7.1.

Allowance distribution between taps of a set

Table 7.1

Tap number	Two taps set	Three taps set
№1 (taper tap)	70%; $\varphi=7^\circ$ ; $l_1=6P$	50%; $\varphi = 4^\circ$ ; $l_1=5P$
№2 (plug tap)	—	30%; $\varphi=10^\circ$ ; $l_1=2,5P$
№3 (bottoming tap)	30%, $\varphi=20^\circ$ ; $l_1=2P$	20%; $\varphi=20^\circ$ ; $l_1=1,5P$

All taps of a set have identical minor diameters  $d_1$ , while the major diameters  $d$  and pitch diameters  $d_2$  are different. For example, for a set of three taps, the diameters are:

$$d_{(№1)} = d_{(№3)} - 0.5P, \quad d_{(№2)} = d_{(№3)} - 0.15P,$$

where  $d_{(№1...3)}$  – is the major diameter of taps №1 ... 3.

$$d_{2(№1)} = d_{2(№3)} - 0.15P, \quad d_{2(№2)} = d_{2(№3)} - 0.07P,$$

where  $d_{2(№1...3)}$  – is the pitch diameter of taps № 1...3.

The geometrical parameters of the cutting teeth of a tap are shown in Fig. 7.8. The **rake**  $\gamma$  is the angle between the tangent to the face of a tap at the given point and the radius drawn to the point. Strictly speaking, rake varies with height of the tooth, since the points lie on different diameters, but for threads with low profile height the thread diameter change is small and the change in angle is small as well.

Due to heavy-load conditions of tapping, the rake angle  $\gamma$ , as a rule, is chosen of positive value. It is recommended for medium-hard steel tapping to take  $\gamma=12...15^\circ$ , for brittle materials (cast iron, bronze, brass), as well as hard steel  $\gamma=0...5^\circ$ , for non-ferrous metals and alloys  $\gamma=16...25^\circ$ .

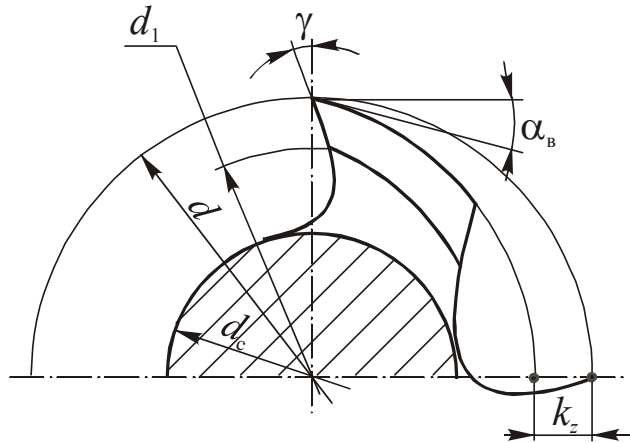


Fig. 7.8 Tap geometrical parameters

The clearance angle on the top of the edge – is the angle between the cutting velocity vector (cutting edge plane) and the tangent to the flank surface. Clearance angles are created by the Archimedean spiral relieving of periphery cutting edges of the teeth. It is recommended to take  $\alpha_{top}=6...12^\circ$  (lower value is for hand taps).

Radial relief value is measured at the face of the following tooth (the same as with relieved mills)

$$k_z = \frac{\pi d}{z_F} \operatorname{tg} \alpha_{top} .$$

Side cutting edge clearance angles for generating cutting patterns are equal to zero, as the thickness of uncut chip is small.

Form relieving for the cutting edges of the entire tooth profile is applied only for taps with profiling cutting patterns, which are used for cutting precise threads with high surface finish.

Blunt taps can be reground along the face, the flanks or both.

**Sizing part** of a tap, which has a full thread profile, is intended for the final formation of a thread. It also guides the tap in a hole, provides tap self-feeding on the thread, cut by the cutting part, and also serves as a stock for tap regrinding. The greatest wear occurs on the first thread after the chamfer.

To reduce friction and to avoid jamming of the tap in a hole, the sizing part major diameter has back taper with a diameter reduction of 0.04...0.08 mm per 100 mm of length.

To reduce friction on a sizing part, taps used for cutting threads in gummy ductile materials have interrupted thread (taps with staggered teeth).

Despite the simplicity of design, various types of taps are found in industry. There are more than 12 versions of machine taps, some of them are shown in Fig. 7.9. A brief description of the common tap designs are given below.



**Spiral point or gun nose or bull nose taps** (Fig. 7.9, a) are primarily used for hand tapping. These taps are made of tool steels in sets of two or three taps with rolled thread.

**Machine and hand taps** are used on drilling machines, lathes and unit-type machines for cutting metric threads M2...M24. The material of the cutting part is HSS. The tap thread is ground and form relieved. Sets of taps can also be used for hand threading. The standard machine taps are single, with relatively short sizing part, with straight flutes and rake angle  $\gamma = 0^\circ$ .

**Taps with staggered teeth** (Fig. 7.9, b) are recommended for cutting thread in gummy ductile materials, since they eliminate tap jamming by reducing friction. The thread teeth are cut away only on the sizing part of a tap. For low-strength ductile materials the teeth are cut away either on a 1/3 of the chamfer length or on the whole chamfer. Practice shows that the effect of reducing the friction is higher, with the thread pitch increasing.

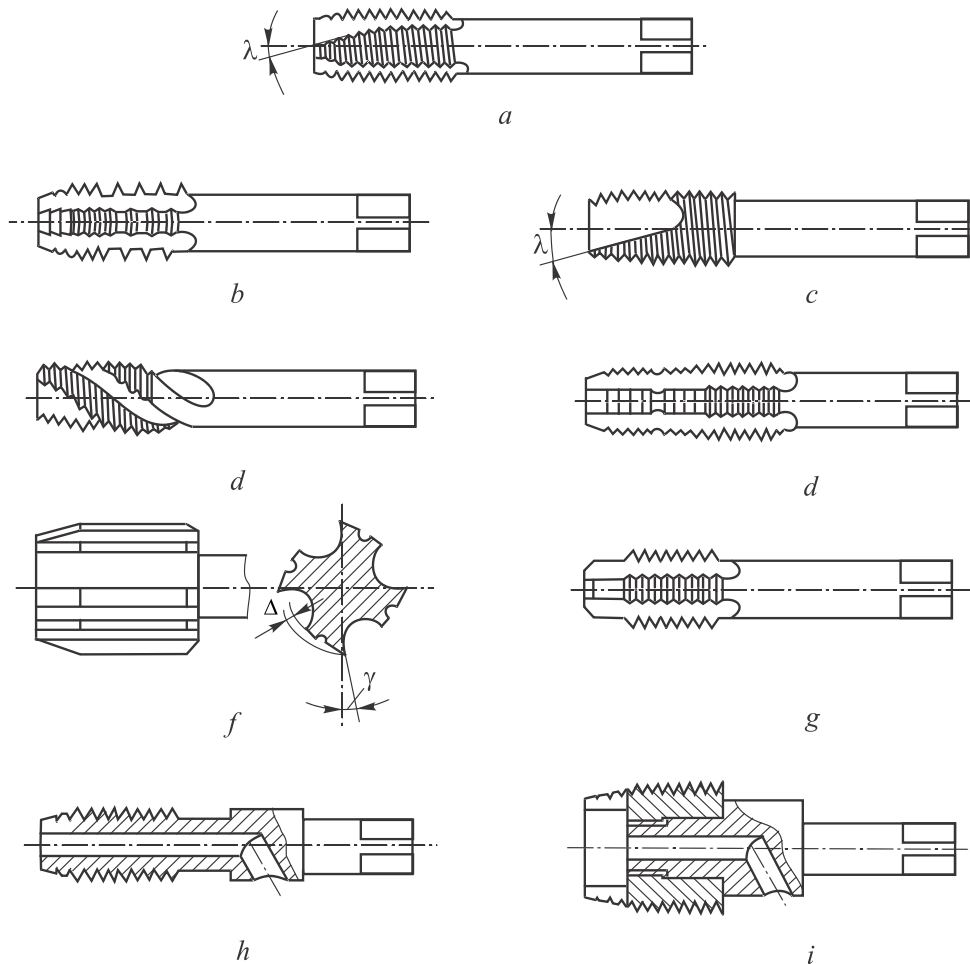


Fig. 7.9 Types of taps: (a) spiral-point; (b) with interrupted thread; (c) short-flute; (d) spiral flute; (e) step tap; (f) tap with burnishing edges; (g) with a pilot; (h) coolant fed; (i) bell-type tap

**Spiral flute taps** (Fig. 7.9, d) are recommended for reliable chip evacuation from blind holes and cutting threads with interruptions. When cutting threads in through holes with the chip evacuation in the direction of feed, it is easier to grind a spiral point with inclination angle  $\lambda$  (Fig. 7.9, a and c).

**Stepped taps** (Fig. 7.9, e) have two cutting parts and allow to implement any combination of profile cutting schemes in a single tap. For example, the first cutting part with truncated teeth can be used for generating scheme, and the second one for the profiling scheme. These taps can be applied for cutting high precision threads. This design is also suitable for hybrid schemes, when the first part performs cutting, and the second smoothens and burnishes the thread.

**Taps with guiding part** (Fig. 7.9, g) are used for tapping holes with accurate mutual position. Taps for through holes have guide pilot positioned in front of the cutting part, and taps for blind holes have a pilot following the sizing part. The guide part, positioned after the sizing part, has increased diameter, and auxiliary guide bushings are required for the operation.

**Nut taps** (Figure 7.10) are used for cutting through holes without reverse rotation of the nuts. For a better tap centering in a hole, taps have long chamfer and short sizing part. The beginning of the cutting part has additional chamfer with  $45^\circ$  and length equal to  $(1 \dots 1.5)P$ , and sometimes is equipped with a smooth front pilot with  $d_{\text{pilot}} = d_{\text{min}} - (0,1 \dots 0,3) \text{ mm}$ .

Due to greater length, and thus complicated manufacture, especially thread grinding, the nut taps are often of assembled design: cutting part and shank are manufactured separately, and then connected together by friction welding, soldering or threading.

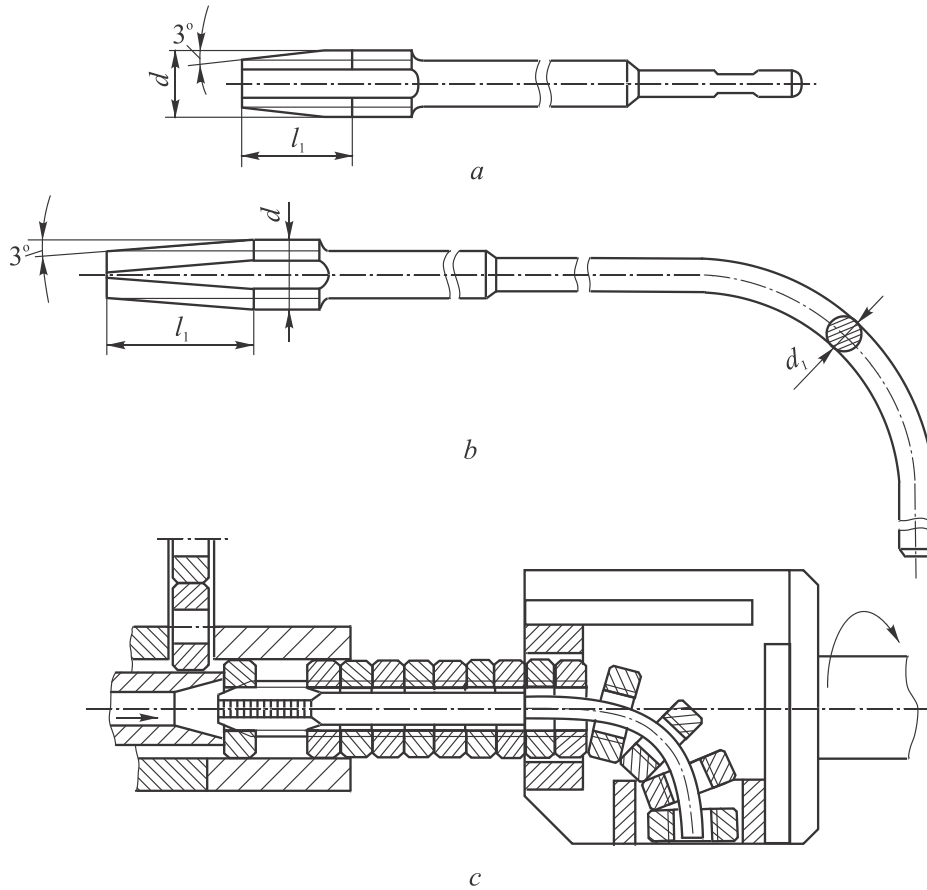


Fig. 7.10 Nut tap: (a) with a straight shank; (b) with a bent-shank; (c) operation

Shanks of the nut taps are made long straight or bent (Fig. 7.10, a, b). Bent shank taps are used for threading nuts on automatic tapping machines with a continuous threading cycle. The nuts are fed from the hopper to the cutting area and as they are tapped, they pass over the curved shank to the receiver (Fig. 7.10 c).

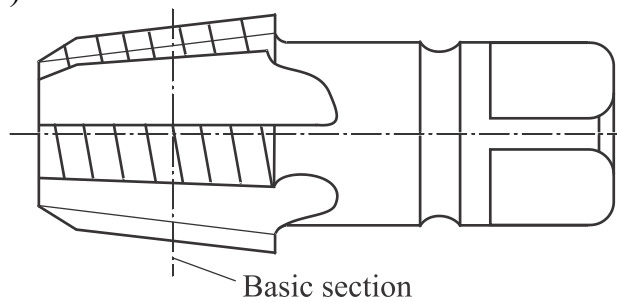


Fig. 7.11 Tap for tapered thread

**Taper thread taps** (Figure 7.11) are used to ensure a tight fit in threaded couplings without the use of sealants. The peculiarity of the taper thread tapping is that the entire cutting part is involved in the threading action. The sizing part of a tapered tap is missing. Tapping is usually performed on ma-

chines with the use of compensation tap holders. Basic parameters are the same as for straight thread tap threads. Cutting teeth are relieved.

**Chaser-inserted and adjustable taps** are used to reduce tool material costs when cutting large diameter threads and to compensate for wear.

### 7.3 Thread dies

**Threading die** is a nut, turned into a cutting tool by drilling clearance holes and forming rake and clearance angles on the teeth.

Dies are used for cutting external threads on bolts, screws, studs, and other fasteners. The most common types are: round, square, hexagonal, pipe thread die, split die.

Fig. 7.12 shows the construction and geometrical parameters of a round die. The elements of a die are: die outer diameter  $D$ , thickness  $B$ , clearance holes diameter  $d_c$ , holes centers diameter  $d_H$ , distance between flutes  $c$ , land width  $b$ , minimum wall thickness  $e$ . The geometrical parameters include: rake angle  $\gamma$ , clearance angle  $\alpha$  and lead angle  $\varphi$  of the chamfer. The outer surface of the die is provided with 3 or 4 tapered holes with a cone angle of  $90^\circ$  for holding die in a holder. A trapezoid groove with an angle of  $60^\circ$  forms a bridge with thickness  $m=0.4\dots 1.5$  mm, which is cut away after two or three regrinding of a die.

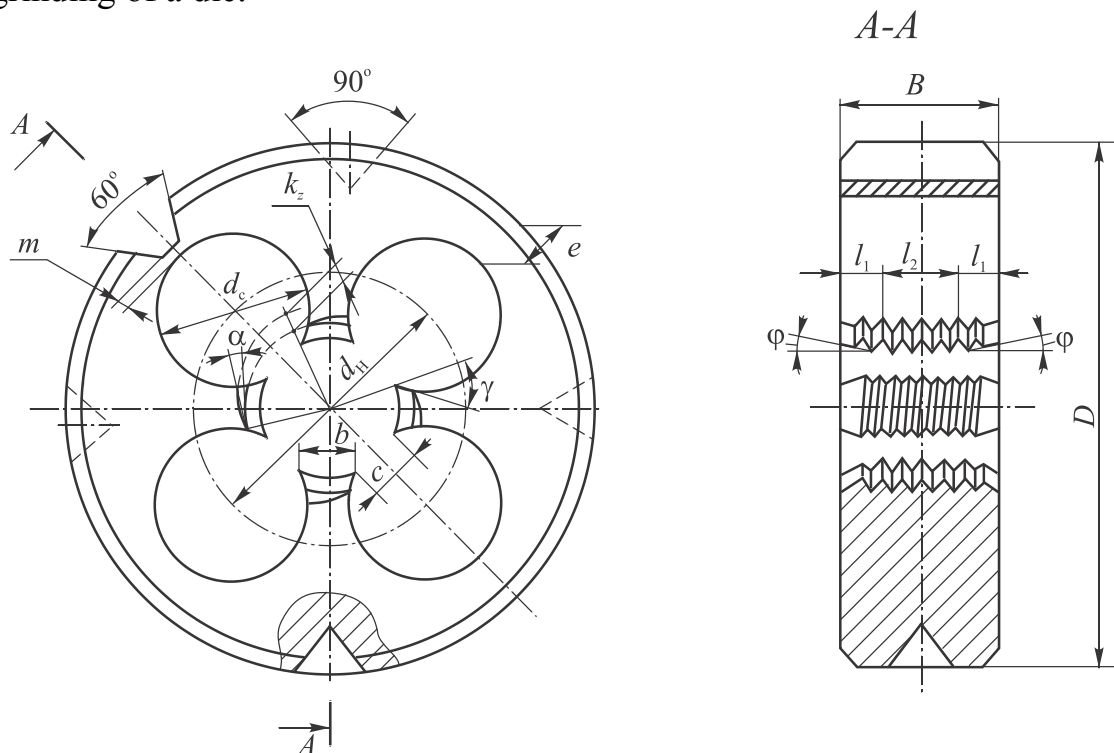


Fig. 7.12 Round threading die elements

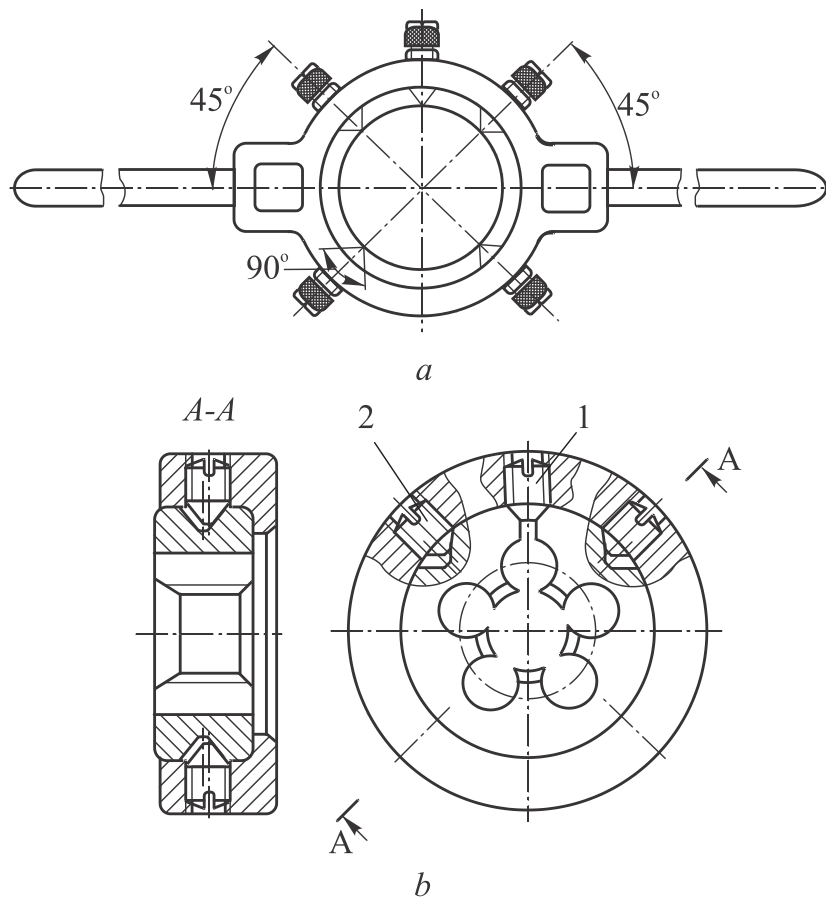


Fig. 7.13 Die holders: (a) HSS; (b) hand driver; (c) ring holder

Dies are held in holders with sliding fit when threading by hand or in a machine (Fig. 7.13, a, b). The fixing screws are offset relative to the axis of conical holes to firmly locate the die with respect to the holder face. Screw (1) is used to adjust the thread diameter of a die after the bridge is removed.

The working part of a die consists of two chamfers with an angle  $2\phi$ , located at both faces of a die, and the sizing part between them (Fig. 7.12).

The recommended angles of a chamfer cone are the following: for threading high-strength materials  $2\phi=20...30^\circ$ , for light non-ferrous metals and alloys  $2\phi=50...70^\circ$ . General purpose dies cone angle  $2\phi=50^\circ$ .

The number of clearance holes relates to the thread major diameter  $d$  (refer to the Table 7.2).

Number of clearance holes of a die

Table 7.2

$d, \text{ mm}$	2...5	6...18	20...30	33...48
$z_c$	3	4	5	6

**The length of the cutting part** is limited, since it is needed to reduce the length of unthreaded portion and is  $l_f=(1.5...3.0)P$ .

**Sizing part** of a die is used for thread calibration. It influences the direction and self-feeding of the tool in the process of cutting. Grinding or form-relieving of the sizing part is impossible. Therefore, the clearance angles of the part are zero. Accuracy of the thread cut by a die is low, not higher than 6h, 8h, due to heat treatment defects.

To reduce friction on the sizing part of a die and the amount of thread distortion, the length of the sizing part is chosen as short as possible, usually  $l_f=(3...6)P$ .

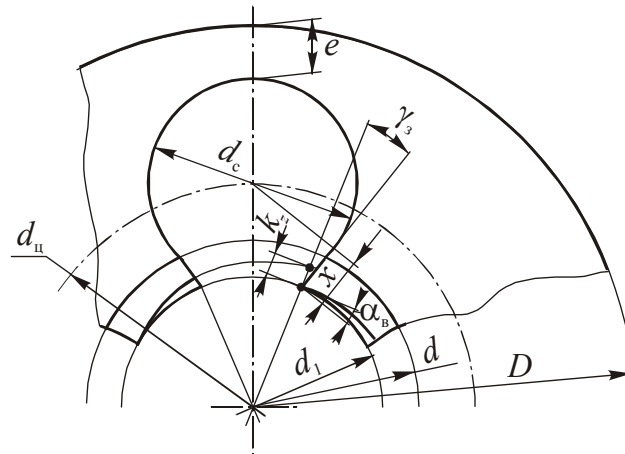


Fig. 7.14 Threading die geometry

#### 7.4 Thread milling cutters and inserted-chaser dies

The following basic types of thread milling cutters are used in engineering practice: multiple-form, single-form, dies and whirling heads. The use of milling cutters instead of turning cutters in cutting external and internal threads provides significant raise of productivity due to: 1) multiple-point cutters with a large total length of the active cutting edges are used (multiple-point cutters); 2) increased chip thickness per tooth (single-point cutters); 3) increase cutting speed for carbide cutters (whirling heads).

**Multiple-point cutters** (see Figure 7.15) are used for sharp-profile external and internal fine pitch threads, located on cylindrical and conical surfaces of workpieces. In fact, they are a set of single-point cutters made into a single package with a teeth profile corresponding to thread profile. Thus, the grooves are annular. The teeth are formed by either straight or helical grooves teeth cut along the cutter axis. Clearance angles are result of Archimedean spiral relieving process.

The process of external thread milling with a straight multiple-form cutter is shown in Fig. 7.16. Here, the cutter axis is set parallel to the workpiece axis. Cutter rotates at a speed  $V_M$  and plunges into the workpiece with the radial feed. Then it is fed for a value of one thread pitch  $P$  along the workpiece axis, while the workpiece is rotated slowly for  $1 \dots 1\frac{1}{4}$  revolution. Here out-feed, equal to  $\frac{1}{4}$  of a revolution, is made to compensate for the initial tool in-feed.

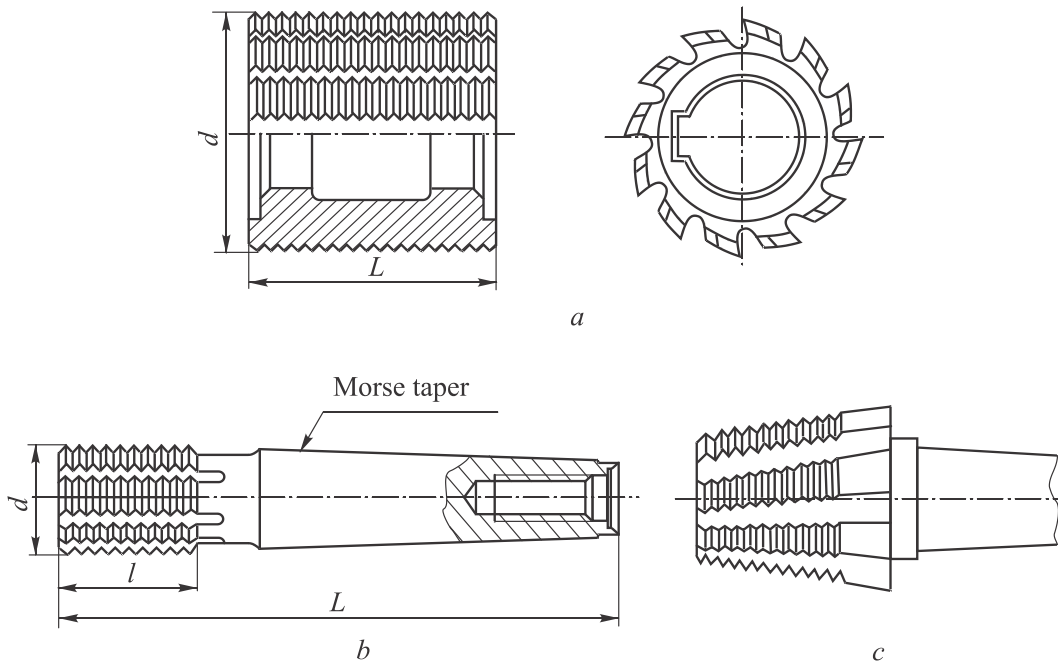


Fig. 7.15 Multiple-form cutters: (a) straight shell; (b) straight shank; (c) for tapered thread

The ratio between the number of workpiece revolutions  $n_w$  and cutter  $n_m$  is determined by the following equations:

$$n_w = \frac{n_m F_z z}{\pi d_2}; \quad n_m = \frac{1000 v_m}{\pi d_m},$$

where  $F_z$  – is feed per tooth;  $z$  – the number of teeth (flute) at the face of a cutter;  $d_2$  – is the thread pitch diameter, mm;  $d_m$  – is the cutter diameter, mm.

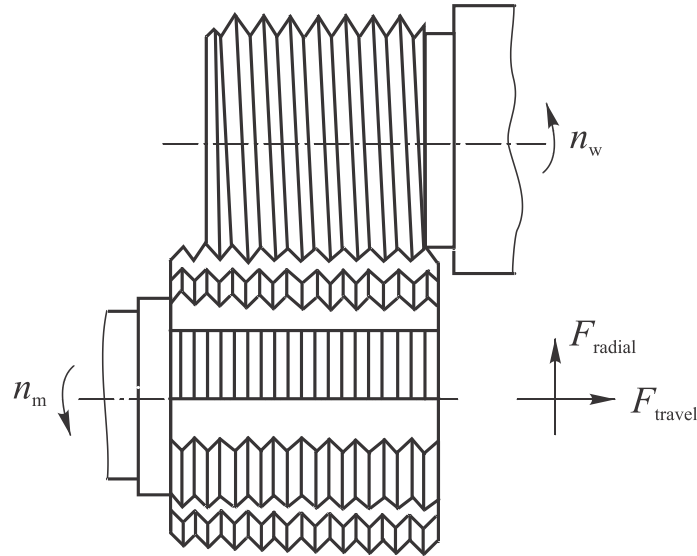


Fig. 7.16 Thread cutting with a multiple-form cutter

The disadvantage of the multiple-form cutters is the distortion of the thread profile angle due to difference between the trajectories of cutting edge cutters (circle) and thread curve in a section perpendicular to the axis of the workpiece (Archimedean spiral). However, the distortion value is low, up to 3...4' for external and 7...9' for internal threads, and usually is within the tolerance limits.

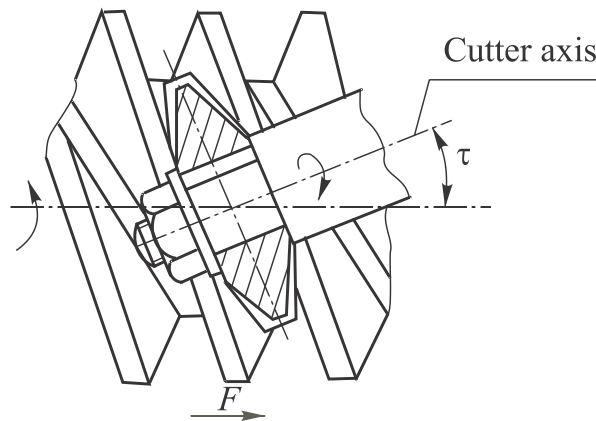


Fig. 7.17 Single-row cutter position with respect to the workpiece

**Single-form cutters** are used for cutting threads with high profile height, diameters and lengths. For example, they are often used for cutting worms, lead screws, etc. Since the cutters are multiple-point cutting tools and cut threads at high feed and in one pass, their performance compared to the turning cutters is much higher.

When a single-form cutter is used, its axis is set at an angle  $\tau$  to the axis of the workpiece, which is helix angle of the thread pitch diameter (Figure 7.17). The single-form cutter rotates during the thread cutting and the work-



piece rotates and traverse along its axis with the feed per revolution equal to thread pitch.

Single-form cutters ensure high productivity and good surface finish. For cutting acme threads, in order to reduce cutting forces and prolong tool life, the milling cutters shown in Figure 7.18 are used. The teeth of the cutter are staggered, thus, each tooth cuts only with one side of the cutting edge, but with doubled thickness of chip.

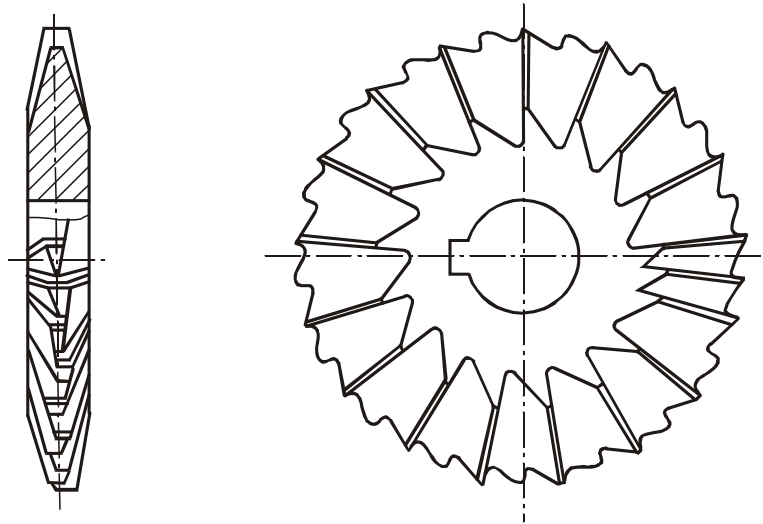


*Fig. 7.18 Single-row cutter for acme thread*

Since the cutter axis is at angle to the workpiece and the teeth are straight-edged, the profile of the thread is distorted. For small values of the  $\tau$  angle the resulting profile error is small, but for higher values of the thread helix, more accurate tooth profile is needed.

**Thread whirling heads** for external thread milling are applicable in heavy mechanical engineering for high-speed cutting of large threads on lead screws with lengths up to 10,000 mm and up to 1000 mm in diameter. The whirling head is shown in Fig. 7.19. It has a rather complex structure and is installed on a lathe carriage at  $\tau$  angle to the axis of the workpiece. Carbide-inserted head envelopes the workpiece and is driven by the separate drive at a speed of 100...450 m/min.

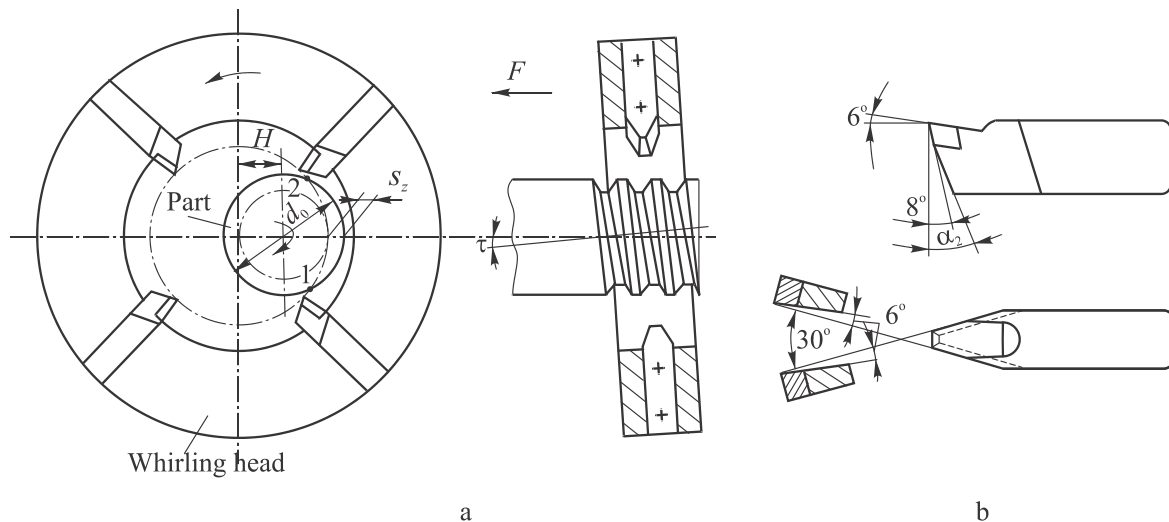


Fig. 7.19 Thread whirling with thread-milling heads: (a) layout; (b) cutter design

The workpiece is counter rotated by the machine tool spindle at a low velocity. The head is fed along the axis of the workpiece with feed rate equal to the thread pitch. Tapping is usually done in one, at least two passes. The head incorporates 2...12 cutters that are, due to the off-center position of the head axis with respect to the workpiece axis (amount of eccentricity is  $H$ ), contact and cut the workpiece periodically. Therefore, chips, removed by the cutters have a variable thickness, equal to zero at the beginning (point 1) and at the end (point 2) of the contact and a maximum thickness  $S_z$  in the middle between these two points. Such a form of chip and relatively short length facilitates the conditions for chip removal from the cutting zone.

Carbide-tipped cutters (Fig. 7.19, b) have  $\gamma = 0...6^\circ$ ,  $\alpha = 6...8^\circ$  with a holder angles  $\alpha_2 = 15...20^\circ$  and side clearance angles  $\alpha = 6^\circ$ . Due to the high cutting speed, proper transportable form of chips and low radial loads the heads can cut quality threads with good surface finish on long stiff shafts. The productivity is 3...4 times higher compared to conventional thread milling and turning.

**Inserted-chaser dies** have a fairly wide application for cutting external and rarely internal threads on the screws, bolts, pipes and other parts. The dies are quite complex in design with cutting elements made in a form of circular or flat chasers, clamped in a head (Fig. 7.20).

Inserted-chaser dies are divided into two main groups: self-opening and adjustable. The former open at the end of tapping operation, thus eliminating the need for reverse rotation (back-tracking), thus reducing the idle time and increasing the productivity. Therefore, these dies have greater application compared to adjustable dies, although the latter are simpler in design.

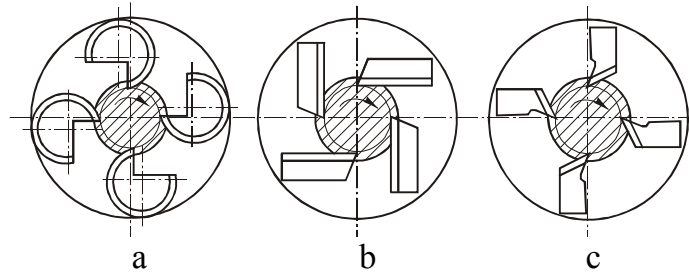


*Fig. 7.20 inserted chaser dies:  
 (a) with circular chasers; (b) with tangential chasers; (c) with radial chasers*

There are two basic types of inserted-chaser dies: revolving, which is applied on turning automatic and semi-automatic machines, and stationary die, which is used on lathes and turret lathes.

The stationary dies are opened automatically at the end of threading, but closed manually by the lever.

The chasers used in dies are circular, tangential and radial. The most widely used chaser is circular, which are easy to manufacture, have precise polished thread and allow a large number of regrinding.

Dies equipped with tangential chasers (Fig. 7.20, b), although allow a large number of regrinding, are displaced by dies with circular chasers, due to complicate manufacture. The dies with radial chasers are even more rarely used (Fig. 7.20, c) due to minimum stock for regrinding, although the design is compact.

## 8. Design and Calculation of Gear Cutting Tools

Gears can be cut either by form cutting or by generating process.

The tooth profile in the method of **form cutting** strongly corresponds to the profile of the grooves between the teeth of the wheel. Form cutting tools include involute gear cutter, involute end mill, shear cutting head and broach. The latter two provide the highest performance, since the metal is removed simultaneously from all the tooth spaces. But at the same time they are the most expensive, difficult to manufacture and thus are applied only in mass production.

The advantage of the method is a simple kinematics of cutting. However, the accuracy of the gear is relatively low due to inevitable inaccuracies in tooth profiling and tool positioning with respect to the workpiece.

In the **generating method** the centroids of a tool and a workpiece roll over each other without slipping, and the profile of the gear teeth is formed as an envelope of the cutting edges positions during gear cutting. The form of the cutting teeth of the generating tools does not match the profile of the tooth spaces and is determined by quite complex calculations. The generating cutting tools are as follows: rack shapers, hobbing cutters, gear-shaper cutters, bevel-shaping cutters, bevel milling heads, etc. The advantage of these tools is versatility, as it is possible to cut gears, of a given module, with different number of teeth. The accuracy of the generating method is higher compared to the form cutting method. Disadvantages include complex kinematics of gear cutting machines and complex design of the cutting tools.

Since the vast majority of gears applied in mechanical engineering are cylindrical with involute tooth profile, this chapter deals with cutting tools used for production of gears of this type.

Design of the cutting tools for non-involute tooth profile cutting, is examined, by the example of spline-cutting hobbing cutter, in Section 6.10.

### 8.1 Involute gear cutters for form cutting

The form cutting tools include: involute gear cutters, involute end mills, shear cutting heads and broaches. The former two tools are widely used in medium production runs and repair service. The latter two types of tools are special purpose and are designed to cut gears of a specific module and number of teeth. They are used in single-purpose machines for large production runs, are difficult to manufacture and have limited application.

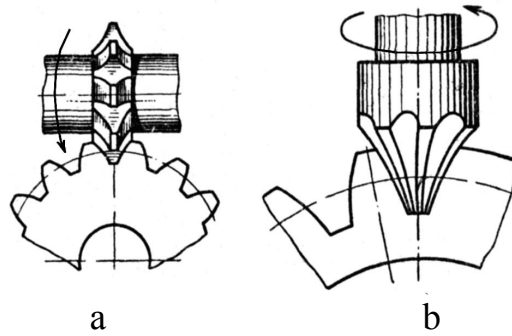


Fig. 8.1 Gear cutting: (a) by an involute cutter; (b) by an involute endmill

**Involute gear cutters** are cutters with profiled cutting edges. They are used for cutting spur and helical gears less ( $m=0.3...26$  mm) on the universal milling machines equipped with indexing device.

In the process of gear cutting the cutter is rotating and the workpiece, held in an indexing device, is fed along its axis. The cutter engages the workpiece at full height of the tooth space and then moves along it. After the space is milled, the workpiece is indexed for successive space.

The main advantage of form cutting tools is easy resharpening. As a tooth relieved tool, involute cutters are reground along the face.

The process of gear cutting is simple in machine setup and kinematics and does not require special gear cutting machines. However, it is time-consuming and provides poor accuracy due to errors of indexing and cutter position with respect to the workpiece. The relieved tooth geometry is nonoptimal, which leads to lower cutting parameters and decreases tool life.

The number of teeth of the cutter is limited as to provide enough stock for regrinding, and therefore affects the productivity and surface finish. Thus, the involute gear cutters are used for cutting wheels of the lowest accuracy grades (9th and 10th).

The analysis shows that the most significant change in the profile of gear teeth is in the range of tooth numbers  $z_1=12...135$ . Therefore, for accurate gear cutting of a specified module it is needed to have a number of mills which is  $n=135-12=123$  pieces. Such a large number of mills is not profitable to have, since many of them may be unclaimed and, in addition, the changes in the profile of two adjacent numbers of teeth are very small, especially for large numbers.

In order to reduce the number of cutters, it is wise to produce sets with limited number of cutters, each intended for cutting wheels with a range of tooth number.

Standard cutter sets contain 8 pieces (numbers) for modules  $m \leq 8$  mm or contain 15 pieces, and sometimes 26 pieces, for  $m > 8$  mm.

The mills grouping in sets is based on equality of length of segments along the outside diameter arc. For this purpose the rack profile and gear profiles for different tooth numbers  $z=12$  and higher are drawn in a large scale.

The sector of profiles difference on the outside diameter is divided into eight equal segments, and the numbers for the corresponding teeth ranges are assigned from 1 to 8 (Fig. 8.2). Thus, each cutter from a set is intended for cutting a certain range of numbers of teeth. Table. 8.1 presents data on these ranges for numbers of mills in the set of 8 and 15 cutters.

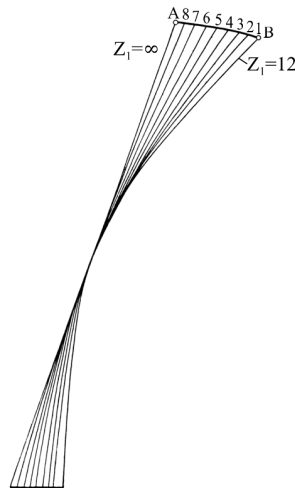


Fig. 8.2 Tooth profiles for different numbers of teeth

The table shows that the greater is the number of a cutter, the wider is the range of teeth numbers, and the number eight cutter can cut gears with  $z=135$  to  $\infty$ , ie including rack.

As the module increases the height of the teeth, and the difference in the curvature of the profile becomes larger. Therefore, the narrower tooth number ranges and a greater number of mills in a set are implemented. Intermediate numbers are designated with the fractional numbers, eg.  $3\frac{1}{2}$  (for a set of 15 cutters) or  $5\frac{1}{4}$  (for a set of 26 cutters). It should be borne in mind that the milling cutter of each number is profiled for the minimum number of teeth of the range.

This minimizes the risk of the meshed gears jamming, as the radius of the profile curvature decreases, and therefore, the width of tooth space increases with the decreasing number of gear teeth.

To simplify the manufacturing and regrinding the involute gear cutters are relieved along the Archimedean spiral. The radial relief value is determined by the well-known equation

$$k_z = \frac{2\pi r_{a0}}{z_0} \operatorname{tg} \alpha_P,$$

where  $r_{a0}$  – is the radius of the cutter outside diameter;  $z_0$  – is number of cutter teeth;  $\alpha_p$  – is the clearance angle on the top of the tooth.

*Cutter number versus tooth numbers range*

Table 8.1

Number of a cutter	Number of cutters in a set		Number of a cutter	Number of cutters in a set	
	8	15		8	15
1	12; 13	12	5	26...34	26...29
1 1/2	–	13	5 1/2	–	30...34
2	14...16	14	6	35...54	35...41
2 1/2	–	15; 16	6 1/2	–	42...54
3	17...20	17; 18	7	55...134	55...79
3 1/2	–	19; 20	7 1/2	–	80...134
4	21...25	21; 22	8	135	135...∞
4 1/2	–	23...25			

Clearanse angles in the normal section on the sides of a cutter tooth (Figure 8.3):

$$\operatorname{tg} \alpha_{Ni} = \frac{r_{a0}}{r_i} \operatorname{tg} \alpha_p \sin \varphi_i, \quad (8.1)$$

where  $r_i$  – is the radius of any  $i$ -th point of the cutting edge;  $\varphi_i$  – is the angle between the tangent to the profile and perpendicular to the axis of the cutter ( $\varphi_i=10...16^\circ$ ).

As follows from the Equation (8.1) and Fig. 8.3 the value of  $\alpha_{Ni}$  is variable. It decreases to  $1^\circ 30'$  at points near the top, even if the  $\alpha_p=12...15^\circ$ .

The rake angle for standard cutters is equal to zero, which impairs cutting conditions, but simplifies the manufacturing, regrinding and tooth profile inspection.

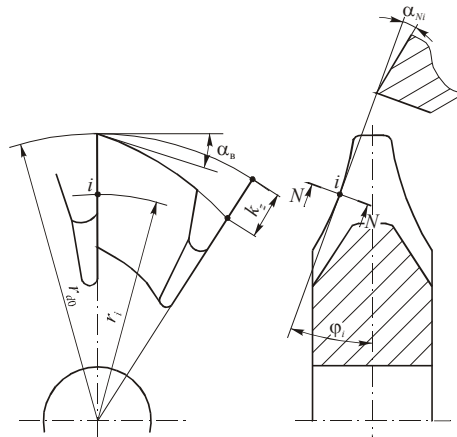


*Fig. 8.3 Clearance angles on the tooth sides*

**Involute end mills** are profiled end mills used for milling spur and helical gears, as well as herringbone gears with coarse modules ( $m=10\dots100$  mm).

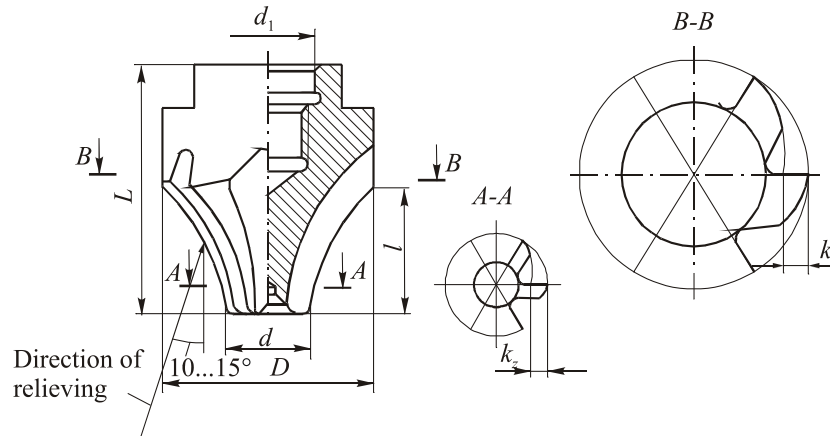


*Fig. 8.4 Involute endmill*

In contrast to involute gear cutters, the involute end mills (Figure 8.4) are threaded to an arbour with, locating on the cylindrical collar of the machine spindle.

Compared to the involute disc cutters, end mills have much smaller dimensions.

Significant disadvantages of the end mills are low productivity and low accuracy of the milled gear.

The low productivity is due to the method of cutting: a small number of teeth, non-rigid mounting, large cutting forces due to the large width of cut and a large angle of contact with the workpiece, so that the feed and cutting speed are usually reduced.

The low accuracy of cut gears is caused by end mill profile errors, errors of reground profile, positioning deviations and errors of the indexing device.

The advantages of the end mills are the possibility of application of universal milling machines for cutting gears of very coarse modules and unique applicability for herringbone gears.

Finger cutter is a special purpose cutting tool and is not commercially manufactured.

## 8.2 Hobs

Gear cutting hobs are generating multiple-point cutting tools of rack type. They are made on the basis of a worm. Rack-type teeth are formed by flutes cut in the worm. Relieving process is used to create clearance angles.



This process also facilitates hob regrinding. Since the racks are positioned on the worm flutes, the rotation of the hob leads to continuous displacement of the racks along hob axis as well. Thus, the hob is a cutting tool with an inherent generating movement or a tool with an infinite rack, which meshes with the gear.

The gear milling is widespread in the industry due to its versatility, high productivity and accuracy. The given hob of a specified module can cut gears with different numbers of teeth, which greatly reduces the number of tools. Due to continuous generating process the high productivity and tooth spacing accuracy is achieved. Hobs are used on special gear-hobbing machines that provide rotation of a cutter and workpiece as well as movement of the cutter along the gear axis.

Hobs are classified by: a) the number of the worm starts – as the single-start and multiple-start; b) the helix hand as right (for cutting spur and right-handed gears) and left-handed (for cutting left-handed helical gears); c) the method of mounting as shell-type and shank-type; d) the design as solid and inserted; e) the method of manufacture as with milled teeth and with ground teeth.

**Hobbing** process is similar to the meshing of two gears. The worm can be considered as a wheel with helical teeth, the number of which is equal to the number of worm starts. The axes of a hob and a gear are crossed in space.

In the process of hobbing the cutter and gear are rotated and the hob is fed along the gear axis. The hob engages the workpiece at the full depth of the gear profile. Rotational speeds of the cutter and the workpiece are strictly related to the feed movement.

Per one revolution of the hob the workpiece is rotated for  $a/z_1$  of a revolution, where  $a$  – is the number of hob starts;  $z_1$  – is the number of gear teeth. All the teeth of a single-started hob are involved in milling of the gear teeth profile, which are generated as the envelope of the cutting edges positions in the sequence of gear cutting. Multiple-start cutters cut a number of gear teeth simultaneously, with the number being equal to the number of the hob starts.

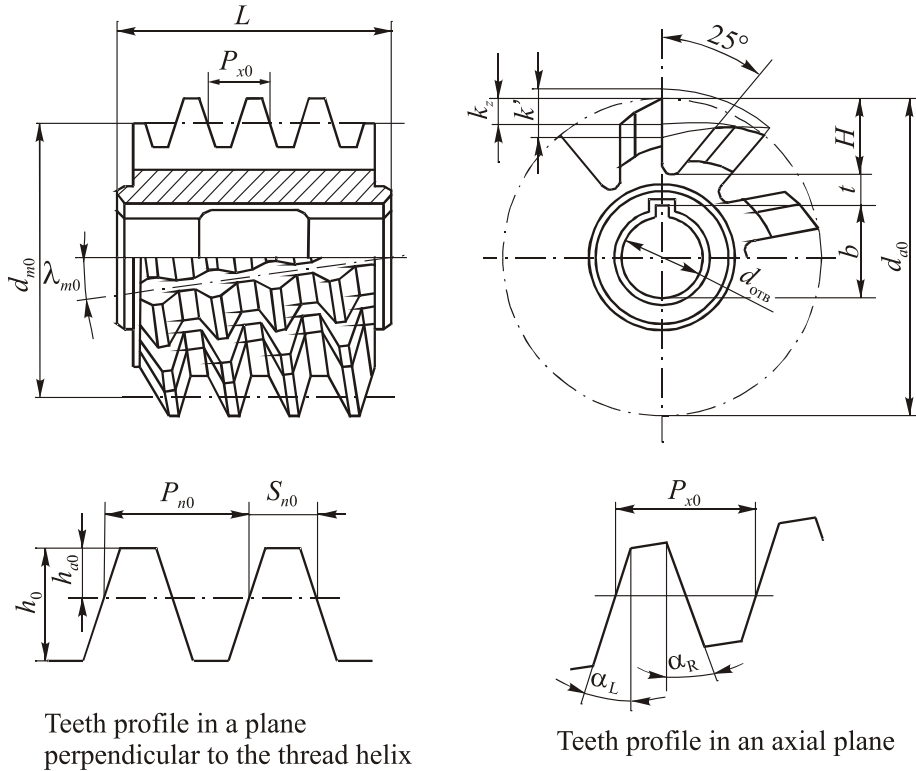


Fig. 8.5 Involute hobbing cutter of an Archimedean type

The **geometrical parameters** of the cutter teeth include a set of rake and clearance angles (Fig. 8.5). In order to ease the manufacture and regrinding, the top cutting edges of a hob usually have  $\gamma=0$ , and clearance angle, formed by relieving process,  $\alpha=10...12^\circ$ . Roughing hobs can have  $\gamma=10...15^\circ$  to facilitate the cutting process.

Clearance angles on the tooth flanks are defined in the normal section  $\alpha_N$ . The analysis shows that the rake and clearance angles on the side cutting edges are much smaller in magnitude than those on the top cutting edge, and are far from the optimal values in terms of tool life. Here, for the standard hob with  $\alpha_0 = 20^\circ$ ,  $\gamma_P = 12^\circ$ ,  $\alpha_P = 10...12^\circ$  these angles are  $\gamma_N = 2^\circ30'$ ,  $\alpha_N = 2^\circ30'...3^\circ$ .

### 8.3 Gear-shaper cutters

Gear-shaper cutter or circular shaper cutter is a cutting tool that represents a toothed gear, which crests and flanks are provided with rake and clearance angles.

Shaping cutters are applied for cutting spur, helical and herringbone gears and internal gears as well. Shaping cutters are essential for cutting gears with small tool over-travel, such as cluster gears or gears with shoul-

ders or flanges. Shaping is a high-production method for cutting gear sectors, racks and narrow gears with a large number of teeth. In addition, shaper cutters are manufacture-friendly and can be manufactured with high accuracy.

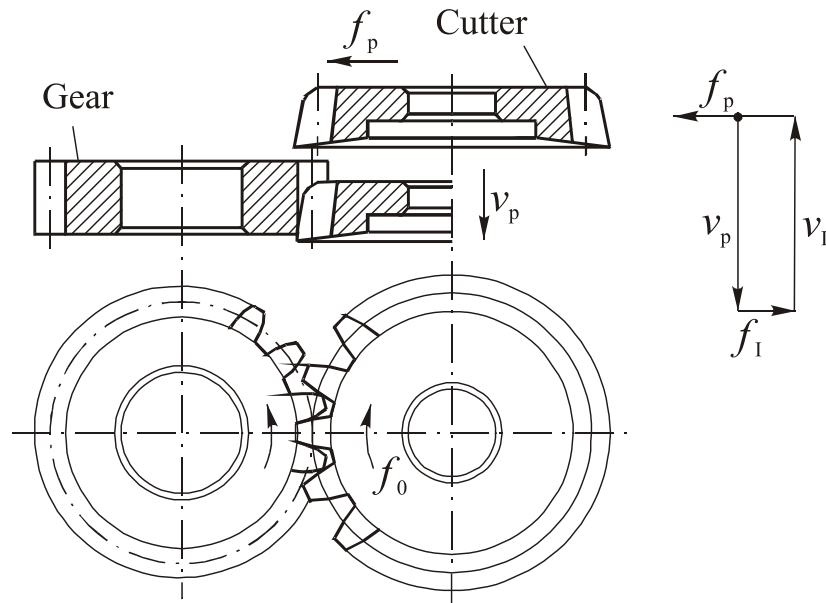


Fig. 8.6 Gear shaping by circular cutters

Fig. 8.6 shows the shaping of a spur gear. The shaping cutter is mounted on a machine spindle and forms a gear in generating cutting. Cutting motion  $V_p$  (primary motion) of a cutter is performed by downward motion of a spindle, it is followed by idle upward movement and consequent rotation of a cutter relative to the workpiece, i.e. generating process is performed. Before the idle stroke ( $V_i$ ) the cutter is retracted from the workpiece for a small distance  $f_i$  to prevent rubbing of the cutter against the workpiece. Thus, the cutter performs reciprocating and rotating motions.

The rotational feed, which determines the thickness of cut on side cutting edges, is implemented by synchronized rotation of the cutter and workpiece, and is measured on the pitch circle as  $f_0$  (mm/double-stroke). In addition, the cutter is radially fed to engage the workpiece at the feed rate  $f_p$  (mm/double-stroke).

Gear teeth profile is generated as the envelope of the shaper cutting edges positions in the sequence of cutting.

Since the shaping process is interrupting with large inertial forces it is impossible to increase high cutting speeds, thus the shaping is less productive compared to hobbing.

The following types of shaping cutters are used in industry: disk-type, cup-type and shank-type (Fig. 8.7). The difference is in the position of the clamping elements, the fasteners of the cup-type shaping cutter are placed in

a special recess to avoid contact with the workpiece faces. Shank-type shaping cutters are small in diameter and are used for cutting internal gears and fine-module gears ( $m < 1$  mm). Helical shaping cutters are used for cutting helical and herringbone gears.

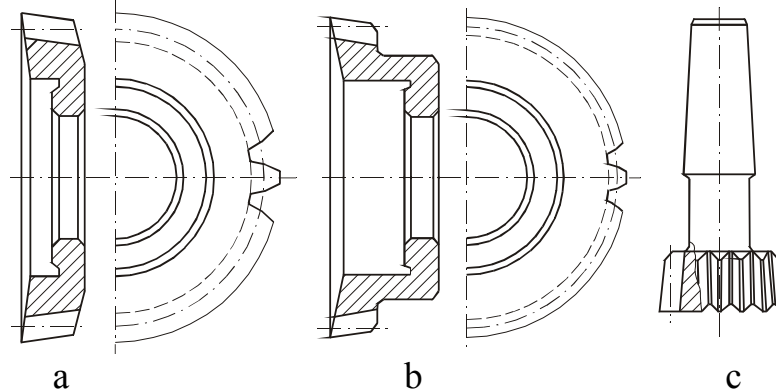


*Fig. 8.7 Gear shaping by circular cutters: (a) disk; (b) cup; (c) shank*

Among disadvantages of shaping cutters there are: complex kinematics of shaping machines, limited range of gear tooth numbers cut by a given cutter as it affects accuracy of the gear tooth profile. Outer diameter of shaping cutters is limited to by the probability of cutter deflection due to console mounting on a machine.

Shaping cutter can be considered as a corrected gear with continuously variable profile correction along the axis of the cutter, decreasing from the front face to the back.

Such correction provides, as it will be shown below, the formation of the clearance angles on the side cutting edges of the cutter. The flank surface adjacent to the top cutting edges is a truncated cone that forms clearance angle  $\alpha_B$  on the top edges, the rake surface is also a truncated cone, where rake angle  $\gamma_B$  is an angle between the cone generator and a plane perpendicular to the cutter axis.

Fig. 8.8 shows a section of a cutter with the three characteristic sections. In the section I-I the profile correction is the maximum positive value, in the section II-II it is equal to zero, and in the section III-III is the maximum negative value. The third section is a limit for a cutter regrinding, which is performed along its face.

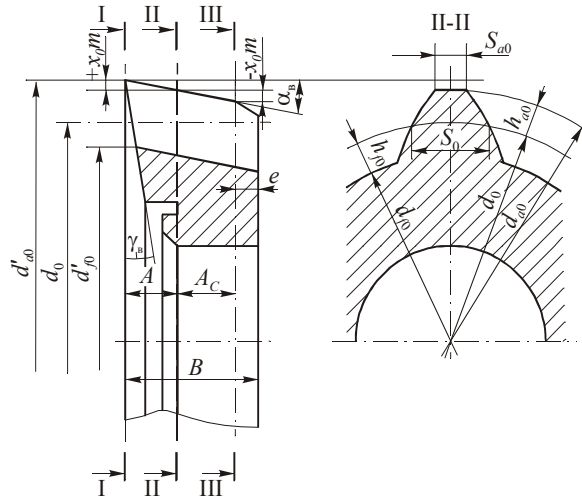


Fig. 8.8 Parameters of a gear shaping circular cutter

The cross-section II-II is called a **reference section**, and the distance from the section to the front end of a cutter is a **reference distance  $A$**  of a new cutter. The distance between sections II-II and III-III is a reference distance  $A_C$  of a completely exhausted (regrinded) cutter.

The process of continuous correction of the shaping cutter can be visualized with the help of hobbing process (Fig. 8.9, a). While the hob and the shaping cutter work are synchronously rotated, the hob is fed radially with the feed  $AB$ , in addition to the axial feed  $OA$ . The rates of the feeds are calculated in such a way that the resulting feed is directed at an angle  $\alpha_B$  to the axis of the shaper cutter. Thus the lateral surfaces (flanks) of the cutter teeth are formed as an **involute helicoid surface**, and the cutter tooth profiles in different sections are the different parts of the involute, offset with respect to the center of the base circle.

The clearance angle in any cylindrical section of the cutter tooth can be found as the angle between the axis and the helical line, which lies on the surface of the cylinder. Helical lines in all cross-sections have the same axial pitch, as they belong to the same helical surface.

Selection of the **number of teeth** for the shaping cutter is performed as follows. One of the most important parameters of a shaper cutter is the number of teeth  $z_0$ . The  $z_0$  depends on the given module, dimensions of the workpiece (diameter and width of a gear), nominal pitch diameter of a gear shaping machine.

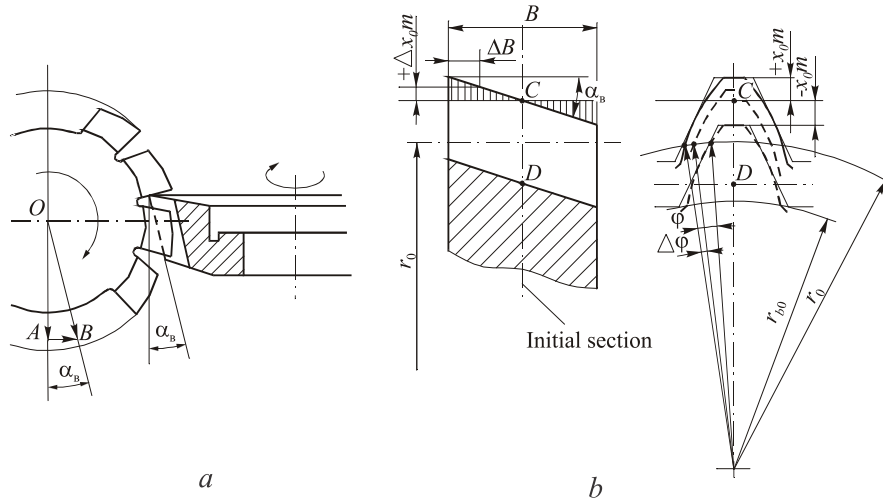


Fig. 8.9 Schemes: (a) hob-milling of a shaper; (b) shaper flanks forming

For the common types of shaping cutters with module  $m=0.2...50.0$  mm, the following series of nominal size are implemented:

- disk-type shaping cutters – 75; 100; 125; 160; 200 mm;
- cup-type shaping cutters – 50; 75; 100; 125 mm;
- shank-type shaping cutters ( $m=1...4$  mm) – 25.38 mm.

The pitch diameters of the most widely used shaping cutters are 75...100 mm and  $z_0=15...75$ . They allow to cut external gears with small heights of transition curves.

## 8.4 Shavers

Shavers are high precision cutting tools, intended for finishing gears. In shaving process the axes of a tool and a workpiece are crossed to provide sliding motion for the process of cutting. The profile of a shaver is serrated to form the cutting edges and space for chips. The cutting process of shaving is a result of the combination of rolling and sliding with the shaver teeth removing thin shavings from the flanks of gear teeth.

The shaving increases the accuracy of the wheels by about one grade. It can correct profile of the teeth, tooth spacing errors, slight errors in teeth direction and run-out. Shaving also improves the teeth surface finish (from  $Ra 2.5...3$  to  $Ra 0.63...0.32$ ). Shavers are applied for spur and helical gears with  $m=0.2...8.0$  mm and hardness of  $HRC 35$ , mainly in order to improve meshing smoothness.

Shaving is done with tools of three types: hob, rack and circular.

**Hob shavers** (Fig. 8.10, a) are applied for cutting worm gears and represent a fluted worm of the same size as the working worm size. Kinematics of a shaver is similar to motions of a worm meshed with worm gear.

**Rack shavers** (Fig. 8.10, b) are designed for shaving cylindrical gears with straight and helical teeth. Helical racks are used for spur gears and spur racks are used for helical gears. Rack teeth profiles carry rectangular grooves, positioned normally to the direction of teeth.

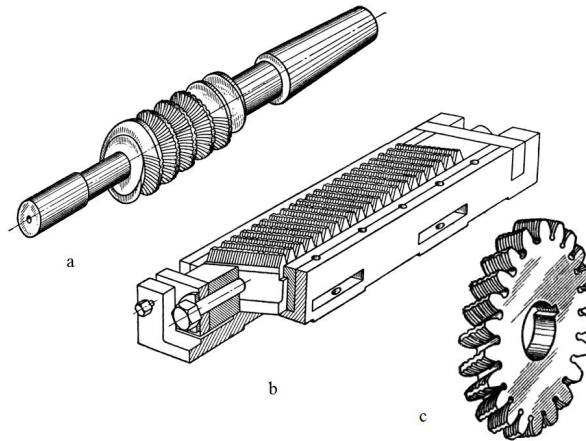


Fig. 8.10 Shavers: (a) hob shaver; (b) rack shaver; (c) circular shaver

It should be noted that the production of rack shaver teeth and shaver mounting is rather complex and time-consuming, and loss of accuracy during the assembly is inevitable. Therefore, this tool is not widely used. In practice, the shaving of spur gears is mostly performed by circular shavers.

**Circular shaver** (Fig. 8.10, c) represents a precision gear made of tool steel. The teeth profiles, like the other types of shavers, are provided with flutes which are formed by shaping. The flutes form cutting edges at the intersection of flutes with the involute flank surfaces of the teeth and provide space for chips.

Helical racks are used for spur gears and spur racks are used for helical gears.

For the cutting process (sliding) the helix angle of the shaver teeth is different from the helix angle of the gear teeth. Thus, the meshed gear and shaver represent gear drive with crossed axes. For spur gears cutting the right-handed helical shavers are commonly used and for helical gears the spur shavers or helical shavers with helix angles different from those of the gear being cut are used.

Shavers are usually made of high speed steels. To shave gears with hardness of  $HRC$  35...48 and higher carbide-inserted shavers with CBN coated teeth are used.

The blunt shavers are resharpened along the teeth flanks and the outside diameter.

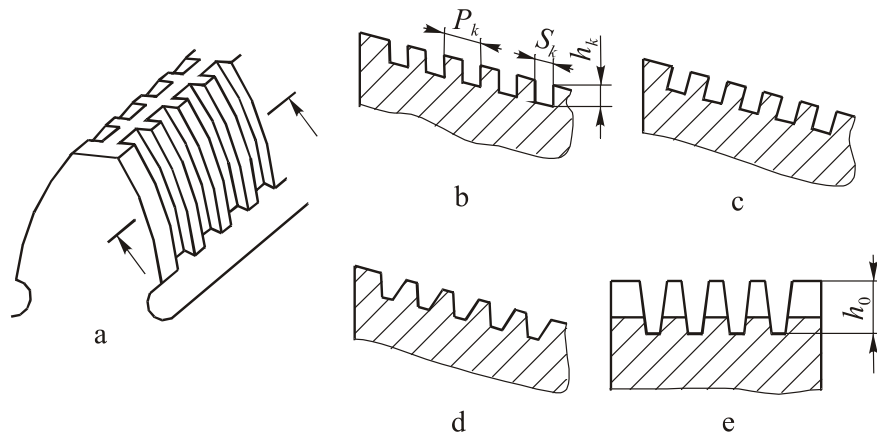


Fig. 8.11 Shaver flutes

Cutting edges of a shaver have zero clearance angles in statics, and are positive in kinematic due to meshing action. The rake angle value depends on the shape of the flute (refer to Fig. 8.11) and feed direction. The flutes shaped normally to the direction of the tooth have  $\gamma=0^\circ$ , regardless of the feed direction.

Flute dimensions shall be sufficient to accommodate chips both for new and resharpened shavers. For standard shaving cutter ( $m=2\dots 8$  mm) flutes have pitch  $P_F=1.8\dots 2.4$  mm, depth  $h_F=0.6\dots 1.0$  mm, width  $S_F=0.5P_F$ .

### 8.5 Generating cutters for parts with non-involute profile

Generating principle, used in the design of involute gear cutting hobs and shaping cutters, is also used to manufacture circular shaped parts with teeth (grooves) located on the outer or inner surface and having a different shape of the profile in a section perpendicular to the axis, as well as parts with repeated profile. Fig. 8.12 shows a few examples of such profiles.

The most common generating cutting tools applied in industry are hobs, shaping cutters, generating cutters. Among their advantages are high productivity and accuracy of the form of manufactured parts. Disadvantages include applicability to the parts of only the given size and high cost of tool manufacture. Thus, these tools are special purpose tools and their application is economically feasible only in large-scale and mass production.

The generating principle is the heart of the process, which is in the mutual rolling action of the tool and workpiece profiles without slipping of their centroids. The centroid of hobs (Fig. 8.13, a) is the starting line  $CT$ , while the



part centroid is the circle  $W$ . When the shaping cutters are used (Fig. 8.13, b) the centroids are two circles:  $CT$  and  $W$ .

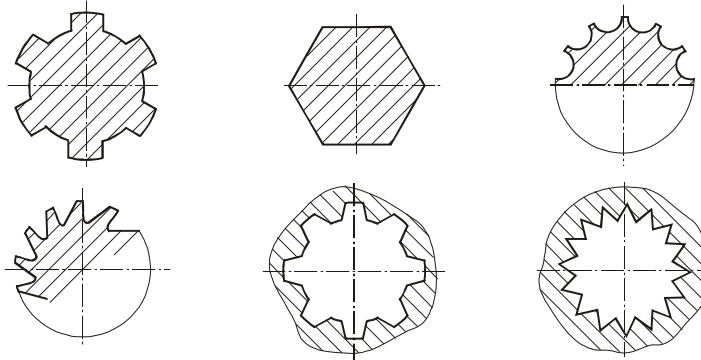


Fig. 8.12 Profiles produced by generating cutting

The most common tools for cutting profiled teeth on the outer surfaces of the parts, such as spline shafts, sprocket gears, ratchet wheels, etc, are hobs.

Shaping cutters are mainly used for cutting teeth on the inner surfaces and the outer surfaces of the parts with integrated flanges and shoulders. The productivity of shaping cutters is lower compared to hobs, but is higher for short lengths of cutting.

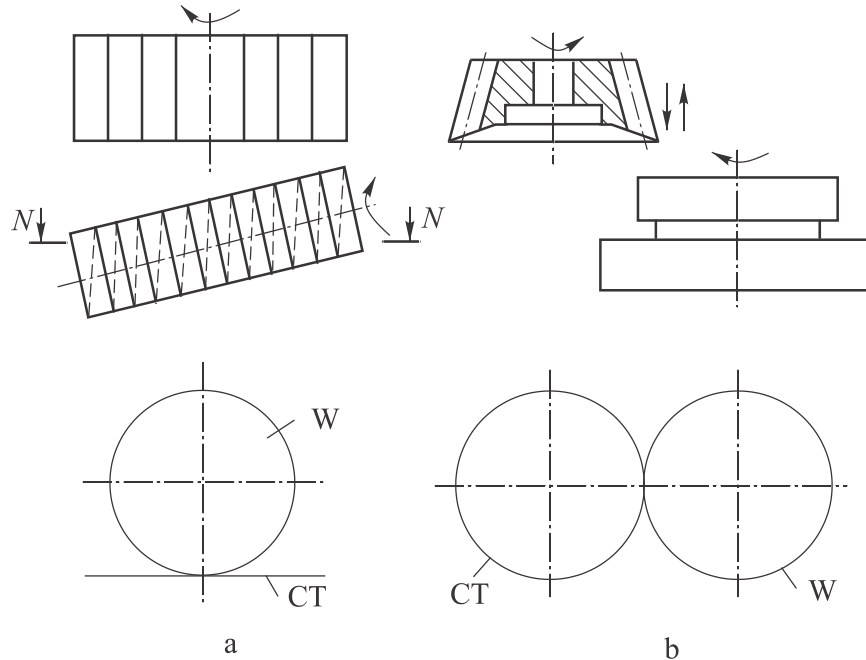


Fig. 8.13 Generating tools and their centroids: (a) hob; (b) shaping cutter

## 8.6 Calculations of spline hobbing cutters

Straight splines with straight-sided teeth are the most common type of splines. The generators of the tooth sides are parallel and being prolonged will touch the virtual circle with a radius equal to half of the thickness of the tooth  $b/2$ .

For the ease of assembly the tops of the teeth are chamfered with  $f \times 45^\circ$ . Therefore, the diameter of the pitch circle  $d_w$  of spline shafts is slightly smaller than the major  $d_a$ .

Splines with major diameter centering have transition curves (fillets) at the base of the tooth, which should be located between the minor diameters of the shaft and the hub. These fillets are replaced by recesses at the tooth root, which also serve as a room for the grinding wheel over travel.

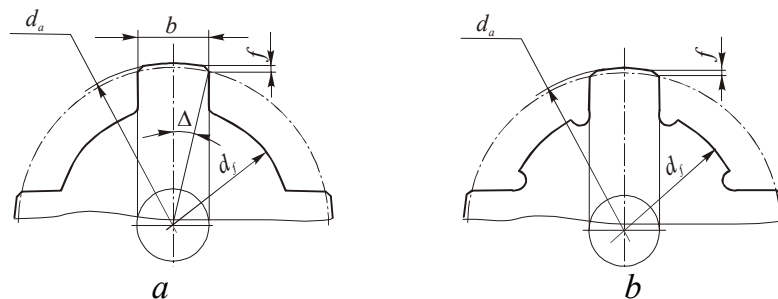


Fig. 8.14 Straight splines centering: (a) major diameter,  $d_a$ ; (b) minor diameter,  $d_f$

Usually, hob profile in the normal section  $N-N$  matches rack profile, engaged with the part profile. Although this is an approximate method of profiling, the error is well within the limits of the part profile tolerance. It should be noted that the error decreases with the hob helix angle  $\tau$ , which is usually smaller than  $6^\circ$ , decreasing.

The analytical method of profiling is examined below.

Fig. 8.15 shows construction of an action line in accordance with the generating conditions. During the generating process the pitch circle  $r_w$  of a part rolls without slipping on the initial line of a hob. The lateral side of a spline tooth takes consequent positions, during its counter-clockwise rotation, while remaining tangent to the virtual circle. Since the side of the tooth does not pass through the center axis of the part, the last (highest) contact point  $A$  is slightly above the initial circle with radius  $r_w$ , and, thus, is the end point of a straight teeth profile and a line of action. The starting point  $B$  of the line of action lies on the line of the hob crests, parallel to the initial line. Thus, the working section of the line of action is the line segment  $BPA$ .

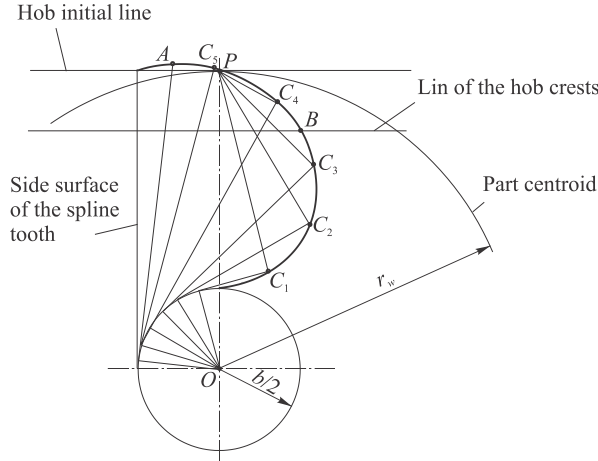


Fig. 8.15 Diagram of the line of action for hob and splined shaft

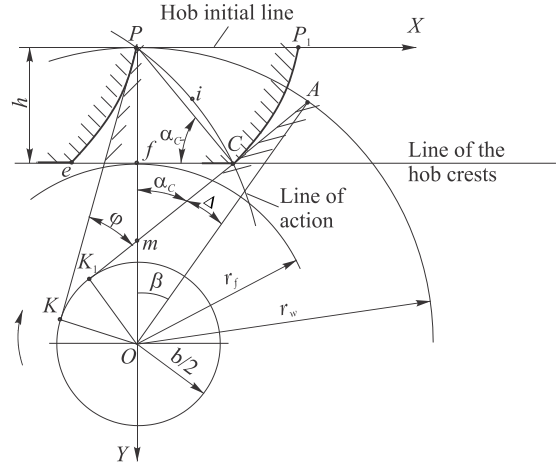


Fig. 8.16 Profiling of a hob for straight splines cutting

To derive the equations of the line of action the diagram shown in Fig. 8.16 is used.

The line of action is found through the determination of the coordinates of the point C that belongs to the line (Figure 8.16):

$$\begin{cases} X_i = (r_w \sin \alpha_i - b/2) \cos \alpha_i; \\ Y_i = (r_w \sin \alpha_i - b/2) \sin \alpha_i. \end{cases} \quad (8.2)$$

Here the variable is the pressure angle  $\alpha_i$ , varying its value the curved line of action can be built.

Similarly, the equation of the hob tooth profile can be found. For any  $i$ -th point of the side cutting edge of a hob the profile equation in general form can be determined as:

$$\begin{cases} X_i = r_w [(\alpha_i - \Delta) - (\sin \alpha_i - \sin \Delta) \cos \alpha_i]; \\ Y_i = r_w (\sin \alpha_i - \sin \Delta) \sin \alpha_i. \end{cases} \quad (8.3)$$

However, Equations (8.3) are inconvenient for practical use, as  $\alpha_i$  is variable and calculated coordinates  $X_i$  and  $Y_i$  can exceed the height of the tooth. Therefore it is better to set value for the ordinate of the profile, rather than the value of the variable  $\alpha_i$ , and then calculate values for  $\alpha_i$  and  $X_i$ .

Assuming that  $Y_i$  is given, the set of Equations (8.3) is solved for  $\alpha_i$ .

It follows from the second Equation of (8.3) that:

$$r_w \sin^2 \alpha_i - r_w \sin \Delta \sin \alpha_i - Y_i = 0.$$

By solving the equation, it can be found:

$$\sin \alpha_i = \frac{r_w \sin \Delta + \sqrt{r_w^2 \sin^2 \Delta + 4r_w Y_i}}{2r_w} = \frac{\sin \Delta}{2} + \sqrt{\frac{\sin^2 \Delta}{4} + \frac{Y_i}{r_w}}. \quad (8.3)$$

Thus, the cutter tooth profile can be constructed from the points by setting the value  $Y_i$  within the height of the tooth  $h = r_w - r_f$ . For a given value on the part drawing  $\Delta$  the  $\alpha_i$ , and then, using Equation (8.3) coordinate  $X_i$  can be found.

The radius of the pitch circle is determined by the initial conditions for the most complete machining of the side of the tooth.

The value of the radius of initial circle is:

$$r_w = \sqrt{\rho_A^2 - 0,187b^2} .$$

In case chamfers  $f$  are applied to the teeth tops (Fig. 8.14) the radius  $\rho_A = r_a - f$ , where  $r_a$  – is the radius of the part major diameter, which is defined by the part drawing.

The fillet height determination is given below.

The radius of the circle  $r_c$ , passing through the point  $C$ , which is the beginning of the transition curve, can be found from Fig. 8.17.

$$r_c = OC = \sqrt{OA^2 + AC^2} = \sqrt{r_f^2 + h^2 \text{ctg}^2 \alpha_c} .$$

The fillet height is  $h_r = r_c - r_f$ . Where radius  $r_f$  is found from the part drawing.

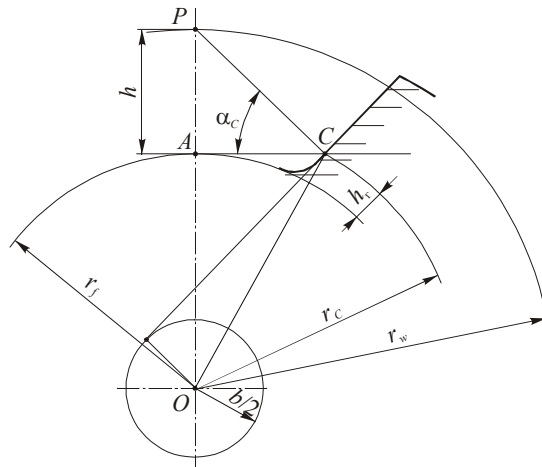


Fig. 8.17 Diagram for fillet height calculation

## 9. Cutting Tools for Automated Production

Cutting tools of special design and auxiliary tooling used in CNC machines and cell-type production are described in this section.

### 9.1 Cutting tools for automated machining

The range of cutting tools used in automated production is almost the same as the one used on universal machines. However, these tools are imposed more strict requirements on the accuracy of the size, form and quality of sharpening.

The indexable inserts of the newly developed cutting tools are widely used not only for turning cutters, but for drills, combination tools, milling cutters, etc.

Indexable spade drills, as well as coolant-fed indexable carbide drills, were widely adopted for hole-making operations, due to ability to quickly change the diameter by replacing inserts in the holder.

To reduce the number of operations the combination instruments such as step drills, core-drill-reamers, drill-taps and etc. are used. Moreover, even entire complex tools with a number of indexable inserts clamped in a housing of complex shape, and intended for machining of different elements of the workpiece surface are applied.

For boring stepped holes a variety of multicutter bars equipped with indexable inserts are used.

In the design of face mills the aggregate-modular principle is used, which implies application of the cartridges equipped with indexable inserts of various shape.

For horizontal milling machines, used in automated lines, a set of milling cutters, mounted on a mandrel (Fig. 9.1, a) and intended for simultaneous machining of multiple surfaces of the workpiece is often used. Due to this design productivity as well as accuracy of the mutual position of the machined surfaces significantly increases.

For three-axis milling on CNC machines the combination mill-drill (Fig. 9.1, b) is used, the cutting edges on the face are similar to the lips of the twist drill in design and are used during axial feed, and the cutting edges on the periphery of the tool are similar to those of the face mills and are used for contour feed.

For machining of complex contours ball nose endmills and bull nose endmills are used (Fig. 9.1, c).

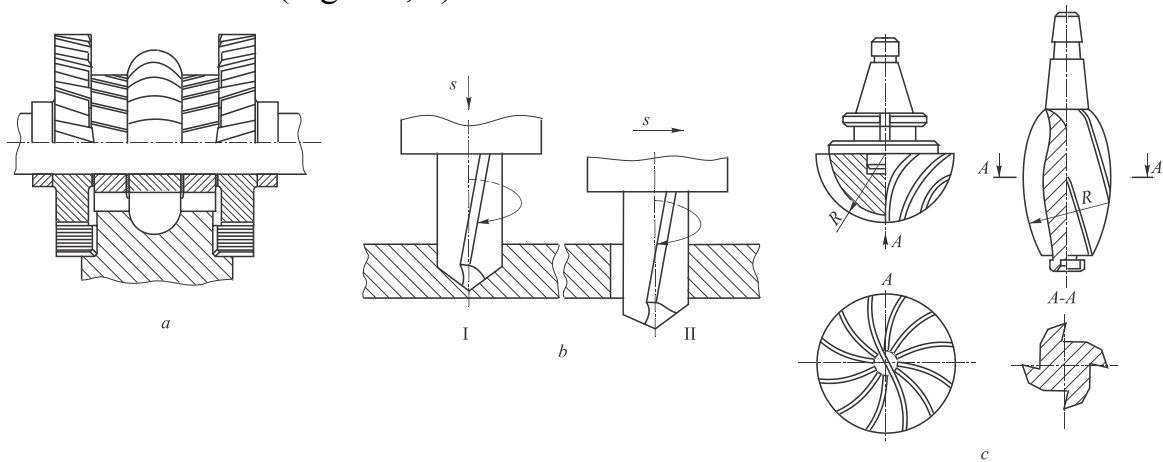


Fig. 9.1 Milling cutters: (a) gang cutters; (b) mill-drill; (c) form milling cutters

In order to provide quick change of the cutting tools and reduction of machine down time, the procedure of setting the cutting tool tools to the required size is performed with special tools off the machine tool. For this purpose the cutting tools are supplied with adjusting elements. For example, the turning cutters are equipped with truss screws, which are screwed into the holder face (Fig. 9.2, a). After adjusting to the size  $L$ , the cutter is clamped in the unit with wedges and screws.

To reduce the time of cutter change various devices, one of which is shown in Fig. 9.2, b, are used. Here the tool (1) clamping is performed with a spring-loaded wedge (2). To replace the cutter it is enough to move the link by the handle (3) to the left, and remove the cutter. Adjustment to the size is also carried out by a self-locking screw (4), supported by a fixed stop (5), mounted in the housing (6).

Adjustment-free replacement of the axial tools (drills, core drills, reamers, etc.) is achieved by means of adjusting screws (Fig. 9.2, c) or adjusting nuts (Fig. 9.2, d), which allow to change the tool overhang  $L$ . Twisting moment in both examples is applied to the key (1), and clamping is performed by the screw (2), which is supported by the sloped flat of the shank.

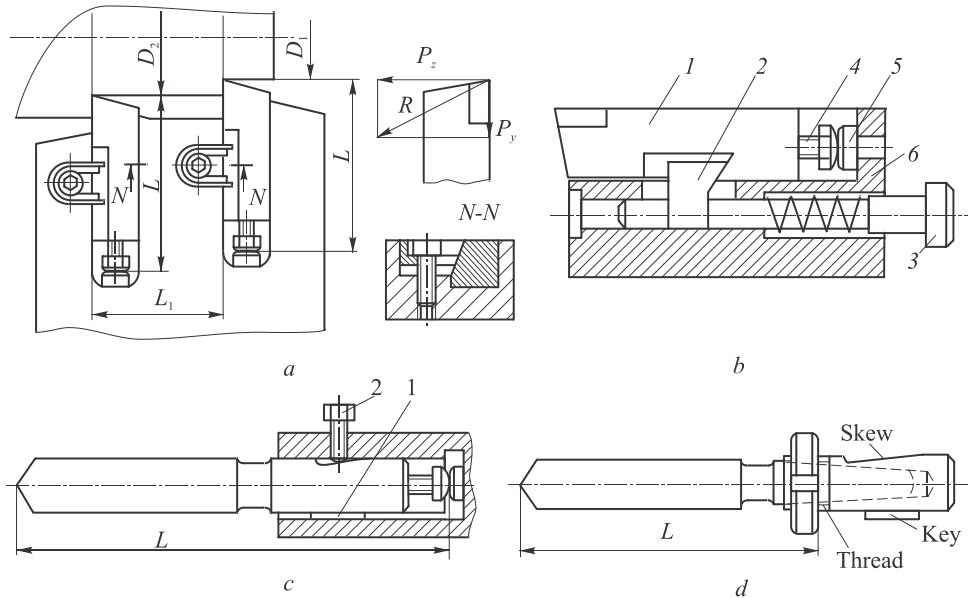


Fig. 9.2 Designs for adjustment-free tool change: (a), (b) for cutters; (c), (d) for axial cutting tools

To prevent the loosening of the tools under variable loads it is essential to design the quick-change tools so that the cutting forces press the holder against the mounting surface of the unit, and not against the adjusting and clamping elements (Fig. 9.2, a).

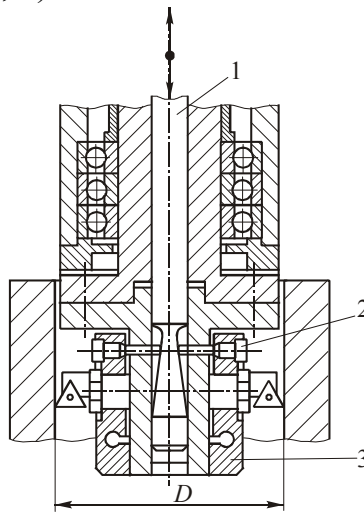


Fig. 9.3 Design of a boring bar with automatic adjustment to the size

To improve the dimensional stability of cutting tools, which is less than the total tool life, a variety of devices for automatic in-cycle size adjustment of the tool is used. An example of such a device is shown in Fig. 9.3. The machine tool gauge monitors the machined hole size and when the size approach to a limit of size calls for adjustment. Then the pull-bar (1) slides

along the spindle axis and by its conical part moves the rods (2) and expands elastic elements of the tool block (3), thus adjusting the hole diameter  $D$ .

## 9.2 Auxiliary tooling for CNC machines and machining centers

Auxiliary tools are various tool holders, chucks, arbours, extensions, adapters, special units and etc. They can significantly extend the field of application of the cutting tools and ensure its operation in automatic mode, and due to unification – to reduce the range of special cutting tools and implement aggregate-modular principle of designing.

The unification of the individual elements of cutting and auxiliary tools has created instrument systems for CNC machines and flexible manufacturing, which can quickly and easily reconfigure for the manufacture of new parts. In this case, auxiliary tools are to: 1) provide high accuracy and reliability of cutting tools mounting in the machine; 2) provide quick change of the tools; 3) expand the nomenclature of the tooling through the use of modular tools made of unified elements.

The largest number of designs for auxiliary tools was designed for multitask CNC machines, which can be divided into lathes group, used for machining of axisymmetric parts, and boring-drilling-milling group, used for machining of case-type parts.

In the first group of machine tools, cutting tools are positioned in turrets or tool posts often with the help of holders with a cylindrical shank, having serrated flats (Fig.9.4). For clamping various types of cutters, the holders have open or closed slots in two mutually perpendicular directions. Axial tool holders have a cylindrical part with conical or cylindrical holes on its face. The clamping of the holders in the machine themselves is performed with a serrated wedge.

The hollow holders with 7:24 tapered shank, straight shank, Morse taper shank or short-taper shank are often used in the machines of the second group. Torque is transferred with the help of dowels, screws, collets, self-locking Morse tapers and etc.

The unified shank with 7:24 taper provides good centering, backlash-free connection to the spindle and allows easy extraction/insertion by a tool changer. To ensure secure grip by a tool changer's gripper the flange of the holder is provided with a "V" groove and two keyway slots and for orientation of the tool relative to the grooves – a 90° angle notch is used.

The pulling of the holder into the spindle is performed by either a screw or a draw bar with spring washers.



The downside of the holders with 7:24 taper shank is large size and weight, and lack of fit on the spindle face.

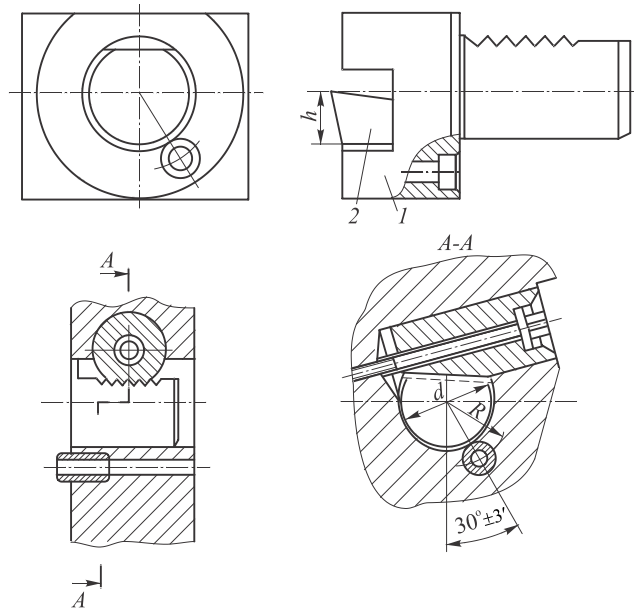


Fig. 9.4 Design of a tool holder with cylindrical shank

Thus, recently, a number of toolholder designs, that offer locating on both the cylindrical and the face surfaces, to substitute the 7:24 holder were searched. The simultaneous fit on both surfaces allows for larger dynamic stiffness with vibration damping in the joint.

The same principle of locating is also applied for assemblies of tool blocks, consisting of cutting and auxiliary tools. In this case, the cylindrical surfaces length should be not less than the diameter in size. Axial run-out of these surfaces should not be more than 1...3  $\mu\text{m}$ , and the radial run-out less than 3...5  $\mu\text{m}$ .

Some schemes of such assemblies are shown in Fig. 9.5.

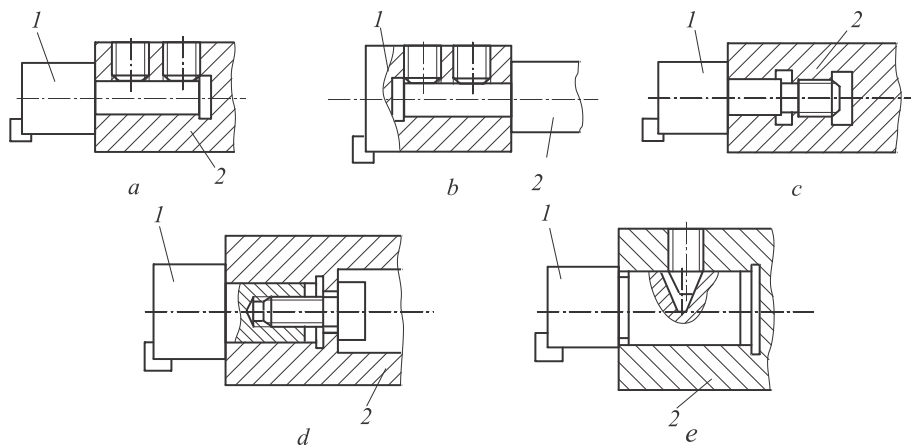
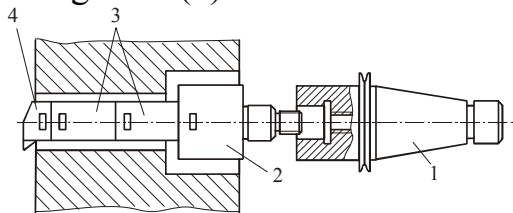


Fig. 9.5 Designs of modules couplings: (1) cutting tool; (2) holder

With clamping screws positioned radially on one side, an internal (Fig 9.5, a) or external (Fig. 9.5, b) coupling of the tool (1) to the mandrel (2) can be used. To create fit on the face interface the threaded versions shown in Fig. 9.5, c, d. A simpler version (Fig. 9.5, e) with a screw with an offset axle is also possible.

Aggregate-modular principle of assembled tool-blocks design can be illustrated by an example of a boring tool shown in Figure 9.6. Here, the block is coupled with a spindle by means of holder (1) with 7:24 taper. The holder couples with the extension (2) of increased diameter for extra rigidity, which is connected to the adapters (3), used to configure the length, and at the end of the block there is a boring head (4).



*Fig. 9.6 Modular boring head assembled of standard modules:  
(1) holder; (2) extension bar; (3) adapter; (4) boring head*

Various adapter sleeves, holders, arbors, collet and three-jaw chucks and etc. are used as auxiliary tools. The auxiliary tools are made of chromium-manganese-titanium alloyed steels with case hardening to HRC 53...57, which ensures high durability. The circular run-out of the mounted in a holder element with respect to the shank should be no more than 5...10  $\mu\text{m}$ .

The disadvantage of assembled tool blocks is rigidity and lower accuracy compared to the solid tools – and the more modular elements are in the block, the higher is the drawback. To raise the accuracy of the blocks, the elements for cutting tool size adjustment are used.

Aggregate-modular principle was used to create tooling system for automated machines, allowing to process complex parts in small batches with automatic change of cutting tool pre-installed in special tool magazines.

These systems consist of two subsystems: the cutting and auxiliary tools, which differ in design depending on the type of equipment and work-piece type.

Figure 9.7 shows an example of the CNC lathe tooling, containing auxiliary and partially cutting tools. Holders with serrated flats (Fig. 9.4, a) are clamped in turrets by means of wedges with locating on cylindrical surface and face. Holder head is provided with open or closed mutually perpendicular slots (1...9) to mount cutters of various types (turning, cut-off, etc.) with different length and direction of the holder with respect to the axis of the mounting hole. Tool holders can be either a right or left-hand design and are ap-

plied depending on the turret location and the direction of the spindle rotation.

The adaptor sleeve (10) allows clamping of cutting tools or auxiliary elements of circular cross-section with diameters of 16...40 mm. For hole making the flat drill (11) with direct mounting in the holder is used. Versions (12) and (13) are provided with Morse tapered holes for mounting a three-jaw chuck (19) and axial cutting tools (drills, core-drills, reamers, etc.). Boring of holes can be performed with either cutters, held in the holders 1...9, or boring bars (14) and (15). Version (16) can be used to clamp taps for threads from M6 to M27 in a chuck. Versions (17) and (18) are adapter sleeves provided with keyway slots. They are used to mount boring bar (20), tap chuck (21) or cutting tools with a short Morse taper (22). These adapter sleeves are a binding link with drilling, milling and boring machines.

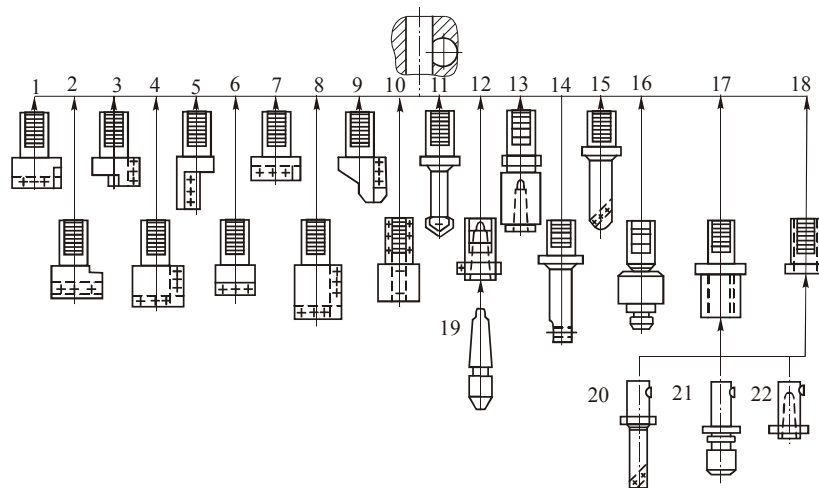


*Fig. 9.7 Tooling system for CNC machines of turning type*

The tool systems for drilling, milling and boring machines are built in the same way. For coupling with the machine spindle the holder shanks with 7:24 taper or Morse taper are used. A fragment of the tooling system and a set of variants for clamping of various cutting tools, such as end mill, drill and boring bar is shown in Figure 9.8. For torque transfer the 7:24 holder has keyway slots for the spindle face-keys. Tool change is performed automatically by the CNC program functions with the help of manipulator, which moves cutting tools from the magazine into the spindle and back.

The mentioned above tooling system for CNC machines turned out to be bulky, expensive and required manual labor for setting tools to the sizes. It was necessary to reduce the number of auxiliary tools features to a minimum and to create more compact designs of cutting tools.

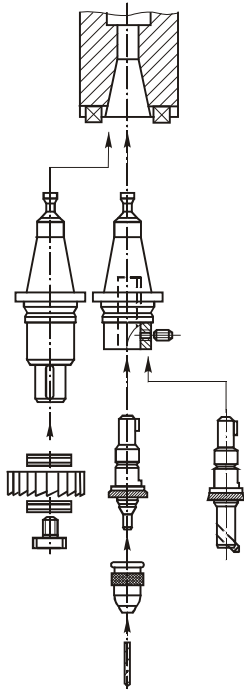


Fig. 9.8 Tooling system for CNC machines of drilling-milling-boring type

A number of companies developed various tooling systems for flexible machining. One of the solutions for CNC lathes was proposed by Sandvik Coromant (Sweden) (Fig. 9.9). It implements compact interchangeable indexable cutting heads used for all types of turning operations. The design incorporates a shortened shank and a head with an opening, shoulder and slot. Inserted heads (1) are clamped in the holder (2), which has special features for fixing the heads. The force applied to the draw-bar (3), elastically deforms shoulders of the shank and forms a rigid coupling of the head to the holder. The exact position of the head is ensured by its location on the face, two sides of the shoulders and the bottom base. The clamping force is created by the spring washers, and the release of the heads is executed by spring washers decompression with the help of hydraulic cylinder.

In addition to cutters (Fig. 9.9, a), tool heads are equipped with other types of cutting tools, as well as chucks for drills, taps, etc. (Fig. 9.9, b, c).

Accuracy of the cutting edge corner positioning after reinstalling the head is  $\pm 2 \mu\text{m}$  in length and  $\pm 5 \mu\text{m}$  in height. Application of heads can reduce the tool weight by about 50%.

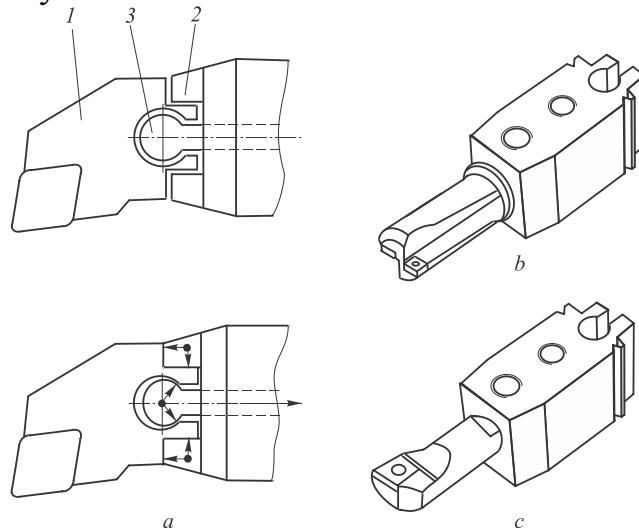


Fig. 9.9 Turning inserts: (a) insert clamping; (b) drill holder; (c) cutter holder

The sets of such heads are placed in storage drums near CNC machines. The heads are coded for automatic tool change and replacement by computer command.

## Conclusion

Cutting of materials is one of the main methods of engineering production. Machining involves material removing to make the product of a given shape and size and ensure accuracy and surface finish. Thus the first three chapters of the book are devoted to the aspects of mechanics of cutting, chip formation, conditions of cutting, tool wear and tool life as well as to description of the basic machining operations.

Information about the patterns of cutting process is the basis for the design of metal-cutting tools, machine tools and manufacturing processes and equipment and is discussed in the chapters from 3 to 9.

The book is written in accordance with the syllabus of the discipline “Material Cutting and Cutting Tools” and is designed for students enrolled in the Bachelor Degree program 150700 “Mechanical engineering”.

## References

1. *Васин С.А., Верещака А.С., Кушнер В.С.* Резание материалов: Термомеханический подход к системе взаимосвязей при резании. – М.: Изд-во МГТУ им. Баумана, 2001. – 448 с.
2. *Высокоскоростная обработка. High Speed Machining (HSM): Справочное пособие.* – М.: ИТО, 2001. – 32 с.
3. *Гинзбург Е.Г., Халевский Н.Т.* Производство зубчатых колес. – Л.: Машиностроение, 1978. – 136 с.
4. *Дибнер Л.Г., Шкурин Ю.П.* Заточка спиральных сверл. – М.: Машиностроение, 1967. – 156 с.
5. *Иноземцев Г.Г.* Проектирование металлорежущих инструментов. – М.: Машиностроение, 1984. – 272 с.
6. *Калашиников С.Н.* Зуборезные резцовые головки. – М.: Машиностроение, 1972. – 162 с.
7. *Кирсанов С.В., Гречишников В.А., Схиртладзе А.Г., Кокарев В.И.* Инструменты для обработки точных отверстий. – М.: Машиностроение, 2003. – 330 с.
8. *Кожевников Д.В., Кулешова И.В., Левин В.И. и др.* Современные конструкции сборного инструмента с многогранными неперетачиваемыми пластинами: Обзор. – М.: НИИмаш, 1979. – 56 с.
9. *Кожевников Д.В.* Современная технология и инструменты для обработки глубоких отверстий: Обзор. – М.: НИИмаш, 1981. – 60 с.
10. *Мазальский В.Н.* Суперфинишные станки. – Л.: Машиностроение, 1988. – 127 с.
11. *Мальшико В.Ю.* Заточка оптимальных углов на резцах // Вестник машиностроения. – 1982. – №5. – С.56–59.
12. *Маслов А.Р.* Приспособления для металлообрабатывающего инструмента: Справочник. – М.: Машиностроение, 1996. – 240 с.
13. *Металлорежущие инструменты/ Г.Н. Сахаров, О.Б. Арбузов, Ю.Л. Боровой и др.* – М.: Машиностроение, 1989. – 328 с.
14. *Попов С.А.* Заточка и доводка режущего инструмента. – М.: Высшая школа, 1986. – 223 с.
15. *Потапов В.А.* Применение механической обработки с минимальным количеством СОЖ на германских заводах// Машиностроитель. – 1999. – №11. – С. 46 – 52.
16. *Прогрессивные методы хонингования/ С.И.Куликов, Ф.Ф.Ризванов, В.А.Ковальчук, С.В.Ковалевский.* – М.: Машиностроение, 1983. – 135 с.

17. Протяжки для обработки отверстий / Д.К. Маргулис, М.М. Тверской, В.Н. Ашихмин и др. – М.: Машиностроение, 1986. – 232 с.
18. Резание и инструмент / Под ред. А.М. Розенберга. – М.: Машиностроение, 1964. – 228 с.
19. *Родин П.Р.* Металлорежущие инструменты. – Киев: Вища шк., 1986. – 456 с.
20. *Романов В.Ф.* Расчеты зуборезных инструментов. – М.: Машиностроение, 1969. – 256 с.
21. *Семенченко И.И., Матюшин В.М., Сахаров Г.Н.* Проектирование металлорежущих инструментов. – М.: Машгиз, 1962. – 952 с.
22. Справочник инструментальщика / И.А.Ординарцев, Г.В.Филиппов, А.Н.Шевченко и др.; Под общ. ред. И.А.Ординарцева. – Л.: Машиностроение, 1987. – 846 с.
23. Справочник конструктора-инструментальщика / Под общ. ред. В.И. Баранчикова. – М.: Машиностроение, 1994. – 560 с.
24. *Хлебалин Н.Ф.* Нарезание конических зубчатых колес/ Под ред. Е.Г.Гинзбурга. – Л.: Машиностроение, 1978. – 160 с.
25. *Эфрос М.Г., Миронюк В.С.* Современные абразивные инструменты / Под ред. З.И.Кремня. – Л.: Машиностроение, 1987. – 158 с.
26. *Якухин В.Г.* Оптимальная технология изготовления резьб. – М.: Машиностроение, 1985. – 184 с.
27. Cutting Tool Applications. George Schneider, 2005
28. Manufacturing Engineering and Technology. Fifth edition. Serope Kalpakjian, Steven R. Schmid, 2006
29. Mechanical Technology. Material Removal Processes. Compendium. Jan Madl, 1996
30. Metal cutting (4th edition). Edward Trent, Paul Wright. 2000, 464 p.
31. Metal cutting mechanics. V.P. Astakhov, 1998, 320 p.
32. Workshop practice (2nd edition). H.S.Bawa. Published by Tata McGraw Hill. 2009

Educational Edition

КИРСАНОВ Сергей Васильевич

# РЕЗАНИЕ МАТЕРИАЛОВ И РЕЖУЩИЙ ИНСТРУМЕНТ

Учебное пособие  
На английском языке

**Published in author's version**

Editor *V.N. Kozlov*

Editor *A.B. Kim*

Translator *A.B. Kim*

Lingvistic Advisor Senior lecturer  
*O.G. Maslennikova*

**Printed in the TPU Publishing House in full accordance  
with the quality of the given make up page**

Signed for the press 00.00.2009. Format 60x84/16. Paper "Snegurochka".  
Print XEROX. Arbitrary printer's sheet 000. Publisher's signature 000.  
Order XXX. Size of print run XXX.



Tomsk Polytechnic University  
Quality management system  
of Tomsk Polytechnic University was certified by  
NATIONAL QUALITY ASSURANCE on BS EN ISO 9001:2008



**TPU PUBLISHING HOUSE.** 30, Lenina Ave, Tomsk, 634050, Russia  
Tel/fax: +7 (3822) 56-35-35, [www.tpu.ru](http://www.tpu.ru)